THE DETECTION AND PREDICTION OF AGRICULTURAL DROUGHT IN THE CANADIAN PRAIRIES

A THESIS

SUBMITTED TO THE FACULTY OF ARTS IN PARTIAL FULFILLMENT OF THE REQUIREMENTS FOR THE DEGREE OF

MASTER OF ARTS

BY
STEVEN QUIRING

DEPARTMENT OF GEOGRAPHY
UNIVERSITY OF MANITOBA
WINNIPEG, MANITOBA

0-612-62829-9

THE UNIVERSITY OF MANITOBA

FACULTY OF GRADUATE STUDIES

*****

COPYRIGHT PERMISSION

THE DETECTION AND PREDICTION OF AGRICULTURAL DROUGHT IN THE CANADIAN PRAIRIES

BY

STEVEN QUIRING

A Thesis/Practicum submitted to the Faculty of Graduate Studies of The University of Manitoba in partial fulfillment of the requirement of the degree

of

MASTER OF ARTS

ACKNOWLEDGEMENTS

This journey has come to an end. It is my distinct pleasure to give recognition to those who played an important role. The completion of this work was due in no small part to the input from my advisor, Dr. Tim Papakryiakou. I have enjoyed being Tim's first graduate student and I hope that I did not cause him too much grief. I would also like to thank my committee members, Dr. Wole Akinremi and Dr. Danny Blair, for their time and thoughtful suggestions. Finally, I would like to thank my family and, especially, my wife Shona for putting up with me during the entire process.

ABSTRACT

This thesis examined four drought indices (Palmer Drought Severity Index (PDSI), Standardized Precipitation Index (SPI), NOAA Drought Index (NDI), and Moisture Anomaly Index (Z)). The comparison revealed that the Moisture Anomaly Index (Z) is the 'best' index for measuring agricultural drought on the Canadian prairies. Not surprisingly, the moisture conditions during the month of June were found to be the most important determinant of yield. A subsequent diagnostic analysis determined that the performance of the Z-index (as an indicator of agricultural drought) is influenced by the number and timing of precipitation events during the growing season. This drought index was used to divide the study region into five relatively homogeneous crop district clusters. Statistics on drought frequency, severity, and spatial extent were calculated using these regions. In Cluster 2 and Cluster 5, approximately one out every six growing seasons experiences moisture conditions that are not suitable for crop production. A spatial analysis showed that there are three preferred patterns of drought on the prairies and a temporal analysis revealed the presence of coherent drought periodicities (in particular quasi-2, 4, and 10-15 year oscillations). Finally, the relationship between global teleconnection indices and the occurrence of agricultural drought was explored through a composite analysis and a Principal Components Analysis. Both of these analyses suggested that North Pacific circulation and SST anomalies during winter, and eastern equatorial SST anomalies during spring may be related to growing season drought. In addition, Atlantic sector teleconnections also appear to be important.

TABLE OF CONTENTS

CHAPTER 4: SELECTION OF THE 'BEST' AGRICULTURAL DROUGHT INDEX

CHAPTER 5: AN AGRICULTURAL DROUGHT CLIMATOLOGY OF THE CANADIAN PRAIRIES

CHAPTER 6: PREDICTION OF AGRICULTURAL DROUGHT ON THE CANADIAN PRAIRIES

CHAPTER 7: CONCLUSIONS AND RECOMMENDATIONS

LIST OF FIGURES

Figure **Page**

LIST OF TABLES

Table **Page**

CHAPTER 1
INTRODUCTION

1.1 Statement of the research problem

Drought is a natural disaster that has a major economic impact on the Canadian prairies because of the vulnerability of the region's agricultural sector to climate variability. This can be illustrated by the 5.8 billion dollars in losses the agricultural sector is estimated to have suffered from the 1988 drought (Wheaton *et al.*, 1992).

The Canadian prairies are dominated by a semi-arid climate where evapotranspiration exceeds precipitation. The precipitation regime is highly variable and unevenly distributed, with the majority of precipitation occurring during the summer months. Growing season precipitation for the Canadian prairies, which provides the majority of water required by crops, averages about 200 mm and crop water demand is approximately 300 mm (Ash *et al.*, 1992). As a result, only a small negative deviation in normal precipitation is required to initiate an agricultural drought. These conditions ensure that droughts are a frequent occurrence in this region.

Drought conditions can usually be found in some part of the Canadian prairies during any given year because of the size of the region and the extreme spatial variability of the weather. Since the beginning of instrumental records (in the 1870's) major droughts (prolonged, widespread, and severe) have occurred in the 1890's, 1930's, 1950's, and 1980's, but paleo-climate research indicates that the climate of the twentieth century may not be representative of the long-term patterns of natural variation in drought frequency and severity. Indeed, prior to

1200 AD, droughts occurred more frequently, lasted longer, and were more severe (Laird *et al.*, 1996).

Droughts are unique among natural disasters because of the long time-frames over which they develop and the difficulty in detecting their onset. A drought index is one tool that can be used to detect the onset and severity of droughts, as well as to study the spatial and temporal patterns of drought. A large number of drought indices have been developed (e.g., Palmer Drought Severity Index (PDSI), Standardized Precipitation Index (SPI), and NOAA Drought Index (NDI)) and they employ a wide variety of approaches to monitor moisture conditions (Appendix A provides definitions of all acronyms that are used).

Drought has been extensively studied on the Canadian prairies and the Great Plains of the United States. Despite this fact, no study has compared the performance of existing drought indices to determine which is most appropriate for measuring agricultural drought on the Canadian prairies. The purpose of this study is to fill this gap in the literature and to document the frequency, severity, and spatial extent of agricultural droughts on the Canadian prairies during the twentieth century. Finally, the predictability of agricultural drought will be examined by building on the existing body of research that has demonstrated that various climate phenomena, such as the El Niño/Southern Oscillation (ENSO) and North Pacific sea-surface temperatures, are strongly linked to precipitation patterns (moisture conditions) over North America. These links are known as teleconnections and have great importance because of the opportunity they offer for long-range climate and drought forecasting.

1.2 Thesis objectives

The main objectives of this study are as follows:

1) to determine the *best* drought index for detecting the occurrence of agricultural drought and measuring its severity on the Canadian prairies;

2) to use the index selected in Objective 1 to identify coherent drought regions in the study area and to describe the patterns of drought frequency, severity, and spatial extent on the Canadian prairies during 1920-1999, and;

3) to explore the relationship between global teleconnection patterns and the occurrence of agricultural drought on the Canadian prairies.

1.3 Relevance of the study

This study has applied value for the agricultural community because it adds to our understanding of climate and drought vulnerability on the Canadian prairies. In addition, knowing which drought index provides the best measure of agricultural drought on the Canadian prairies will encourage agencies, like the Prairie Farm Rehabilitation Administration (PFRA) and the Canadian Wheat Board (CWB), to adopt this index on an operational basis for monitoring growing season moisture conditions. Finally, exploring the relationship between teleconnections and severe drought events on the Canadian prairies will help to elucidate those physical mechanisms involved in drought formation and which control the length and severity of droughts. As a result, the onset of drought may be detected earlier and more accurately, allowing for appropriate measures to be implemented to minimize loss, thereby safeguarding the agricultural economy from climate uncertainty.

CHAPTER 2
LITERATURE REVIEW

2.1 Introduction

This literature review is presented in nine sections. The first section provides a working definition of agricultural drought. The second section examines the climate and drought history of the prairies. The third section details the impact of drought. The fourth section describes the physical processes that cause droughts. The next section discusses factors affecting crop yield and this is followed by a section that describes crop water-use efficiency. The seventh section provides an introduction to the drought indices used in this study. The final two sections define and describe teleconnections and discuss their utility for drought prediction.

2.2 Defining agricultural drought

The occurrence of drought at irregular intervals is a normal and natural part of the variability of the climate system. In fact, droughts occur in all climatic-zones throughout the world.

Drought is a complex phenomenon that is difficult to accurately describe because its definition is spatially variant and context dependent. As a result, there are more than 150 definitions of drought in the literature (Glantz, 1982). At the simplest level, drought can be defined as a moisture deficit (Wilhite *et al.*, 1987). More accurately, drought can be defined as "an interval of time, generally of the order of months or years, when the moisture supply of a region falls short of the climatologically expected (normal) or climatologically appropriate moisture supply" (Palmer, 1965). It should be noted that there is a difference between aridity and drought. Aridity is a permanent climate characteristic that refers to low average annual rainfall, or very little available water (Rosenberg, 1978). Drought is a temporary feature of the climate, when rainfall is below what is normally expected or appropriate. Droughts may be exacerbated by other factors, including extreme heat, low humidity, and high winds (Rosenberg, 1978).

Drought definitions can be broken down into three main categories: meteorological, hydrological, and agricultural. Meteorological drought refers to any significant negative departure from 'normal' precipitation. Hydrological drought is more concerned with deficiencies in streamflow, groundwater, and lake and reservoir levels and agricultural drought is based on prolonged water stress due to inadequate soil moisture and its effects on plant health and productivity (e.g., crop yield, biomass production) (Nkemdirim and Weber, 1999).

The relationship between the three main categories of drought is illustrated in Figure 2.1. Drought will first become evident when precipitation falls below normal levels for an extended period of time. This first stage is known as meteorological drought. If these conditions persist, the vegetation will be influenced as soil moisture becomes depleted and there is insufficient recharge. This stage is classified as agricultural drought. Eventually, if precipitation levels remain below normal for an extended period of time (many months or years), we then enter the third stage of the drought evolution --- hydrological drought, when discharge and groundwater supply is affected. There is typically a significant lag between the first and third stages of drought, therefore, a 'short' drought (e.g., one that persists for three to six months) may not affect the hydrological system.

There are many definitions of agricultural drought, including a shortage of moisture in the rooting zone of crops, and a state of deficient moisture conditions which produces a lasting adverse effect upon plants, particularly those of economic importance. In this study, agricultural

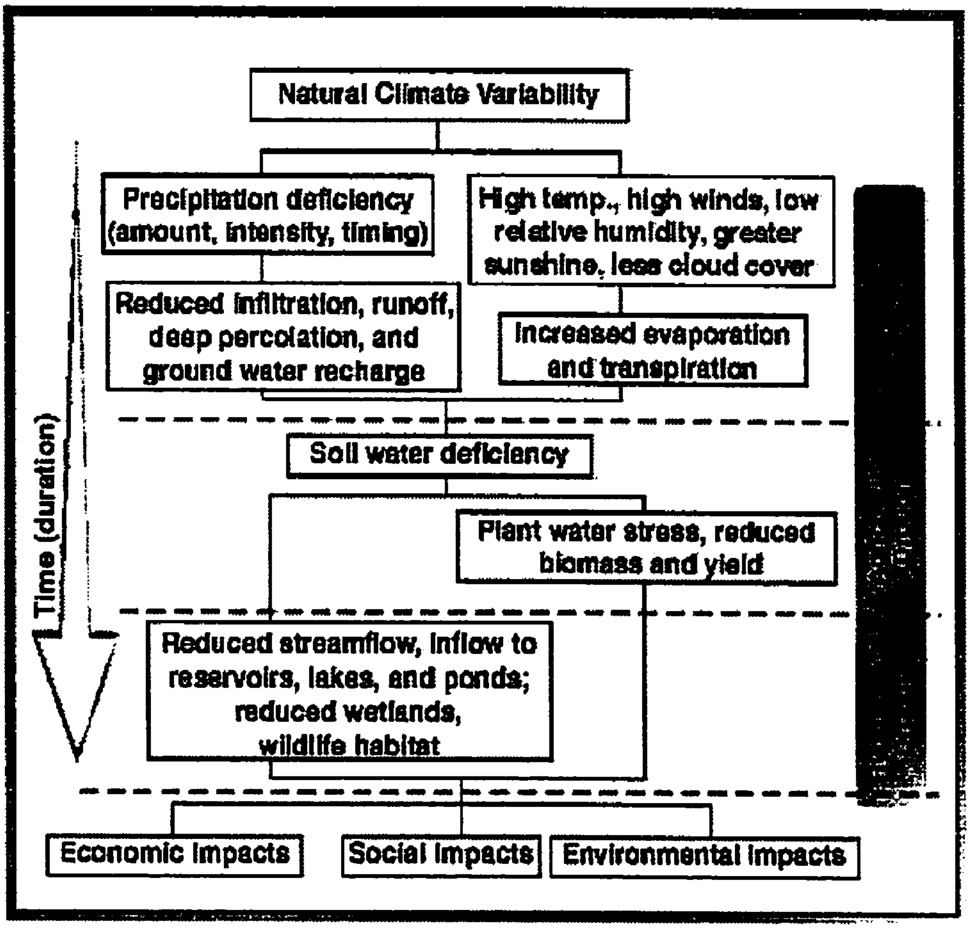

Figure 2.1 Schematic diagram of the three main categories of drought *(NDMC, 1999)*

drought is specifically defined as an interval of time, generally of the order of months or years when the moisture supply of a region consistently falls below the climatically appropriate moisture supply such that crop production or range productivity is adversely affected (Palmer, 1965; Rosenberg, 1978). Ultimately, agricultural drought is a supply and demand problem. Demand is determined by the plant and supply is determined by soil moisture, which is recharged through rainfall (Wilhite *et al.*, 1987).

There are a number of other terms that should be defined for the sake of clarity. Drought frequency can simply be defined as the number of times during a particular period that a drought of a given magnitude occurs. Drought intensity is the magnitude of the moisture departure from normal (irrespective of the length of time for which this state persists).

Droughts have both spatial and temporal aspects. That is, their effects are felt over a particular area for a certain length of time. Of course, the affected area can either increase or decrease as the drought evolves. Drought severity is determined from and influenced by the duration of the drought, its spatial extent, the magnitude of the moisture deficit, and by the impact on people (social, physical, or economic impacts) (Wilhite *et al.*, 1987). Generally, the greater the severity of the drought, the larger the area involved. It is almost impossible to have a severe drought that only affects a very small area, due to a link between severe droughts and large-scale atmospheric circulation anomalies (Rosenberg, 1978).

2.3 Climate and drought history of the Canadian prairies

Although instrumental records for most of the prairies are only available since the 1870s, the climate of the region during the Holocene (the last 10,000 years) has been extensively studied using a variety of paleo-climate data sources such as tree rings, pollen records, and lake sediments.

The climate of the Canadian prairies during the Holocene can be divided into four distinct phases. The first phase, prior to 9000 years BP (before present), was dominated by rapid vegetation changes due to the processes of soil development and postglacial migration of plants (Herrington *et al.*, 1997). During the second phase, from 9000-6000 years BP, the climate was much warmer and drier than it is today and as a result the northern boundary of the prairies was approximately eighty kilometers farther north (Herrington *et al.*, 1997). In the third phase, from 6000-4000 years BP, the climate was cooler and wetter than it is today causing the Boreal forest to advance southward. Finally, a series of ice advances and retreats have occurred since 4000 BP. Notably, the climate warmed during the Medieval Warm Period (approximately 950-1450 AD). This was followed by a rapid cooling that took place during the Little Ice Age (approximately 1500-1850 AD). More recently, a series of distinct phases are also evident in the climatic record. According to Gullet and Skinner (1992), a general warming of the climate occurred from the late 1890s to the 1940s. This was followed by a cooling trend that occurred from the 1940s through the 1970s, and the warming resumed in the 1980s.

Research has revealed that there have been many periods of intense drought on the Canadian prairies and throughout the Great Plains during the Holocene. The episodes of drought that have occurred during the last century appear fairly mild and infrequent when compared to the droughts that ravaged the prairies prior to 1200 AD (Laird *et al.*, 1996). It is hypothesized that droughts occurred more frequently, for longer intervals (decades), and were more intense than the infamous drought of the 1930s (Stahle *et al.*, 2000). A 2,300 year drought reconstruction for the Northern Great Plains using lake salinity records inferred from fossil diatoms suggests that extreme droughts were much more frequent during 200-370 AD, 700-850 AD, and 1000-1200 AD (Laird *et al.*, 1996). Unfortunately, for the period prior to the nineteenth century, little agreement exists among the different drought histories that have been reconstructed for the Northern Great Plains (Stockton and Meko, 1983; Laird *et al.*, 1996; Sauchyn and Beaudoin, 1998; David *et al.*, 1999; Stahle *et al.*, 2000). It can be concluded that drought frequency has been relatively uniform during the last 750 years, although this may not be representative of the long-term variability present in the Northern Great Plains climate record (Laird *et al.*, 1996).

The drought history of the Canadian prairies since the beginning of the nineteenth century is less ambiguous. Minor droughts occurred on the Canadian prairies in 1804-5, 1820, the 1860s, 1910, 1917-1921, and 1976-1977 (Kemp, 1982; Maybank *et al.*, 1995). Major droughts occurred on the Canadian prairies in the 1880s, 1890s, 1930s, late 1950s and early 1960s, and most recently in the 1980s (Maybank *et al.*, 1995). The length of these droughts has varied from one to four years, with an average duration of two years (Maybank *et al.*, 1995).

The first major drought of the twentieth century began in 1929, and by 1933 severe drought gripped all of the Canadian prairies. The drought did weaken somewhat during 1934 and 1935, but in 1936 excellent crops were ruined by extreme July heat coupled with a lack of precipitation. Many stations set temperature records in 1936-1937 by recording more than forty-five days with maximum temperatures greater than 30°C (Maybank *et al.*, 1995). The result was a complete crop failure in 1937. In fact, the two-year period from 1936-1937 was the most severe period of drought, in terms of severity and extent, during the entire twentieth century and its effects were felt in all three prairie provinces (Maybank *et al.*, 1995).

The next major drought occurred in 1961. This drought is the most severe and extensive single-year drought to occur on the Canadian prairies during the last one hundred years (Maybank *et al.*, 1995). It began in September 1960, when soil moisture levels became depleted due to a lack of fall precipitation. Drought conditions persisted through the spring and intensified in June and July because of the hot-dry weather. The drought, by this time, encompassed the entire southern agricultural region of Alberta, Saskatchewan, and Manitoba. This drought had its biggest impact in the agricultural and hydro-electrical sectors and net farm income decreased by three hundred million dollars from the previous year (Maybank *et al.*, 1995; Bonsal *et al.*, 1999).

Like the 1930s, the 1980s were a decade ravaged by drought. In the summer of 1980, ranchers lost millions of dollars because of the impact of the drought on pasture and livestock (Maybank *et al.*, 1995). Late summer precipitation did help to save some of the crops in Manitoba and Saskatchewan, but both the forestry and hydro-electrical sectors still felt the negative effects of the prolonged drought.

Drought struck again in 1984, this time due in part to an extremely mild winter. In February, the majority of prairie meteorological stations reported less than 5 cm of snow and most of it had melted by the end of the month (Maybank *et al.*, 1995). The dry spring resulted in low crop yields over much of the prairies.

Drought conditions returned to the Canadian prairies with a vengeance in 1987. The winter of 1987-1988 and the spring and summer of 1988 experienced above normal temperatures and below normal precipitation. Mean temperatures were between two and four degrees above normal across most of the prairies for March, April, and May (Cohen *et al.*, 1992). June 1988 was the hottest month ever recorded at many climate stations on the Canadian prairies. During the summer (June, July, and August), temperatures were an average of four to seven degrees higher than normal across most of the prairies (Herrington *et al.*, 1997). This, coupled with the fact that many stations had less than half the normal June rainfall, produced a wedge of severe drought that extended northward almost to the fringe of the Boreal forest in June 1988 (Cohen *et al.*, 1992). The drought weakened slightly by August, but the soil moisture deficit remained well into the fall and winter of 1988. Yields in Saskatchewan and Manitoba were only 50-60% of normal and Manitoba was forced to import hydroelectric power because rivers and lake-levels had reached record lows. The 1987-1988 drought also had many other impacts, including those on duck populations, forest fires and dust storms.

Nkemdirim and Weber (1999) used the PDSI to compare the drought of the 1930s with the drought of the 1980s. They found that nine out of the eleven years between 1929-1939 and six of the eleven years between 1979-1989 were drought years. In addition, the region affected by mild to extreme drought in the 1930s was 16% larger than in the 1980s. However, the area affected by extreme drought was 10% larger in the 1980s. The spatial pattern of drought during the 1930s can be described as patchy, while during the 1980s the pattern of drought was much more spatially coherent or zoned.

Although the droughts of the 1930s were more frequent and persistent than those of the 1980s, individual events were generally less severe. The 1961 drought is the single most severe hydro-climatological event of the twentieth century, but it did not cause as much hardship as the droughts of the 1930s and 1980s due to its short duration. The severe droughts of the 1980s were less socially destructive than the 1930s because technological and cultural advances insured that people were better able to adapt and cope with the drought.

2.4 Impacts of drought on the Canadian prairies

Water is an integral part of the economy and therefore a shortage of water has far-reaching impacts that span many sectors. The impacts of drought can broadly be described as either economic, environmental, or social in nature, and these impacts may arise from both direct or indirect means.

The majority of economic damage that results from drought events occurs in the agricultural sector (or sectors closely related to it). The most obvious economic loss is from decreased crop and livestock production. Drought also increases the risk of disease outbreaks in both plants and animals. Prolonged drought may result in bankruptcy, increased unemployment, higher prices for food, food shortages, and retarded economic growth. Forestry production may be affected through loss of timber due to wildfires, insects, disease, or seedling mortality. In addition, the travel and tourism industry may lose revenue, manufacturers of farm equipment may be faced with reduced sales, and transportation costs may increase if rivers and lakes become un-navigable.

Environmental damage occurs when plants, animals, or the natural environment (habitat, air, water, and soil) are affected by drought. Environmental losses are much more difficult to quantify than economic losses. Many parts of the environment affected by drought events (e.g., air quality, damage to plant species) quickly return to normal when the drought ends, while for other parts of the environment (e.g., soil loss, landscape damage, loss of biodiversity) the damage is essentially permanent.

Social implications mainly involve public health and safety, population migration, and reduced quality of life. Many of the impacts of drought classified as economic or environmental may have a social component as well. Public health and safety often becomes an issue during droughts because of concerns about forest fires, water quality issues, food shortages, or mental and physical stress. Population migration can also be significant if a severe drought persists for a long period of time. Indeed, drought was responsible for the migration of over a quarter of a million people during the 1930s (Maybank *et al.*, 1995). Finally, the most common social problem that arises due to drought is a reduced quality of life due to the discomfort, uncertainty, and stress that those people affected by the drought may experience.

Not all impacts of drought are negative. For example, agricultural producers outside of the affected region may benefit from higher prices. Generally, however, drought is seen as a natural disaster that causes significant damage to the economy. The most recent destructive drought on the Canadian prairies occurred in 1988. Crop production during this year was only 50% of the long-term average in Saskatchewan and 60% in Manitoba. Federal drought assistance programs and insurance companies paid out over 1.8 billion dollars in claims as a result of widespread crop failure and export losses cost the economy an additional 4 billion dollars (Herrington *et al.*, 1997). As a result, more than 10% of farmers and farm workers left the agricultural sector (Herrington *et al.*, 1997).

The drought of 1988 also caused environmental degradation through massive amounts of soil erosion and increased frequency of dust storms (Cohen *et al.*, 1992). Impacts on forestry included higher than normal seedling mortalities, outbreaks of tent caterpillars and spruce budworms, and an active forest fire season (the cost of fighting fires in Manitoba and Saskatchewan reached 56 million dollars) (Cohen *et al.*, 1992).

In 1986-1987 Manitoba produced 24 billion kWh of power from its hydroelectric generating stations. The 1988 drought significantly reduced the flow on the Saskatchewan, Red, and Nelson River systems and as a result only 18 billion kWh were produced in 1987-1988 and

15.2 billion kWh in 1988-1989 (Maybank *et al.*, 1995). Expressed in dollar value, the losses from the resulting reduction in exports of electricity for Manitoba reached nearly 80 million dollars per year.

Because of the complexity of drought and the central role that water resources play in the prairie economy, the occurrence of drought produces a ripple effect in other sectors. This study only focuses on the direct impact of drought on agricultural production in the prairies.

2.5 Physical processes that cause drought

There are four major mechanisms responsible for precipitation: frontal activity (dynamically induced vertical motions of stable saturated air), convective activity (vertical motions of unstable air), orographic lifting (as a result of local topography), and vertical motions of air associated with frictional convergence (Nicholson, 1986; Janowiak, 1988; Janicot, 1992). The amount of precipitation that falls is highly variable over time and space and this is especially true for the Canadian prairies. Variability in the amount of precipitation received at any location occurs as a result of spatial and temporal variability in one or more of the precipitation mechanisms (Monteverdi, 1978).

The main cause of drought is a lack of precipitation. The inter and intra-annual variability of precipitation, coupled to some extent with temperature, affects the frequency and intensity of droughts (Maybank *et al.*, 1995). In general, this variability is controlled through three mechanisms: 1) land and ocean temperatures, 2) atmospheric circulation patterns and the location of mid-latitude storm tracks, and 3) surface boundary conditions (e.g., soil moisture levels, snow cover) (Herring, 2000). Each of these parameters is linked through a complex series of feedback loops to all of the other parameters. So, a change in any one of the parameters will influence the behaviour of each of the other parameters. The most severe and prolonged droughts occur when a number of the physical mechanisms responsible for drought act in concert (Barry and Chorley, 1987).

Surface boundary conditions force the climate system through variations in their optical (albedo) or thermal (latent versus sensible heat) properties (Maybank *et al.*, 1995). These conditions include the presence or absence of snow and ice, soil moisture levels, and the distribution of vegetation. Snow cover is a critical variable of the climate system because of its high reflectivity, high emissivity, and low water vapour pressure and conductivity (Maybank *et al.*, 1995). The presence or absence of snow cover can completely transform both the micro and meso-climate of the affected area. The addition of a snow cover immediately changes the energy budget, and alters the water and radiation exchanges. Important variables that influence drought occurrence and drought persistence include the amount of snow that accumulates during the winter, the spatial distribution of the snow cover, and the timing and rapidity of spring melt.

Soil moisture can play a role in both preventing and prolonging summer droughts (Herring, 2000). When there is an ample supply of soil moisture, water evaporates as the ground is heated (latent heat flux). This warm moist air rises into the atmosphere and eventually condenses forming clouds and possibly results in precipitation. The incoming heat is used to evaporate the moisture and thus the surface remains cooler. If there is not enough soil moisture when the ground is heated, all of the energy is used to warm the soil making it hotter and drier (sensible heat flux). This process can be best described using the Bowen ratio, which represents the ratio of the sensible to latent heat fluxes.

Soil moisture also affects the albedo and thermal diffusivity of the soil. Higher soil moisture results in a lower albedo, while lower soil moisture means a higher albedo. The thermal diffusivity of the soil (the rate of heat flow into the soil) will initially increase as the soil begins to dry out, but then decreases when the soil becomes very dry. This causes the air temperature to rise, which increases drying and evapotranspiration rates. High temperatures are both a cause and a product of drought. In other words, drought begets drought (Namias, 1960).

Advection (from the Pacific Ocean and the Gulf of Mexico) is the single most important source of water vapour for rainfall on the Canadian prairies. Regional evapotranspiration, however, has been shown to contribute between 24-35% of the moisture for rainfall over the Canadian prairies during the summer (Raddatz, 2000). Regional evapotranspiration also affects the availability of convective energy and this impacts the frequency and intensity of convective storms. These results indicate that regional evapotranspiration is an important factor in the persistence of summer droughts and wet spells. The Canadian prairies are a source region for water vapour for the rest of the atmosphere (a net exporter of water vapour), which is consistent with the climate of a semi-arid region where annual ET regularly exceeds precipitation.

Atmospheric circulation patterns are important causal agents of drought. The prevailing atmospheric flow for the prairies is from west to east, but much of the moisture is removed from Pacific air masses as they pass over the Rocky Mountains. In addition, the cooler temperatures of the Pacific Ocean, as compared to the Gulf of Mexico, mean that the Pacific air masses tend to be drier. Air masses usually move northwards from the Gulf of Mexico during the summer, carrying abundant amounts of moisture. Under drought conditions this flow of moisture from the Gulf is cut off due to the presence of a large, quasi-stationary high-pressure system that develops over the Great Plains. This high-pressure system forms when the Intertropical Convergence Zone (ITCZ) shifts northward (often during a La Niña). The jet stream also shifts north and a high-pressure system develops over, or just west of, the Great Plains. This is referred to as a blocking event. Conversely, during wet years, more moisture than normal is transported from the Gulf to the Great Plains. The jet stream shifts south of its normal position, with a branch extending into southern California. A low-pressure zone is created when the jet stream is deflected by the Rocky Mountains.

Blocking is the primary way in which the atmospheric circulation contributes to drought conditions. A blocking event is defined as an "anomalous atmospheric condition which prevents moisture-laden weather systems from moving over a region for an extended period of time" (Kavvas and Anderson, 1996). Atmospheric blocking events typically have a split jet stream (extending at least 45 degrees of longitude), significant meridional mass flow (as opposed to zonal), and they persist for at least ten days (Kavvas and Anderson, 1996). One variety of blocking event is known as an *Omega Block* and is characterized by a large stationary high-pressure system that forms as a result of stationary mid-latitude Rossby waves. The origin of these quasi-stationary waves is not fully understood, but it is believed that they are associated with sea-surface temperature anomalies in the Pacific (Kavvas and Anderson, 1996).

The persistence of these stationary high-pressure systems can initiate droughts. Blocking events increase the likelihood of drought because of the physical processes that take place while they remain in place (e.g., the soil moisture-temperature-precipitation feedback process). For this reason, drought conditions can last much longer than the anticyclone from which they usually originate (Kavvas and Anderson, 1996).

Land and ocean temperatures can also contribute to drought conditions. Research has demonstrated that there is a direct relationship between sea surface temperature (SST) anomalies in the Atlantic and Pacific and large-scales circulation patterns that are responsible for wet or dry spells (Herring, 2000). In other words, a *teleconnection* exists. For example, when SSTs in the equatorial Pacific are warmer than normal, higher than normal amounts of precipitation are expected along the west coast and central regions of North America (Herring, 2000). Conversely, when SSTs in the Pacific are cooler than normal, one expects lower than normal precipitation.

SST anomalies mainly result from changes in atmospheric winds, solar radiation, and deep-ocean circulation (Maybank *et al.*, 1995). Once a SST anomaly is produced, it tends to persist for months or even years because of the thermal inertia of the oceans. Thus, any circulation anomalies that result from these SSTs will likely persist for a similar period of time. This means that SSTs are an important causal mechanism that can contribute to the length and severity of drought.

The physical processes that cause drought can be illustrated using examples from the Canadian prairies. During the growing season, the mid-troposphere general circulation is normally characterized by an upper-level ridge located to the west of the Canadian prairies. This results in a northwesterly flow and associated advection of negative vorticity and subsidence over the region (Bonsal *et al.*, 1999). Prolonged dry periods are often due to enhanced meridional flow over North America with an unusually persistent and stronger than normal western ridge which blocks the flow and displaces cyclonic tracks north of the study region (Bonsal *et al.*, 1999). Conditions on the surface, under the ridge, are dominated by anitcyclonic circulation and atmospheric stability (Dey, 1982). At higher levels, the jet stream is positioned in a northwest-southeast direction over the northern prairies (Bonsal *et al.*, 1999). Wet summers are produced by the opposite conditions, where there is a more zonal flow, a slight troughing to the west of the study region, and the position of the jet stream and storm tracks to the south, along the Canada-United States border.

During 1988, the jet stream and storm tracks were displaced well to the north of their normal location. These large-scale circulation anomalies persisted from April to mid-July. A study using General Circulation Models (GCM) demonstrated that tropical SST anomalies were responsible for these circulation anomalies in the mid-latitudes (Trenberth and Guillemot, 1996). These SST anomalies, coupled with the 1988 La Niña, disrupted the atmospheric heating patterns in the tropics by shifting the location of the ITCZ to the north and changing its intensity (Trenberth and Guillemot, 1996). This provided a direct link between the drought conditions on the prairies and the anomalous SSTs via large-scale atmospheric circulation anomalies.

Bonsal and Lawford (1999) have found that the occurrence of extended dry spells (periods of greater than 10 days with no precipitation) in the growing season are significantly more frequent during El Niño events, particularly during the mature stage (the second summer) of the El Niño. This finding seems to be contrary to the findings of Trenberth and Guillemot (1996) and others (Garnett and Khandekar, 1992; Garnett *et al.*, 1998; Herring, 2000). Bonsal and Lawford (1999), however, do note that their study only focuses on extended periods of consecutive dry days (precipitation frequency) and not on precipitation amounts.

Certain North Pacific SST anomaly patterns are often observed during the mature stages of El Niño and La Niña events. It is hypothesized that these North Pacific SSTs may be related to a phase of the PNA pattern. Positive (negative) PNA tends to occur during the winter following the onset of El Niño (La Niña) events. The North Pacific SST anomalies may be generated by the surface conditions associated with the Aleutian Low. The Aleutian Low is stronger (weaker) during the positive (negative) phase of the PNA (Bonsal and Lawford, 1999). Although it is difficult to isolate the influence of ENSO from that of the North Pacific SSTs, it is believed that certain SST anomalies may help to reinforce (sustain) the ridging conditions over the study region (Bonsal *et al.*, 1993). Note that these conditions are not always present in severe drought situations. For example, the droughts in 1961 and 1980 have been shown to be associated with North Pacific SSTs but not ENSO events (Bonsal and Lawford, 1999). The timing of El Niño and La Niña events may have an influence on North Pacific SSTs and growing season droughts as well. That is, North Pacific SST anomalies and growing season droughts tend to occur more consistently when El Niño and La Niña events occur in consecutive years (Bonsal and Lawford, 1999).

Modeling studies show that antecedent soil moisture conditions are also important in initiating and maintaining a growing season drought (Trenberth and Guillemot, 1996). These anomalous surface boundary layer conditions have the potential to induce persistent anomalies through changes in latent and sensible heat fluxes from the surface. The Bowen ratio for the Canadian prairies was approximately 1.0 during the drought of 1988, while during the wet summer of 1993 the Bowen ratio was less than 0.2 (Trenberth and Guillemot, 1996; Bonsal and Lawford, 1999).

In summary, it is evident that ENSO, North Pacific SSTs, PNA, and surface boundary layer conditions are all related to drought. However, it is also recognized that there are other physical processes that control drought. Further investigation is necessary to understand the role of other atmospheric and oceanic teleconnections.

2.6 Factors affecting crop yield

There are five main factors that affect the quality and quantity of Canadian prairie wheat yields: climate, soil, plant diseases, insects, and weeds (Bushuk, 1982; Riha *et al.*, 1996). These will be discussed in turn.

Moisture is an important moderator of crop growth. Average annual precipitation values range from about 300 mm in southern Alberta and southwestern Saskatchewan to over 500 mm in eastern Manitoba. About one quarter of the precipitation falls in the form of snow from November until the end of March. Since much of the moisture from snow is lost in the spring as runoff, winter precipitation is of little value for crops. Hence, precipitation during the growing season is vital. Growing season precipitation actually accounts for up to two-thirds of the total annual precipitation (Bonsal *et al.*, 1999) (Table 2.1). The period of maximum rainfall is usually from the middle of June to early July (Bonsal *et al.*, 1999). On average, June has the highest monthly rainfall followed by July, August, and May. In dry years, the lack of soil moisture can reduce average yields by as much as 50% (Bushuk, 1982). Other factors such as large amounts of solar radiation, low humidity, and frequent high winds increase the rate of soil moisture loss.

Table 2.1 Growing season (May-July) precipitation statistics by crop district (1920-99)

CD	Mean	Median	Max	Min	Standard Deviation	Variance	Coeff. of Variation
AB1	145.33	135.54	318.44	65.15	50.4	2540.0	34.7
AB2	156.76	147.04	310.82	68.45	54.6	2977.3	34.8
AB3	207.39	182.06	511.65	72.40	88.2	7777.8	42.5
AB4	149.48	144.80	294.49	76.37	47.3	2236.7	31.6
AB5	176.09	162.05	282.37	81.36	50.8	2580.9	28.9
AB6	214.56	209.57	363.55	97.01	61.6	3790.4	28.7
AB7	187.19	191.67	311.96	71.43	51.1	2606.9	27.3
AB8	220.01	214.81	378.82	79.47	61.6	3798.0	28.0
AB9	254.84	248.38	450.99	106.25	74.8	5601.5	29.4
AB10	190.61	190.05	301.62	86.90	50.1	2507.1	26.3
AB11	225.33	223.95	405.83	105.01	55.8	3112.4	24.8
SK1a	193.20	188.24	344.25	64.05	61.7	3802.9	31.9
SK1b	193.66	195.47	363.50	63.37	61.6	3792.2	31.8
SK2a	181.40	175.90	342.17	66.91	64.1	4111.4	35.4
SK2b	180.18	182.70	313.88	58.29	57.1	3257.9	31.7
SK3an	167.70	169.12	290.29	48.87	51.9	2692.9	30.9
SK3as	177.90	181.09	309.85	53.76	56.7	3211.6	31.9
SK3bn	161.55	161.94	316.09	45.48	54.0	2914.1	33.4
SK3bs	159.21	162.80	300.73	43.21	55.0	3025.1	34.6
SK4a	159.67	158.34	307.32	26.86	54.3	2944.8	34.0
SK4b	152.91	147.63	327.60	49.37	50.9	2594.8	33.3
SK5a	183.20	176.32	353.82	60.15	59.8	3579.1	32.7
SK5b	184.58	177.62	510.80	15.00	70.0	4900.3	37.9
SK6a	168.73	161.59	300.80	45.79	54.5	2964.6	32.3
SK6b	161.88	151.45	283.02	65.80	48.9	2390.7	30.2
SK7a	149.08	140.00	286.84	74.07	46.9	2200.1	31.5
SK7b	163.78	163.52	300.53	71.84	46.4	2156.2	28.4
SK8a	179.73	183.48	339.15	66.40	54.7	2989.4	30.4
SK8b	170.75	160.36	374.71	55.16	57.3	3286.5	33.6
SK9a	174.62	175.68	278.10	62.68	51.1	2605.6	29.2
SK9b	172.33	167.30	295.24	59.25	47.4	2242.8	27.5
MB1	207.77	211.80	421.12	59.36	67.1	4506.3	32.3
MB2	199.86	191.05	357.14	72.77	62.7	3926.5	31.4
MB3	197.04	187.69	334.82	89.94	58.6	3437.4	29.8
MB4	199.45	197.81	357.50	57.75	56.0	3134.8	28.1
MB5	191.78	188.19	373.05	49.25	63.4	4022.6	33.1
MB6	197.66	196.89	364.90	75.28	59.3	3520.2	30.0
MB7	205.58	197.39	330.31	91.65	55.2	3042.3	26.8
MB8	211.02	212.18	364.46	83.12	63.5	4029.4	30.1
MB9	211.23	217.96	380.17	90.45	58.9	3469.7	27.9
MB10	188.15	190.73	343.54	62.00	67.8	4592.9	36.0
MB11	207.77	202.99	427.20	104.50	59.1	3489.3	28.4
MB12	176.05	175.97	331.89	64.20	55.7	3102.9	31.6
MEAN	***185.05***	***181.42***	***345.47***	***67.59***	***57.6***	***3382.9***	***31.3***

The timing of moisture delivery is also important. During the latter stages of growth, the wheat plant requires large quantities of water. The period of highest crop water demand occurs during the mid-June to early July period, coincident with the period of highest precipitation (Bonsal *et al.*, 1999). Too much precipitation can be detrimental to crop yields. If an excess of precipitation falls just prior to planting, farmers may have trouble getting onto their fields to seed and seedlings may not establish deep root systems, making them more susceptible to moisture stress later in the growing season. Excess amounts of precipitation during harvest are also detrimental because they lead to decreases in yield quality and quantity. The occurrence of frost, hail, and wind storms can also significantly decrease yields. The frost-free period averages only 115 days which limits which crops can be grown. Heat and sunlight are also necessary for plant growth, but they do not usually exhibit a great deal of inter-annual variability and thus do not normally affect crop growth on the Canadian prairies.

The soil is another element that helps to determine yield quality and quantity. Cereal crops remove nitrogen, potassium, calcium, phosphorus, and micronutrients from the soil as they grow (Bushuk, 1982). Some soils are more fertile than others, and, crops grown on more fertile, well-drained soils will produce higher yields than those crops grown on less fertile, poorly-drained soils. Soil characteristics not only vary across the prairies, but also from field to field.

Cereal crops continue to be prone to insects and disease despite advances in biological engineering, and insecticide and fungicide treatments (Bushuk, 1982). The most common insects on the prairies include the wheat stem sawfly, cutworms, grasshoppers, and Bertha armyworms, and common diseases include rust, smut, and root rot (Bushuk, 1982). All of these organisms can cause substantial yield losses and reductions in grain quality. Weeds can also reduce yield quantity and quality because they rob crops of moisture and nutrients. Therefore, weed control is an essential feature of water conservation.

Absolute correspondence between a drought index and yield is not expected since these and other factors affect the actual yields realized for each crop district (Akinremi *et al.*, 1996). However, the occurrence of insects and disease often increases during drought conditions and this feedback leads to further reductions in yield (Wilhite *et al.*, 1987).

2.7 Crop water-use efficiency

Water supply is the most significant factor in determining the distribution and growth of plant species (Bouten, 1995). Plant growth is directly correlated with evapotranspiration (Figure 2.2) and is also related to precipitation. Plants need an enormous amount of water — up to one thousand times as much as their biomass production (Bouten, 1995). Water-use efficiency can be defined as the crop yield per unit of water used (evapotranspiration) (Eastin and Sullivan, 1984). A typical grassland/crop requires about 500 kg of water for transpiration to produce 1 kg of dry matter (Volkmar and Woodbury, 1995).

Wheat has five phenological stages of development: emergence, jointing, heading, soft dough, and ripening, and crop water demand typically ranges from 30-100% of potential evapotranspiration (PE) depending on the phenological stage (Ash *et al.*, 2000). In the first stage, from planting to emergence, crop water demand is about thirty percent of PE. As the crop continues to develop, there is an increase in leaf-area and biomass and this creates an increasingly large crop water demand. When the crop completely covers the ground, water demand is required at the rate of one hundred percent of PE.

The difference between the amount of water a crop can potentially use (the crop water demand) and the amount it actually receives during the growing season is the moisture shortfall

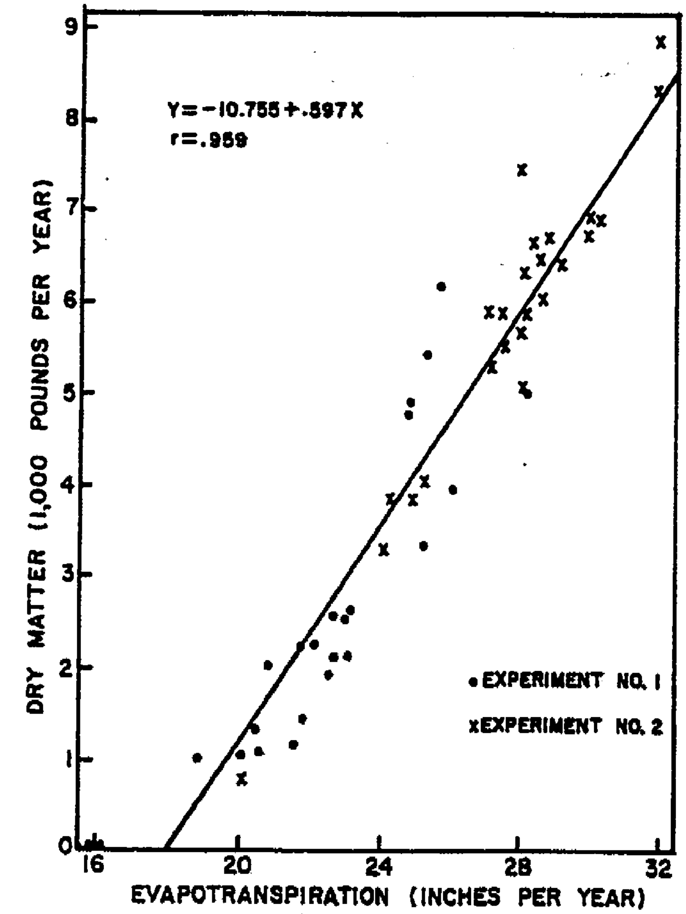

Figure 2.2 Relationship between wheat yields and evapotranspiration (*Allison, Roller, and Ranney)*

or *crop moisture stress*. Research indicates that both the magnitude and the timing of moisture stress are important. Yields are largely determined by plant moisture stress during the *heading* and *soft dough* stages (Figures 2.3, 2.4) (Arora *et al.*, 1987; Wilhite *et al.*, 1987).

The amount of water available to a crop in any given year is determined by the amount and distribution of rainfall, the horizontal transport of moisture, the rate of evaporation, the water holding capacity of the soil, and the amount of soil moisture at planting (Bouten, 1995). A wheat crop requires an average of 275 mm to 325 mm of water from planting to maturity on the Canadian prairies (Ash *et al.*, 2000). The growing season is defined as the period between planting and harvest. On the Canadian prairies the growing season varies between 100-120 days with planting usually taking place between April 30-May 20 and harvest taking place between August 11-22. Growing season rainfall only makes up about two-thirds of the crop water demand for most regions of the prairies (Ash *et al.*, 2000). The remainder of the crop water requirement must be supplied by the soil.

Soil moisture is recharged by autumn rains, snow melt, and spring rain prior to planting. The available water-holding capacity of soil varies according to the type of soil. For example, a coarse-textured soil can hold about 175 mm of available water over a depth of 1.2 m, while medium and fine-textured soils can hold approximately 225 to 250 mm (Ash *et al.*, 2000). In the Canadian prairies, average crop moisture stress at heading varies from nearly zero in the Red River Valley and Interlake regions of Manitoba, to -35 mm in south-central Saskatchewan (Figure 2.5). The average moisture stress has increased by the time the crop reaches the soft dough stage because the moisture supply does not meet the crop water demand (Figure 2.6). The spatial variation in moisture stress has important implications. Studies in southern Saskatchewan have shown that every millimetre of water used by a wheat crop increases yield by 9 kg/ha (0.13

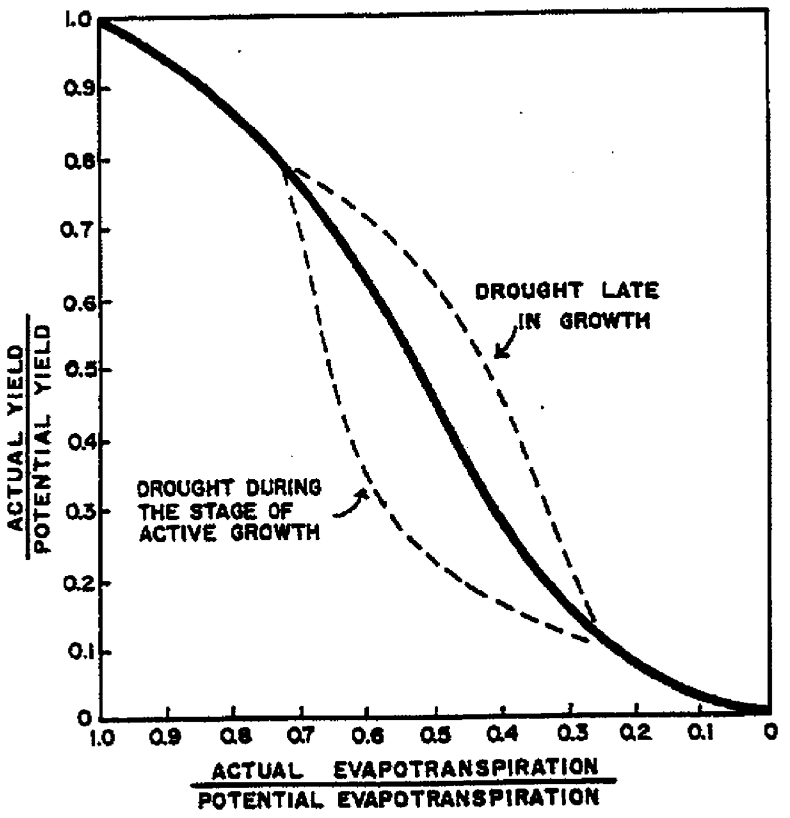

Figure 2.3 Generalized relationship between yield and adequacy of water availability (*Allison, Roller, and Ranney*)

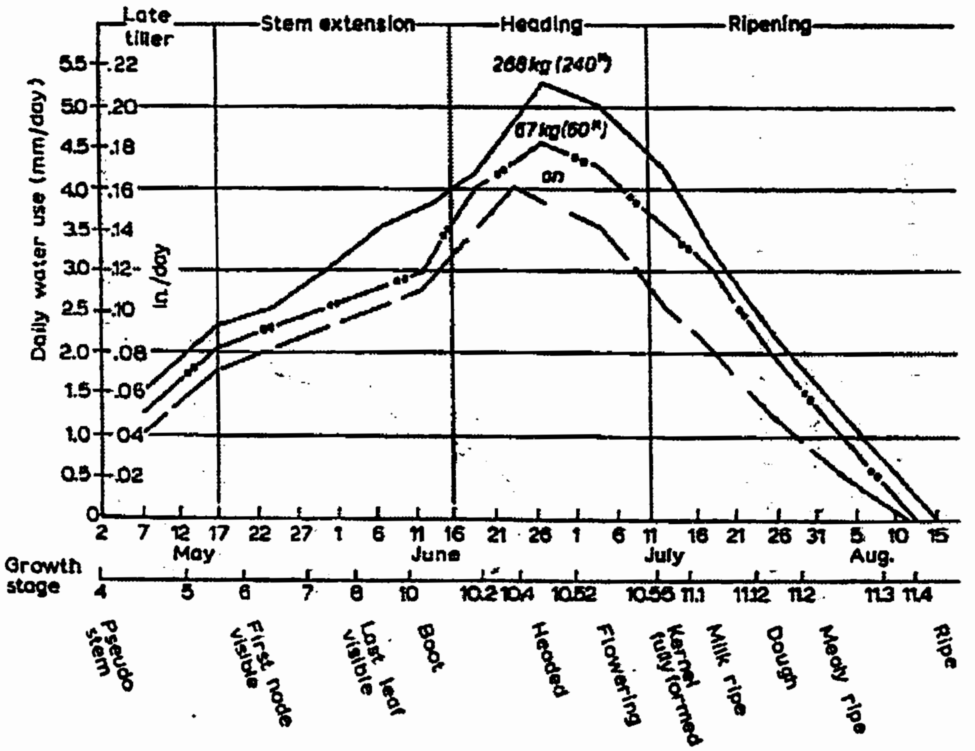

Figure 2.4 Daily water use by dryland winter wheat grown under favourable conditions with 0, 67, and 268 kg ha^{-1} N rates *(Brown, 1971)*

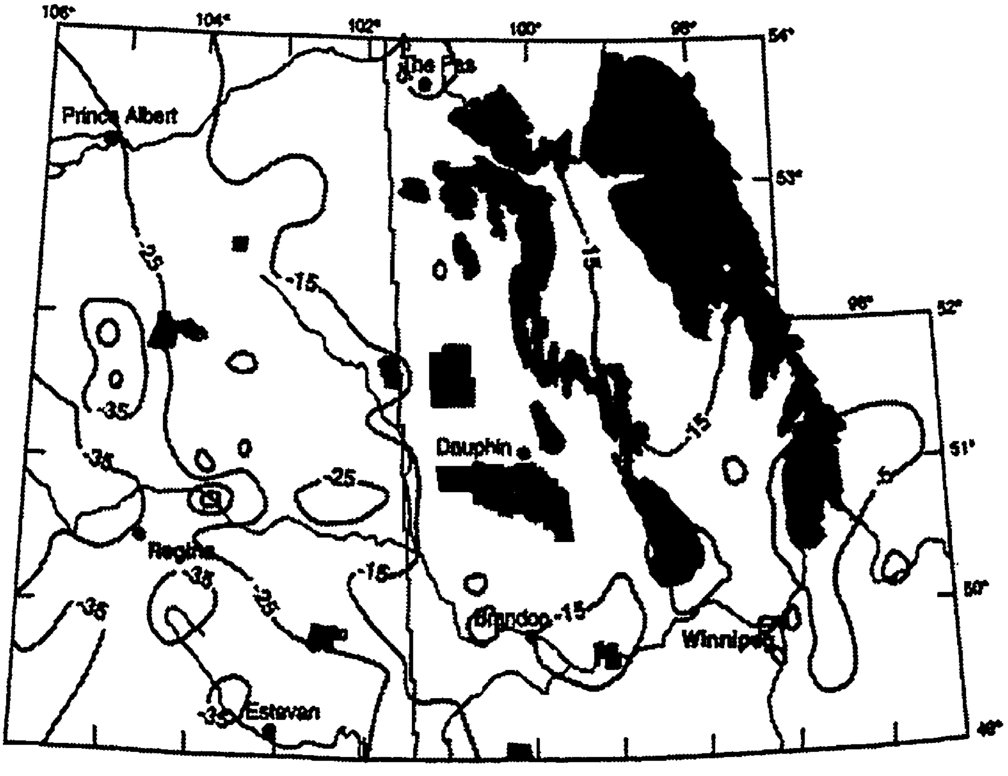

Figure 2.5 Average plant moisture stress during heading (mm) *(ACE, 2000)*

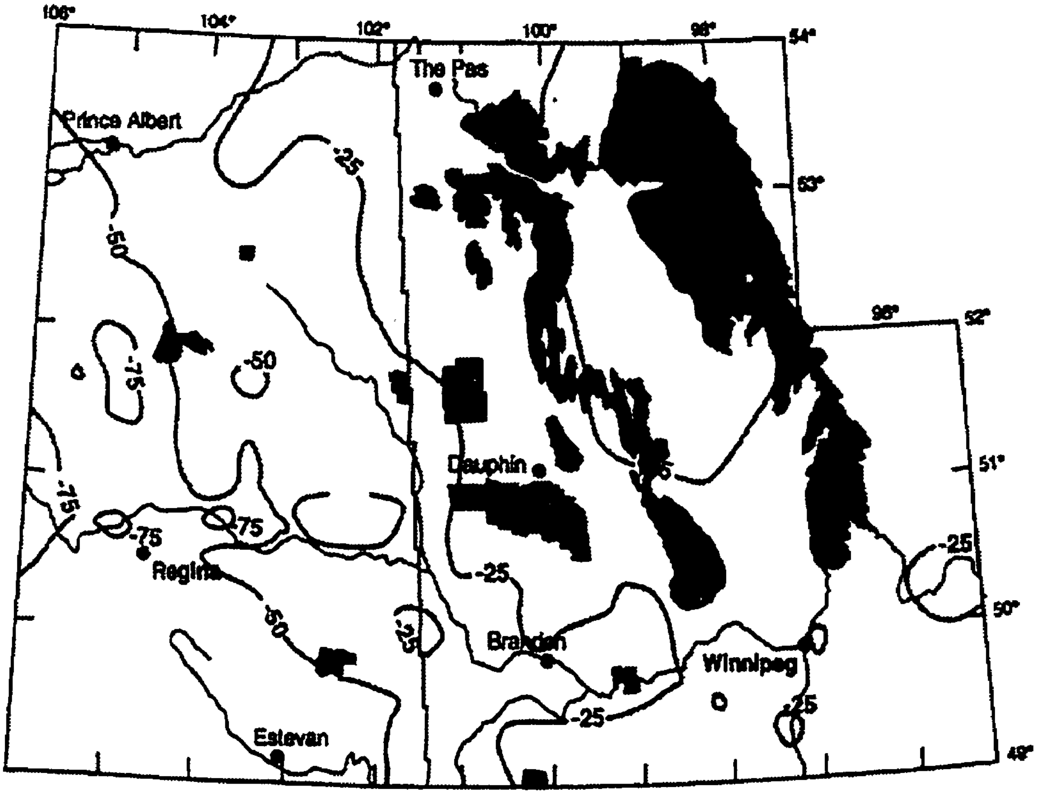

Figure 2.6 Average plant moisture stress during soft dough (mm) *(ACE, 2000)*

bu/ac). Thus, the difference in moisture stress between south-western Manitoba and central Saskatchewan of 25 mm translates into a yield difference of 225 kg/ha (3.3 bu/ac) (Saskatchewan Agriculture and Food, 2000).

A drought index needs to focus on the changing water demands during each phenological stage to accurately predict yield (Wilhite *et al.*, 1987). If a drought index is employed without regard to the phenological sensitivity, this will limit the correlation between the index and yield. For example, if drought occurs when the crops water demand is relatively small, there may be very little negative impact on the crop. The heading and soft dough stages of development (which usually occur in late June and July) are the most sensitive to water stress. Therefore, it is important for drought indices to consider the months of June and July as the most important for determining wheat yields.

2.8 Drought indices

Drought indices are used to quantify the moisture condition of a region by assimilating complex data sets into a single number. Drought indices should really be viewed as moisture supply indices because they can be used to measure both moisture surplus and moisture deficit. These indices are important for not only quantifying the severity of drought in a particular region, but also for determining the spatial extent of drought, detecting drought onset and termination, and comparing moisture supply conditions between regions (Alley, 1984). There are many different drought indices commonly employed for monitoring moisture conditions, they include: Percent Normal, Standardized Precipitation Index (SPI), Palmer Drought Severity Index (PDSI), Moisture Anomaly Index (Z), Crop Moisture Index (CMI), Surface Water Supply Index (SWSI), Reclamation Drought Index, Deciles, Rainfall Anomaly Index, BM Index, NOAA Drought Index (NDI), and the NDVI-based Vegetation Condition Index.

Many of the above indices are employed operationally to monitor drought conditions for the United States, Canada, and Australia. Many drought indices exist because no single index is suited for all purposes. Some indices are designed for measuring agricultural drought while others may be more applicable for quantifying meteorological or hydrological drought. As discussed previously, the concept of drought is an elusive one, with no single definition being suitable for all applications. A drought index is an oversimplification of reality because it assimilates a wide variety of data into a single expression. This is both a benefit and a hindrance.

One of the main purposes of a drought index is to provide information for decision-makers in government, corporations, and the public. Drought indices are often applied to forecast water availability and crop yields and can also be used to compare past conditions with contemporary ones to gain perspective.

The following three sections examine how each of the drought indices selected for inclusion in this study are derived and calculated.

2.8.1 Palmer Drought Severity Index and Moisture Anomaly Index

The Palmer Drought Severity Index (PDSI) (also referred to as the Palmer Drought Index or simply the Palmer) was developed by W. C. Palmer in 1965. The PDSI is one of the most widely used drought indices and is employed in a whole host of applications, in part due to the fact that it was one of the earliest drought indices.

The PDSI is currently used by the United States Department of Agriculture (USDA) in their *Weekly Weather and Crop Bulletin*. It is also used to determine federal drought assistance and most states employ some form of the PDSI in their drought contingency plans. The PDSI has also been employed for drought prediction (Lohani and Loganathan, 1997). The PDSI is widely used in the scientific literature to examine the spatial and temporal characteristics of drought, the severity of drought, and to make comparisons between different regions (Alley, 1984; Soule, 1992; Kumar and Panu, 1997; Nkemdirim and Weber, 1999). The PDSI has been used to determine forest fire hazard and the frequency of dust storms (Cohen *et al.*, 1992).

The PDSI was designed to measure meteorological drought, but it can also be used to measure hydrological drought. The PDSI is a soil moisture/water balance algorithm that requires a time series of daily temperature and precipitation data and information on the available water content (AWC) of the soil and the latitude of the site (region) for which it is being calculated. The PDSI involves a relatively complex calculation. A water balance is computed (usually monthly) using historic records of temperature and precipitation (Alley, 1984). Soil moisture storage is handled by dividing the soil into two layers. It is assumed that the top layer of the soil can hold a maximum of 25 mm of water. The capacity of the second layer of the soil is based on the characteristics of the soil being considered. The second layer will not be recharged until the capacity of the first layer has been entirely filled. The PDSI uses the Thornthwaite method (Thornthwaite, 1948) to compute potential evapotranspiration (PE). Evapotranspiration losses from the soil occur if PE > P (where P is the precipitation for the month). Evapotranspiration loss from the surface layer of the soil (L_s) is assumed to take place at the potential rate. It is assumed that evapotranspiration loss from the underlying layer of the soil (L_u) depends on the initial moisture conditions in this layer, PE, and the combined available water content in both layers.

The first step to calculate the monthly PDSI is to determine the monthly departure from normal moisture:

$$d_i = P_i - P_i' \qquad [1]$$

where d, is the magnitude of the moisture departure for month i. P is the actual precipitation in month i, and P' is the *climatologically appropriate* precipitation for month i and is derived by:

$$P_i' = ET' + R' + RO' - L' \qquad [2]$$

In [2], ET' is the expected or *climatologically appropriate* evapotranspiration, R' is the expected or *climatologically appropriate* soil water recharge, RO' is the expected or *climatologically appropriate* runoff, and L' is the expected or *climatologically appropriate* water loss from the soil. The variables ET', R', RO', and L' are derived as follows:

$$ET' = \alpha\, PE \qquad [3]$$

$$R' = \beta\, PR \qquad [4]$$

$$RO' = \tau\, PRO \qquad [5]$$

$$L' = \delta\, PL \qquad [6]$$

where PE is the potential evapotranspiration, PR is the potential recharge, PRO is the potential runoff, and PL is the potential loss from soil. The constants (α, β, τ, δ) are derived for each month of the year from historical averages in the following manner:

$$\alpha = ET/PE \qquad [7]$$

$$\beta = R/PR \qquad [8]$$

$$\tau = RO/PRO \qquad [9]$$

$$\delta = L/PL \qquad [10]$$

The Moisture Anomaly Index, Z_i, is the product of d and the weighting factor K for the month i:

$Z_i = d_i K_i$ [11]

The PDSI, indicated by X_i, is a combination of Z_i, the moisture anomaly index for the current month, and the PDSI value for the previous month:

$X_i = Z_i/3 + 0.897X_{i-1}$ [12]

The weighting factor K_i in [11] is initially determined using an empirically derived coefficient, K', which is then adjusted using a regional correction factor to account for the variation between locations:

$K_i = [14.2/ (\Sigma D_i K_i)]\ K'$ [13]

where D is obtained during the calibration period by determining the mean of the absolute values for each month of the year.

The average of the annual sum of monthly DiKi values was initially calculated to be 17.67 (Palmer, 1965). This value has since been adopted as a regional correction factor so that all ΣDiKi values equal 17.67. This allows for comparisons of droughts between different regions (Palmer, 1965). In [13] a value of 14.2 is used instead of 17.67 following Akinremi *et al.* (1996). Akinremi *et al.* (1996) tested the regional correction factor proposed by Palmer (1965) against the one they derived by averaging the values of 142 stations across the Canadian prairies. The use of Palmer's value returned a higher PDSI value than with the one calculated by Akinremi *et al.* (1996). They felt that Palmer's value inflated the drought index for the Canadian prairies.

In what follows, both the Moisture Anomaly Index (Z) [11] and the PDSI [12] will be assessed relative to reported wheat yields. While both of these indices are derived using the same data, their monthly values are quite different. The Z index is a measure of the monthly moisture status compared to the normal or climatically appropriate moisture budget for any given month. The monthly values for the Z index are not affected by moisture conditions in the previous month (it has no 'memory'). This means that monthly Z values can vary dramatically from month to month. The PDSI is an autoregressive process of the first order because its value for each month is linearly related to the previous month. Questions have been raised as to the appropriateness of the weighting of antecedent conditions in the PDSI [12]. The current month's PDSI is calculated using only one-third of the current month's moisture status. The PDSI is a slow varying drought index that is most appropriate as a measure of hydrological drought because of its consideration of antecedent conditions (Strommen and Motha, 1987). This long-term memory goes back several years and contributes to the occasionally erratic behaviour of the PDSI (Guttman, 1998). The Moisture Anomaly Index is likely more appropriate for considering meteorological or agricultural drought.

2.8.2 Strengths and weaknesses of the PDSI and Moisture Anomaly Index

The PDSI has a number of important limitations and caveats attached to its use. The PDSI uses a simplistic water balance model and adopts the threshold method for runoff estimation. Furthermore it does not use a physically-based method for calculating PE (e.g., the Priestly-Taylor equation) (Akinremi *et al.*, 1996). The relationship between ET and PE is based on a large number of factors including the soil texture, rooting structure, and the physiology of the plant. This means that while the PDSI is more physically based than some of the other drought indices (e.g., SPI and NOAA Drought Index), it falls short in certain important areas. In addition, the PDSI does not consider snow accumulation, snow melt, or frozen soil which can be particularly important in regions such as the Canadian prairies (Akinremi *et al.*, 1996). The PDSI is usually calculated using a monthly time-step. This means that it may not be able to accurately account for short-term water deficits.

The PDSI makes the assumption that there is a single water holding capacity (AWC) across the entire region for which it is calculated (Strommen and Motha, 1987). This is not realistic when dealing with large areas such as crop districts or climate divisions, since the PDSI disregards seasonal and annual changes in the water holding capacity of the soil layers (Alley, 1984).

It should be noted that the PDSI does not incorporate a lag between the introduction of excess water as precipitation and its appearance as runoff. A more accurate reflection of what is actually taking place could be produced if between 50-75% of the runoff (RO) was lagged. Observed monthly stream discharges cannot be reproduced without this correction (Alley, 1984).

Another caveat is that the drought classes proposed by Palmer (Table 2.2) are entirely arbitrary (Alley, 1984). The descriptions attached to each category and the breaks between categories are not based on any empirical experiments.

Table 2.2 PDSI drought classification *(Palmer, 1965)*

PDSI Value	Category
> 4.0	Extremely wet
3.0 to 3.99	Very wet
2.0 to 2.99	Moderately wet
1.0 to 1.99	Slightly wet
0.5 to 0.99	Incipient wet spell
0.49 to -0.49	Near normal
-0.5 to –0.99	Incipient dry spell
-1.0 to –1.99	Mild drought
-2.0 to –2.99	Moderate drought
-3.0 to –3.99	Severe drought
< -4.0	Extreme drought

On the other hand, there are many benefits to be gained from using the PDSI to represent drought conditions and for detecting the onset and severity of droughts. The PDSI is easy to interpret and can be generated in a timely and economically viable manner from an existing weather network (Strommen and Motha, 1987). The PDSI allows for statistics to be calculated on the frequency, intensity, and duration of droughts for any region and any given time period (Strommen and Motha, 1987). The PDSI also uses a regional correction factor that is designed to allow for regional comparisons.

It is also argued that the PDSI is an 'objective' drought index because Palmer compared its performance with actual soil moisture conditions while developing it (Strommen and Motha, 1987). Like all models, the PDSI is based on a series of assumptions. The assumptions, however, are all clearly delineated so that the user can understand how the index is calculated and the areas where the index does not accurately reflect reality.

2.8.3 Standardized Precipitation Index

The Standardized Precipitation Index (SPI) was developed by McKee *et al.* (1993, 1995) to provide a moisture supply index that performed better than the PDSI. The SPI is based on statistical probability and was designed to be a spatially invariant indicator of drought that recognizes the importance of time-scales in monitoring moisture supply. The SPI is a standardizing transform of the probability of observed precipitation and it can be computed for any duration chosen by the user (Guttman, 1999). Shorter durations of weeks or months can be used to apply this index to agricultural interests, and longer durations of years can be used to apply this index to water supply and water management interests (Guttman, 1999).

The SPI can be calculated for any location using the long-term precipitation record for that location. This long-term record is fit with a probability density function and subsequently transformed using an inverse normal (Gaussian) function, with mean zero and variance of one (Guttman, 1999). This results in the mean SPI for any given location and desired time period being zero (Hayes, 1999). Positive values of the SPI indicate greater than median precipitation, while negative values indicate less than median precipitation. This normalization procedure treats all climates (whether wet or dry) in the same way and therefore allows for comparisons between them (Hayes, 1999). The drought classification developed by McKee *et al.* (1993) for the SPI is shown in Table 2.3. According to this system, a drought event is said to occur whenever the SPI is continuously negative and reaches an intensity of less than -1.0. The magnitude of the drought can be calculated by the cumulative sum of all months within a drought event (McKee *et al.*, 1993, 1995). Because the SPI is standardized, the percentage of time that the SPI is in each drought category can be calculated. The SPI spends 24% of the time in mild drought, 9.2% in moderate drought, 4.4% in severe drought, and 2.3% in extreme drought (Hayes, 1999). The percentage that the SPI indicates as "extreme drought" is consistent with what can be typically expected for an extreme event according to Hayes (1999).

Table 2.3 SPI drought classification *(McKee et al., 1993)*

SPI Value	Category
> 2.0	Extremely wet
1.5 to 1.99	Very wet
1.0 to 1.49	Moderately wet
-0.99 to 0.99	Near normal
-1.0 to –1.49	Moderately dry
-1.5 to –1.99	Severely dry
< -2.0	Extremely dry

It is necessary to standardize the procedure for computing the SPI so that all users calculate values that are spatially and temporally comparable. If different probability distributions are used to calculate the SPI, different values for the index will be obtained. Guttman (1999) experimented with using different probability distributions for calculating the SPI from a time-series of precipitation. He concluded that the Pearson Type III distribution provides the best model. To facilitate the implementation of this model as the standard in the scientific literature, a copy of this program has been made available through the Internet. The calculation of all SPI values for this research will be accomplished using this FORTRAN program.

2.8.4 Strengths and weaknesses of the SPI

The SPI, like the PDSI, has been developed so that it is an easy-to-interpret and spatially invariant measure of drought. It can be used to calculate the frequency, intensity, and duration of droughts. One of the major benefits of the SPI is that because it is probability based, the rarity of the current drought as well as the probability of receiving enough precipitation to end a drought can be calculated (Hayes, 1999). Also, the SPI can be utilized for many different applications because it can be calculated for any time scale the user requires.

An important drawback of the SPI is that its accuracy is highly dependent on the sample size (Guttman, 1999). The longer the time scale that is considered, the less accurate the index becomes because its probability is being calculated using fewer cases. The SPI is a moving average process for periods longer than a month and it is not physically-based. Unlike the PDSI, it does not consider any factors other than precipitation in producing its drought index values.

Guttman (1998) compared the PDSI against the SPI using spectral and cross-spectral analysis and proved that there is high coherence between the PDSI and SPI. This can be attributed to the importance of precipitation in the calculation of each index. For periods of less than one year the PDSI was found to lag the SPI, while for periods of about one year the two indices were found to be in phase. Guttman (1998) recommends using the SPI rather than the PDSI because it is simple to calculate, spatially invariant, probabilistic, and the time period for which it is calculated can be adapted to serve the interests of various users. Conversely, the PDSI is complex, spatially variant, difficult to interpret, and temporally fixed.

2.8.5 NOAA Drought Index

The NOAA Drought Index (NDI) was developed by Strommen and Motha (1987) as an early warning system for agricultural drought in developing countries. It was created to provide a simple and inexpensive way to monitor agricultural drought. The index can be applied, however, by a wide variety of users with a few simple modifications (Titlow, 1987).

The first step in calculating the NDI, is to compute the mean monthly precipitation values. Typically, at least thirty years of data is required to calculate this index (Titlow, 1987). Then the mean precipitation values for each week of the year should be derived using a spline fit. The first eight weeks of actual and average precipitation are then summed and compared. If actual precipitation is greater than 60% of normal precipitation, then the last week (week 8) is considered to have little or no water stress (Titlow, 1987). Next the first week (week 1) is dropped and a new week (week 9) is added, to create another eight-week block for comparison. If any eight-week block receives less than 60% of normal precipitation, it is said to be experiencing stress. Once this occurs, weeks are no longer dropped when additional weeks are added and the summation now takes place for the entire block (more than eight weeks). A drought does not end until the moisture deficit is eliminated (Titlow, 1987). When actual precipitation once again exceeds 60% of normal, the evaluation period reverts to an eight-week block. This method of calculation is used so that antecedent moisture conditions are considered.

2.8.6 Strengths and weaknesses of the NDI

The NDI has not been as extensively utilized in the literature as PDSI, Z, and SPI. The NDI is the simplest of the drought indices selected for consideration in this study since it only requires daily precipitation data and monthly precipitation normals to be calculated. The FORTRAN code used to calculate the NDI can be easily modified to adjust the drought thresholds to whatever level the user deems most appropriate. The main strength of the NDI, other than its simplicity, is the fact that it is calculated on a weekly time step. This should, of course, be of value in a study that is interested in agricultural drought. The duration and frequency of droughts can also be calculated using this index.

On the other hand, the NDI is not designed for comparison between regions and its method of calculating drought recovery is unrealistic. During drought situations, no week is dropped until the entire block of weeks exceeds the predefined drought threshold (e.g., 60% of normal precipitation for that time period). Obviously, this is an artificial way to determine when a drought has actually ended. Also, because the NDI is expressed as a percentage (actual precipitation compared to normal precipitation), it does not impart any information on the rarity of a given drought event.

2.9 Teleconnections

One of the most promising developments in drought (climate) forecasting and understanding climate variability is the inclusion of teleconnections in predictive models. Indeed, most research interested in examining climate variability is in one way or another based on teleconnections (Nicholls and Katz, 1991). The term teleconnection refers to a persistent pattern of anomalies within the atmosphere or oceans that link regions that are often separated by great distance. Teleconnection patterns are often defined as preferred modes of low-frequency variability, typically lasting for weeks, months, or even years, and are associated with changes in planetary-scale wave patterns. Hence, they commonly affect very large areas, including entire ocean basins and continents. All teleconnections are naturally occurring aspects of the quasi-chaotic atmospheric system and it is generally thought that they arise as a result of internal atmospheric dynamics (Glantz, 1991). It is becoming increasingly apparent that sea-surface temperatures and ocean circulation patterns also play a vital role in the creation and persistence of teleconnections. However they are created, teleconnections are often associated with widespread and anomalous temperature and precipitation patterns, in response to anomalous pressure and wind patterns, which are, in turn, usually associated with anomalous jet-stream locations and intensities.

The discovery of what we now recognize as teleconnections is attributed to Sir Gilbert Walker (Walker, 1923, 1924), who, in his attempts to explain drought-producing variations in the Indian monsoon, identified a number of low-frequency circulation systems within the global climate. However, the term teleconnection was not actually used until 1935, when Angstrom used it to describe an "atmospheric seesaw" now known as the North Atlantic Oscillation (NAO) (Glantz, 1991). The importance of teleconnections was not widely appreciated until the early 1970s, following intensive research into the 1972-73 El Niño event (Glantz, 1991).

Without doubt, the El Niño/Southern Oscillation (ENSO) is the most widely known and extensively studied teleconnection pattern. As is the case with most teleconnections, ENSO involves large-scale ocean-atmosphere interactions. Indeed, it has become abundantly clear that the tropical-Atlantic and tropical-Pacific SST patterns strongly influence the atmospheric circulation of the tropics (Lamb and Peppler, 1991; Rasmusson, 1991). These effects then pass through the rest of the global climate system as a series of planetary-scale waves (Mo and Livezey, 1986).

Consequently, an understanding of the physical mechanisms that allow local anomalies to be extended globally is essential to understanding climate variability (Gray and Sheaffer, 1991; Tribbia, 1991). Walker's pioneering work initiated the understanding of these processes, and laid the groundwork for those studies which have since contributed to our understanding of the connections between mid-latitude temperature and precipitation anomalies and large-scale circulation systems, including those studies by Bjerknes (1969), Namias (1978b, 1980), Wallace and Gutzler (1981), Yarnal and Diaz (1986), Ropelewski and Halpert (1986, 1987), Barnett and Preisendorfer (1987), White *et al.* (1993), Yin (1994), Hurrell (1996), Shabbar and Barnston (1996), Shabbar and Khandekar (1996), Stone *et al.* (1996), and Cordery and McCall (2000), to name but a few.

A great many teleconnections have been documented in the literature. Table 2.4 contains a brief description of the teleconnections selected for inclusion in this study. These teleconnections were chosen because they were believed to be the most pertinent to the Canadian prairies. For the sake of simplicity, the sunspot number is also included in Table 2.4, even though, it is not traditionally defined as a teleconnection index.

Table 2.4 A description of selected teleconnection patterns *(CPC, 2001; NOAA, 2001; McFarlane et al., 2000; Thompson and Wallace, 2000; King et al., 1998; Beamish et al., 1997; Mantua et al., 1997)*

Name of teleconnection pattern	Period of prominence	Description
East Atlantic pattern (EA)	All months except May to August	North-south dipole of pressure anomalies positioned in the southeastern Atlantic; linked to the position of the subtropical ridge
East Atlantic Jet (EAJET)	April to August	North-south dipole of anomalies; centred over the eastern North Atlantic and Northern Africa/the Mediterranean; negative phase is associated with weakened westerlies and blocking events over Greenland and the UK
Western Pacific pattern (WP)	All months	North-south dipole of pressure anomalies; centred over the Kamchatka peninsula and southeastern Asia (in summer and fall a third centre is added over the Beaufort sea); negative phase is associated with a zonal Pacific jet
Eastern Pacific pattern (EP)	all months except August and September	North-south dipole of pressure anomalies; centred near Alaska/west coast of Canada and Hawaii; positive phase is associated with a deeper than normal trough and enhanced westerlies
North Pacific pattern (NP)	March to July	Two anomaly centres; one spans western and central North Pacific and the other is centred over eastern Siberia; positive phase = southward shift and intensification of jet stream and enhanced anticyclone over western NA
Pacific/North American pattern (PNA)	All months except June and July	Pattern of height anomalies at 700 mb level; centres with similar sign are found south of the Aleutian Islands and over the southeastern U.S. and centres of opposite sign are located near Hawaii and over the inter-montane region of North America; positive phase = more meridional circulation
Sunspot number	All months	The total number of sunspots that are observed during a year
Pacific Decadal Oscillation (PDO)	All months	The leading principal component of monthly SST anomalies in the North Pacific Ocean, poleward of 20°N; during the summer the positive (warm) phase is associated with above normal temperatures along the west coast of North America and in south Florida and the central part of North America experiences below normal temperatures; above normal precipitation occurs over most of the interior of NA
Arctic Oscillation (AO)	All months	Ring-like mode of annular variability; positive phase features below normal pressure over the pole and above normal pressure over the mid-latitudes, enhanced polar vortex, stronger

		westerlies, and above normal temperatures over Eurasia and central NA, colder than normal in eastern NA
Tropical/North Hemisphere pattern (TNH)	November to February	Two anomaly centres; one centred over the Gulf of Alaska and the other over Hudson Bay; related to the location and eastward extent of the Pacific jet
Pacific Transition (PT)	May to August	Wave-like pattern of anomalies which extends from the Gulf of Alaska to the Labrador Sea and is aligned along 40° N; negative phase linked to a reduced ridge over NA
Southern Oscillation Index (SOI)	All months	Standardized difference between sea level pressure in Tahiti and Darwin; strongly negative = El Niño; strongly positive = La Niña
Aleutian Pressure Index (ALPI)	December through March	Measures the relative intensity of the Aleutian Low; a positive index value reflects a relatively strong, or intense Aleutian Low
Pacific Circulation Index (PCI)	December through March	The cumulative summation of negative northwesterly atmospheric circulation frequency anomalies; positive value reflects increased westerly and southwesterly atmospheric circulation off the west coast of Canada
Atmospheric Forcing Index (AFI)	December through March	The first component from a principal components analysis on the ALPI, PDO, and the northwesterly atmospheric circulation anomalies for the North Pacific; positive values represent intense Aleutian lows, above average frequency of westerly and southwesterly winds, cooling of sea surface temperatures in the central North Pacific, and warming within North American coastal waters
Pacific SST: Niño-1+2 (0°-10°S & 90°-80°W) Niño-3 (5°N-5°S & 150°W-90°W) Niño-4 (5°N-5°S & 160°E-15°W) Niño-3.4 (5°N-5°S & 170°W-120°W)	All months	Expressed as temperature departures from the monthly long-term mean; strongly positive = El Niño; strong negative = La Niña
North Atlantic SST- (5°N-20°N & 60°W-30°W) South Atlantic SST- (0°-20°S & 30°W-10°E) Tropical SST (10°N-10°S)	All months	Expressed as temperature departures from normal

Several teleconnections require a more detailed description than can be provided in the preceding table. One of these is the NAO which is the leading mode of variability in the North Atlantic. The NAO consists of a north-south dipole of pressure anomalies with one centre located over Greenland and the other centre of opposite sign over the middle of the North Atlantic (between 35°N and 40°N). Recently, it has been suggested that this teleconnection may be hemispheric (a ring-like or annular mode of variability) rather than regional in nature (Thompson and Wallace, 1998; Thompson and Wallace, 2000; Thompson *et al.*, 2000). This 'new' paradigm, which has been labeled the Arctic Oscillation (AO), only arrived on the teleconnection scene within the last three years when Thompson and Wallace (1998, 2000) and Thompson *et al.* (2000) used the term to describe the leading Empirical Orthogonal Function (EOF) of winter sea-level pressure (SLP) anomalies poleward of 20°N. Interestingly, these authors suggest that the AO is essentially identical to the more familiar North Atlantic Oscillation (NAO), or, perhaps more correctly, that the NAO is simply a regional component of the larger-scale, hemispheric AO. The claims of Thompson and Wallace, and their followers, remain somewhat controversial, and are being re-evaluated by many others (Kerr, 1999; Deser, 2000). In any case, there is a great deal of agreement between the NAO and AO teleconnection indices ($R^2 = 0.98$) and so for the purposes of this study the AO will be used (Thompson and Wallace, 1998).

The PDO is an El Niño-like teleconnection pattern, based on anomalous sea-surface temperature conditions in the Pacific. The term "Pacific Decadal Oscillation" was coined by Hare in 1996, in association with his research into connections between Alaska salmon production cycles and Pacific climate (Mantua *et al.*, 1997). As indicated by its name, the PDO is much more persistent than ENSO. Mantua *et al.* (1997) found that major climatic regime shifts occurred in the North Pacific in 1925, 1947, and 1977. These interdecadal shifts were found to be linked to significant changes in SSTs, air temperature, pressure, and the biota throughout the Northern Hemisphere. The authors also noted that ENSO and the PDO were clearly related both spatially and temporally, although this is still a matter of some debate.

Sunspots and the 22-year Hale Magnetic Cycle have been linked to drought periodicities in numerous studies (Stockton and Meko, 1983; Oladipo, 1987; Padmanabhan and Ramachandra Rao, 1990). Despite this fact, no physical mechanism by which sunspots influence the occurrence of drought had been identified.

2.10 Drought prediction using teleconnections

Generally, the upper limit for weather forecasting is about two weeks due to the inherently chaotic atmospheric system, and the limitations of our understanding of atmospheric processes and the initial state of the atmosphere (Cane, 1991; Maybank *et al.*, 1995). It is important to keep in mind that teleconnections do not assist in the production of long-range *weather* forecasts but, instead, long-range *climate* forecasts. That is, teleconnections facilitate the forecasting of the average weather conditions to be expected over some period of time, typically on the order of months or seasons. Thus, climate forecasts are less resolved both spatially and temporally than weather forecasts. Teleconnections allow the time-frame of predictability to be lengthened, largely because of the thermal inertia of the oceans, the long life-cycle of SST anomalies, and the phase-locking of the SST variations to the annual cycle (Nicholls and Katz, 1991). In other words, the coupling between the atmosphere and the more slowly varying oceans facilitates climate prediction over time scales of months, seasons, years, and even decades (Sutton and Allen, 1997; Uppenbrink, 1997).

The long-range forecasting methods currently in operation can be divided into three main categories (Barnston *et al.*, 1994). The first category contains models that are purely statistical in nature, including canonical correlation analysis (CCA), principal oscillation patterns (POP), empirical orthogonal functions (EOF), and stepwise multiple regression. Some statistical techniques involve looking at trends in the general circulation of the atmosphere and using kinematics or extrapolation. Other statistical techniques involve predicting climatological persistence using contingency tables (Namias, 1978b).

Analogue models are another method used to produce long-range forecasts. These models compare current meteorological conditions to similar conditions of the past, therefore, a long and complete meteorological record is required for this method to be most effective (Namias, 1980).

The final category contains those long-range forecasting methods that are either purely dynamic and those that utilize a combination of dynamic and statistical techniques. These models attempt to simulate the complex physical interactions within the ocean-atmosphere system. The intermediate coupled model (ICM) is a dynamically based model that employs simplified models of the ocean and atmosphere. The hybrid coupled model (HCM) uses an ocean general circulation model with a statistical, or simplified dynamical atmosphere model. The coupled general circulation model (CGCM) uses a dynamical ocean general circulation model and an atmospheric general circulation model (Kirtman *et al.*, 1997).

As understanding of physical processes increases, dynamically-based models have the potential to be more valuable than analogue or statistical methods. Currently, however, these approaches deliver roughly the same amount of forecast skill (Barnston *et al.*, 1994). The best forecasting models currently have an overall prediction skill of around 0.6 (where 1.0 indicates a perfect forecast). The limits of predictability and the associated skill levels, especially in extratropical climates, vary by region, season, and lead time due to the nature of the global teleconnections (Wilhite *et al.*, 1987; Barnston *et al.*, 1994). Although this marginal skill level is regarded as useful, there needs to be improvement before these long-range forecasts have much operational value. For a forecast to have operational value it must have sufficient skill so that decisions made based on these forecasts make economic sense. In addition, long-range forecasts need to be readily accessible, application specific, easy to understand, and available in a timely manner so that steps can be taken to reduce the impact of the drought (Wilhite *et al.*, 1987). For example, forecasts could be applied to determine fertilizer applications, cropping decisions, irrigation scheduling, when to plant and harvest, and the management of feed supplies and water resources (Wilhite *et al.*, 1987).

Canada lags somewhat behind the other major grain-growing nations in its efforts to produce long-range climate forecasts. This may be because the influence of many of the major global teleconnections on Canadian climate is not as clear as in other parts of the world (most notably Australia). Nevertheless, some significant teleconnection-related research has been done. For example, Shabbar and Khandekar (1996) analyzed the impact of the ENSO on the temperature field over Canada. Shabbar and Barnston (1996) used canonical correlation analysis (CCA) to forecast three-month mean surface temperature and precipitation across Canada. Their predictors were quasi-global SST, Northern Hemisphere 500 mb geopotential heights, and antecedent temperature values.

Furthermore, a number of studies have linked North Pacific SSTs to winter weather over North America. For example, Namias (1969, 1972, and 1986) demonstrated that the occurrence of a large area of anomalously cold water in the central North Pacific combined with a large area of anomalously warm water off the coast of California and down into Central America produces a unique Rossby wave pattern. This Rossby wave pattern results in warm and dry conditions over western North America and cool and wet conditions over eastern North America. If the SST pattern is reversed, the related weather patterns tend to be reversed, too.

Knox and Lawford (1990) used the PNA, the NAO, and NP teleconnection indices to investigate the relationship between Northern Hemisphere circulation and pressure patterns at the 500 mb level. They established that prairie precipitation is strongly related to the phase of the PNA. Wet months are associated with the negative phase and dry conditions are associated with the positive phase. They also found that the NAO and NP are strongly related to spring precipitation on the prairies.

Bonsal *et al.* (1993) used North Pacific SST anomalies to predict the occurrence of extended growing-season dry-spells on the Canadian prairies. Their study verified the previous work of Knox and Lawford (1990), and showed that dry-spells on the prairies are associated with positive height anomalies in the mid-troposphere. Anomalies in North Pacific SSTs, North American snow cover, or soil moisture conditions may be responsible for these changes in the large-scale circulation patterns. Bonsal *et al.* (1993) also found that the severity of the dry-spells was influenced by the duration and persistence of the SST anomaly, and the height of the 500 mb ridge. Interestingly, it was noted that when the SST anomaly persisted for longer than nine months a dry-spell always occurred.

Garnett *et al.* (1997) examined a variety of teleconnection relationships for the Canadian prairies. A relationship was found between SSTs in the eastern equatorial Pacific in April and July precipitation on the prairies. This is particularly important because July precipitation very much affects both the quantity and the quality of the Red Spring wheat yield. In a subsequent study, Garnett *et al.* (1998) developed a predictive model, using PNA and ENSO, that explained up to 64% of the summer temperature variation and 47% of the summer precipitation variation. They suggest that these regression models can be used to develop a skillful forecast of summer weather over the Canadian prairies with a lead-time of two to four months.

Quiring and Blair (2000) studied the relationship between various global teleconnections and Red Spring wheat yield in Saskatchewan at the crop-district level. They developed a group of statistical models that were able to explain more than 62% of the variance in wheat yield using a combination of simultaneous and lagged teleconnection and meteorological variables. However, there was a great deal of spatial variability, in terms of the degree of explanation provided by the models, across Saskatchewan. North Pacific and North Atlantic sector teleconnections were found to be most closely correlated to wheat yields in Saskatchewan. The Pacific Transition (PT), the East Atlantic Jet (EAJET), and the North Atlantic Oscillation (NAO) were particularly significant. Many of the teleconnections found to be important for predicting variations in yield had spatially coherent patterns. That is, the crop districts where particular teleconnections were found to be statistically significant tended to be grouped together. This study once again highlighted the importance of North Pacific sector teleconnections (e.g., PNA, PT, NP), ENSO, and SSTs for long-range forecasting on the Canadian prairies. It also illustrated that Atlantic sector teleconnections such as the NAO and EAJET may have more importance to the Canadian prairies than the literature suggests.

Bonsal and Lawford (1999) found a relationship between ENSO and the number of dry spells on the Canadian prairies. They observe that during the second summer following the mature stage of an El Niño (La Niña) there is an increased (decreased) likelihood of dry spells occurring. However, as was noted earlier, this relationship does not appear to agree with the finding of other researchers.

In Australia, a number of studies have used teleconnections to forecast drought. For example, Chiew *et al.* (1998) found that there is a clear link between ENSO and Australian drought, but it is not sufficiently strong to accurately predict drought on an operational basis.

Cordery and McCall (2000) also used the SOI to create a drought forecast for Australia. They used a method of data partitioning to selectively choose the years for which they made their forecasts. This allowed them to explain up to 65% of the variance in precipitation using forecast models with up to a one-year lead time.

Over the last decade, improvements in the ability to forecast the climate have been substantial. Models now have the capability to make moderately successful forecasts with a two-season lead (Barnston *et al.*, 1994). Further developments in seasonal climate prediction depend on the maintenance and expansion of the worldwide observation system that covers both the ocean and the atmosphere, especially in certain large areas of the ocean and parts of the Southern Hemisphere (Uppenbrink, 1997). Unfortunately, GCMs do not yet accurately reproduce the processes of the atmosphere for desired lead times, and they are limited in their predictability based on the accuracy of the initial conditions and the inability to reflect the lower-frequency components of the ocean-atmosphere system (Shabbar and Barnston, 1996). Thus, linear statistical approaches still provide better forecast-skill. Statistical models are also much less costly to run and serve the purpose of setting the baseline skill level to which dynamical models must be compared (Barnston *et al.*, 1994).

Largely as a result of research noted in this literature review, there appears to be general agreement that fluctuations in North Pacific and North Atlantic sector teleconnections, ENSO, and SSTs provide the best opportunities for the creation of reliable long-range forecasts of Canadian climate. To date, no studies have examined the relationship between teleconnections and agricultural drought on the Canadian prairies. Most of the research has only been concerned with the relationships between teleconnections and temperature or precipitation. Thus, this study attempts to fill this gap in the scientific literature.

CHAPTER 3
STUDY AREA, DATA SOURCES, AND METHODOLOGY

3.1 Introduction

This chapter is presented in four sections. The first section identifies the study area. The second section describes the time frame of the study. The third section outlines the data requirements, sources, and collection procedures for the climate, crop yield, teleconnection, and drought index data. The final section discusses the methodological techniques that were used to: 1) calculate the drought indices, 2) select the 'best' agricultural drought index, 3) perform a diagnostic analysis, 4) produce an agricultural drought climatology of the Canadian prairies, and 5) explore the relationship between teleconnections and agricultural drought.

3.2 Spatial setting

The study area is the agriculturally-active region of the Canadian prairies (i.e., crop-growing region of Manitoba, Alberta, and Saskatchewan) (Figure 3.1). The Canadian prairies are located close to the centre of the North American continent. The Prairie ecozone covers an area of 520,000 km^2 in southern Manitoba, Saskatchewan, and Alberta (approximately 49-54° N latitude and 96-114° W longitude) (Raddatz, 1998). This region was predominately covered by grassland prior to settlement in the nineteenth century. Today, as much as 60% of the Canadian prairies has been converted to agricultural usage (Raddatz, 1998). The remainder of the region is divided between native and perennial grasslands that are used for pasture, land that is lying fallow, and land that is not used for agricultural production (Raddatz, 2000).

The landscape of the Canadian prairies is dominated by plains and gently rolling terrain,

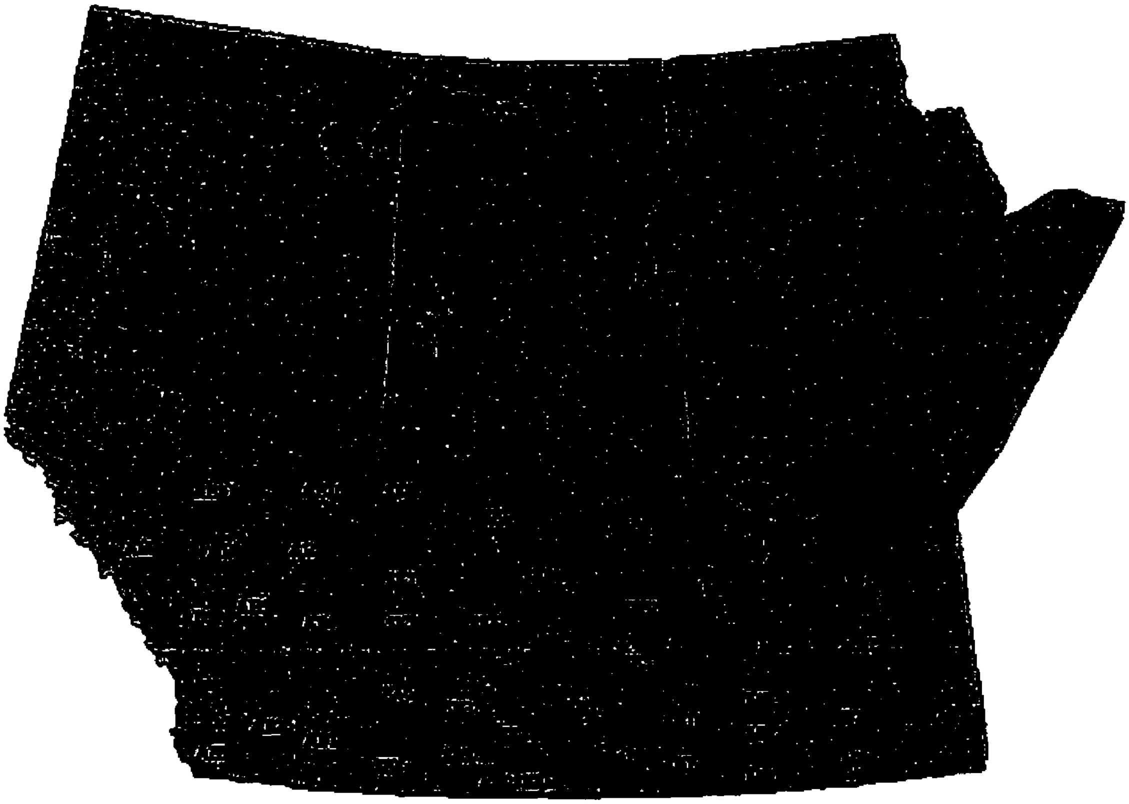

Figure 3.1 The study region- Alberta, Saskatchewan, and Manitoba crop districts/census agricultural regions

punctuated by rivers and deep glacial melt water channels. The Cypress Hills, near the U.S. border in Alberta and Saskatchewan, and the Manitoba escarpment are the only two areas where relief is an important climatic control. The region can be divided into three ascending levels of plains: the Manitoba lowlands, the Saskatchewan plains, and the high plains of Alberta (elevations >1500 m in southwest Alberta) (Cohen *et al.*, 1992). The major river systems in the prairies are the Saskatchewan, the Assiniboine, and the Red. The Saskatchewan basin includes the North and South Saskatchewan, Red Deer, Bow, and Oldman Rivers and is an important source of irrigation for Alberta and Saskatchewan. Most of the flow in prairie rivers originates as snow from the Rocky Mountains along the western boundary of the watershed. Southern Alberta and Saskatchewan both contain several large closed internal drainage basins (~80,000 km^2) which have no surface outflow (Herrington *et al.*, 1997). Many shallow lakes, sloughs, potholes, and depressions cover the landscape. The number and size of these wetlands is highly dependent on the precipitation during recent years (Winter and Rosenberry, 1998). The soils of the prairies are primarily glacial or lacustrine in origin and they range from grey wooded to brown and black (Cohen *et al.*, 1992). The Rocky Mountains provide a formidable barrier that prevents unmodified air masses from the Pacific Ocean from being pushed across the prairies by the prevailing westerlies, by either blocking or modifying their flow (Herrington *et al.*, 1997).

The prairies display many of the characteristics of a typical continental climate with hot summers and cold winters. Another important determinant of the climate of the prairies is the exposure to air masses from many different source regions. The absence of topographic barriers to the north, east, and south allows air masses to approach from all directions. Air masses that move down from the north can bring frigid air sweeping across the prairies, air masses from the south often are warm and heavily laden with moisture, and warm-dry winds can sweep down off the mountains in the west. The result is that the prairies are prone to extreme short-term temperature variability (Blair, 1997).

Latitude is also vital to the climate of the prairies because it produces strong seasonality due to changes in the amount of solar insolation. Annual precipitation ranges from 300 to 550 mm. The driest conditions in the prairies tend to be found in the south and the southwest, while the wettest areas are found in the north and northeastern prairies (Herrington *et al.*, 1997). About two-thirds of the precipitation falls during the summer months (May to August) (Cohen *et al.*, 1992). Snow also makes up a significant portion of the total precipitation and the continuous snow cover lasts four to five months. There is a great deal of spatial variation in precipitation variability, and thus drought susceptibility, across the prairies (Longley, 1952).

The boundaries of the study region are defined by the boundaries of the crop reporting regions for the three Prairie Provinces. These boundaries are used for the collection and dissemenation of agricultural data at the sub-provincial scale. In Saskatchewan, the boundaries are known as Crop Districts. In Manitoba they are called Agricultural Regions and in Alberta the boundaries are Census Agricultural Regions. All of these regions will all be referred to as crop districts from this point forward.

The crop districts are small enough that, from a climatological perspective, they are relatively homogeneous, but they are large enough that they contain a sufficient number of climate stations to produce reliable regional averages. A total of 43 crop districts from across the Canadian prairies have been selected for consideration. There are 12 crop districts in Manitoba, 20 in Saskatchewan, and 11 in Alberta. A number of crop districts in northern Alberta have been excluded from the analysis because they are outside of the main crop-growing region.

Although the boundaries of the crop districts in Saskatchewan remained static between

1961-1999, crop districts in Manitoba underwent boundary changes. The crop districts in Manitoba were redrawn in 1976 and unfortunately the new boundaries can not easily be rectified with the old (Code, 1998). Therefore, yield data only exists for Manitoba after the new crop district boundaries were adopted in 1977.

Data for Alberta is available under two different boundary systems, namely Census Agricultural Regions and Crop Districts. Both of these systems have a different number of regions for which data is collected. Crop districts in Alberta are much larger than those in Saskatchewan and Manitoba. This creates a problem for the calculation of drought indices because as crop districts increase in size, they are less likely to be climatologically homogeneous. For this reason, drought indices were calculated in Alberta using the Census Agricultural Regions because the size of these regions corresponds much more closely to that of the crop districts in Manitoba and Saskatchewan.

Yield data for Alberta was only available using the crop district boundaries. Therefore, it was necessary to derive the yields for the Census Agricultural Regions by applying the crop district data to the census regions that shared the same area. Because the boundaries for the Census Agricultural Regions were generally determined by cutting the Crop Districts into two or three separate regions, the crop yield data for the each Crop District can be applied to each of these Census Agricultural Regions (Table 3.1).

Table 3.1 Conversion of Alberta Crop Districts to Census Agricultural Regions

Crop District	Census Agricultural Region
1	1, 4
2	2, 5
3	3, 6
4a	7
4b	10
5	8, 9, 11

Admittedly, this is a crude approach to dealing with the problem because it assumes that average yield and amount of production was uniform across the entire area covered by the old crop district. This approach was adopted because it avoids the problems associated with using regions that are too large to be climatologically homogeneous, and it ensures that there are a sufficient number of years of yield data to test the drought indices.

3.3 Temporal setting

This study examines the occurrence and predictability of agricultural drought on the Canadian prairies during 1920-1999. A paucity of data in some crop districts during 1900-1920 prevented an examination of the entire twentieth century. Some spatial and temporal gaps still exist in the temperature and precipitation data since 1920, but the data quality is sufficient to allow for the calculation of drought indices for all crop districts.

The first objective of this study is to determine which of the drought indices provides the 'best' measure of agricultural drought on the Canadian prairies. Crop yield data was used to measure the performance of the drought indices and to determine which was most appropriate as a measure of agricultural drought. All of the drought indices were calculated for the entire 1920-1999 period, but due to the availability of crop yield data they were only validated for 1961-1999 in Alberta and Saskatchewan, and 1977-1999 for Manitoba. The relationship between teleconnections and drought was explored using 1961-1999 data.

3.4 Data requirements, sources, and collection procedures

3.4.1 Meteorological data

A complete record of daily temperature and precipitation data for each crop district was extracted from the Atmospheric Environment Service (AES) CD-ROM for the 1920-1999 period for 1020 stations across the prairies (Figure 3.2) (Appendix B contains a complete list of stations). These stations were then used to calculate the mean daily temperature and precipitation for each crop district for the entire period of record.

The first step in calculating the average temperature and precipitation values for each crop district was to determine which climate stations were located within which crop districts. This was done by plotting the locations of the stations in ArcView GIS using the latitude/longitude coordinates and station names. Stations that fell in a particular crop district were then extracted using a spatial clip function. As a result, forty-three different files were created (one for each crop district) with each file containing a list of all the stations within its borders. This station list was then edited to remove all of those stations that had less than five years of data. These stations were eliminated because they did not have a long enough record to warrant consideration. The station list was also examined for redundancy. This was done to ensure that each location was only represented by a single station to avoid uneven spatial weighting within the crop district. It was sometimes necessary to use more than one station at each location if their records were of different lengths, to get as close to a complete record as possible.

Daily maximum and minimum temperature, rain, snow, and total precipitation were then extracted for each station from the AES CD-ROM. All of the station data (29,220 days) for each crop district were merged into a single file and then aggregated to produce an average daily temperature and total precipitation value for each day. The total number of missing days for each crop district are shown in Table 3.2. Long periods of missing data were filled-in by using the closest station from a neighbouring crop district. Most of the missing data were filled-in using this technique. However, there were still some missing values for shorter periods (a few days) and these were estimated for temperature using a linear interpolation between surrounding values, and for precipitation by using the series mean. No more than 93 values (out of 29,220) were filled-in for any one variable using linear interpolation (temperature) or the series mean (precipitation). The total number of days that were filled-in using linear interpolation (maximum and minimum temperatures) or the series mean (rain and total precipitation) for each crop district is shown in Table 3.2.

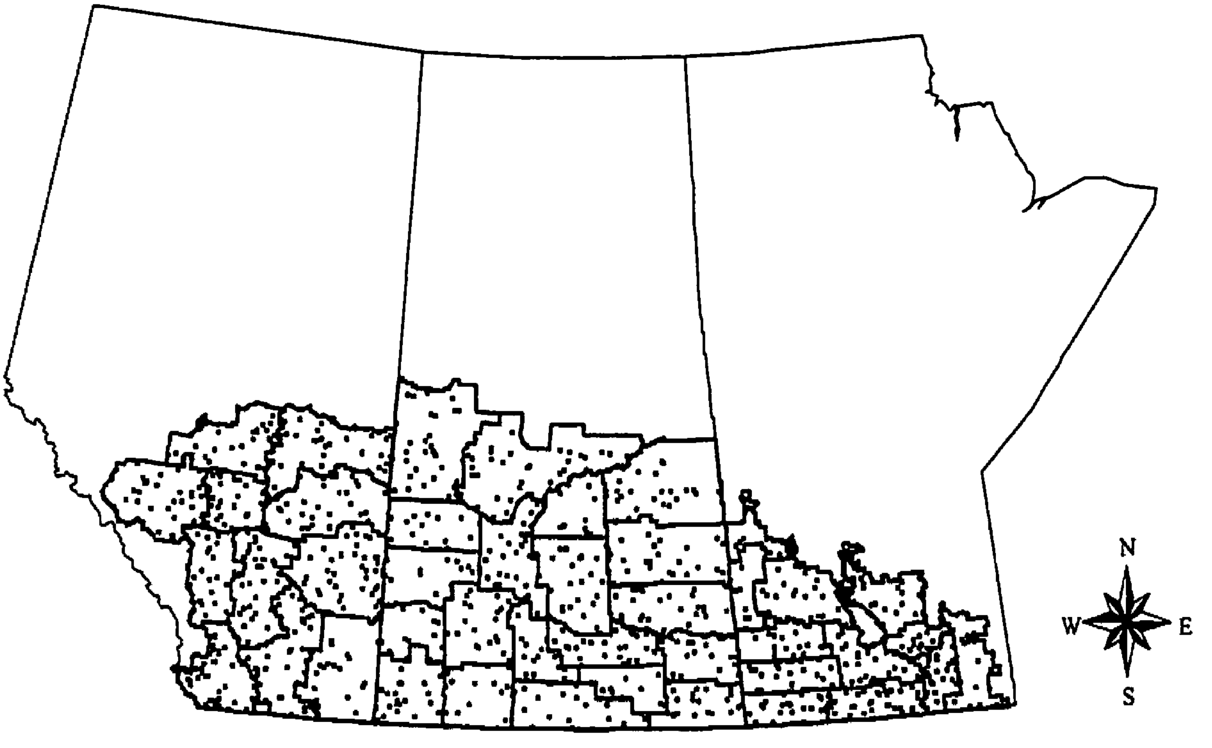

Figure 3.2 Location of the climate stations selected for use in this study

Table 3.2 Total number of missing days between 1920-1999 and the number of missing days filled-in for each variable using linear interpolation (MAX, MIN) or the series mean (RAIN, PPT)

Crop District	Total number of missing days	MAX	MIN	RAIN	PPT
SK9b	0	0	0	0	0
SK9a	0	0	0	0	0
SK8b	247	1	0	0	0
SK8a	0	2	2	0	0
SK7b	30	6	6	0	0
SK7a	0	2	2	0	0
SK6b	0	0	0	0	0
SK6a	214	0	0	0	0
SK5b	29	3	3	0	0
SK5a	0	0	0	0	0
SK4b	0	5	5	1	0
SK4a	0	0	0	0	0
SK3bs	0	1	2	0	0
SK3bn	0	0	0	0	0
SK3as	1038	40	33	0	0
SK3an	339	0	0	0	0
SK2b	0	0	0	0	0
SK2a	62	10	15	0	0
SK1b	0	1	1	0	0
SK1a	248	15	13	0	0
MB1	30	2	3	0	0
MB2	0	0	0	0	0
MB3	0	0	0	0	0
MB4	2942	93	68	6	6
MB5	7911	9	9	2	2
MB6	967	11	5	0	0
MB7	1134	0	0	0	0
MB8	0	0	0	0	0
MB9	1803	0	0	0	0
MB10	0	2	4	0	0
MB11	11245	0	0	0	0
MB12	2568	0	1	0	0
A1	0	0	0	0	0
A2	0	0	0	0	0
A3	0	0	0	0	0
A4	212	0	0	0	0
A5	0	0	0	0	0
A6	0	0	0	0	0
A7	0	8	7	0	0
A8	0	0	0	0	0
A9	0	2	3	0	0
A10	0	0	0	0	0
A11	0	0	0	0	0

3.4.2 Crop yield data

The Red Spring wheat (*Triticum aestivum* L.) yield data for the forty-three crop districts for 1961-1996 was supplied by the Canadian Grain Commission (CGC), and the data for 1997-99 was provided by Alberta Agriculture, Food, and Rural Development, Saskatchewan Agriculture and Food, and Manitoba Agriculture. A summary of the crop yields for each crop district is presented in Tables 3.3, 3.4, and 3.5.

Table 3.3 Summary of crop yield data for Manitoba crop districts

Crop District	Mean Yield (bu/ac)	Standard Deviation	Years
MB1	28.2	6.20	23
MB2	29.8	6.17	23
MB3	31.5	4.79	23
MB4	31.6	5.31	23
MB5	33.0	5.54	23
MB6	31.2	4.81	23
MB7	34.1	7.31	23
MB8	33.6	7.63	23
MB9	32.5	6.84	23
MB10	28.9	5.45	23
MB11	32.3	5.89	23
MB12	31.8	5.29	23
MEAN	**31.5**	**5.9**	

Table 3.4 Summary of crop yield data for Saskatchewan crop districts

Crop District	Mean Yield (bu/ac)	Standard Deviation	Years
SK1a	24.2	6.08	39
SK1b	25.7	5.98	39
SK2a	22.7	6.58	38
SK2b	26.9	5.77	39
SK3an	23.3	6.81	39
SK3as	22.9	6.80	39
SK3bn	24.0	6.88	39
SK3bs	23.3	7.47	39
SK4a	21.0	7.06	39
SK4b	23.2	7.96	39
SK5a	26.7	5.86	39
SK5b	28.0	5.89	39
SK6a	25.1	6.08	39
SK6b	25.5	7.11	39
SK7a	26.9	6.72	39
SK7b	27.3	6.17	39
SK8a	29.3	7.73	39
SK8b	29.1	6.61	39
SK9a	27.4	6.43	39
SK9b	28.3	4.82	39
MEAN	**25.5**	**6.5**	

Table 3.5 Summary of crop yield data for Alberta crop districts

Crop District	Mean Yield (bu/ac)	Standard Deviation	Years
AB1	22.7	7.73	39
AB2	33.1	7.46	39
AB3	31.2	7.51	39
AB4a	28.8	5.65	39
AB4b	30.9	5.26	39
AB5	39.9	9.44	39
MEAN	**31.1**	**7.2**	

A number of conversions were necessary to insure that all of the data were in the same units. Table 3.6 provides a list of the equations that were used to convert yield and production data from metric to imperial units.

Table 3.6 Summary of conversions used for wheat yield and production statistics

FROM	TO	CONVERSION
Kilograms/Hectare	Bushels/Acre	Multiply by 0.01487
'000 MT	'000 Bushels	Multiply by 36.7437
1 Tonne	X Bushels	Equals 36.7437
1 Acre	X Hectares	Equals 0.40469

3.4.3 Teleconnection data

Many of the teleconnection indices used in this study were selected because they are known to be statistically-related, at least occasionally, to the North American climate. Others were selected for exploratory purposes. That is, although the literature does not seem to contain any evidence that they are connected to the Canadian prairie climate, it was deemed worthwhile to determine whether or not they have anything to offer to long-range forecasting for the study area. A number of other indices, including Asian and European-sector indices were excluded from the analysis because they were not thought to be important to the study region.

Most of the monthly teleconnection data was obtained from the Climate Prediction Center (CPC) of the National Oceanographic and Atmospheric Administration (NOAA) in Washington, D.C.. The CPC routinely monitors thirteen prominent teleconnection patterns that can be identified in the Northern Hemisphere (NH) extra-tropics throughout the year, including: EA, EAJET, EP, NP, PNA, TNH, PT, SOI, Pacific SSTs (specifically the Niño-1+2 (N12), Niño-3 (N3), Niño-4 (N4), and Niño-3.4 (N34)), North and South Atlantic SSTs, and tropical SSTs.

The CPC uses the Rotated Principal Component Analysis (RPCA) of Barnston and

Livezy (1987) and applies it to 700 mb geopotential height anomalies to calculate its teleconnection indices (i.e., those defining atmospheric-circulation patterns). Ten patterns, or eigenvectors, are selected for each month from the height anomaly fields for the three-month period centred on that month. The RPCA procedure is based on the entire flow field and not just height anomalies at a few selected locations. The amplitude of each teleconnection pattern is determined by using a least-squares regression analysis. The amplitudes are determined such that the combined sum of their products explains the maximum spatial structure of the observed height anomaly field during the month. For each pattern, the amplitudes are then assembled into a continuous time series and standardized for each month independently.

The Aleutian Low Pressure Index (ALPI) data (up to the end of 1999) was provided by Beamish using the calculation procedure developed by Beamish *et al.* (1997). The Pacific Circulation Index (PCI) data (up to the end of 1999) was provided by King using the calculation procedure developed by King *et al.* (1998). The Atmospheric Flow Index (AFI) data (up to the end of 1999) was provided by McFarlane *et al.* (2000). The sunspot data was provided by NOAA (2001). The Arctic Oscillation data (AO) data was provided by Thompson and Wallace (2000), and the PDO data (up to the end of 1999) was provided by Mantua using the calculation procedure developed by Mantua *et al.* (1997).

Monthly teleconnection values from the current crop year and lag teleconnection values from the winter prior to planting were all considered during the exploratory analysis. The monthly values for each of the teleconnections were combined to form seasonal variables. Winter was represented by calculating the average value for December, January, and February, and spring was the average of March, April, and May. These lag values are important because they represent conditions leading up to the growing season and offer the best opportunity for making a climate forecast with a reasonable lead-time.

3.5 Methodology

This section describes how the drought indices were calculated, how the 'best' drought index was selected, and how the links between global teleconnection variables and drought conditions on the Canadian prairies were explored.

3.5.1 Calculating the drought indices

Four different drought indices were selected for inclusion in this study: the Palmer Drought Severity Index (PDSI), the Moisture Anomaly Index (Z), the Standardized Precipitation Index (SPI), and the NOAA Drought Index (NDI). The PDSI and Z indices were calculated using the FORTRAN code provided by Akinremi (1996) (source code for each drought index is contained in Appendix C). This program requires a time series of daily temperature and precipitation data and information on the available water content (AWC) of the soil and the latitude of the site (region) for which it is being calculated. The daily temperature and precipitation files for 1920-1999 were created for each crop district according to the method described in Section 3.4.2.

The entire data set (1920-1999) was used to calculate the CAFEC (climatologically appropriate for existing conditions) coefficients (e.g., ET, PET). The AWC for each crop district was calculated using an area-weighted method from maps of Alberta, Saskatchewan and Manitoba that were developed by De Jong and Sheilds (1988). Each of the maps was scanned and then imported and georectified in ArcView GIS. The crop district layer was overlayed and the AWC for each crop district was calculated based on an area-weighted average of the AWC classes. The latitude for each crop district was determined by calculating the centroid of each crop district polygon in ArcView GIS. The latitude and AWC values and the filenames of the input/output files were all manually changed prior to compiling and running the program for each crop district.

The SPI was calculated using the FORTRAN code provided by Guttman (1999). This program requires a time series of daily precipitation data for 1920-1999 for each crop district. This data file was produced according to the method described in Section 3.4.2. The NOAA drought index was calculated using the FORTRAN code provided by Titlow (1987). This program requires a time series of daily precipitation data for 1920-1999 for each crop district and monthly mean precipitation values. These data files were produced according to the method described in Section 3.4.2.

3.5.2 Selecting the 'best' index of agricultural drought

In this study, the term agricultural drought is defined as an interval of time, generally of the order of months or years, when the moisture supply of a region consistently falls below the climatically appropriate moisture supply such that crop production or range productivity is adversely affected. Thus, it is appropriate to use crop yield to determine which drought index is most appropriate for measuring agricultural drought on the Canadian prairies. This method was chosen because it is a straightforward and effective means of evaluating the drought indices and because it has precedence in the literature (Kumar and Panu, 1997).

Red Spring wheat yield (*Triticum aestivum* L.) was chosen as the index crop to be used for comparing the performance of the four drought indices because it is the most abundant wheat class grown on the Canadian prairies. Red Spring wheat yield accounts for almost 70% of the total wheat production in the region (Babb *et al.*, 1997), and it is grown extensively in all of the 43 crop districts considered in this study. This approach relies on the underlying assumption that moisture supply is the single most important factor in determining yield and that all of the other factors that affect yield (e.g., insects, disease, weather-related damage) do so in a uniform manner across all crop districts. The reliance on this assumption introduces a certain amount of error due to the spatial variability of crop moisture stress and the other yield-limiting factors.

The selection of the best index of agricultural drought was carried out in three stages. The first stage involved the creation and comparison of growing season drought index variables. Growing season drought index variables were created by summing the monthly or weekly values for May, June, and July for each of the four drought indices. The second stage involved the use of a series of linear regression equations and stepwise regression models to objectively determine which drought index variables were the most statistically significant. The best index of agricultural drought was then selected based on the results of the first two stages. It was subsequently evaluated and fine-tuned to increase the strength of the correlation with Red Spring wheat yield (this is discussed in more detail in Section 3.5.3).

All of the crop-yield and drought index data used in this part of the study is from the 1961-1999 time period for Alberta and Saskatchewan, and 1977-1999 for Manitoba. Those years that were extremely wet were not considered during any stage of the drought index comparison because too much moisture may decrease yields (recall Section 2.7). The SPI was used as an objective measure of growing season moisture and those years that had an aggregate growing season SPI value greater than 2.0 were excluded from further analysis.

During the first stage, a common growing season drought index variable was created and compared for each of the drought indices. Given the importance of growing season moisture conditions, a growing season drought index variable was created for each of the four drought indices by summing the monthly or weekly values of the indices for May, June, and July. A linear regression was then developed for each crop district with the growing season drought index variable as the independent variable and Red Spring wheat yield as the dependent variable. The best drought index was selected by comparing the coefficient of determination values (R^2) between indices. The goodness-of-fit for any given model is measured by the coefficient of determination, R^2, which is defined as the ratio of variation attributable to the regression relation (explained variance) compared to the total variation in the response variable.

In the second stage, a stepwise multiple regression was used to determine which variables were statistically significant. The candidate regressor variables for each drought index included the monthly and weekly January to July variables as well as the growing season drought index variable and an antecedent moisture condition variable. The antecedent moisture condition variable provides an indication of the amount of soil moisture at planting, calculated by summing all of the index values from the fall and winter prior to planting (September to April).

In multiple regression, the variation of a single dependent variable is explained by a number of predictor variables. The concept of least-squares is used to obtain the best-fit surface through multi-dimensional space (Shaw and Wheeler, 1994). Using standard procedure as a guide, the criteria chosen for the stepwise regression models were as follows: probability of F for entry $<= 0.05$, and probability of F for removal $>= 0.1$. The stepwise regression method was used because it provides an objective and automated method to find the best-fit surface and it also allowed for all possible combinations of antecedent and growing season variables to be considered. The stepwise regression procedure selected the statistically significant variables for each crop district. The assumption is that the more important a particular variable is, the more times it will be selected by the stepwise regression procedure.

During the fine-tuning stage, a series of experiments were carried out to determine the optimum way in which to utilize the best drought index. Different combinations of growing season variables (April, May, June, July, August) were considered. Crop moisture demand varies throughout the growing season and June and July are the most important months in terms of crop water-use. A number of variables were derived by using different combinations of growing season months (weeks). First, the drought index values for the months of April, May, June, and July were considered separately, and then all months were input together. Finally, experimentation with a number of different growing season drought index variables was undertaken to determine whether April and May should be included. A number of different combinations of variables were also produced to determine whether giving additional weight to June and July would increase the correlation with crop yield.

A pairwise difference test was then performed on the two most significant variables to insure that the differences in the coefficient of determination values (R^2) were indeed significant at the .05 level. The results of these tests are reported and discussed in detail in Chapter 4.

3.5.3 Performing a diagnostic analysis

The purpose of performing a diagnostic analysis on the drought index that was selected as the most appropriate for measuring agricultural drought was to examine, in detail, the strengths and weaknesses of this index. The analysis was broken down into two parts: a spatial analysis, and temporal analysis.

The spatial analysis was carried out by mapping the correlations between the drought index and Red Spring wheat yield. Other factors were also mapped in an attempt to explain the spatial pattern of these correlations. A correlation analysis was also carried out using location and precipitation, to explain why the model performed well in some crop districts, but poorly in others.

The temporal analysis examined the year-to-year variations in model performance within three representative crop districts. The three crop districts were selected on the basis of how well they were able to explain the variations in Red Spring wheat yield. One represented those crop districts that showed good correlation with the drought index, one represented those crop districts that were near the overall mean, and one represented those crop districts that performed poorly. The actual yield residuals were plotted against the predicted yield residuals for each crop district and a number of years were selected for in-depth analysis. The daily temperature and precipitation data and monthly Z-index values were plotted for particular years when the predicted yield differed greatly from the actual yield and the graphs were used to attempt to explain why the model did not perform well. Years when the actual yield closely agreed with the predicted yield were also examined in the same manner. These results are reported in Chapter 4.

3.5.4 Producing an agricultural drought climatology

The purpose of producing an agricultural drought climatology for the Canadian prairies is to satisfy the second objective (Section 1.2). The agricultural drought climatology was produced in a number of sections. In the first section, the study area was divided into a number of drought regions and these regions were subsequently used to describe the frequency, severity and extent, spatial patterns, and temporal patterns of agricultural drought on the Canadian prairies.

A cluster analysis was performed to reduce the number of units to be described by the agricultural drought climatology. Ward's method of cluster analysis was used to determine which crop districts were most similar based on the growing season Z-index values for all 43 crop districts. After reviewing the dendrogram, it was decided to divide the study region into five smaller areas. Each of these five regions is made up of between six and thirteen crop districts, as determined by the cluster analysis procedure. The membership and characteristics of each of these drought regions was then analyzed in detail using descriptive statistics. The five drought regions were used in all of the subsequent analyses.

The frequency of droughts (and floods) was calculated for each drought region by determining the number of times that an event of a given magnitude occurred during the 1920-1999 study period. Two different drought and flood thresholds were subjectively chosen based on a visual examination of the time series Z-index plots. In particular, the frequency was calculated for events that had a Z-index value of less than or equal to -5 (moderate drought), and less than or equal to -7 (extreme drought).

The spatial extent of each drought event was determined by calculating how many crop districts were experiencing a drought with a Z-index value of less than or equal to -3. This number was then expressed as a percentage of the total number of crop districts within the cluster. This method provides a good approximation of the total area covered by a particular drought event because the crop districts are relatively uniform in size. A more accurate measure of drought area could be determined by calculating drought index values at a great many point locations and then interpolating a surface based on these points. The average of all of the Z-index values for every crop districts within each cluster was calculated and used to indicate the drought severity of that cluster. Generally, as drought severity increases, the area that is affected also increases. Therefore, drought severity and spatial extent were described together.

The Moisture Anomaly Index values for each crop district were mapped for each growing season from 1920 to 1999, to analyze the spatial patterns of drought. A series of choropleth maps for each of the crop districts was created by classifying the Z-index values into seven categories. The categories used to create these growing season maps are based on the original drought categories proposed by Palmer (recall Table 2.2). However, for display purposes the number of categories has been trimmed from eleven to seven (Table 3.7).

Table 3.7 Revised Moisture Anomaly Index classification (after *Palmer, 1965*)

Z-index Value	Category
> 5.0	Very wet
3.0 to 4.99	Moderately wet
1.0 to 2.99	Slightly wet
0.99 to - 0.99	Near normal
-1.0 to - 2.99	Mild drought
-3.0 to - 4.99	Moderate drought
< - 5.0	Severe drought

The choropleth maps were created in ArcView GIS by importing the Z-index data table and linking it to the crop district boundary file. The maps were then visually interpreted to determine what spatial patterns of drought were evident.

The Fast Fourier Transform (FFT) (Burt and Barber, 1996) technique was used to analyze the temporal patterns of drought, or drought cycles, that may be present in the eighty years of available data by transferring the data from the time domain to the frequency domain. The graphical representation of such transformation is the spectral density curve, plotting frequency or period versus spectral density power. The density can be seen as the 'level of relevance' of each frequency or period. The higher the density, the more important a particular frequency or period will be. Spectral density plots were produced for a representative crop district from each of the five drought regions.

A series of cross amplitude graphs were also produced for each of the pairs of regions. The cross amplitude graphs plot frequency or period against amplitude. Amplitude and density can be interpreted in the same way, because the amplitude of a wave is a function of the initial density power causing its displacement. The amplitude corresponds to both of the drought regions' amplitudes being summed together, hence the higher the amplitude peak, the greater the degree of agreement between the two regions. For this reason, the cross amplitude graph can be used to indicate where the two regions have similar important frequencies (or periods).

Both the spectral density and cross amplitude plots were created using a Tukey-Hemming spectral window with a span of seven to remove the background noise and irregular variation from the drought index time series.

3.5.5 Exploring the relationship between global teleconnections and drought

The relationship between global teleconnection patterns and the occurrence of agricultural drought on the Canadian prairies was examined to satisfy the third objective (Section 1.2). The analysis was carried out in two stages. The first stage was a composite analysis where five of the most severe growing season droughts were used to create composites of a number of ocean and atmospheric variables such as geopotential height, outgoing longwave radiation, ocean temperature, and the jet stream. These composites were used to illustrate some of the circulation and SST anomalies that occur coincident with severe growing season droughts, and in the seasons leading up to the drought. The composite analysis also provided a better understanding of surface boundary layer conditions associated with severe drought events. The second stage was a Principal Components Analysis (PCA) that was used to help in identifying the teleconnection patterns that play a role in creating and sustaining drought conditions on the prairies in the seasons leading up to a severe growing season drought event. Examining severe droughts is particularly important because these are the events that tend to have a strong coherent climate signal. Thus, there are likely to be strong causal links between these events and atmospheric and oceanic anomalies.

A composite analysis of the atmospheric circulation, boundary layer conditions, and SSTs associated with severe droughts was undertaken using the climate visualization tools provided by

NOAA-CIRES Climate Diagnostics Center[1]. The five most severe growing-season drought events to occur since 1948 were used in the composite analysis. The selection of severe drought events was restricted to the post-1948 period since the majority of data sets that are available from the Climate Diagnostics Center (CDC) are only available for 1948 to 1999. Accordingly, the five drought years that were selected for analysis were 1961, 1988, 1958, 1967, and 1977. These five years were used to create all of the composite mean and composite anomaly maps for the growing season using June-July data, for spring using March-April-May data, and for winter using December-January-February data. Composite anomaly maps were created for a variety of atmospheric and oceanic data sets including precipitation rate, surface temperature, outgoing long-wave radiation (OLR), potential evaporation rates, soil moisture, relative humidity, SSTs, geopotential height, atmospheric pressure, and upper level winds (jet stream). These composites were subsequently analyzed to determine the surface conditions and persistent atmospheric and oceanic anomalies that are associated with severe drought events.

Obviously, one of the weaknesses of using this type of composite analysis is that it does not accurately represent the conditions during a particular drought event because it aggregates the conditions associated with all five events. The occurrence of these five drought events could have been caused by different forcing functions. However, this analysis is not meant to document the particular conditions of the atmosphere and oceans during individual drought events that have occurred on the prairies, but rather to look for similarities and patterns in the most severe drought events.

The Principal Components Analysis (PCA) was used to help identify the teleconnection patterns that play a role in creating and sustaining drought conditions on the prairies in the

1 Available at: http://www.cdc.noaa.gov/PublicData/web_tools.html

seasons leading up to a severe growing season drought event. The results of the PCA are important because they can be used to support the findings of the composite analysis. PCA is a mathematical technique that can be used to produce new combinations of the original data, to reduce the number of variables under analysis, or to explore the relationships between a number of variables to identify groups of interrelated variables (Shaw and Wheeler, 1994). For this study, PCA was used to explore the relationships between a number of teleconnection variables and the drought index variable and to identify which teleconnection patterns were identified as being interrelated to the drought index variable by being grouped with it.

There are two main methods that can be used to perform this type of analysis. The first is Factor Analysis. This procedure assumes that the observed correlations are largely influenced by the various factors that are common to all variables (there is common variance). It also assumes that some of the variance is specific to each of the variables (there is unique variance). In order to use Factor Analysis you must understand the relationship between the variables sufficiently so that you can specify the number of factors, and the amount of common variance that is associated with each factor (Shaw and Wheeler, 1994). In PCA it is assumed that there is no variation that is not accounted for by the cumulative effect of all possible components (all variance is common). PCA is an exploratory tool that does not require you to have a complete understanding of the relationship between the variables (Shaw and Wheeler, 1994). Due to the exploratory nature of this analysis, it was determined that the PCA method was most appropriate.

PCA can be calculated using a correlation or covariance matrix. The standard procedure is to use the correlation matrix. This assumes that the correlation matrix is reliable and that all of the variance in each variable is explained by the components that are common to all variables (i.e., there is no unique variance, only common variance) (Shaw and Wheeler, 1994). The PCA technique does not have any distributional requirements and allows for multicollinearity among the variables. This is particularly important because there is multicollinearity among some of the teleconnection variables.

The first principal component is, by definition, the linear combination of variables that explains the largest amount of variance in the data. The second component is the linear combination of variables that explains the second greatest amount of variability, and is uncorrelated with the first variable. The eigenvalue is the sum of all of the squared variable loadings for each component. Generally only those components whose eigenvalues are greater than unity, or which explain at least a proportion of 1/p (p = number of variables) of the total variance are considered (Shaw and Wheeler, 1994). The nature of each component can be identified by examining the variables whose loadings are greater than 0.4, or less than -0.4 (Shaw and Wheeler, 1994). In this study, only those variables whose loadings were greater than 0.5, or less than –0.5 were considered for the sake of clarity. The square of each loading indicates the percentage of variation in the component accounted for by the respective variable.

Rotating the PC matrix maximizes the loadings on each component. The purpose of the rotation is to simplify the interpretation by maximizing the loadings of strongly correlated variables and minimizing the loadings of weakly correlated variables. In this analysis the Varimax rotation procedure was used. Varimax is a commonly used rotation procedure that produces an orthogonal positioning of axes where the correlation between any two is zero. Therefore, each of the principal components is uncorrelated with the others.

The PCA was carried out using ten years of data. It used four of the same years that were used in the composite analysis as well as an additional six major drought years (Table 3.8). All ten drought years were selected from 1961-1999 based on the severity (mean growing season Z-index value for the prairies) and spatial pattern of the drought events. Only those years that featured a spatial pattern where drought dominated the entire study region were considered for inclusion. This is based on the premise that different spatial patterns of drought may be caused by different mechanisms.

Table 3.8 The ten drought years utilized by the PCA

Year	Z-index
1961	-5.6
1967	-2.6
1972	-1.0
1977	-2.4
1979	-1.4
1980	-2.1
1984	-1.9
1985	-2.3
1988	-4.7
1989	-1.6

The PCA was carried out for two seasons (winter and spring). Monthly teleconnection variables were combined to create a single mean variable for each season (e.g., monthly December, January, and February values were averaged to produce a single winter value). This analysis did not consider the relationship between growing season teleconnections and moisture conditions on the Canadian prairies because concurrent relationships are of little value for drought prediction. The two seasons that were used in the PCA correspond to those used in the composite analysis to allow both sets of findings to be related to one another.

The list of eligible teleconnection variables was reduced to only include the most important teleconnection patterns to simplify the interpretation of the PCA. The selection was based on previous research and the authors knowledge of the teleconnection patterns (Quiring, 1999). The list was trimmed to only include one measure of each teleconnection (e.g., only

Niño-3 SSTs were used to represent ENSO). Several teleconnections are not measured on a monthly basis (e.g., ALPI, sunspots) and so these variables were included in the season in which they are measured. For example, since ALPI is measured over the December to March period, it was included in the winter analysis. The mean growing season Z-index value for the prairies was included in all seasons to determine which teleconnections were related to it. All of the teleconnections included in the winter analysis are shown in Table 6.2 and all of the teleconnections utilized in the spring analysis are shown in Table 6.4.

All of the components with an eigenvalue greater than 1.0 were extracted for each season using the Varimax rotation technique. The eigenvalues, percent of variance explained, and cumulative percent of variance explained were calculated for each component. The components were then interpreted by analyzing the factor loadings.

The PCA will supplement the composite analysis by identifying the teleconnection patterns that are important precursors of drought in the two seasons prior to the onset of major growing season drought events. The PCA will quantify the relationship between a number of the most important teleconnections and the growing season drought index. When the drought index has high loadings on particular PCs, this indicates that the other variables that have strong loadings on the same PC are related to the drought index. If both the composite analysis and PCA analysis show similar results, this will help to verify that these teleconnections are related to the occurrence of severe drought events and should be considered for inclusion in operational long-range forecast models. All of the results are presented in Chapter 6.

CHAPTER 4
SELECTION OF THE 'BEST' AGRICULTURAL DROUGHT INDEX

4.1 Introduction

In this chapter the performance of four of the most important and widely used drought indices (Palmer Drought Severity Index (PDSI), Moisture Anomaly Index (Z), Standardized Precipitation Index (SPI), NOAA Drought Index (NDI)) will be compared to determine which is the most appropriate for measuring agricultural drought on the Canadian prairies. A performance-based analysis of the most widely used drought indices will help to determine which index should be employed in drought research for the Canadian prairies. This is followed by a diagnostic evaluation of the performance of the best agricultural drought index. The diagnostic evaluation will focus on identifying the causes of the spatial and temporal variations in model performance. The fulfilment of the first objective is probably the single most important component of this study because the results of subsequent objectives are reliant on the premise that the drought index being used provides an accurate and representative measure of agricultural drought on the prairies.

4.2 Drought index comparison

The comparison of the four drought indices was carried out in three stages. The first stage involved the creation and comparison of a growing season variable for each drought index using a correlation analysis. The second stage involved testing the drought indices using a series of stepwise regression analyses. The best drought index was determined based on the results from the first two stages. It was then evaluated and fine-tuned to increase the correlation with

Red Spring wheat yield.

4.2.1 Evaluation of the growing season drought index variables

Before a linear regression was developed for each crop district with the growing season drought index variable as the independent variable and Red Spring wheat yield as the dependent variable, the linear trend in average annual yield over the study period was removed (Figure 4.1). This trend has been noted in the work of other researchers and can be attributed to farming innovations such as the development of advanced varieties of wheat that are better able to cope with moisture stress, increased use of fertilizers, improved weed control, and better tillage practices (Babb *et al.*, 1997). The yield data was regressed against year-of-harvest for each crop district to remove the underlying trend. The average R^2 for the 43 crop districts was 0.24, significant at the .05 level. The unstandardized residual values for each of the linear regression equations were calculated and these values were subsequently used for evaluating the performance of the drought indices. This procedure eliminates some of the variation in the yield data that is not related to moisture supply.

The results of the regression analysis for each of the drought indices versus yield (as outlined in Section 3.5.2) are summarized at the provincial level and presented in Figure 4.2. Notably, the mean R^2 values for Saskatchewan are greater than Manitoba and Alberta for all of the growing season drought indices except the NOAA Drought Index (NDI). Alberta has the highest R^2 values for the NDI and the second highest for the other three drought indices. Manitoba has the lowest values for all drought indices.

The growing season Moisture Anomaly Index (Z) variable explains the greatest amount of variance in Red Spring wheat yield for all three provinces. The Standardized Precipitation Index (SPI) ranks second in terms of the amount of variance explained. The Palmer Drought

Figure 4.1 Scatter plots of Red Spring wheat yield versus year for all 43 prairie crop districts

Saskatchewan SK1a-SK7b

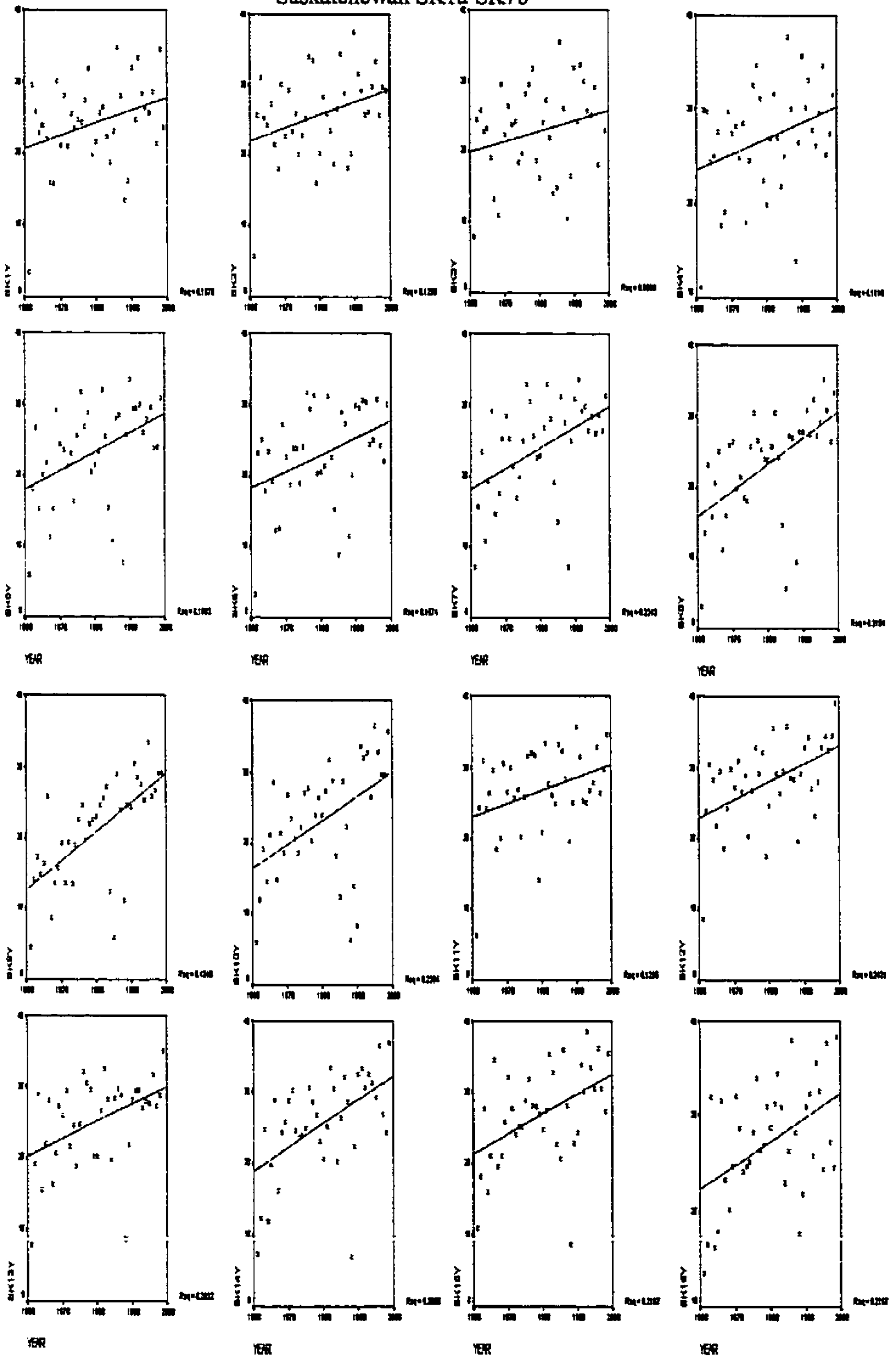

Saskatchewan SK8a-SK9b

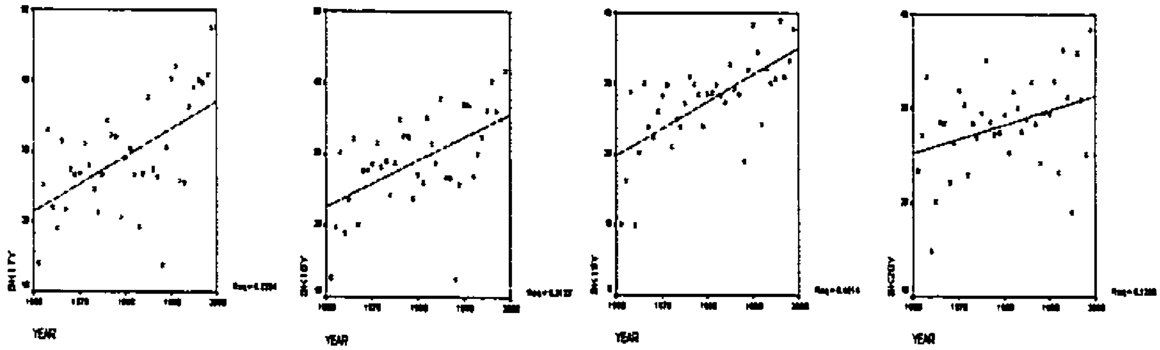

Manitoba MB1-MB12

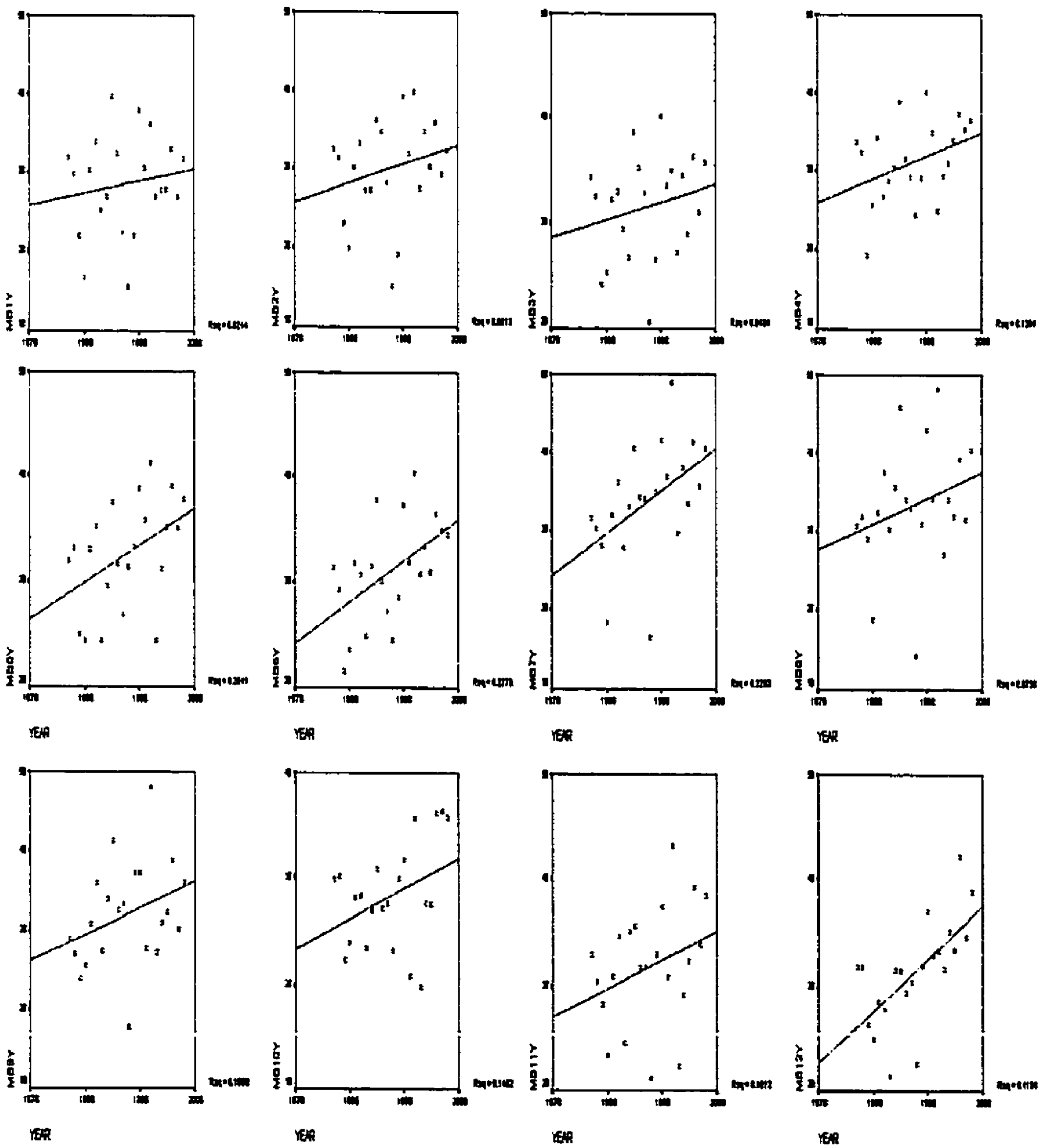

Alberta AB1-AB5

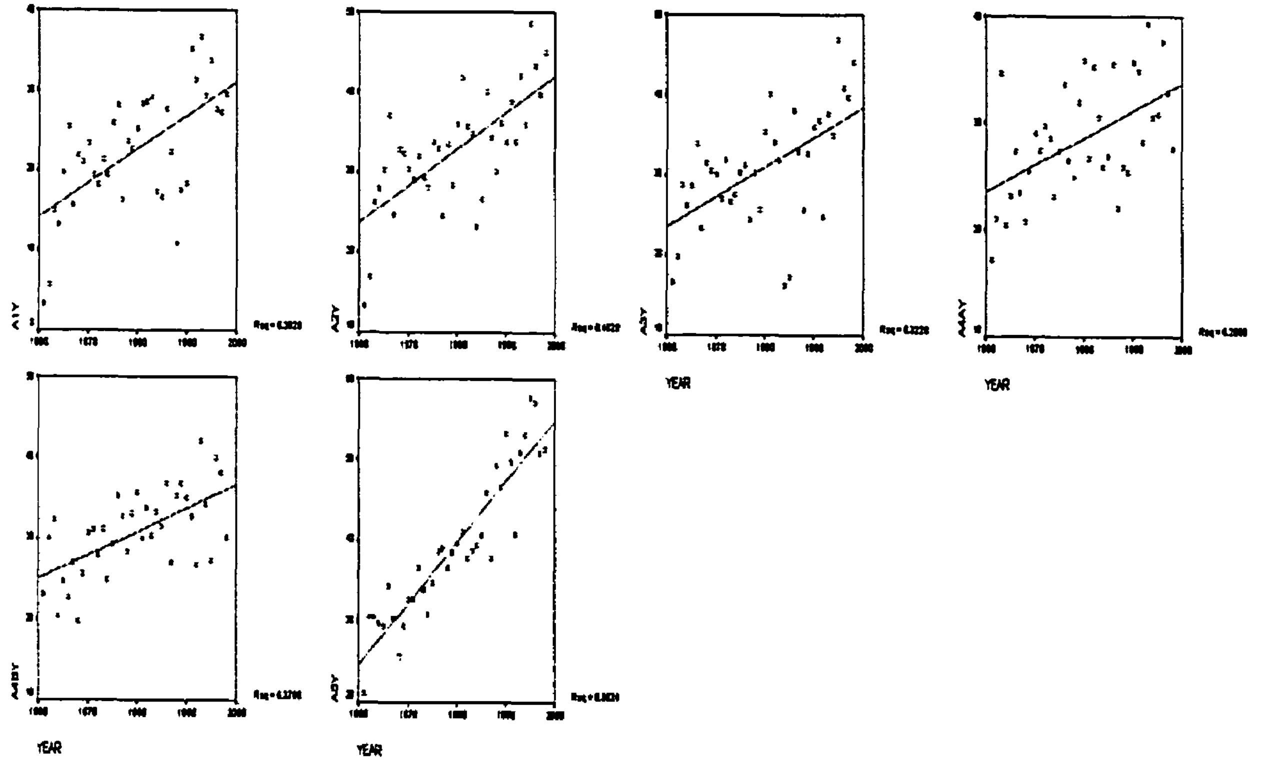

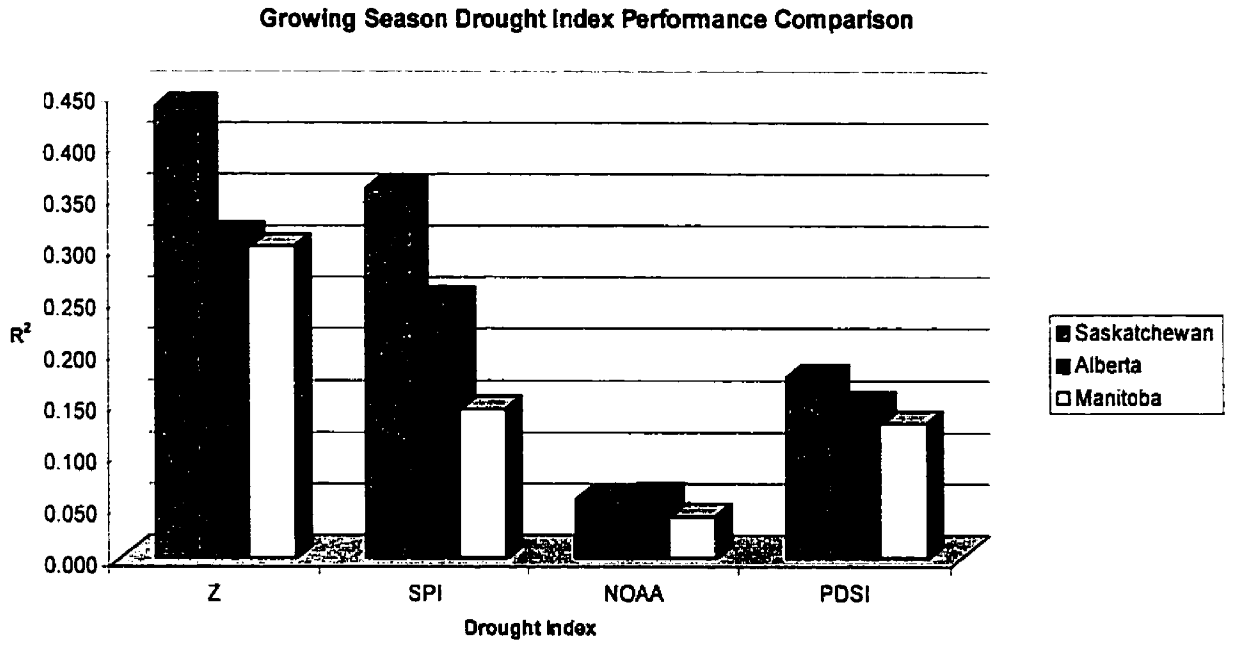

Figure 4.2 Summary of the coefficient of determination (R^2) between the growing season drought variables and Red Spring wheat yields for each of the Prairie Provinces

Severity Index (PDSI) ranks third and the NDI ranks a distant fourth. Overall, the Z-index explains almost 45% of the variation in Red Spring wheat yield in Saskatchewan and this declines to approximately 31% and 30% in Alberta and Manitoba, respectively.

While a statistically significant relationship exists between the growing season agricultural drought variables and yield, there are many other factors that play a role in determining yield outcomes. The influence of these other factors (which have been discussed in detail in Section 2.6) may explain why none of the drought indices explained more than 45% of the variance in crop yield at the provincial level. While the actual magnitude of the correlations is important, for the purposes of this study it is more important to compare the performance of each of the drought indices to determine which performs the best.

It is evident that the amount of variance in Red Spring yields explained by the drought indices is not constant over the prairies. Systematic differences in the amount of variance explained in Saskatchewan as compared to Alberta and Manitoba may result from regional differences in climate, soil conditions, moisture stress, and data quality. There is an even greater degree of spatial variability present at the crop district level (Tables 4.1, 4.2, and 4.3). In Manitoba, the R^2 values between the Z-index and Red Spring wheat yield ranged from 0.593 in MB8 to 0.001 in MB5; in Saskatchewan the R^2 values ranged from 0.603 in SK7a to 0.115 in SK8B; and in Alberta they ranged from 0.574 in AB1 to 0.024 in AB11. Similar variability between crop districts is also present in the other three drought indices. This demonstrates that although there is a strong positive correlation between the drought indices and Red Spring wheat yield in most crop districts, there are some crop districts where this relationship is weak. This will be discussed further in Section 4.3.

Table 4.1 Coefficient of determination (R^2) between Red Spring wheat yield and growing season drought indices for Manitoba crop districts

CD	Z	SPI	NOAA	PDSI
MB1	0.399	0.132	0.012	0.151
MB2	0.493	0.161	0.043	0.464
MB3	0.393	0.239	0.000	0.152
MB4	0.004	0.029	0.047	0.006
MB5	0.001	0.011	0.006	0.006
MB6	0.265	0.139	0.020	0.065
MB7	0.479	0.177	0.012	0.157
MB8	0.593	0.433	0.049	0.106
MB9	0.242	0.073	0.004	0.045
MB10	0.376	0.165	0.170	0.280
MB11	0.294	0.107	0.087	0.045
MB12	0.080	0.068	0.030	0.088
MEAN	**0.302**	**0.145**	**0.040**	**0.130**

Table 4.2 Coefficient of determination (R^2) between Red Spring wheat yield and growing season drought indices for Saskatchewan crop districts

CD	Z	SPI	NOAA	PDSI
SK1a	0.370	0.310	0.069	0.108
SK1b	0.398	0.476	0.000	0.116
SK2a	0.587	0.547	0.096	0.281
SK2b	0.355	0.361	0.026	0.064
SK3an	0.541	0.507	0.073	0.193
SK3as	0.597	0.514	0.185	0.299
SK3bn	0.516	0.346	0.051	0.277
SK3bs	0.563	0.379	0.114	0.328
SK4a	0.472	0.469	0.014	0.146
SK4b	0.448	0.257	0.041	0.329
SK5a	0.412	0.392	0.040	0.100
SK5b	0.331	0.302	0.002	0.019
SK6a	0.501	0.351	0.055	0.167
SK6b	0.582	0.496	0.192	0.358
SK7a	0.603	0.302	0.065	0.393
SK7b	0.302	0.209	0.039	0.102
SK8a	0.115	0.102	0.021	0.012
SK8b	0.371	0.218	0.039	0.120
SK9a	0.364	0.386	0.003	0.032
SK9b	0.314	0.212	0.008	0.049
MEAN	**0.437**	**0.357**	**0.057**	**0.175**

Table 4.3 Coefficient of determination (R^2) between Red Spring wheat yield and growing season drought indices for Alberta crop districts

CD	Z	SPI	NOAA	PDSI
AB1	0.392	0.259	0.034	0.263
AB2	0.331	0.366	0.017	0.087
AB3	0.425	0.370	0.123	0.242
AB4	0.368	0.265	0.078	0.321
AB5	0.432	0.217	0.078	0.218
AB6	0.574	0.425	0.140	0.296
AB7	0.410	0.368	0.043	0.096
AB8	0.045	0.037	0.011	0.016
AB9	0.095	0.037	0.045	0.019
AB10	0.350	0.379	0.094	0.063
AB11	0.025	0.037	0.003	0.014
MEAN	**0.313**	**0.251**	**0.061**	**0.149**

4.2.2 Stepwise regression results

The drought indices were also evaluated using a stepwise multiple regression. The stepwise model selected those drought variables that were statistically significant at the pre-determined level (probability of F for entry <= 0.05, and probability of F for removal >= 0.1). (refer to Section 3.5.2 for details). Figure 4.3 shows the number of times that variables from each drought index were selected as statistically significant.

The model was run for all 43 crop districts. There were five crop districts for which no variables were found to be statistically significant at the selected level of significance and therefore no model was generated. A total of 61 variables were selected as statistically significant in the remaining 38 crop districts. The distribution of the drought index variables was as follows: 35 of the variables were from the Z-index, 12 were from the SPI, 11 from the NDI, and 3 from the PDSI. A breakdown of which Z-index variables were selected is shown in Figure 4.4 (where Z refers to the drought index and the number refers to the month).

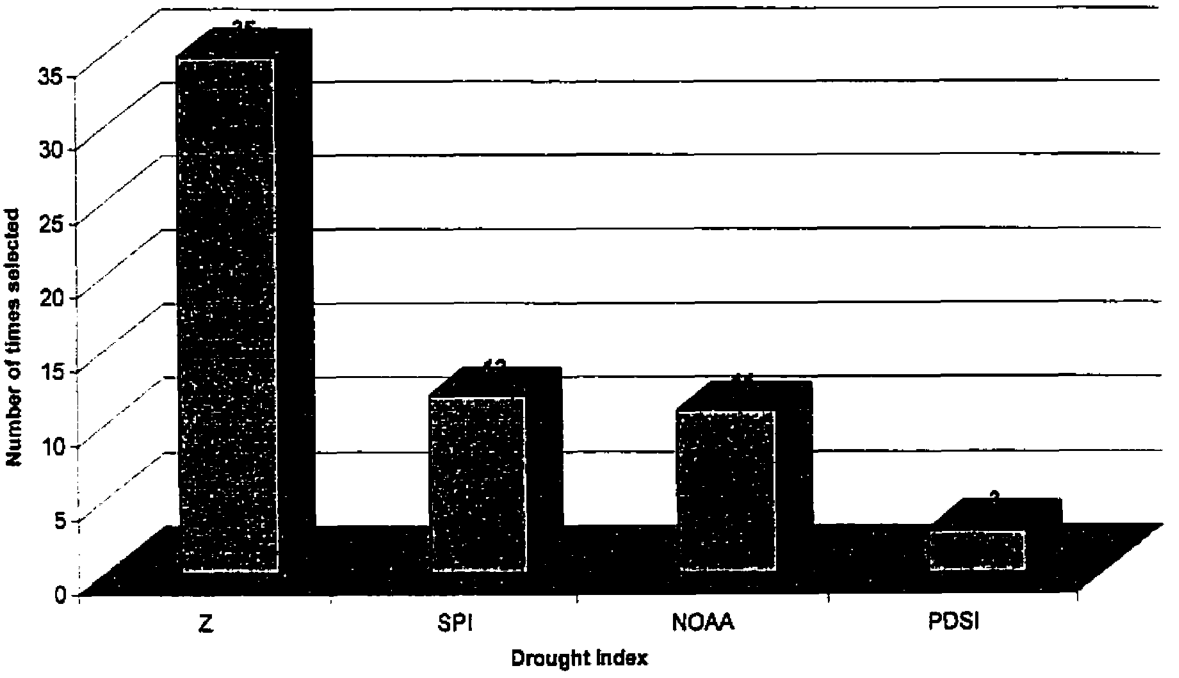

Figure 4.3 Number of times that variables from each drought index variable were selected by the stepwise regression procedure

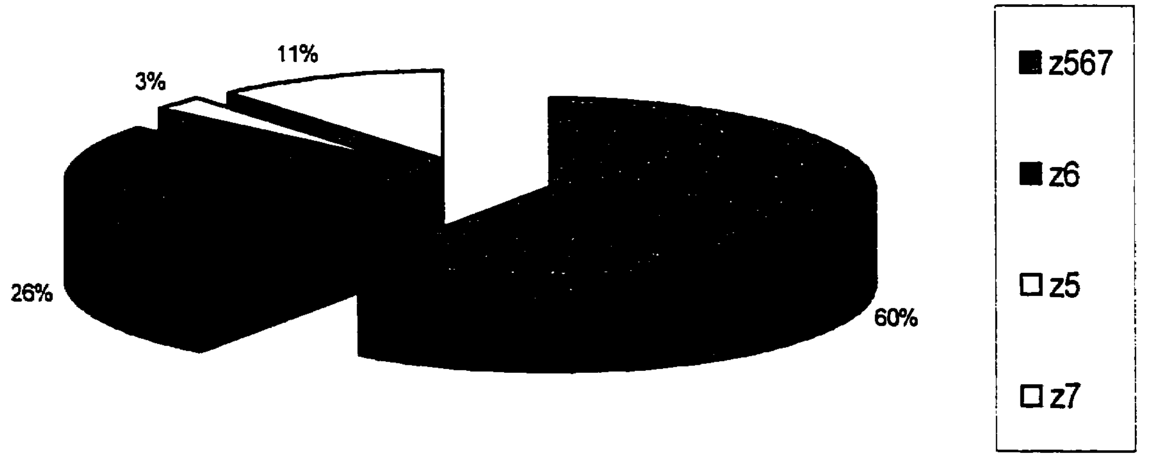

Figure 4.4 Distribution of Moisture Anomaly Index (Z) variables selected by the stepwise models

The single most important Z-index variable was Z567; it was selected a total of 21 times (60% of the total Z-index variables selected). The Z567 variable (the growing season drought variable) is derived by adding the Z values for May, June, and July. The second most frequently select Z-index variable was the June Z-index value (Z6); it was selected a total of 9 times (26% of the total Z-index variables selected). The third most frequently select Z-index variable was the July Z-index value (Z7); it was selected a total of 4 times (11% of the total Z-index variables selected). Finally, the May Z-index value (Z5) was selected once (3% of the total Z-index variables selected). Tables 4.4 to 4.6 show the details of the stepwise regression results for the remaining drought indices.

Table 4.4 Frequency of variable selection for SPI

Variable	Number of times selected
Growing Season (SPI567)	5
June SPI (SPI6)	3
May SPI (SPI5)	2
July SPI (SPI7)	2
TOTAL	**12**

Table 4.5 Frequency of variable selection for NDI

Variable	Number of times selected
Week 17 (W17)	3
Week 24 (W24)	3
Week 19 (W19)	1
Week 21 (W21)	1
Week 22 (W22)	1
Week 23 (W23)	1
Week 26 (W26)	1
TOTAL	**11**

Table 4.6 Frequency of variable selection for PDSI

Variable	Number of times selected
July PDSI (PDSI7)	2
May PDSI (PDSI5)	1
TOTAL	**3**

Overall, the results indicate that the Z-index is the best index for measuring agricultural drought because it had the largest number of variables that were selected as statistically significant. More than 57% of the variables chosen (35 out of 61) were Z-index variables. The second most frequently selected drought index was the SPI, being selected 12 times. The NDI was the next most frequently selected drought index, used 11 times. Finally, the PDSI was only selected three times by the stepwise regression models. These results are fairly consistent with the findings from Section 4.2.1. According to the frequencies, the Z-index is the best index for measuring agricultural drought and the SPI ranks second. However, the NDI index now ranks third among the drought indices. In fact, the NDI does almost as well as the SPI and does much better than the PDSI in terms of the number of times it was selected as statistically significant. It is possible that the improved performance of the NDI is due to the fact that creating an aggregated growing season variable for this index is not appropriate. Although the NDI is calculated on a weekly basis, its value is actually derived from the moisture condition for the previous eight weeks. Thus, the current week's moisture condition only accounts for $1/8^{th}$ of the NDI value. This eight-week calculation window means that there is a great deal of overlap when you add all of the growing season weeks together. Weekly values may be more appropriate because the moisture conditions during some weeks are more important than others.

Similarly, the poor performance of the PDSI can probably be attributed to the fact that it also is heavily reliant on previous values of the PDSI. The moisture conditions from the current month of the PDSI only accounts for one third of that month's PDSI value. The monthly values of the PDSI were only selected as statistically significant 3 times out of the total of 61. It can be concluded that the PDSI is not an appropriate drought index to use when you are interested in measuring agricultural drought. The PDSI is a better indicator of hydrological drought.

The aggregated growing season variables proved to be the single most important variables for the Z-index and the SPI. June was the individual month that was most frequently selected variable for both the SPI and Z-index. The next most important variable for the Z-index was July, and then May. For the SPI, both the July and May variables were selected an equal number of times. For the NDI, the first week of May and the last week of June were the most frequently selected variables. A summary of all of the drought indices, according to the month or season they represent, is presented in Table 4.7.

Table 4.7 Frequency of variable selection for all drought indices by month/season

Variable	Number of times selected
Growing Season	26
May	8
June	18
July	9
TOTAL	**61**

Growing season drought index variables were the most frequently selected variable type (almost 43% of the variables chosen spanned the growing season). June was the next most important time period and the single most important month. June variables represented nearly 30% of all variables chosen. The results show that July (~15%) and May variables (~13%) were less important. None of the variables for the months of January to April and none of the variables representing the antecedent moisture conditions (representing the conditions from harvest of the previous year until planting of the current year) were selected as statistically significant in any crop district. It is somewhat surprising that antecedent moisture conditions play such a small part in determining crop yield given the importance that farmers place on soil moisture levels at planting. Results of a separate correlation analysis indicate that all of the antecedent condition (or soil moisture recharge) variables explains less than 10% of the variance in yield (Table 4.8).

Table 4.8 Coefficient of determination (R^2) between Red Spring wheat yield and antecedent moisture condition variables by province

Province	Z	SPI	PDSI
Manitoba	0.143	0.125	0.025
Saskatchewan	0.071	0.046	0.063
Alberta	0.039	0.048	0.085
MEAN	**0.084**	**0.073**	**0.057**

This section showed that the Z-index is the best index for measuring agricultural drought. It also highlighted those times of the year when moisture supply has the largest impact on crop yield. Thus, it can be concluded that while the entire growing season is important, the month of June is the single most critical time period.

4.2.3 Fine-tuning the best drought index

The results of the first two stages of the drought index comparison have shown that the Z-index is the most suitable index for measuring agricultural drought on the Canadian prairies. During this final stage, an analysis will be carried out to determine whether there is a way to improve the correlation between the Z-index and Red Spring wheat yields.

Given what we know about crop water use, it is not surprising that the strongest correlation was between the drought index values during the growing season and yield. To maximize these correlations, it is important to consider what months should be included. Planting on the Canadian prairies typically occurs during the early part of May. As was mentioned in the previous chapter, too much moisture during May can be detrimental to crop growth because it discourages the development of an extensive root structure. This means that the plant is less able to deal with water stress later in the year. Of course, if there is not enough available soil moisture during the month of May then the crop will not germinate properly and low yields will result. The two months most important from a water-use perspective are June and July since by the beginning of August, crop water-use declines as the crop ripens and harvest normally occurs during this month. The results of the correlation analysis and the stepwise regression models support this premise.

An analysis of the growing season Z-index variable was performed to compare using an aggregate of May, June, and July values versus only using an aggregate of June and July. A pairwise significant difference test was performed and the results showed that there was not a statistically significant difference in the mean coefficient of determination value between the two variables (Tables 4.9, 4.10, and 4.11). That is, the removal of the May value from the growing season aggregate did not change the mean R^2 value in a statistically significant manner. In fact, there was actually a small increase in the mean R^2 value for each province when the May variable was excluded. Thus, the June-July growing season Z-index variable (Z67) was adopted as the best index of agricultural drought.

Table 4.9 Coefficient of determination (R^2) for two Z-index growing season drought variables: Manitoba crop districts

CD	Z567	Z67	Difference (Z67-Z567)
MB1	0.399	0.386	-0.013
MB2	0.493	0.459	-0.034
MB3	0.393	0.362	-0.031
MB4	0.004	0.054	0.050
MB5	0.001	0.017	0.016
MB6	0.265	0.165	-0.100
MB7	0.479	0.653	0.174
MB8	0.593	0.644	0.051
MB9	0.242	0.363	0.121
MB10	0.376	0.257	-0.119
MB11	0.294	0.308	0.014
MB12	0.080	0.138	0.058
MEAN	**0.302**	**0.317**	**0.016**
TOTAL			***0.187***

Table 4.10 Coefficient of determination (R^2) for two Z-index growing season drought variables: Saskatchewan crop districts

CD	Z567	Z67	Difference (Z67-Z567)
SK1a	0.370	0.451	0.081
SK1b	0.398	0.421	0.023
SK2a	0.587	0.651	0.064
SK2b	0.355	0.312	-0.043
SK3an	0.541	0.608	0.067
SK3as	0.597	0.704	0.107
SK3bn	0.516	0.575	0.059
SK3bs	0.563	0.600	0.037
SK4a	0.472	0.573	0.101
SK4b	0.448	0.478	0.030
SK5a	0.412	0.448	0.036
SK5b	0.331	0.487	0.156
SK6a	0.501	0.521	0.020
SK6b	0.582	0.560	-0.022
SK7a	0.603	0.522	-0.081
SK7b	0.302	0.395	0.093
SK8a	0.115	0.234	0.119
SK8b	0.371	0.327	-0.044
SK9a	0.364	0.497	0.133
SK9b	0.314	0.420	0.106
MEAN	**0.437**	**0.489**	**0.052**
TOTAL			***1.042***

Table 4.11 Coefficient of determination (R^2) for two Z-index growing season drought variables: Alberta crop districts

CD	Z567	Z67	Difference (Z67-Z567)
AB1	0.392	0.547	0.155
AB2	0.331	0.376	0.045
AB3	0.425	0.379	-0.046
AB4	0.368	0.378	0.010
AB5	0.432	0.496	0.064
AB6	0.574	0.524	-0.050
AB7	0.410	0.459	0.049
AB8	0.045	0.072	0.027
AB9	0.095	0.086	-0.009
AB10	0.350	0.364	0.014
AB11	0.025	0.024	-0.001
MEAN	**0.313**	**0.337**	**0.023**
TOTAL			***0.258***

A variety of other experiments were carried out to see if the relationship between the Z-index growing season drought variable and Red Spring wheat yield could be further improved. In particular, since previous analyses suggested that June is the single most important month in terms of moisture condition, tests were conducted to consider whether introducing a weighting factor that gave more weight to the June conditions could increase the R^2 value. These tests demonstrated no statistically significant improvement by using the June-weighted variable over the original growing season drought index variable (Z67).

4.2.4 Summary of drought index comparison

The results of the preceding analysis have shown that the Z-index and the SPI are the two drought indices most useful for measuring agricultural drought on the Canadian prairies. The Z-index had the best results in both the correlation and stepwise regression analyses. Not surprisingly, Red Spring wheat was particularly sensitive to growing season moisture conditions. In particular, yield was found to be most reliant on the moisture conditions in June. July was the second most important month for determining yield, and May was ranked as the least important. Antecedent moisture conditions were shown to only explain a very small amount of the variance in wheat yields.

A more detailed examination of the Z-index during the growing season revealed that considering the moisture conditions for the month of May did not increase the amount of variance in Red Spring wheat yields that were explained by just using moisture conditions for June and July. Therefore, the best index for measuring agricultural drought on the Canadian prairies is the June-July Z-index variable (Z67).

4.3 Diagnostic analysis

This section contains a more detailed discussion of the spatial and temporal patterns of variability associated with the relationship between the Z-index and Red Spring wheat yield. In the first part of this section the spatial patterns of drought index performance will be illustrated and explained. Then the relationship between actual and predicted yield will be analyzed for three representative crop districts (one crop district with a high R^2 value, one with an average R^2 value, and one with a low R^2 value). This will provide insight into the causes of temporal variations in model performance.

4.3.1 Spatial Analysis

The values of the coefficient of determination (R^2) for the best index of agricultural drought (Z67) and Red Spring wheat yield are mapped in Figure 4.5. The highest R^2 values tend to be found in the central and southern crop districts and lower R^2 values tend to be found in the northwestern and northeastern crop districts. A further examination of these patterns is important because it will help to illuminate the strengths and weaknesses of the Z-index.

The first step was to map the mean growing season precipitation and average yield for each crop district (Figures 4.6 and 4.7). The highest mean growing season precipitation totals are found in northwestern Alberta (those crop districts that are closest to the Rocky Mountains) and in central Manitoba. The lowest mean growing season precipitation totals are found in southern Alberta and Saskatchewan and those crop districts that are along the Alberta/Saskatchewan border. The region of the lowest average yields stretches across southern Saskatchewan and into southern Alberta. The region of highest average yields is in northwestern Alberta. Many of the crop districts in central Manitoba and western Alberta also have relatively high mean yields. A

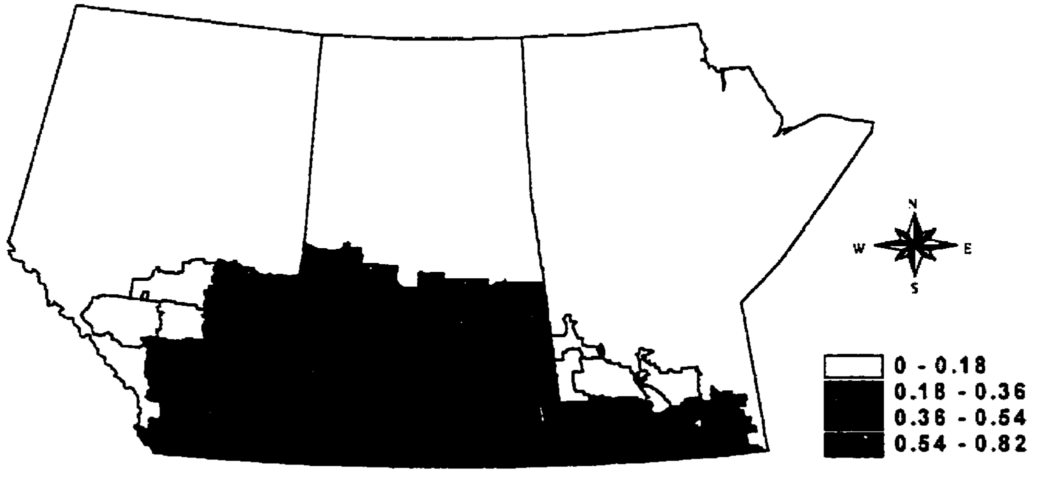

Figure 4.5 Coefficient of determination (R^2) values for the relationship between the best index of agricultural drought (Z67) and Red Spring wheat yield

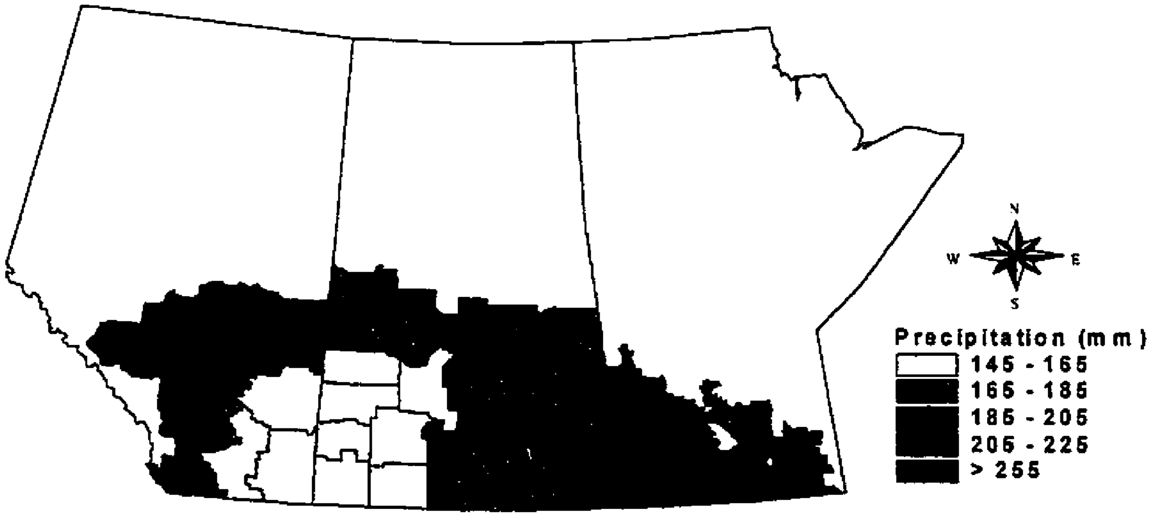

Figure 4.6 Mean growing season precipitation by crop district

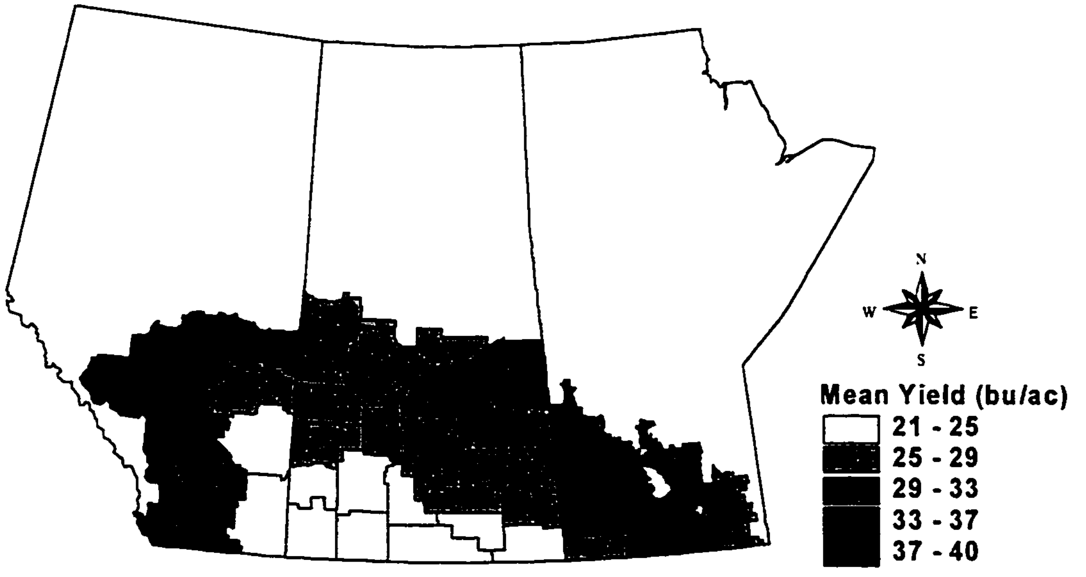

Figure 4.7 Mean Red Spring wheat yield by crop district

visual examination of Figures 4.5, 4.6, and 4.7 reveals similar spatial patterns. The areas of lower average yields and mean precipitation tend to be those where the agricultural drought index performs better. Conversely, the areas with higher yields and growing season precipitation tend to be those where the agricultural drought index performs poorly.

The spatial patterns of model performance were also analyzed by sorting the crop districts by a particular variable and then graphing the R^2 values. For example, to determine whether the mean growing season precipitation had an influence on the strength of the relationship between Red Spring wheat yield and Z67, all of the crop districts were ranked according to the mean growing season precipitation and then the R^2 values were plotted (Figure 4.8). The general trend indicates that as the mean growing season precipitation increases, the correlation coefficient decreases. The same trend is evident when the crop districts are ranked by the magnitude of the maximum and minimum precipitation events. These trends seem to indicate that Z67 is not as effective at modelling variations in yield in those crop districts that consistently receive relatively large amounts of moisture (i.e., moisture is no longer an important limiting-factor of yield).

Another way to examine the relationship between growing season precipitation and the spatial variability of model performance is by mapping the coefficient of variation (standard deviation/mean) for precipitation. This statistic provides a measure of the relative dispersion (variability) of the growing season precipitation between 1920-1999. The higher the coefficient of variation, the more variable the growing season precipitation is for a particular crop district (Figure 4.9). The spatial pattern of the coefficient of variation resembles that of the model performance shown in Figure 4.5. Many of the crop districts found to perform poorly, such as those in the northwestern portion of Alberta, have a relatively low coefficient of variation. Conversely, those crop districts that performed well, such as those in the central and southern

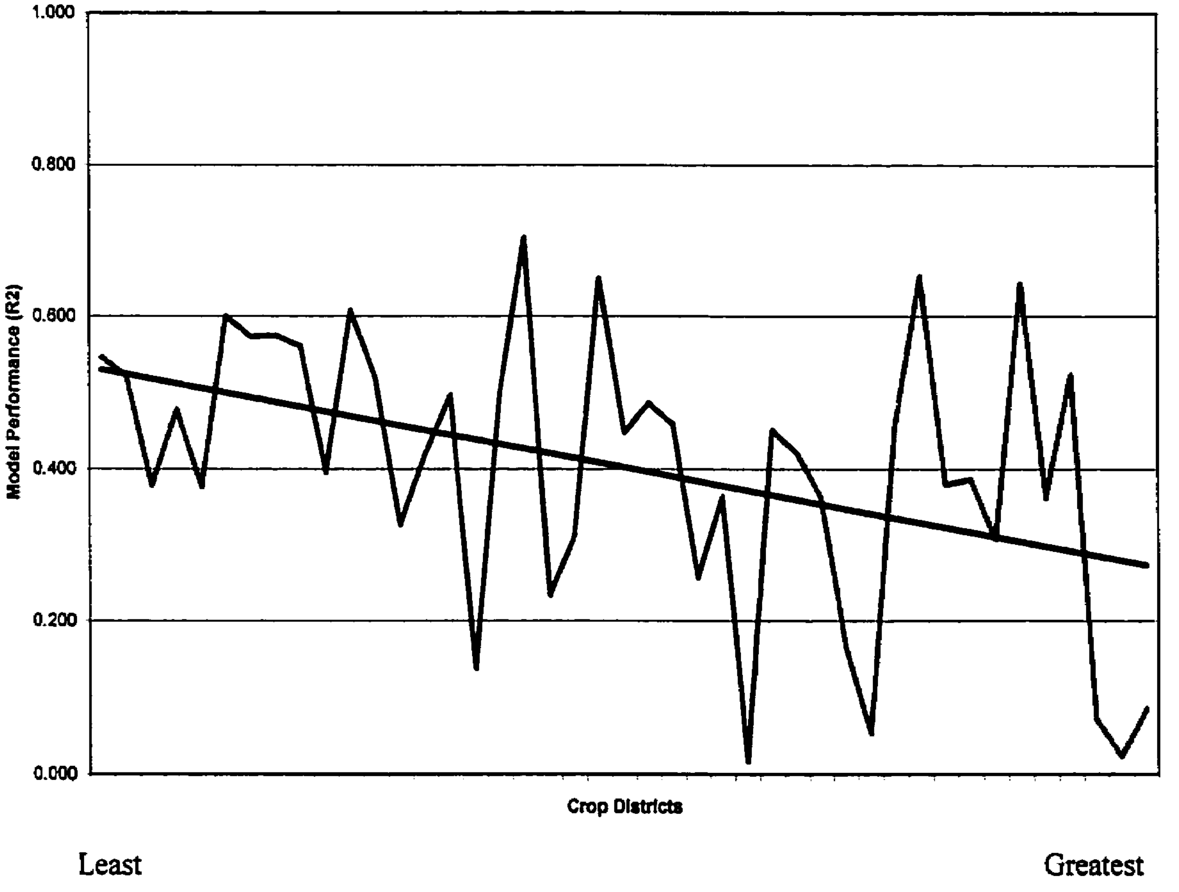

Figure 4.8 Model performance (R^2) for crop districts sorted by mean growing season precipitation from least to greatest

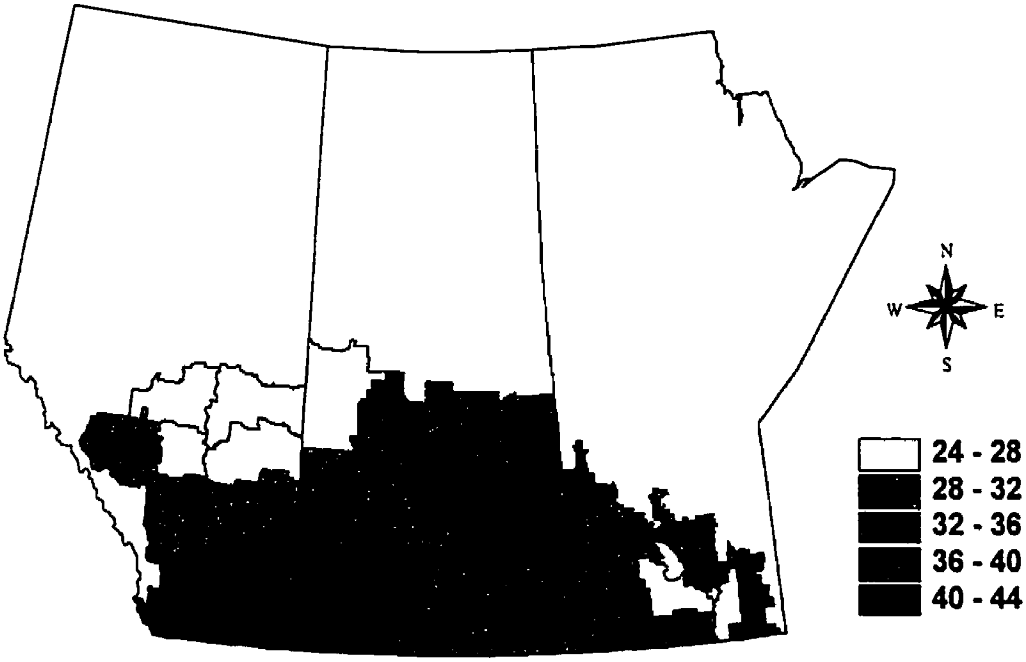

Figure 4.9 Coefficient of variation for growing season precipitation by crop district

areas of the study region, have a relatively high coefficient of variation. The one crop district that behaves somewhat erratically is the southwestern most crop district (AB3). Many of the climate stations that were used to calculate the daily precipitation values for this crop district are located in the foothills of the Rocky Mountains at elevations of greater than 1000 m. Some stations have elevations greater than 2000 m. The effect of being in such close proximity to the mountains is that the precipitation characteristics of this crop district do not fit the overall pattern that is present over the rest of the study region.

Generally, as mean precipitation increases, the coefficient of variation decreases. As the mean amount of growing season precipitation decreases, the link between Red Spring wheat yield and Z67 grows stronger because of the heightened importance of growing season moisture. Crop districts that receive higher amounts of growing season precipitation (and where precipitation is less variable) tend to have a weaker coupling between the Z-index and crop yield. Therefore, other factors that affect yield, such as length of the growing season, disease, insects, and soil fertility, may have increased importance in these crop districts.

Other relationships besides climate, like the available water content (AWC) of the soil, were also explored to see how they influenced model performance. A higher AWC value means that more moisture can be stored in the soil. Thus, it should be less drought prone. However, the crop districts with higher AWC values tend to be located in areas that receive small amounts of growing season precipitation and so there is not a statistically significant relationship between AWC and model performance (not shown).

Latitude explains approximately 20% of model performance (20% of the variance in the relationship between Red Spring wheat yield and Z67). As latitude increases, model performance tends to decrease (Figure 4.10). Latitude can be treated as a proxy variable for soil

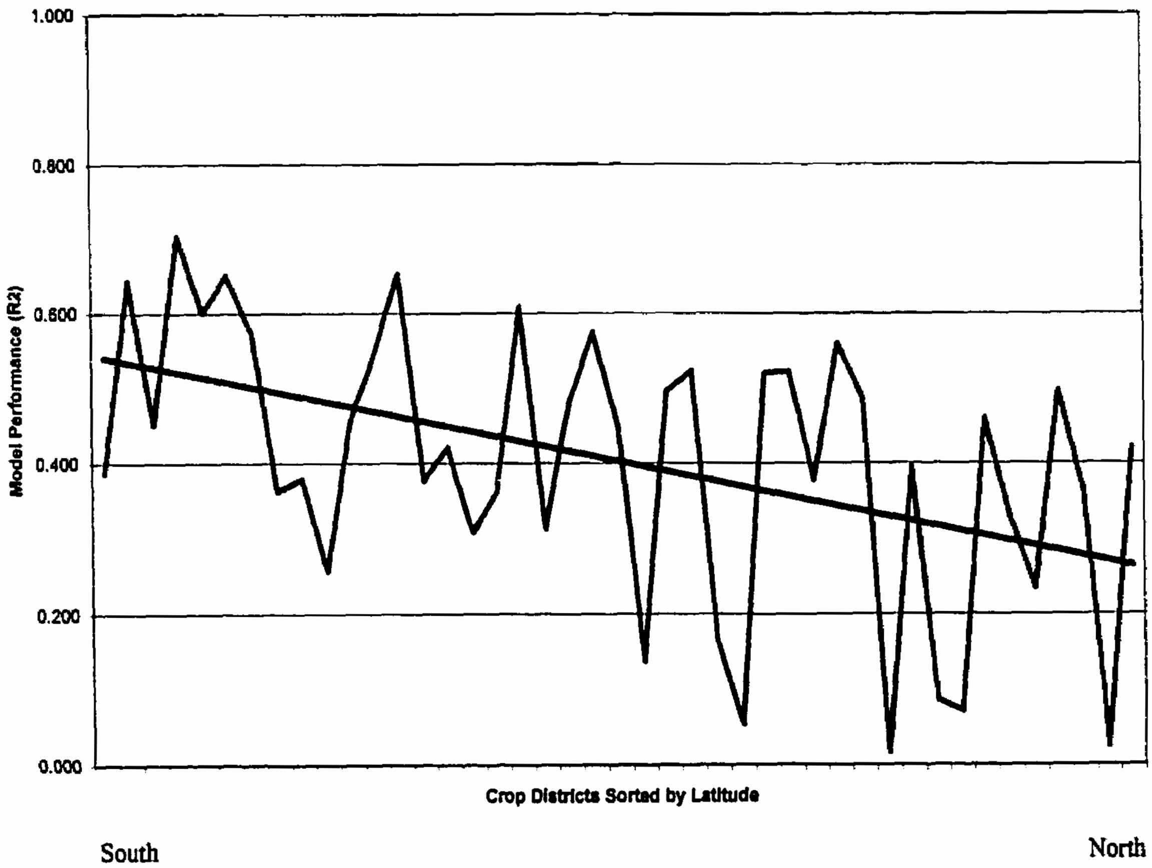

Figure 4.10 Model performance (R^2) for crop districts sorted by latitude from south to north

fertility, growing season length, and available heat since each of these factors has a strong north-south gradient in the study region. Southern crop districts tend to have more fertile soils, a longer growing season, and more available heat. These factors do not normally limit crop growth in the south, but certainly can be important in the more northerly crop districts.

Approximately 40% of the spatial variation in the relationship between Z67 and annual yield can be explained by considering mean precipitation and latitude. Both of these variables are inversely related to model performance. Therefore, the crop districts that tend to do the best are the ones that have a more southerly location and a low maximum growing season precipitation value. It is not entirely surprising that these variables are influential in determining model performance, but because precipitation, environmental conditions, and yield are all, to some degree, interrelated caution should be used when interpreting their relationships to each other and to model performance. Crops cannot grow without precipitation and as the variability of the precipitation regime increases, yield variability also tends to increase. While latitude can be treated as a proxy variable for the north-south gradient in soil conditions, growing season length, and heat, there is also a north-south component in the pattern of precipitation. The crop yield models could be improved if additional data sets were available that measured some of the other important factors that affect crop yield such as insects, extreme meteorological events (hail, wind, frost), and disease.

4.3.2 Temporal analysis

It is also important to examine the relationship between actual and predicted yield over the entire time series because this will help to illuminate the strengths and weaknesses of the Z-index. Three representative crop districts have been selected for further analysis. Crop district SK3as was selected because there is a strong relationship between yield and Z67 in this crop district and the R^2 value is 0.704 (Figure 4.11). Crop district AB11 was selected for analysis because there is a very poor relationship between Red Spring wheat yield and Z67 in this crop district and the R^2 value is only 0.024 (Figure 4.12). MB2 was the third crop district chosen because it represents an average relationship between yield and Z67 with an R^2 value of 0.459 (Figure 4.13). In addition to plotting the actual versus predicted yield departures (from the mean) for three crop districts, a select number of years will be analyzed to assess why the model performed well in some years and poorly in others.

4.3.2.1 Temporal analysis of SK3as

Figure 4.11 shows the relationship between actual and predicted yield for crop district SK3as. There is a good agreement between the predicted and actual yield departures for most years. In particular, there is very close agreement between the model and the actual values during 1962, 1969, 1974, 1975, 1981, and 1997. There are also a number of years when there is poor agreement between the predicted and actual values such as 1977, 1985, and 1994.

In SK3as, there was a large difference between the actual and predicted yield for 1977. The predicted yield departure was -1.58 (bu/ac) and the actual yield departure was 7.17 (bu/ac). Figure 4.14 displays the daily maximum temperature and precipitation for the May to August period in 1977 and Figure 4.15 shows the Z-index values for January to August. According to these figures, May and July were both wetter than normal months while June was drier than normal. The reasons for the discrepancy between the actual yield and those predicted by the model might be attributable to the wet conditions in May that provided ample soil moisture for the crop to germinate and grow. Rains that fell during the middle of June, coupled with a few weeks of lower June temperatures may have allowed the crops to make it through the month

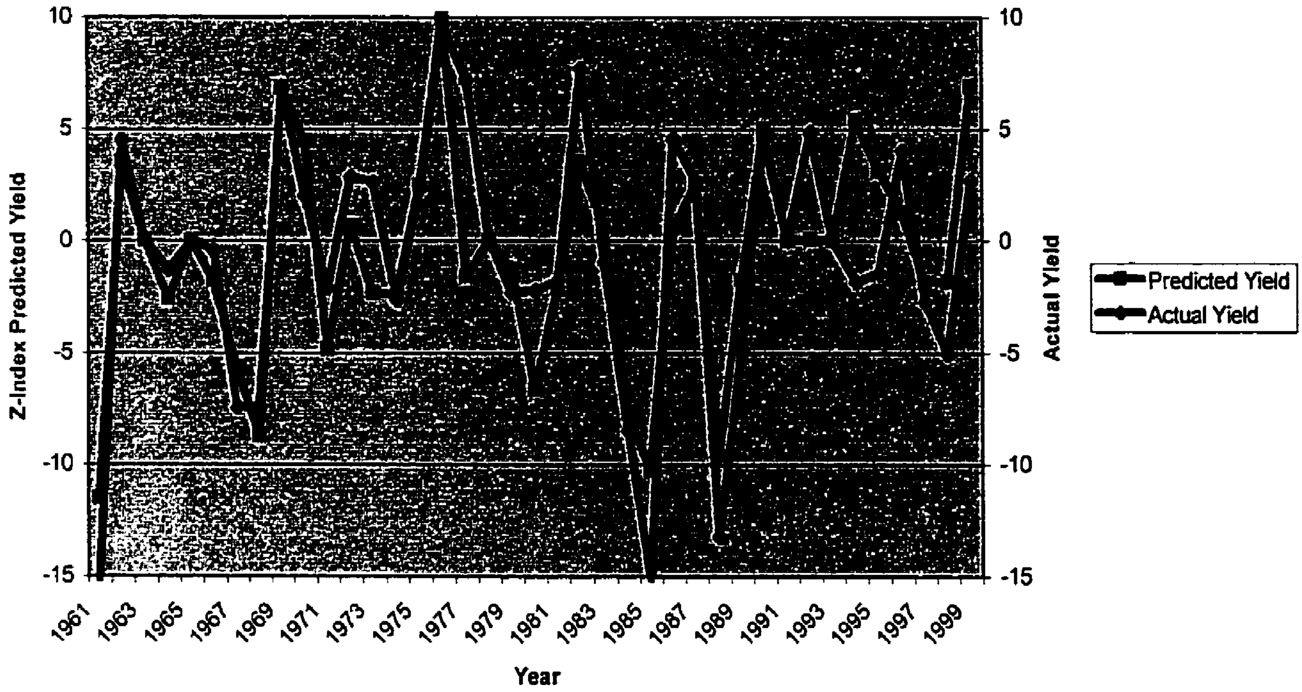

Figure 4.11 Actual versus predicted yield departures for crop district SK3as based on a linear regression model using Z67

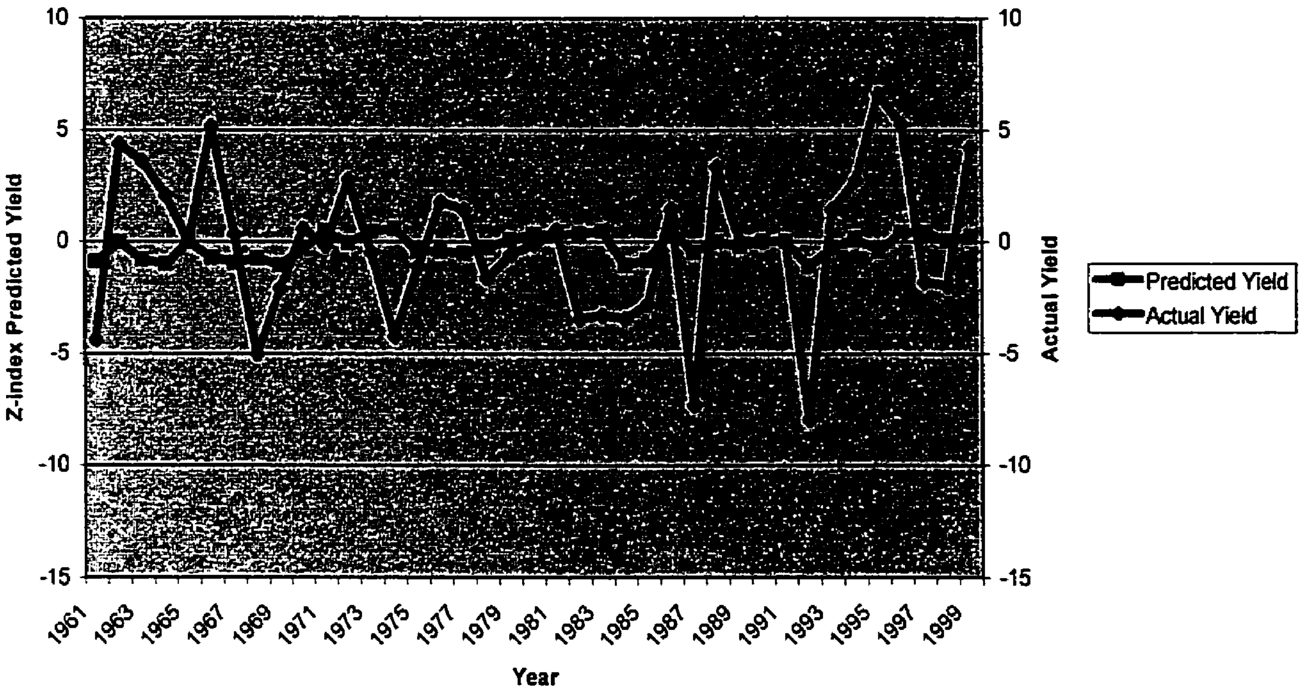

Figure 4.12 Actual versus predicted yield departures for crop district AB11 based on a linear regression model using Z67

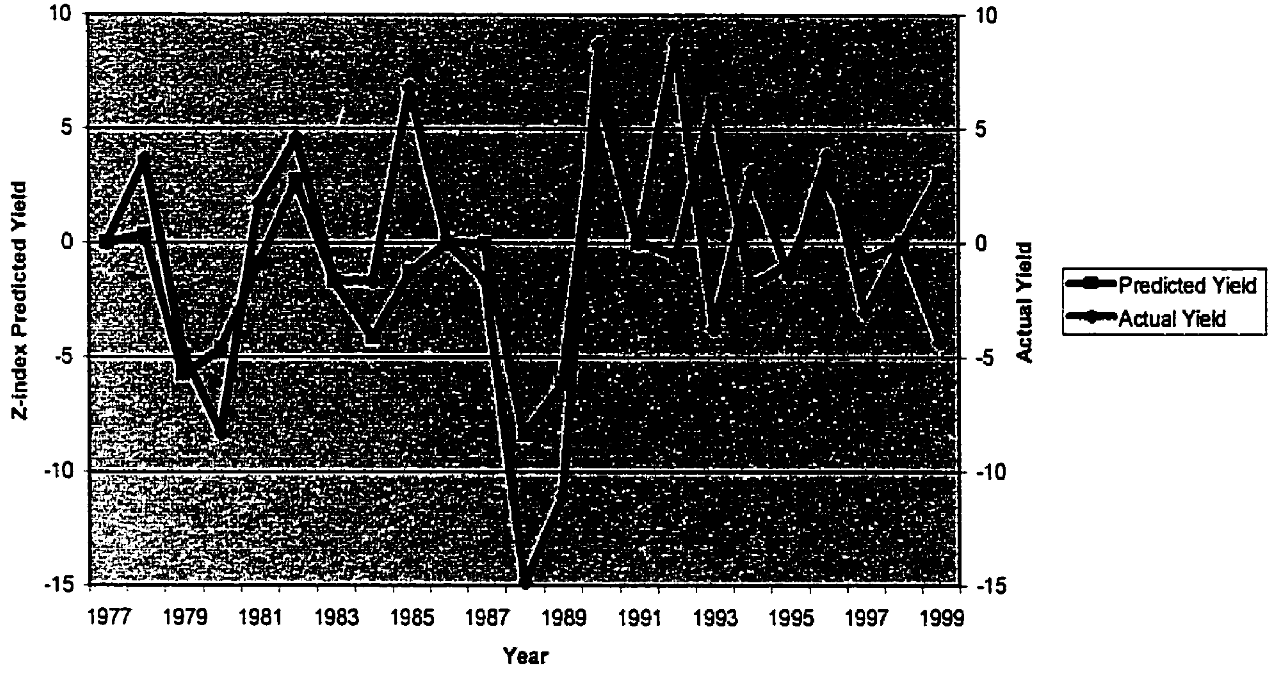

Figure 4.13 Actual versus predicted yield departures for crop district MB2 based on a linear regression model using Z67

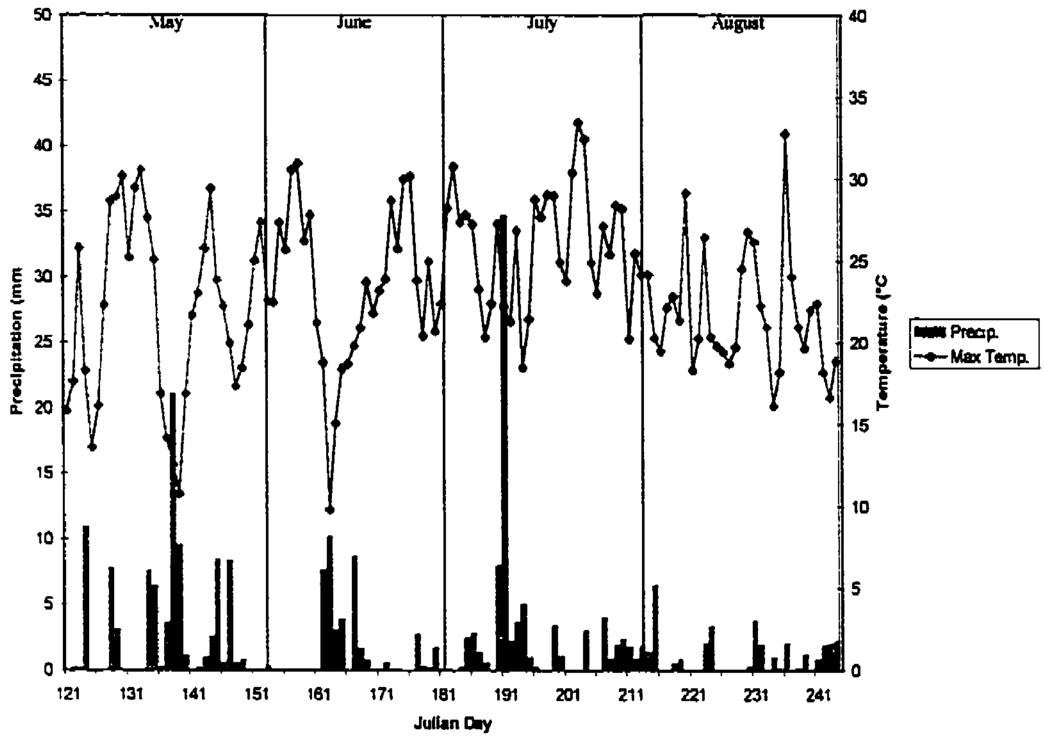

Figure 4.14 Daily maximum temperature and precipitation for crop district SK3as: May 1 to August 31, 1977

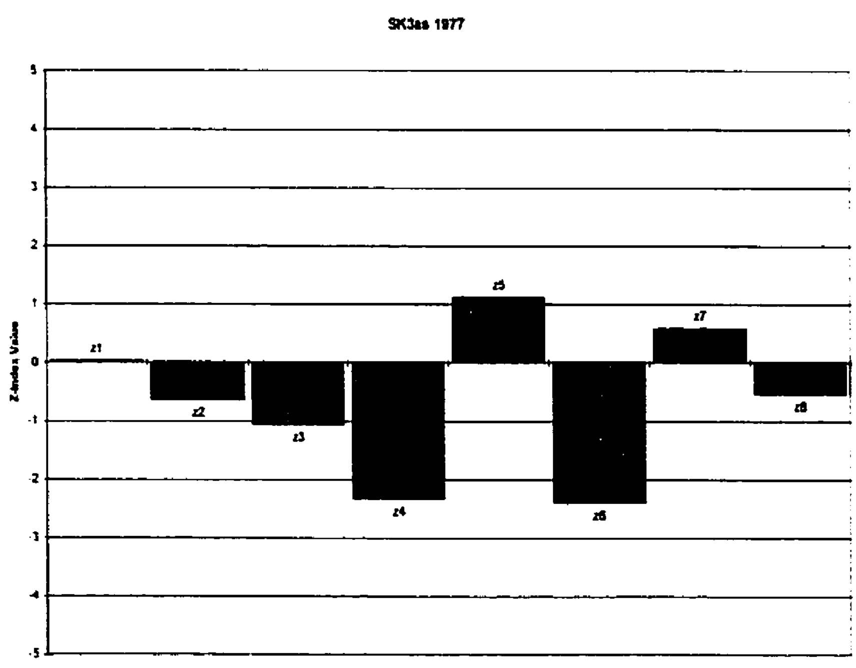

Figure 4.15 Monthly Z-index values for crop district SK3as: January to August, 1977

without experiencing too much stress. The slightly wetter than normal conditions in July probably helped to make up for the June conditions. The June-July Z-index (Z67) value was -1.82 and because of the difference between June and July, this does not really accurately reflect the growing season conditions. In addition, a slightly drier than normal August insured that harvest could take place without difficulty or significant loss of yield. Even given these considerations, yields should only be slightly better than normal. Therefore, factors other than moisture stress (e.g., lower than normal pestilence or disease) must be responsible for the high yields in this year.

Yields were also not well predicted in 1985. Actual yield departures were -15.2 (bu/ac) and the model only predicted the yield departures to be -10.2 (bu/ac). Figure 4.16 shows the daily maximum temperature and precipitation for the May to August period in 1985 and Figure 4.17 shows the Z-index values for January to August. Severe drought conditions are present during both June and July. The June-July Z-index (Z67) value is -6.63. The reason for the discrepancy between the actual yield and those predicted by the model may be attributed to the fact that the model routinely underpredicts the impact of severe drought years (e.g., 1961, 1985, and 1988). Although the model seems to be able to accurately predict large positive yield departures, it does not fare well with the large negative yield departures. Perhaps if there was a longer period of record that included more severe drought years, the model would have done better at accounting for the effects of severe drought. It is also possible that the response of yield to moisture conditions may not be linear below a certain threshold.

The third year in which there is a large difference between the actual and predicted yield in SK3as is 1994. The predicted yield departure was 5.39 (bu/ac) and the actual yield departure was -1.82 (bu/ac). The daily maximum temperature and precipitation for the May to August period for 1994 are presented in Figure 4.18 and the Z-index values for January to August are presented

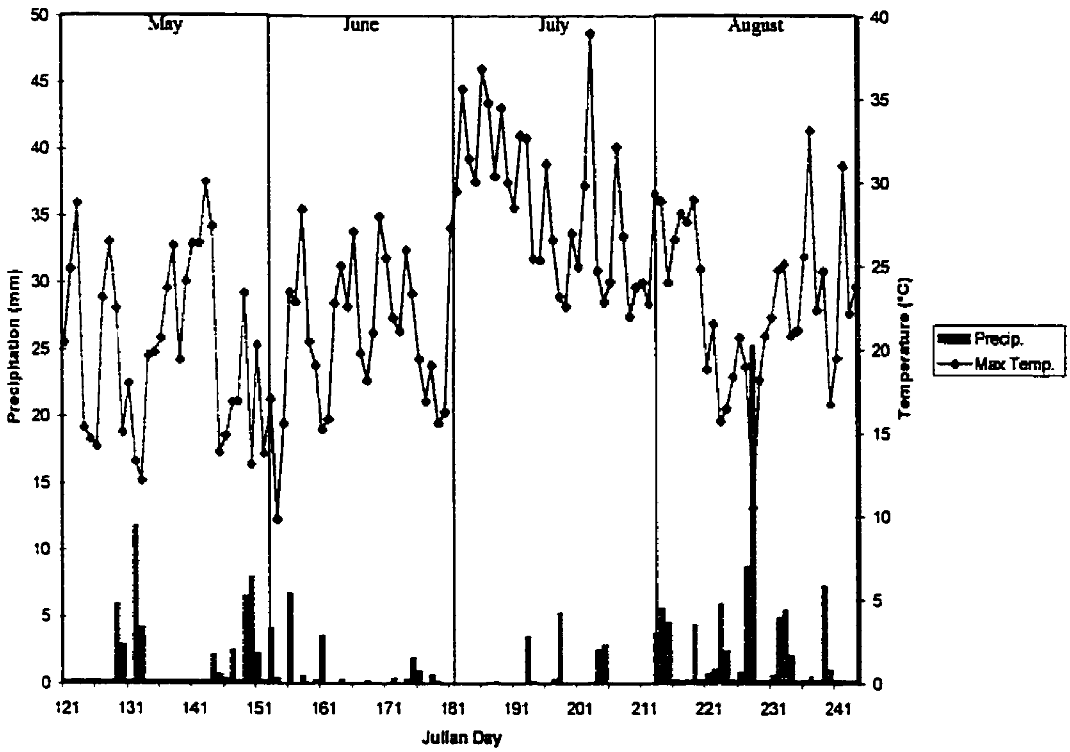

Figure 4.16 Daily maximum temperature and precipitation for crop district SK3as: May 1 to August 31, 1985

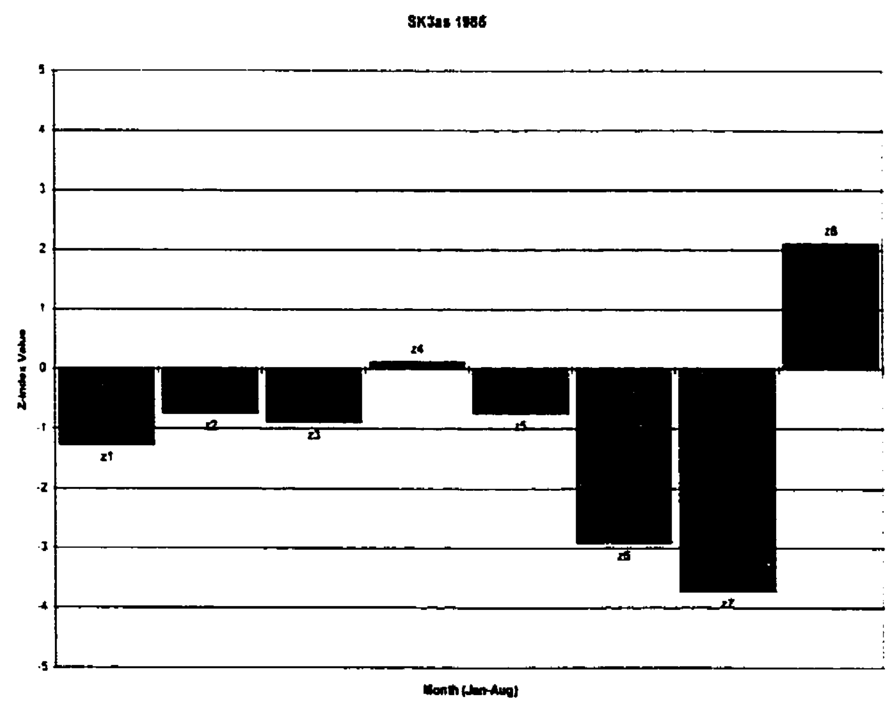

Figure 4.17 Monthly Z-index values for crop district SK3as: January to August, 1985

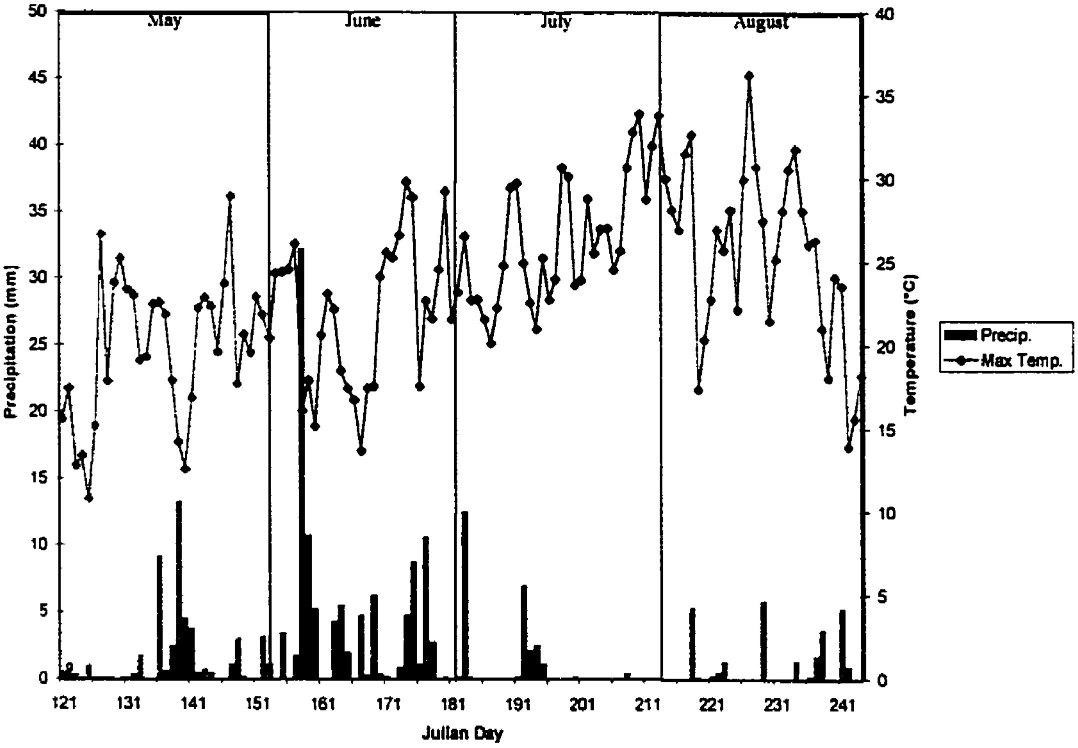

Figure 4.18 Daily maximum temperature and precipitation for crop district SK3as: May 1 to August 31, 1994

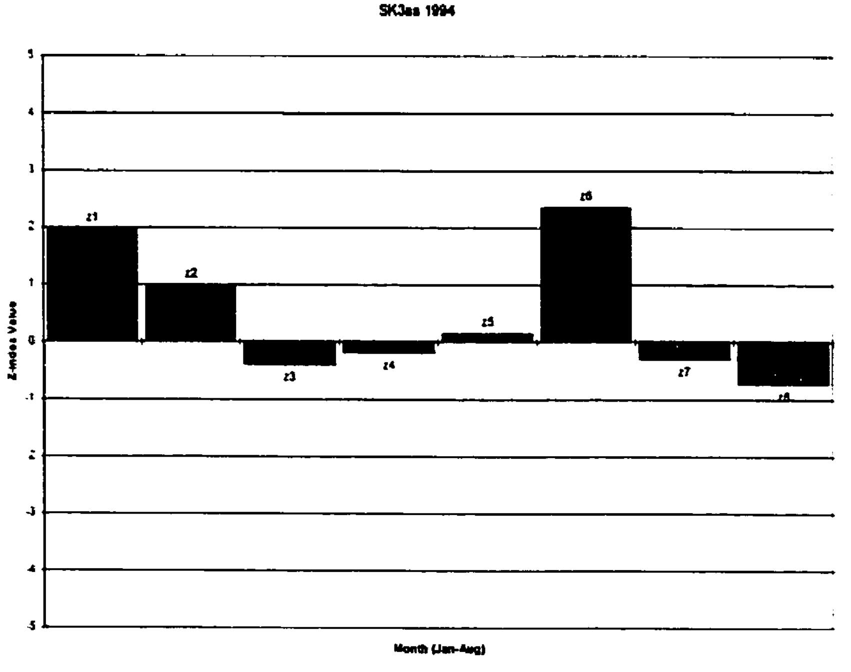

Figure 4.19 Monthly Z-index values for crop district SK3as: January to August, 1994

in Figure 4.19. The month of June was significantly wetter than normal and July was slightly drier than normal. The June-July Z-index (Z67) value was 2.04 and this is mainly due to the wet conditions in June. The difference between actual and predicted yield is likely caused by the July conditions. From Figure 4.18 it is evident that very little rain fell after July 2 and there were also very few precipitation days. The July Z-index value should really be much lower to accurately reflect the moisture stress that was experienced by the crop. The wetter than normal June conditions would not have provided the crop with enough moisture to sustain it until harvest or to produce above normal yields.

There were many years in SK3as when there was good agreement between actual and expected yield; one example is 1990. The predicted yield departure was 4.99 (bu/ac) and the actual yield departure was 4.61 (bu/ac). The daily maximum temperature and precipitation for the May to August period for 1990 are presented in Figure 4.20 and the Z-index values for January to August are presented in Figure 4.21. June was only slightly drier than normal and July was significantly wetter than normal and as a result the June-July Z-index (Z67) value was 1.82. The close agreement between actual and predicted yield is likely due to the relatively normal conditions in May and June followed by wet conditions in July. Precipitation during the entire growing period is fairly consistent and has no big gaps. There is a good mixture of several large precipitation events and many smaller events. The first part of August is warm and dry which promotes rapid ripening of the crop.

4.3.2.2 Temporal analysis of AB11

Figure 4.12 shows the relationship between actual and predicted yield for crop district AB11. It is rather obvious from this graph that there is little or no relationship between yield and

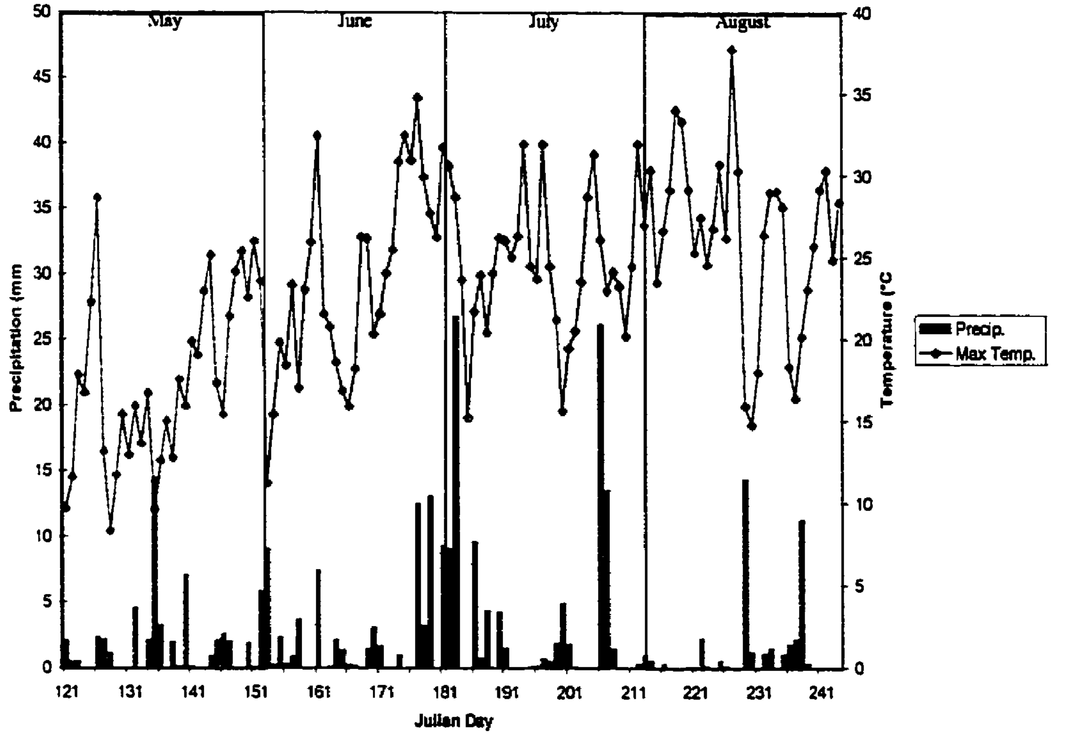

Figure 4.20 Daily maximum temperature and precipitation for crop district SK3as: May 1 to August 31, 1990

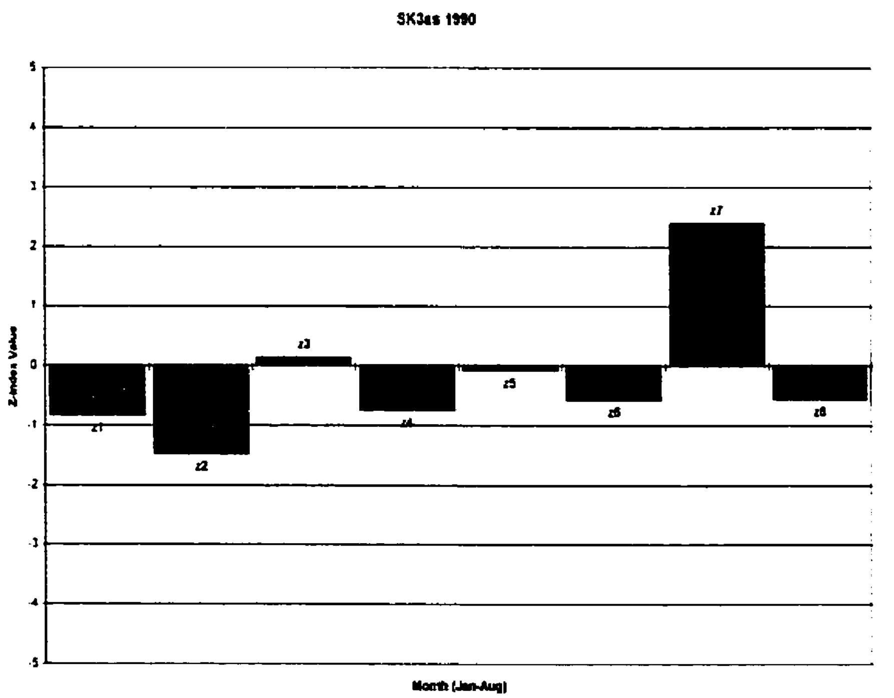

Figure 4.21 Monthly Z-index values for crop district SK3as: January to August, 1990

Z67. This graph was included because it provides a good contrast to SK3as. In addition, it serves to illustrate that there is a great deal of variability in model performance across the prairies. A detailed analysis of individual years was not carried out for this crop district because the R^2 value between yield and the June-July Z-index value was nearly zero. Instead, this section will contain a general discussion of some of the reasons why crop predictions are so problematic in this crop district (and others in Alberta).

One reason for the poor performance of the Z-index in the northwestern portion of Alberta is due to the relatively high mean growing-season precipitation. As was discussed in Section 4.3.1, crop districts that receive higher amounts of growing season precipitation tend to have a weaker coupling between the Z-index and crop yield. Therefore, other factors that affect yield such as length of the growing season, disease, insects, and soil fertility may have increased importance in these crop districts. In addition, some of the poor model performance in this crop district in particular, and in Alberta in general, may be attributable to the change in crop district boundaries and the resulting adjustment in yield values for the crop districts. Yield values in Alberta were actually measured for much larger regions and then applied to a number of smaller regions imbedded within their boundaries. Obviously, this may negatively affect the relationship between crop yield and the Z-index for some crop districts in Alberta if the crop yields are not homogenous across the larger regions.

Irrigation also could affect the model performance. Irrigation is more extensively used in Alberta than any other prairie province (Table 4.12). However, the majority of Alberta irrigation occurs west of Calgary and around Lethbridge and Medicine Hat and so is probably not an important factor in this particular crop district. It may affect the accuracy of the models in other Alberta crop districts. It should also be noted that irrigation is normally only used for specialty (e.g, potatoes) and high-value cash crops and not cereal crops such as wheat.

Table 4.12 Irrigated area by province from 1996 Census and provincial data

PROVINCE	CENSUS (ha)	PROV. DATA (ha)	DIFFERENCE (ha)
AB	516,600	473,168	43,432
SK	97,378	130,348	32,970
MB	22,190	26,600	4,410
TOTAL	**636,168**	**630,116**	

Source: MB: Gaia Consulting (1997); SK: Sask Water (1997); AB: AAFRD (1999)

Model performance could also be affected by the quality of the climate data that is being used to calculate the Z-index value. The quality of the temperature and precipitation data is determined by the number of climate stations that are available at any given period of time. The more stations used, the better the quality of the data is likely to be. It is also important that the stations be spread as uniformly as possible over the crop district. Problems could arise if the majority of climate stations are all from one part of the crop district and the Red Spring wheat is being grown in a different part of the crop district. Obviously, this consideration is not unique to this crop district.

4.3.2.3 Temporal analysis of MB2

Figure 4.13 shows the relationship between actual and predicted yield for crop district MB2. MB2 is an example of a crop district where the relationship between Z67 and yield is of average strength (close to the overall mean). From the graph it is evident that there is generally a fair amount of agreement between the actual and predicted yield departures. The years where there is the least difference between predicted and actual yield are 1979, 1983, 1995, and 1996. The model performs poorly in a number of years, particularly in 1985, 1988, 1992, 1993, and

1999.

There is a fairly large discrepancy between the actual and predicted yield in MB2 during 1985. The predicted yield departure was -1.28 (bu/ac) and the actual yield departure was 6.77 (bu/ac). The daily maximum temperature and precipitation for the May to August period for 1985 are presented in Figure 4.22 and the Z-index values for January to August are presented in Figure 4.23. June was slightly wetter than normal and July was significantly drier than normal and as a result the June-July Z-index (Z67) value was -1.46. The difference between actual and predicted yield in this crop district is difficult to explain. Obviously the moisture conditions are more than adequate for crop growth through the end of June. However, during the month of July there is very little total precipitation and very few precipitation days (events). This lack of rain during a critical growth stage should have caused yields to be lower than normal. Part of the discrepancy between actual and predicted yield may be explained by the heavy rains that occurred at the beginning of August. It is possible that these rains may have helped the crops to recover from the moisture stress experienced in July. The August rains would be particularly important if planting had occurred later than normal in 1985. If planting had occurred close to the end of May, the crop would not have reached maturity until the end of August. Therefore, the rains that fell in June would have insured that the crop got well established. The dry hot weather in July would have speeded the growth of the crops and the rain at the beginning of August would then have come just as the crops were filling out. Since date of planting data is not readily available to the author, this is merely speculation. It is also possible that factors other than weather may be responsible.

Model performance during 1988 was also problematic. The predicted yield departure was -8.36 (bu/ac) while the actual yield departure was -14.8 (bu/ac). The daily maximum temperature

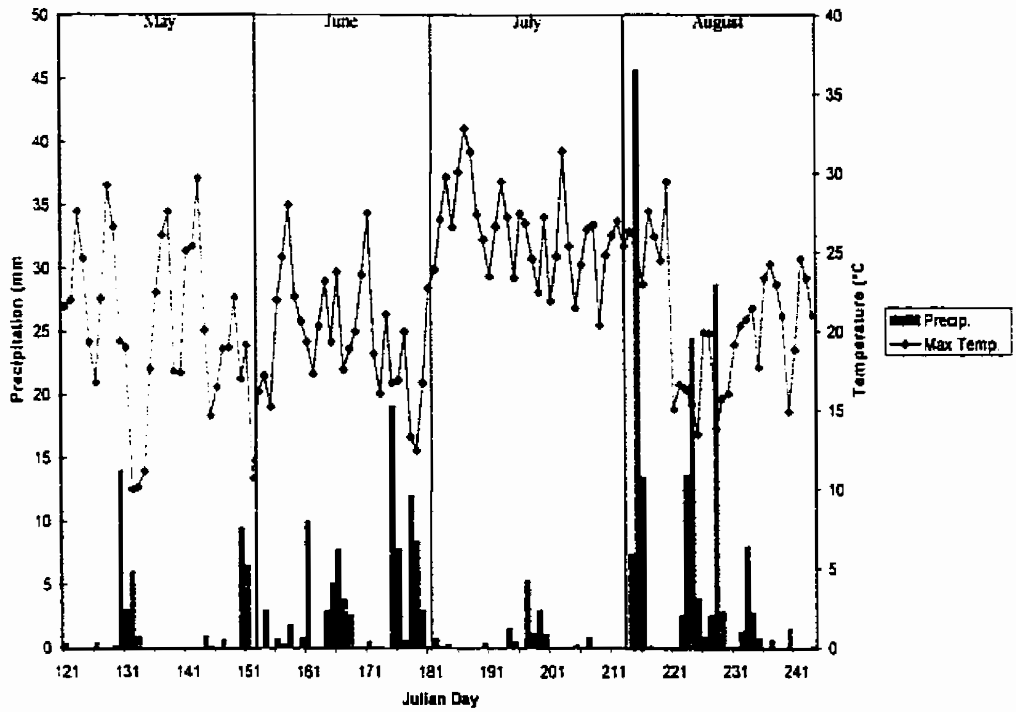

Figure 4.22 Daily maximum temperature and precipitation for crop district MB2: May 1 to August 31, 1985

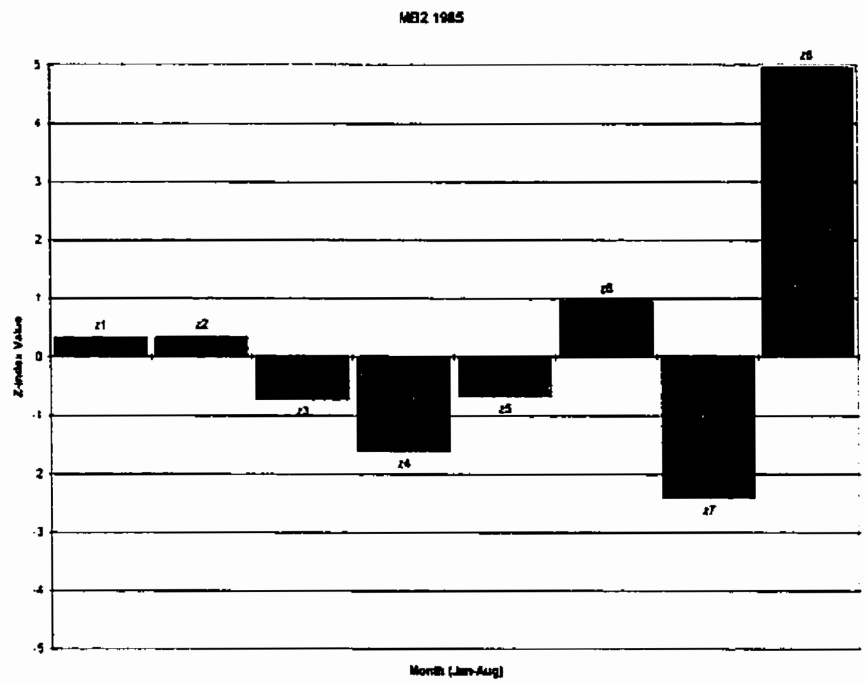

Figure 4.23 Monthly Z-index values for crop district MB2: January to August, 1985

and precipitation for the May to August period for 1988 are presented in Figure 4.24 and the Z-index values for January to August are presented in Figure 4.25. Every month of the year was moderately to severely dry and this drought peaked in intensity in June with a Z-index value of nearly -5. The June-July Z-index (Z67) value was -5.74. The difference between actual and predicted yield for 1988 is due to severe underprediction by the model. As was previously mentioned, the model does not seem to be able to accurately predict the large negative yield departures.

A third example of a year when there is a large difference between the actual and predicted yield in MB2 is 1993. The predicted yield departure was 6.19 (bu/ac) and the actual yield departure was -3.74 (bu/ac). The daily maximum temperature and precipitation for the May to August period for 1993 are presented in Figure 4.26 and the Z-index values for January to August are presented in Figure 4.27. The month of June was slightly wetter than normal and July was significantly wetter than normal. As a result, the June-July Z-index (Z67) value was 3.06. The difference between actual and predicted yield is likely caused by the extremely cool and wet July conditions. Along with a large amount of rain, there were also a large number of precipitation days. In fact, some amount of rain fell almost every day in July. The growing conditions in June should have been conducive to producing a healthy crop. However, in July persistent rains and below normal temperatures likely limited crop growth. The cool wet conditions persisted into August and this probably delayed maturity and reduced yield.

The model also performed quite well during many years in MB2 and 1996 is one example. The predicted yield departure was 2.85 (bu/ac) and the actual yield departure was 3.83 (bu/ac). The daily maximum temperature and precipitation for the May to August period for 1996 are presented in Figure 4.28 and the Z-index values for January to August are presented in Figure

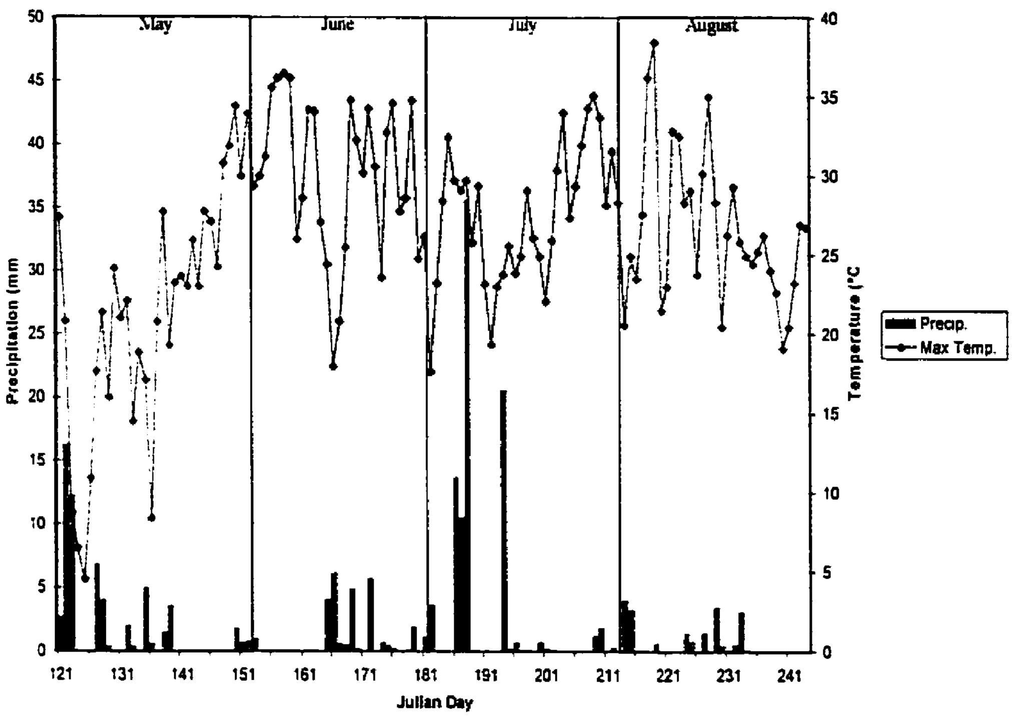

Figure 4.24 Daily maximum temperature and precipitation for crop district MB2: May 1 to August 31, 1988

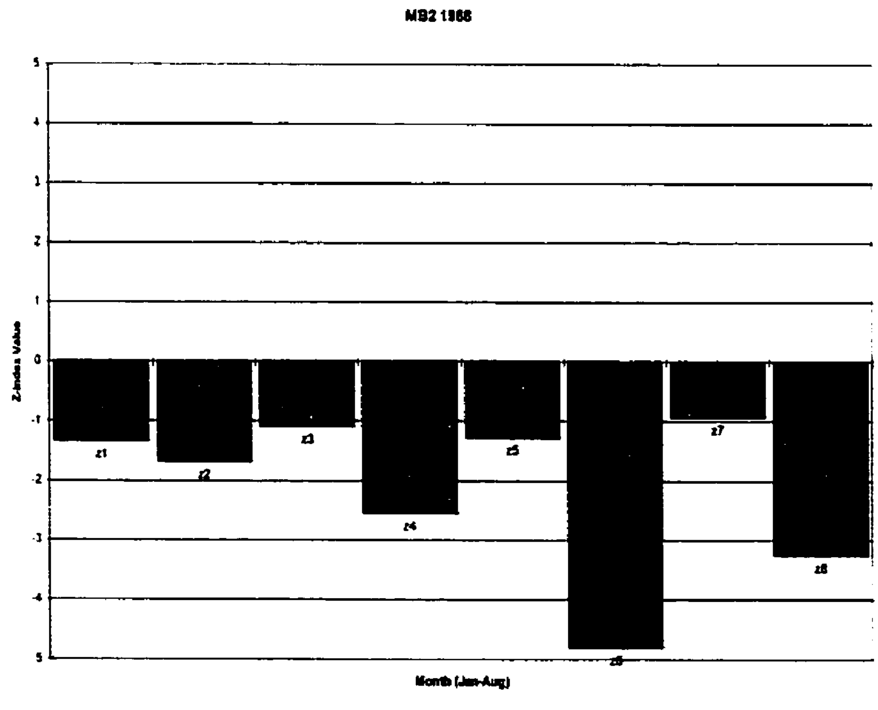

Figure 4.25 Monthly Z-index values for crop district MB2: January to August, 1988

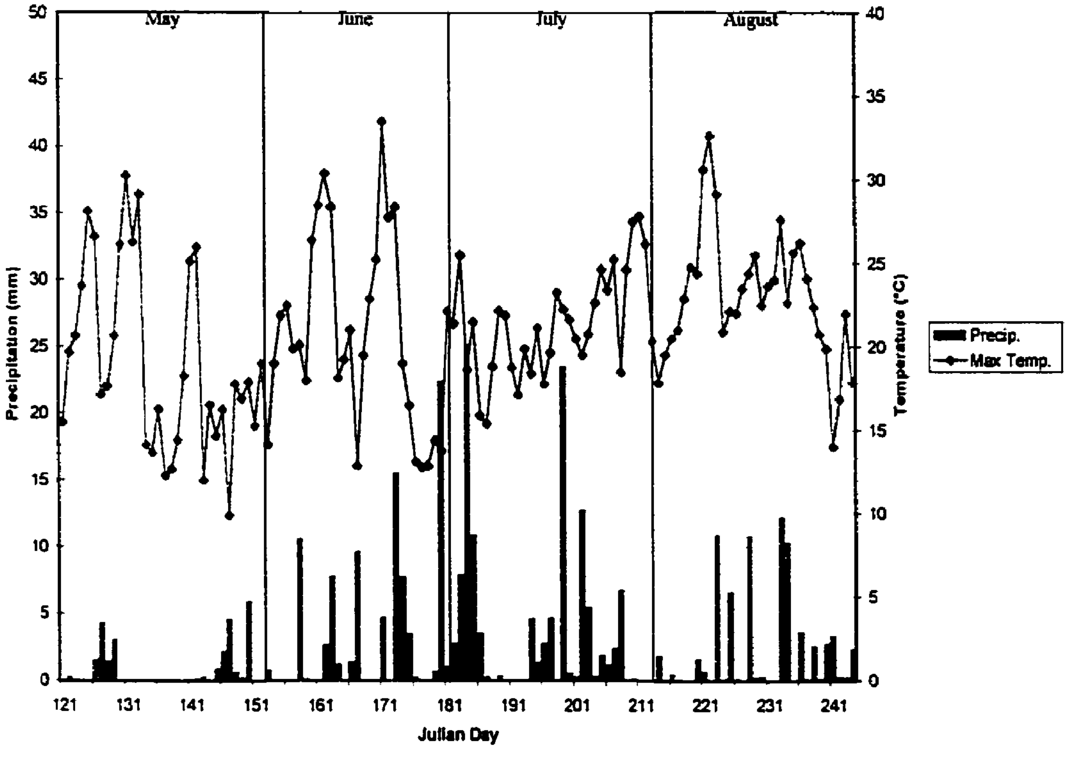

Figure 4.26 Daily maximum temperature and precipitation for crop district MB2: May 1 to August 31, 1993

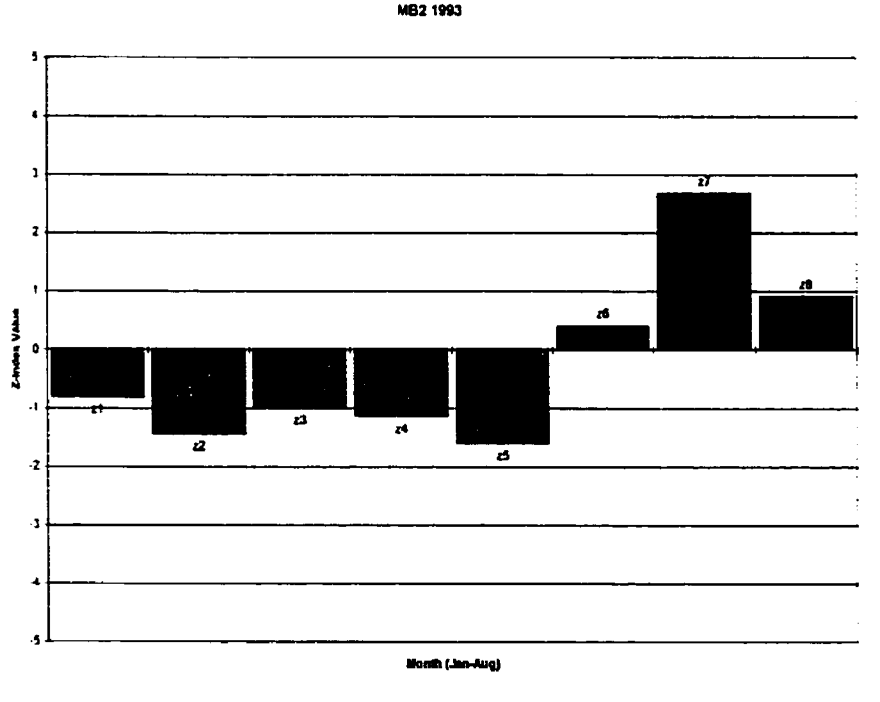

Figure 4.27 Monthly Z-index values for crop district MB2: January to August, 1993

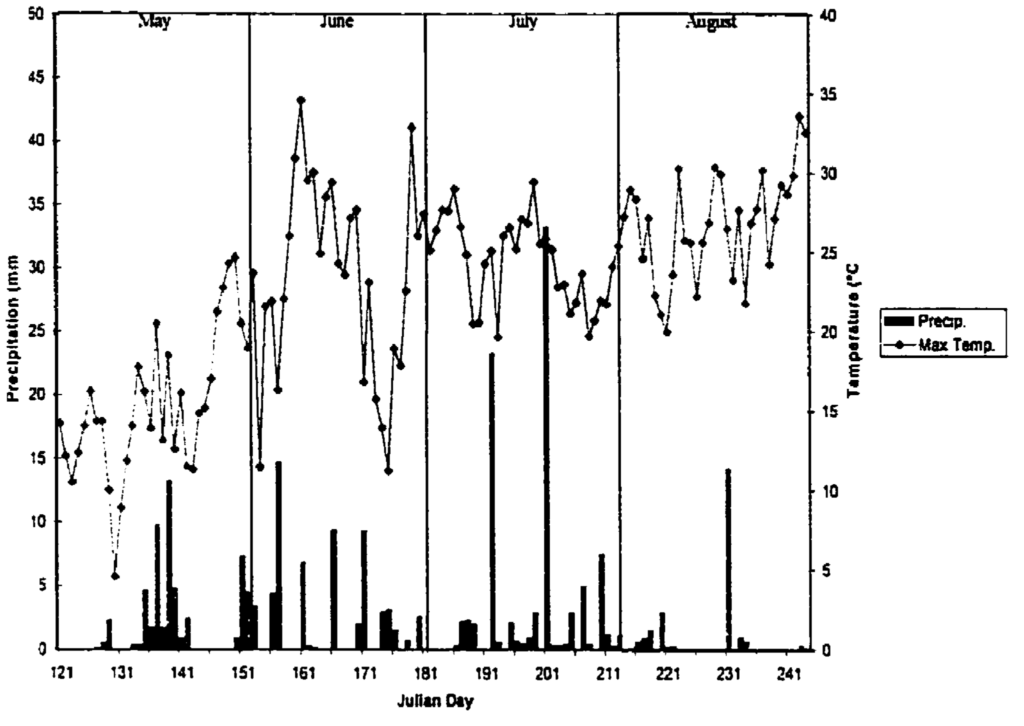

Figure 4.28 Daily maximum temperature and precipitation for crop district MB2: May 1 to August 31, 1996

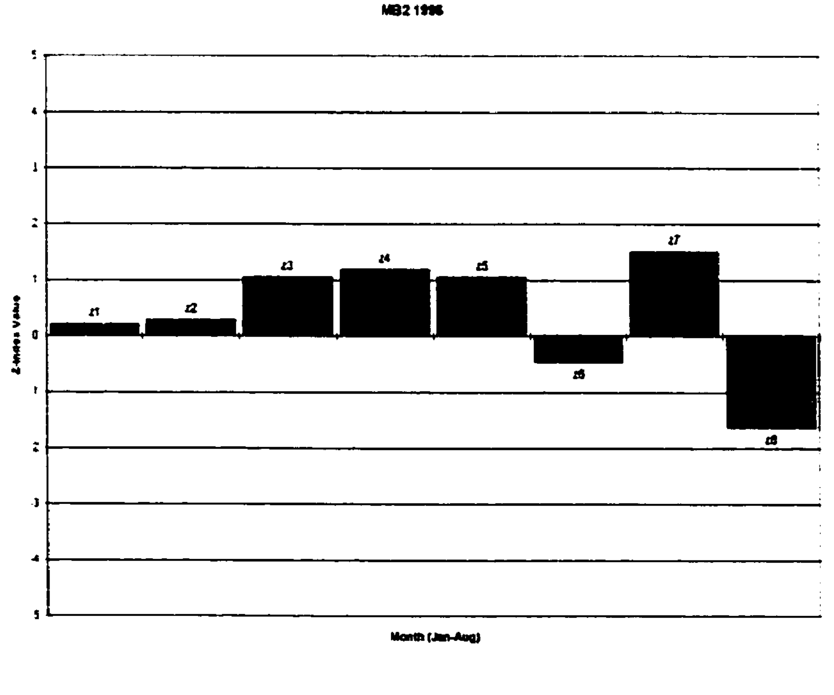

Figure 4.29 Monthly Z-index values for crop district MB2: January to August, 1996

4.29. June was only slightly drier than normal and July was moderately wetter than normal and as a result the June-July Z-index (Z67) value was 1.04. The close agreement between actual and predicted yield is likely due to the relatively normal conditions in June followed by slightly wet conditions in July. Precipitation during the entire growing season is relatively consistent. Two large precipitation events in July cause it to be a wetter than normal month. The warm, dry conditions in August are ideally suited for having the crop mature and be harvested with out any problems.

Overall, it is likely that the performance of the model would be better in all Manitoba crop districts if crop yield data was available for the same the length of time as Saskatchewan and Alberta.

4.3.2.4 Summary of temporal analysis

Many of the years where the model performs poorly can be attributed to an unequal distribution of precipitation. In some cases several large events will skew the precipitation totals. Poor model performance is also associated with years with large gaps when no precipitation falls (particularly at the end June and the beginning of July). The timing of precipitation and its distribution (and intensity) throughout the growing season is just as critical, if not more critical, than the total amount of growing season precipitation. Also, large changes between June and July (dry June, wet July, and vice versa) can cause the model to perform poorly since the net effect produces a Z-index variable that is near zero.

The moisture conditions during the months of May and August also play a role in determining how accurately the model can predict Red Spring wheat yield. Extremely large or small amounts of May precipitation can cause yields to be lower than would otherwise be expected. August moisture conditions tend to be inversely correlated with yield since rain that falls at this point of the growing season does not significantly contribute to yield. Extremely large amounts of August precipitation can significantly decrease yield by delaying the harvest, causing crops to lodge, and causing grain that has been swathed to sprout, thus lowering the quality of yield.

Model error may result from having an insufficient number of climate stations to produce a reliable spatial average of temperature and precipitation, or an unequal spatial distribution of where crops are grown within a crop district. Perhaps with a longer period of record with more severe drought years the model would do better at accounting for severe drought. It is also possible that the response of yield to moisture conditions is not linear below a certain threshold.

The single most important factor that is not accounted for by the Z-index is the timing of precipitation events and the distribution of precipitation during the growing season. It is likely that the amount of variance that is explained in Red Spring wheat yields could be significantly increased if this index was calculated on a weekly basis and if it was weighted so that those weeks when the crop requires the most water receive special weighting.

4.4 Chapter summary

The intent of this study was not to create a new drought index, or even to make significant modifications to existing indices. The first objective is to evaluate a selection of drought indices that are readily available and that have been adopted by a wide range of users to determine which is the most appropriate for agricultural application on the Canadian prairies.

The Moisture Anomaly Index (Z) was determined to be the 'best' index for measuring agricultural drought. The Z-index performed better than the other three drought indices in both the growing season drought correlation analysis and the stepwise regression analysis. The results showed that the SPI is also useful for measuring agricultural drought on the Canadian prairies. The Z-index is based on Palmer's calculation of the monthly water budget. The parameters for the moisture budget (e.g., ET, PET, RO, and S) are calculated from the temperature and precipitation for the current month. This month is then compared to the climatically appropriate or normal conditions for that month. A value is assigned to each month based on whether it is wetter or drier than normal. The larger or smaller the value, the more extreme the month.

Not surprisingly, Red Spring wheat was determined to be sensitive to growing season moisture conditions. In particular, yield was found to be most reliant on the moisture conditions in June. July was the second most important month for determining yield, and May was ranked as the least important. Antecedent moisture conditions were shown to only explain a very small amount of the variance in wheat yields. A more detailed examination of the Z-index during the growing season revealed that considering the moisture conditions for the month of May did not increase the amount of variance in Red Spring wheat yields explained by just using moisture conditions for June and July. Therefore, the best index for measuring agricultural drought on the Canadian prairies is the June-July Z-index variable (Z67).

There is a great deal of spatial variability across the prairies in the strength of the relationship between Red Spring wheat yield and Z67. This index may not be suitable for use in all crop districts, particularly those in northwestern Alberta (CDs 8, 9, 11) and in the northern portion of the grain growing region in Manitoba (CDs 5, 11). Almost half of the variation in model performance can be attributed to variations in mean precipitation and latitude. Both of these variables are inversely related to model performance. Therefore, crop districts with a more southerly location and lower growing season precipitation tended to perform the best. The crop yield models could be improved if additional data sets were available that measured some of the other important factors that affect crop yield, such as insects, extreme meteorological events (hail, wind, frost), and disease.

There is also considerable temporal variability in model performance in most crop districts. Many of the years where the model performs poorly can be attributed to an unequal distribution of precipitation. The timing of precipitation and its distribution in the growing season is extremely critical to crop yield. Large variations between June and July Z-index values can also cause the model to perform poorly. The moisture conditions during May and August also play a role in determining how accurately the model can predict Red Spring wheat yield. Obviously, other sources of model error also exist, but overall the growing season Z-index provides a reasonable measure of agricultural drought on the Canadian prairies.

CHAPTER 5
AN AGRICULTURAL DROUGHT CLIMATOLOGY OF THE CANADIAN PRAIRIES

5.1 Introduction

In the previous chapter we determined that the Moisture Anomaly Index is the best index for measuring agricultural drought on the Canadian prairies. In this chapter, the Z-index will be used to produce an agricultural drought climatology for the prairies for 1920-1999. Specifically, the Z-index will be used to divide the study area into a number of smaller relatively homogeneous drought regions. These drought regions will then be used to discuss the patterns of drought frequency, severity, and spatial extent. A series of growing season drought maps will be created for the 1920-1999 study period to illustrate the spatial patterns of drought and then spectral analysis will be carried out to investigate the temporal patterns of drought.

5.2 Creation of drought regions

The study region was divided into a five relatively homogeneous drought regions using Ward's cluster analysis (Figure 5.1) (refer to Section 3.5.4). The location of these five regions are shown in Figure 5.2. It is evident from the coherent spatial pattern in Figure 5.2 that group membership appears to be primarily controlled by geography (location). That is, the climate processes responsible for determining the growing season Z-index values operate on a regional-scale. Thus, moisture conditions during the growing season in any given crop district are likely to be most similar to the moisture conditions in neighbouring crop districts. This is not entirely surprising given that with the exception of the Rocky Mountains, topography (elevation) does not

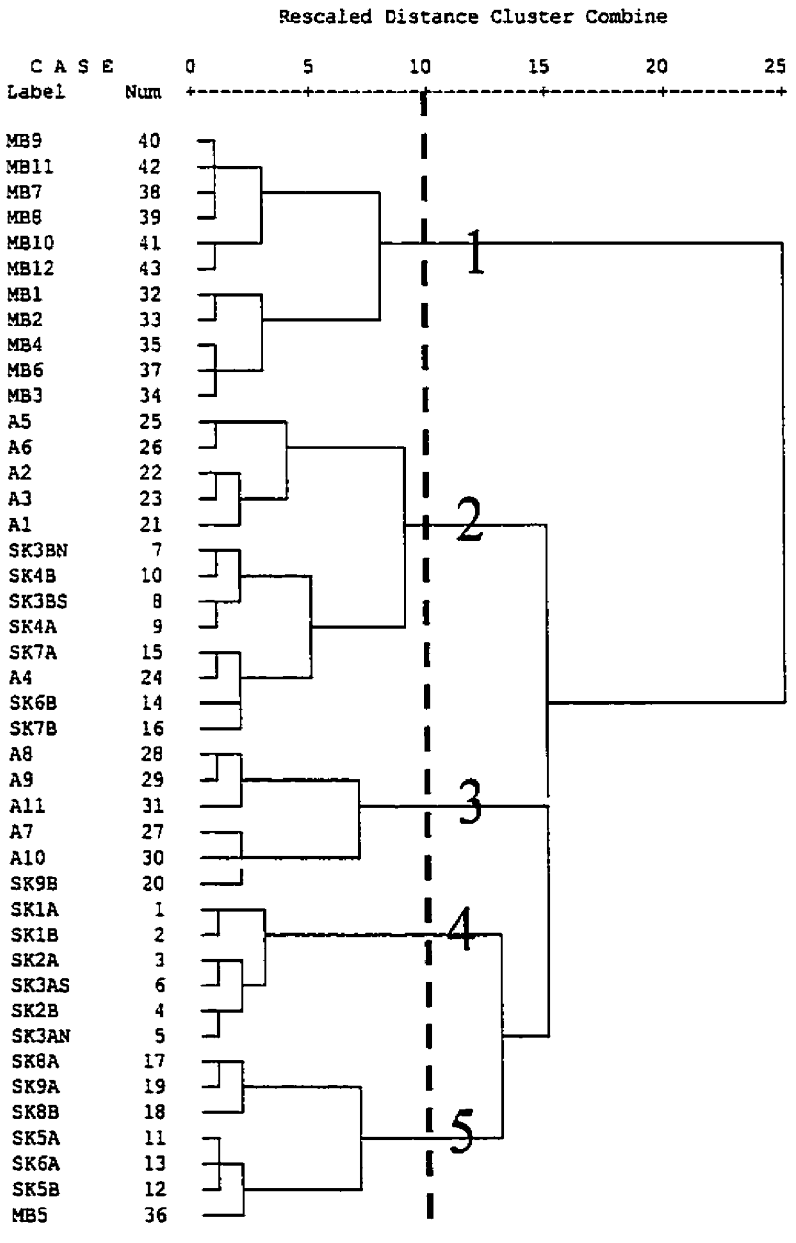

Figure 5.1 Dendrogram created by using Ward's method of cluster analysis on the growing season Z-index values for Canadian prairie crop districts

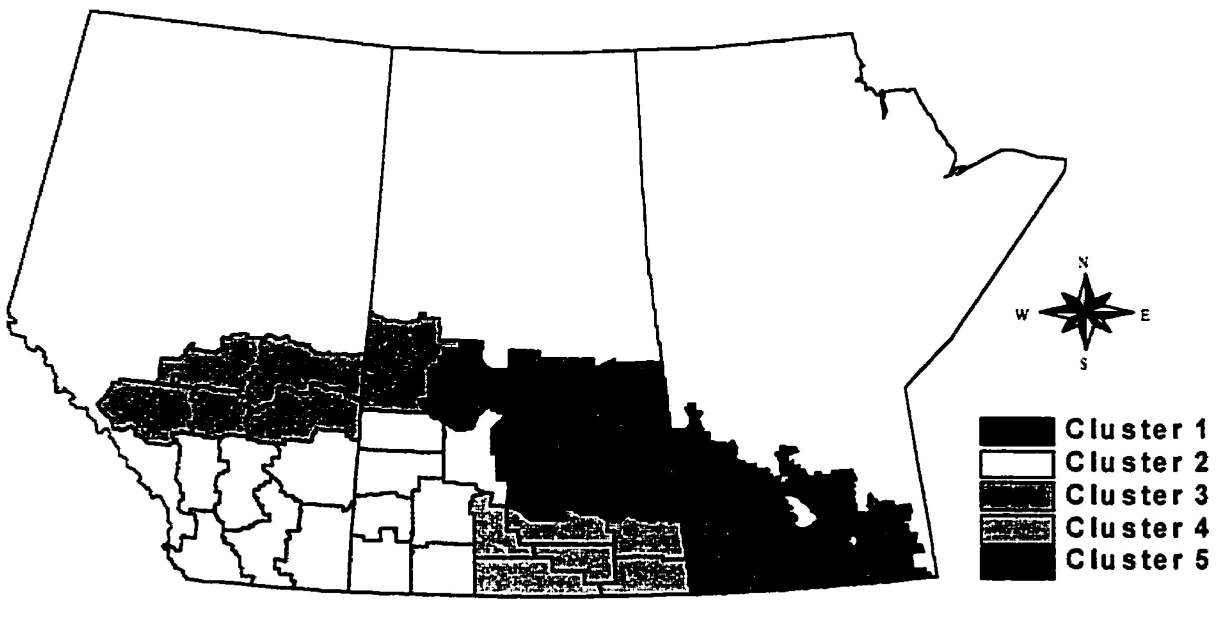

Figure 5.2 Location and membership of five homogeneous drought regions as determined by cluster analysis

play a major role in determining the climate of the Canadian prairies. Thus, the movement of air masses and the operation of many climate processes tends to be fairly homogenous over great distances. Therefore, the rationale for the location and membership of these regions can be attributed to aspects of the climate that do vary over the Canadian prairies such as the location of the jet stream and storm tracks, the proximity of the crop districts to the Rocky Mountains, and the influence of latitude.

Cluster 1 is located on the eastern side of the study region. All of the Manitoba crop districts except for MB5, located in the northwestern corner of Manitoba, belong to Cluster 1. Namely the eleven crop districts that make up Cluster 1 are: MB1, MB2, MB3, MB4, MB6, MB7, MB8, MB9, MB10, MB11, MB12. Two tables of summary statistics for the five clusters have been prepared. The results in Table 5.1 were calculated by determining the standard deviation, the variance, and the maximum and minimum Z-index values for each year of the 1920-1999 study period from the crop districts within each cluster. All of these yearly values were then averaged. The results in Table 5.1 give an indication of the amount of variation within each cluster. Cluster 1 had an average yearly standard deviation of 1.72 and an average yearly variance of 3.39. Both of these values rank as the second smallest and therefore Cluster 1 is the second most homogeneous cluster (all of the crop districts within Cluster 1 tend to have fairly similar Z-index values) in the study region. The homogeneity of each cluster is also illustrated by the clustering distance shown in Figure 5.1. The shorter the clustering distance, the more homogeneous the group. The homogeneity of each region can also be assessed by examining Figure 5.3. The more tightly the time series of Z-index values are grouped together, the more homogeneous the cluster will be. The second table of summary statistics (Table 5.2) created for each of the five drought regions presents the overall results. It was calculated by considering the

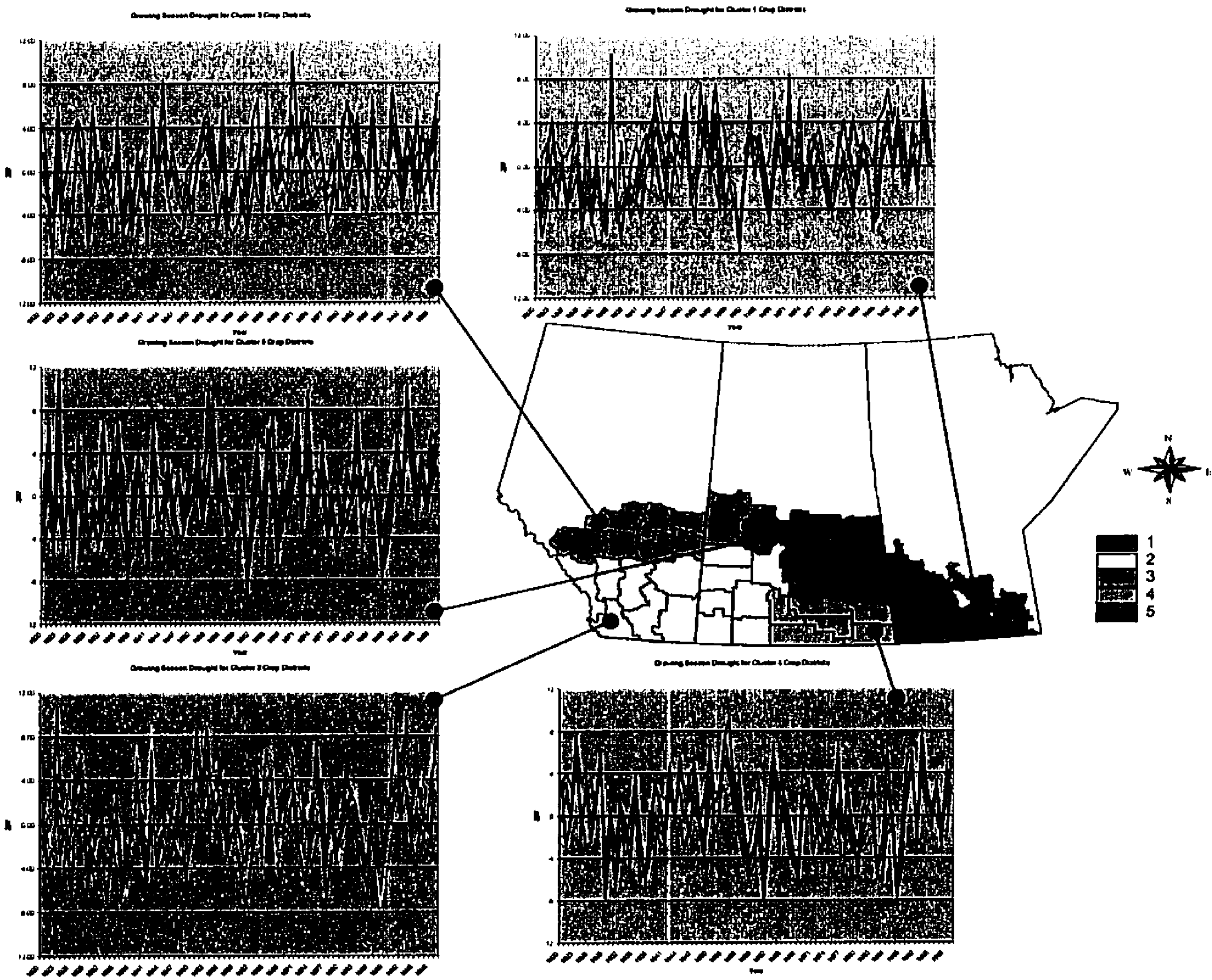

Figure 5.3 Moisture Anomaly Index values for each crop district plotted by cluster: 1920-1999

Z-index values for all years and crop districts within each cluster. The standard deviation and variance values provided in Table 5.2 shows the degree of variability of the drought regime for each cluster. The maximum and minimum values in Table 5.2 show the magnitude of the most extreme wet and dry events recorded by each cluster during the study period. Cluster 1 has the lowest standard deviation (3.04) and variance (9.22), meaning that it experiences less severe wet and dry events than the other clusters in the study region.

Table 5.1 Summary of average yearly maximum and minimum drought index values, and mean yearly standard deviation and variance for each cluster

Cluster	Max	Min	Standard Deviation	Variance
1	2.82	-2.65	1.72	3.39
2	3.48	-2.99	1.95	4.13
3	2.77	-2.65	2.05	4.76
4	1.99	-2.12	1.56	2.82
5	2.73	-2.42	1.85	3.99
MEAN	**2.76**	**-2.57**	**1.83**	**3.82**

Table 5.2 Overall summary of drought index values for each cluster: maximum, minimum, standard deviation, and variance

Cluster	Max	Min	Standard Deviation	Variance
1	10.29	-7.94	3.04	9.22
2	11.01	-7.54	3.49	12.17
3	10.97	-8.14	3.17	10.05
4	9.58	-8.19	3.38	11.40
5	11.75	-9.10	3.51	12.31
MEAN	**10.72**	**-8.18**	**3.32**	**11.03**

Cluster 4 is located in the southeastern corner of Saskatchewan and is composed of six crop districts (SK1a, SK1b, SK2a, SK2b, SK3an, and SK3as). Cluster 4 is the most homogenous of all of the clusters within the study region. It has the smallest standard deviation (1.56) and variance (2.82) (Table 5.1). This is perhaps due to the fact that Cluster 4 covers the smallest area. Normally, the smaller the region the more likely it is to be homogeneous. Cluster 4 has an overall standard deviation of 3.38 and a variance of 11.40. These values are very close to the mean for all the clusters within the study region.

Cluster 5 is located in the northeastern corner of Saskatchewan and Manitoba. It is composed of six crop districts from northeastern Saskatchewan (SK5a, SK5b, SK6a, SK8a, SK8b, and SK9a) along with one crop district from Manitoba (MB5). Cluster 5 has a moderate level of homogeneity as compared to the other clusters. The average yearly standard deviation is 1.85 and the variance is 3.99 (Table 5.1) and this compares favorably with the mean standard deviation of 1.83 and the mean variance of 3.82. Cluster 5 has the most variable and extreme drought regime of all of the clusters in the study region. It has the highest overall standard deviation of 3.51 and a variance of 12.31 (Table 5.2). It also has the largest recorded maximum and minimum Z-index values.

Cluster 2 draws its membership from southern Alberta and southwestern Saskatchewan. It is made up of thirteen crop districts (AB1, AB2, AB3, AB4, AB5, AB6, SK3bn, SK3bs, SK4a, SK4b, SK6b, SK7a, and SK7b). The large number of crop districts within Cluster 2 may contribute to it being the second most heterogeneous cluster in the study region. It has an average yearly standard deviation of 1.95 and a variance of 4.13 (Table 5.1). Cluster 2 is only slightly less variable and extreme then Cluster 5. It has an overall standard deviation of 3.49 and a variance of 12.17 (Table 5.2). It is not completely unexpected that this cluster experiences extreme conditions due to the fact that many of the crop districts that make-up this cluster are part of a particularly drought prone region known as Palliser's Triangle.

Finally, Cluster 3 draws its membership from northern Alberta and northwestern

Saskatchewan. It is made of a total of six crop districts (AB7, AB8, AB9, AB10, AB11, and SK9b). Cluster 3 has the highest amount of within cluster variance (most heterogeneous cluster) as illustrated by having the highest standard deviation of 2.05 and variance of 4.76 (Table 5.1). Much of the variance between crop districts in Cluster 3 can be ascribed to the influence of the Rocky Mountains on precipitation (and therefore drought) patterns. Crop district AB8, in particular, exhibits a great deal of inter- and intra-growing season variability. However, in terms of overall variability (susceptibility to drought), this cluster is slightly below the mean of the other clusters with a standard deviation of 3.17 and a variance of 10.05 (Table 5.2).

5.3 Drought frequency

The frequency of droughts (and floods) for each cluster was calculated by determining how many times an event of a given magnitude occurred during the 1920-1999 study period. Two different drought and flood thresholds were subjectively chosen based on a visual examination of the time series Z-index plots shown in Figure 5.3. The total number of drought events with Z-index values less than or equal to -5 and less than or equal to -7 were counted and the results are summarized in Table 5.3. For the sake of comparison, this table also shows the number of flood events (extremely wet events) with Z-index values greater than or equal to 5 and greater than or equal to 7. Because there are a different number of crop districts in each cluster, the results presented in Table 5.3 are slightly misleading. Obviously, since Cluster 2 is composed of thirteen crop districts it will likely have a greater number of drought (and flood) events. Therefore, the number of drought events were standardized by dividing the total number of drought events that occurred during the study period by the number of crop districts within each cluster (Table 5.4).

Table 5.3 Summary of the number of drought and flood events exceeding a given threshold recorded within each cluster

Cluster	Count > 5	Count <-5	Count > 7	Count < -7
1	42	41	17	2
2	96	71	30	7
3	33	25	4	3
4	35	35	7	5
5	49	43	19	9

Table 5.4 Summary of the standardized number of drought and flood events exceeding a given threshold recorded within each cluster

Cluster	Standardized count > 5	Standardized count <-5	Standardized count > 7	Standardized count < -7
1	3.82	3.73	0.18	1.55
2	7.38	5.46	0.54	2.31
3	5.50	4.17	0.50	0.67
4	5.83	5.83	0.83	1.17
5	7.00	6.14	1.29	2.71

According to Table 5.4, Cluster 5 has the highest average number of moderate and extreme growing season droughts per crop district. Cluster 5 had an average of 6.14 growing season droughts per crop district that were more severe than a -5 (moderate drought) and an average of 2.71 events that had a Z-index value more severe than -7 (severe drought). This supports the overall standard deviation and variance statistics from Table 5.2 that indicated that this is the region with the most variable and extreme drought regime. An average of 6.14 growing season droughts per crop district during the 80-year study period indicates that there were moderate to severe drought conditions during approximately 7.7% of the study period (or one out of every thirteen years).

After Cluster 5, Cluster 2 experienced moderate to severe drought conditions most frequently. It had an average of 5.46 growing season droughts that were more severe than -5 and an average of 2.31 droughts per crop district that were more severe than -7. The drought frequency results for this cluster agree with the overall drought statistics in Table 5.2 which indicated that Cluster 2 has the second highest susceptibility to drought. Moderate to severe drought conditions occurred during 6.8% of the study period (or approximately one out of every fourteen years).

Cluster 4 had an average of 5.83 growing season droughts that were more severe than -5 and an average of 1.17 droughts per crop district that were more severe than -7. This ranked it as the third most drought susceptible cluster. Cluster 4 actually had a slightly higher average number of moderate growing season droughts than Cluster 2, but it had a much lower average number of extreme growing season droughts and therefore it was ranked behind Cluster 2. Moderate to severe drought conditions occurred during 7.3% of the study period (or approximately one out of every fourteen years).

Cluster 1 had an average of 3.73 growing season droughts that were more severe than -5 and an average of 1.55 droughts per crop district that were more severe than -7. This drought frequency ranked it as the fourth among the prairie clusters. Moderate to severe drought conditions occurred during 4.7% of the study period (or approximately one out of every twenty-one years).

Cluster 3 had an average of 4.17 growing season droughts that were more severe than -5 and an average of 0.67 droughts per crop district that were more severe than -7. This ranked it as the least drought susceptible cluster. Cluster 3 actually had a slightly higher average number of moderate growing season droughts than Cluster 1, but it had a much lower average number of extreme growing season droughts and so it was ranked behind Cluster 1. Moderate to severe drought conditions occurred during 5.2% of the study period (or approximately one out of every nineteen years).

All of the clusters had a higher average number of extreme drought events (< -7) than extreme flood events (> 7), except for Cluster 3. Clusters 1 and 4 had an approximately equal number of moderate drought (< -5) and flood (> 5) events. Clusters 2, 3, and 5 all had a higher number of moderate flood events than drought events. Cluster 2 had an average of 7.38 flood events (> 5) per crop district and Cluster 5 had an average of 7.00. This means that moderate to severe flood conditions occurred during 9.2% of the study period for Cluster 2 and 8.8% for Cluster 5. This once again illustrates that these two crop districts have a highly variable precipitation regime. When the average number of moderate to severe drought and flood events are combined together it is evident that approximately 16% of the study period for Clusters 2 and 5 (one out of six years) have growing season moisture conditions that are not well-suited for agriculture.

5.4 Drought severity and spatial extent

Figure 5.4 shows the mean drought severity and spatial extent of each growing season drought for all five cluster-regions. The drought severity has been plotted in reverse order on the secondary Y-axis (smallest value at the top) to better illustrate the relationship between drought severity and spatial extent. Generally, as drought severity increases, the area that is affected also increases. Therefore, there is an inverse relationship between drought severity (negative Z-index value) and the spatial extent of a drought event. The linear correlation between drought severity and spatial extent is consistently around -0.80 (correlations are negative because the Z-index expresses drought as a negative number) for all clusters (Cluster 5 has a correlation of -0.81;

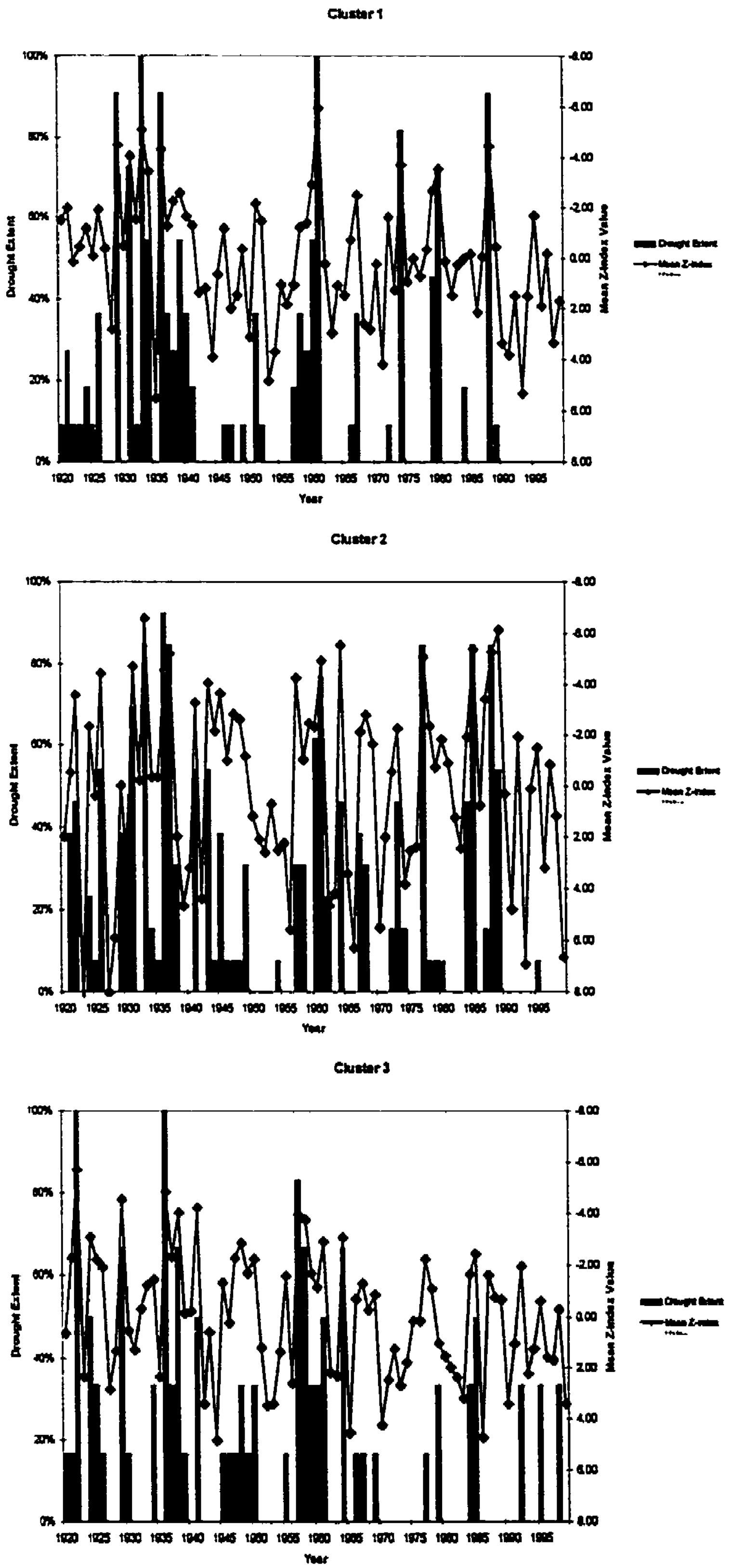

Figure 5.4 Mean Z-index value and spatial extent of drought for each cluster

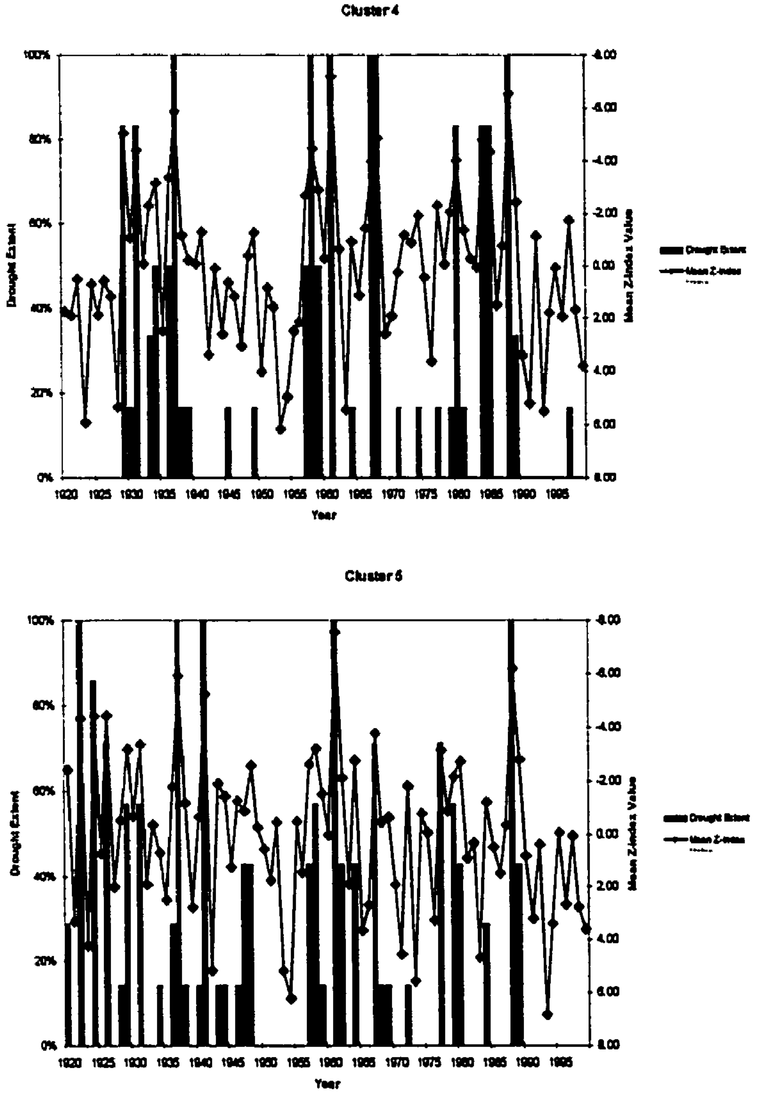

Figure 5.4 Mean Z-index value and spatial extent of drought for each cluster (cont.)

Cluster 4 = -0.79; Cluster 3 = -0.80; Cluster 2 = -0.81: Cluster 1 = -0.80). Therefore, it seems that this relationship is not influenced by the variability of a cluster's precipitation regime.

Cluster 1 is one of the clusters that has the least variable precipitation regime and is the least prone to drought. There are only two years during the study period (1934, 1961) when all crop districts in this cluster were experiencing moderate to severe drought conditions. In total, moderate drought conditions were present in at least one crop district in Cluster 1 during 37 years.

Cluster 2 is one of the most drought prone regions on the Canadian prairies, but there were no years during the study period when moderate to severe drought conditions were present in all crop districts. This is somewhat surprising given what we know about this cluster from previous sections. This may simply be due to the fact that this region is composed of thirteen crop districts, which is significantly more than all of the other clusters. Cluster 2 had 44 years where there was at least one crop district that was experiencing moderate to severe drought conditions. No other cluster had more than 37 years when there was at least one crop district experiencing drought conditions.

Cluster 3 had only two years (1923, 1936) where 100% of the crop districts that make up this cluster were experiencing drought conditions. There were a total of 37 years when at least one crop district in Cluster 3 was experiencing drought conditions.

There are six years (1936, 1958, 1961, 1967, 1968, and 1988) when drought conditions are present in all of the crop districts in Cluster 4. However, there were only 29 years when at least one crop district was experiencing drought conditions in Cluster 4.

Cluster 5 is the most drought prone cluster. There are five years (1923, 1936, 1961, and 1988) when moderate to severe drought conditions are present in all of the crop districts within this cluster. Overall, there were a total of 34 years when drought conditions were present in at least one of the crop districts in Cluster 5.

The relationship between drought severity and the spatial extent of drought events can also be analyzed by looking at the Canadian prairies as a whole (Figure 5.5). Overall, there is a linear correlation of -0.88 between drought severity and the spatial extent of drought events. That is, approximately 77% of the variance in the spatial extent of drought events can be explained by the mean Z-index values (drought severity) for all crop districts on the Canadian prairies. The increase in the correlation between drought severity and spatial extent over the values for each individual drought region can be attributed to using all 43 crop districts.

None of the drought events that occurred during the study period were concurrent in all crop districts across the prairies. The most severe drought occurred in 1961 (mean Z-index value of -5.67) and covered approximately 86% of the prairies. Other major droughts occurred in 1988, 1929, 1937, and 1936. Table 5.5 lists the severity and spatial extent of the twenty most severe droughts that occurred during 1920-1999. Overall, drought conditions were present in at least one crop district during 62 years. That is, there was a moderate to severe drought in at least one crop district during 77.5% of the study period.

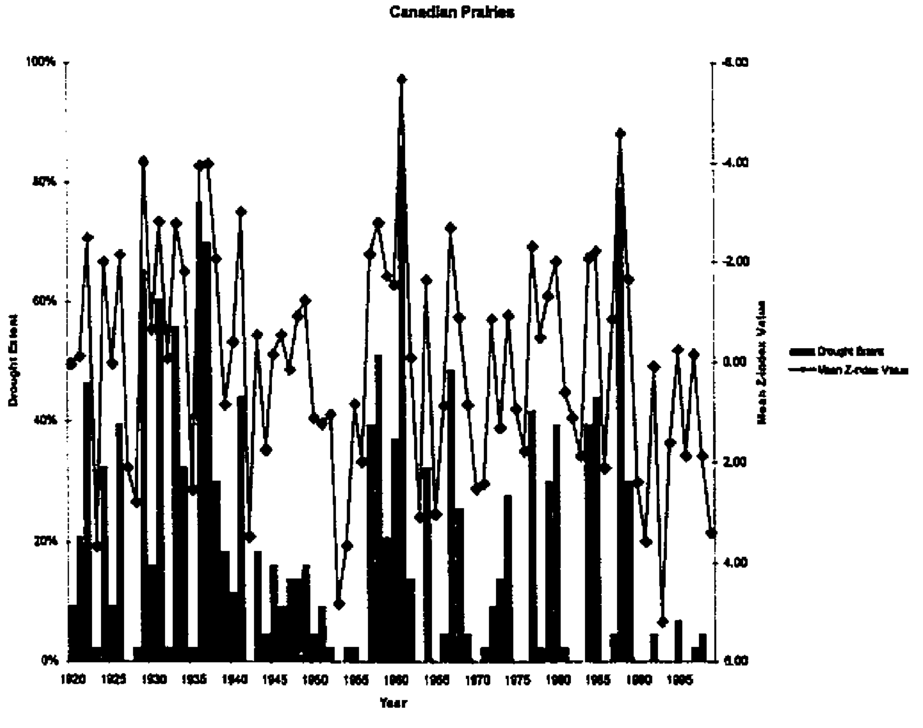

Figure 5.5 Mean Z-index value and spatial extent of drought for the Canadian prairies

Table 5.5 Summary of the severity and spatial extent of the twenty most severe prairie droughts during 1920-1999 (sorted by drought severity (mean Z-index value))

Year	Mean Z-index Value	Drought extent (% of area < -3)
1961	-5.67	86.05%
1988	-4.58	79.07%
1929	-4.01	65.12%
1937	-3.97	69.77%
1936	-3.94	76.74%
1941	-3.00	44.19%
1931	-2.81	60.47%
1958	-2.79	51.16%
1933	-2.77	55.81%
1967	-2.70	48.84%
1922	-2.47	46.51%
1977	-2.32	41.86%
1985	-2.21	44.19%
1957	-2.15	39.53%
1926	-2.14	39.53%
1984	-2.07	39.53%
1938	-2.05	30.23%
1980	-2.01	39.53%
1924	-2.01	32.56%
1934	-1.80	32.56%

5.5 Spatial patterns of drought

The Moisture Anomaly Index values for each crop district were mapped for each growing season from 1920 to 1999 to illustrate the spatial patterns of drought (Figure 5.6). Three distinctly different spatial patterns of drought are evident from a visual analysis of the growing season drought maps. The first pattern will be referred to as linear and it is associated with a coherent linear arrangement or pattern to how the Moisture Anomaly Index values are distributed across the Canadian prairies. This spatially coherent pattern takes a variety of forms. For example, during some years there was a distinct band of drought (or wet conditions) that stretched across the study region. One example of this type of pattern occurred in 1943, when a

Figure 5.6 Annual growing season Moisture Anomaly Index (Z-index) maps: 1920-1999

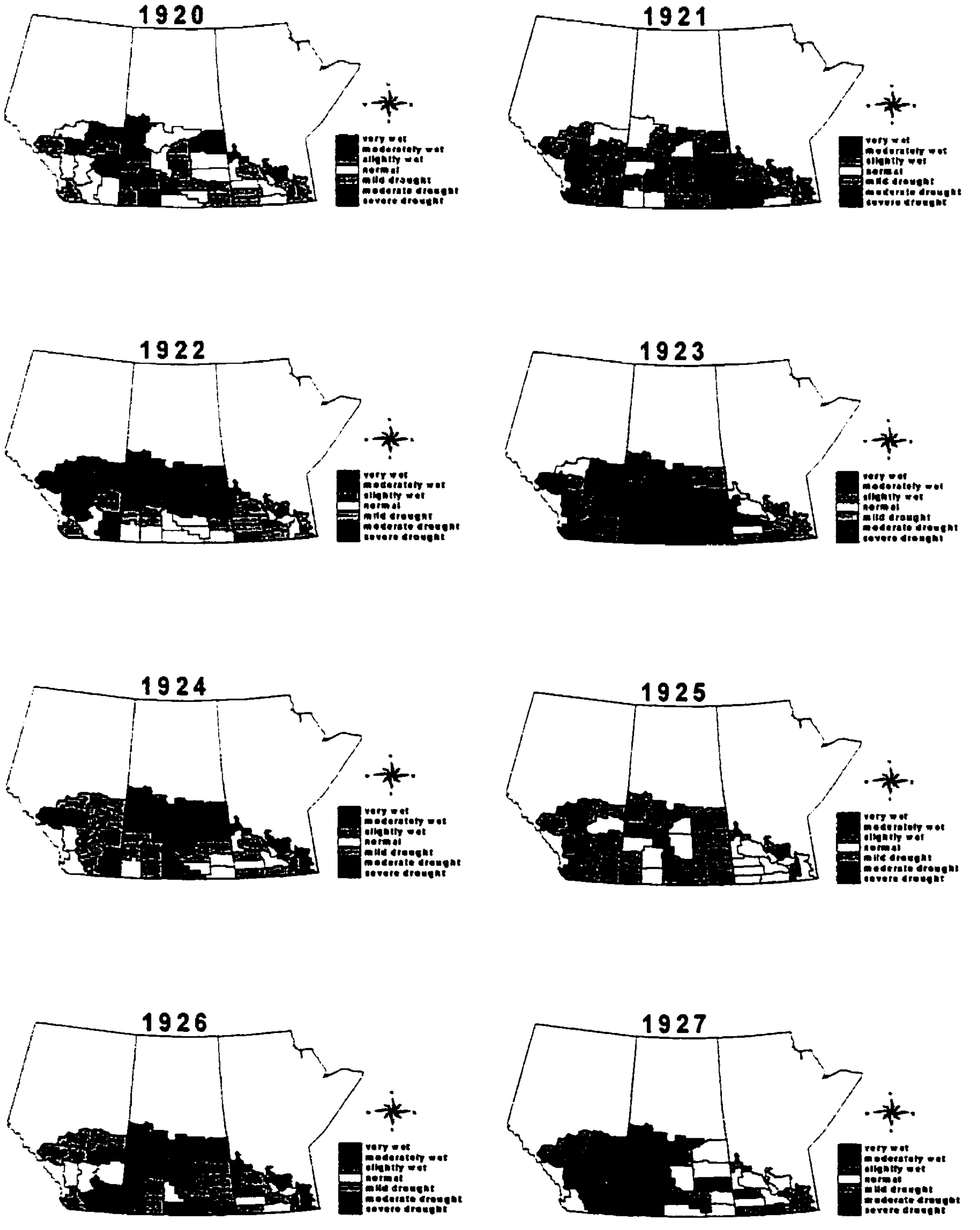

Figure 5.6 Annual growing season Moisture Anomaly Index (Z-index) maps: 1920-1999 (cont.)

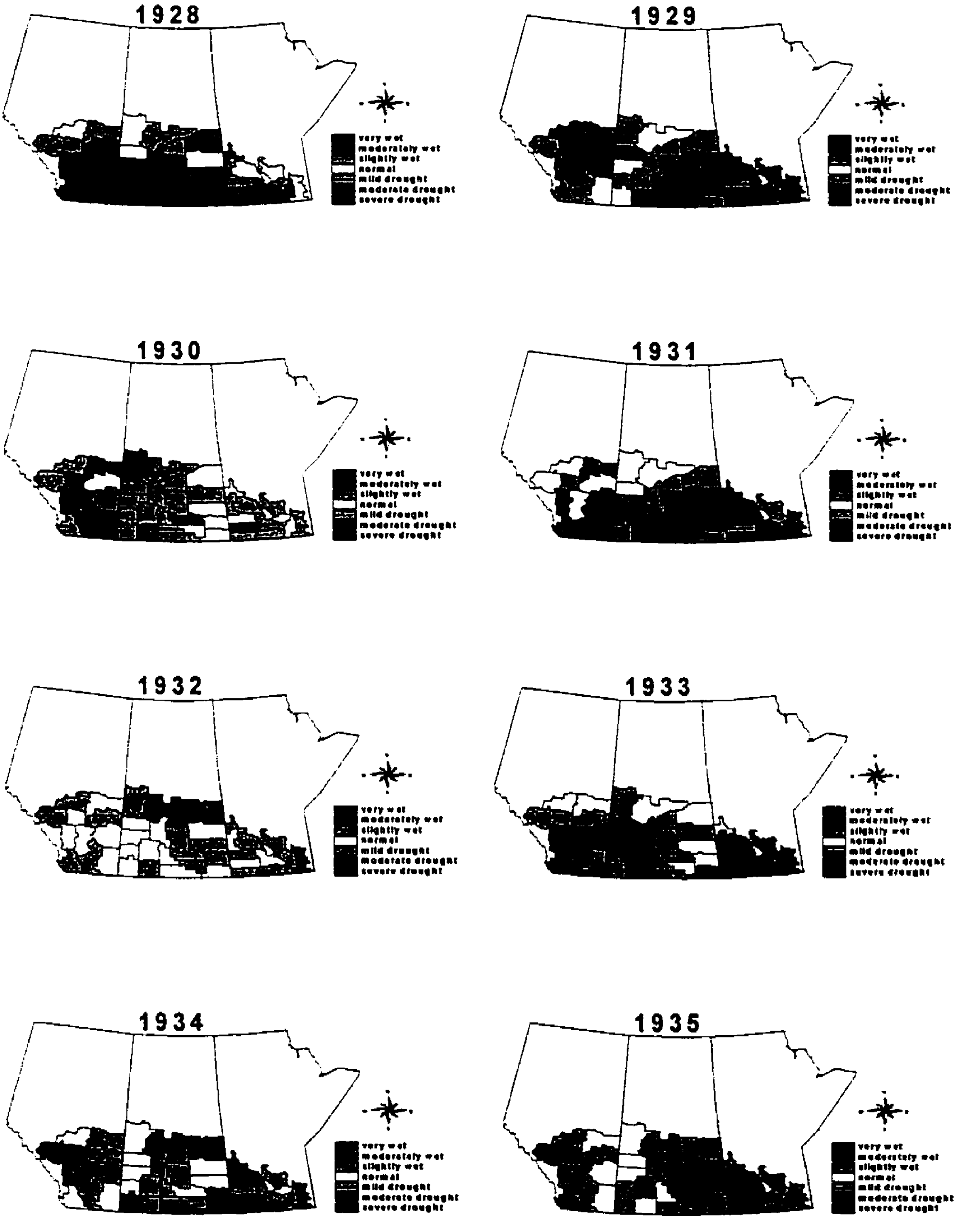

Figure 5.6 Annual growing season Moisture Anomaly Index (Z-index) maps: 1920-1999 (cont.)

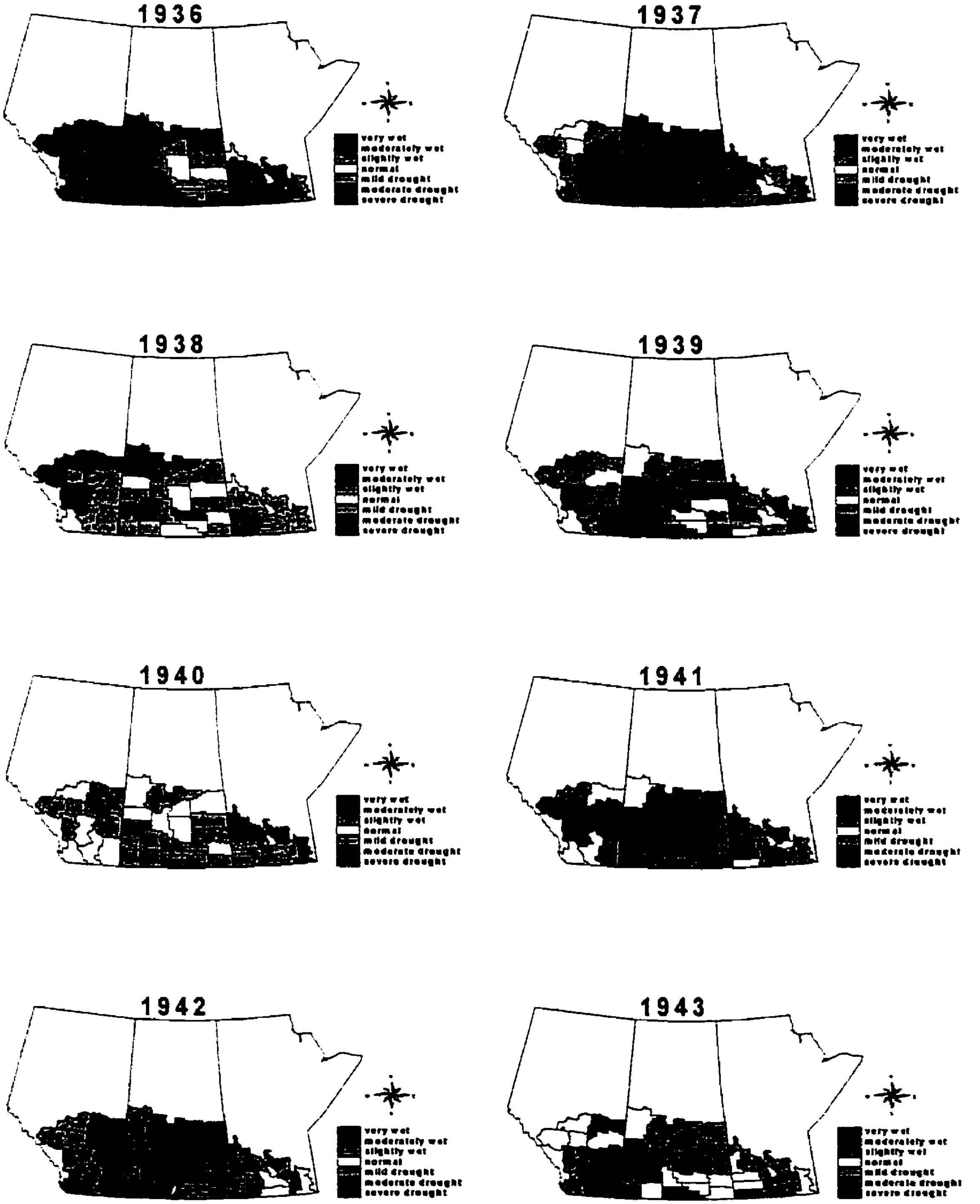

Figure 5.6 Annual growing season Moisture Anomaly Index (Z-index) maps: 1920-1999 (cont.)

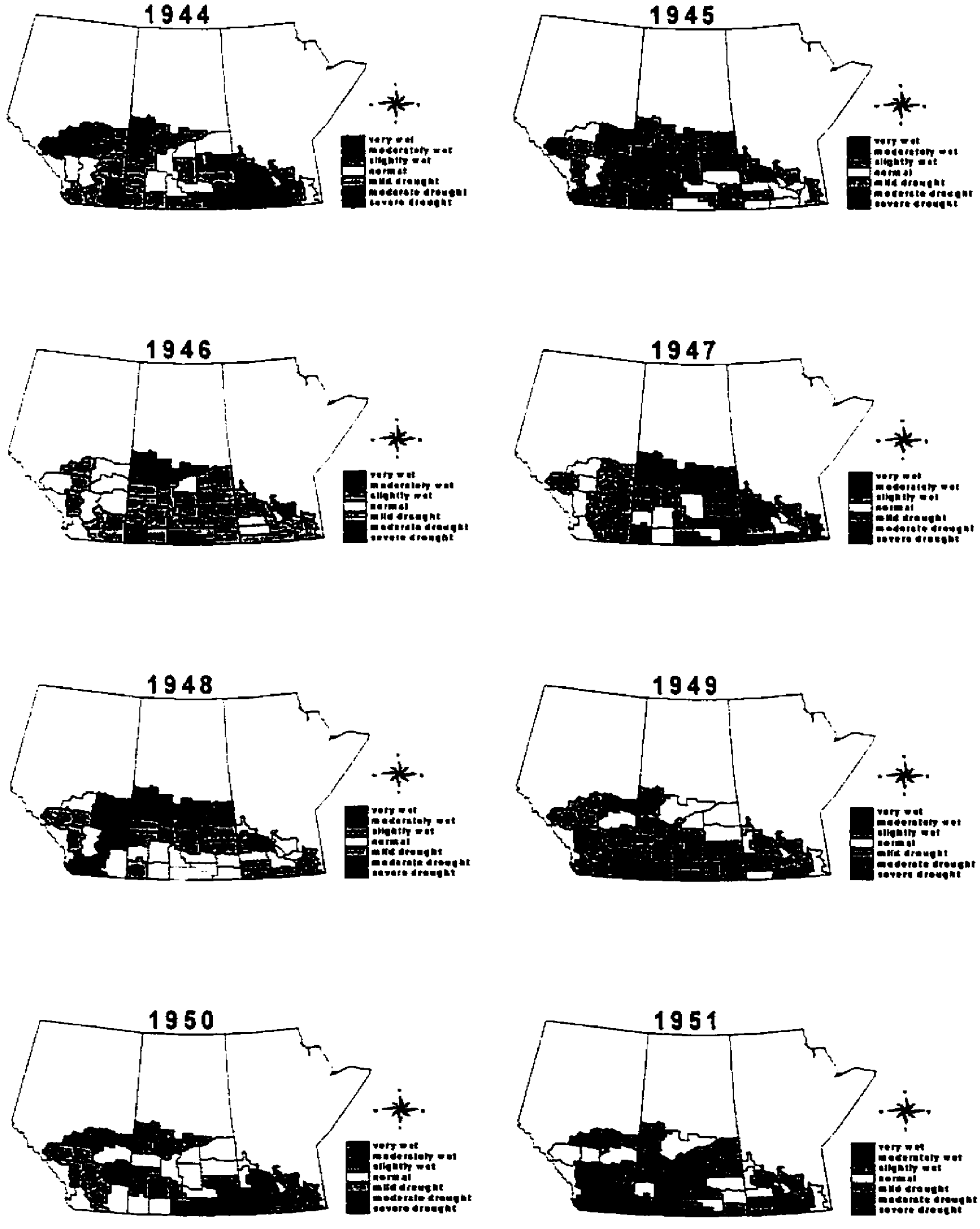

Figure 5.6 Annual growing season Moisture Anomaly Index (Z-index) maps: 1920-1999 (cont.)

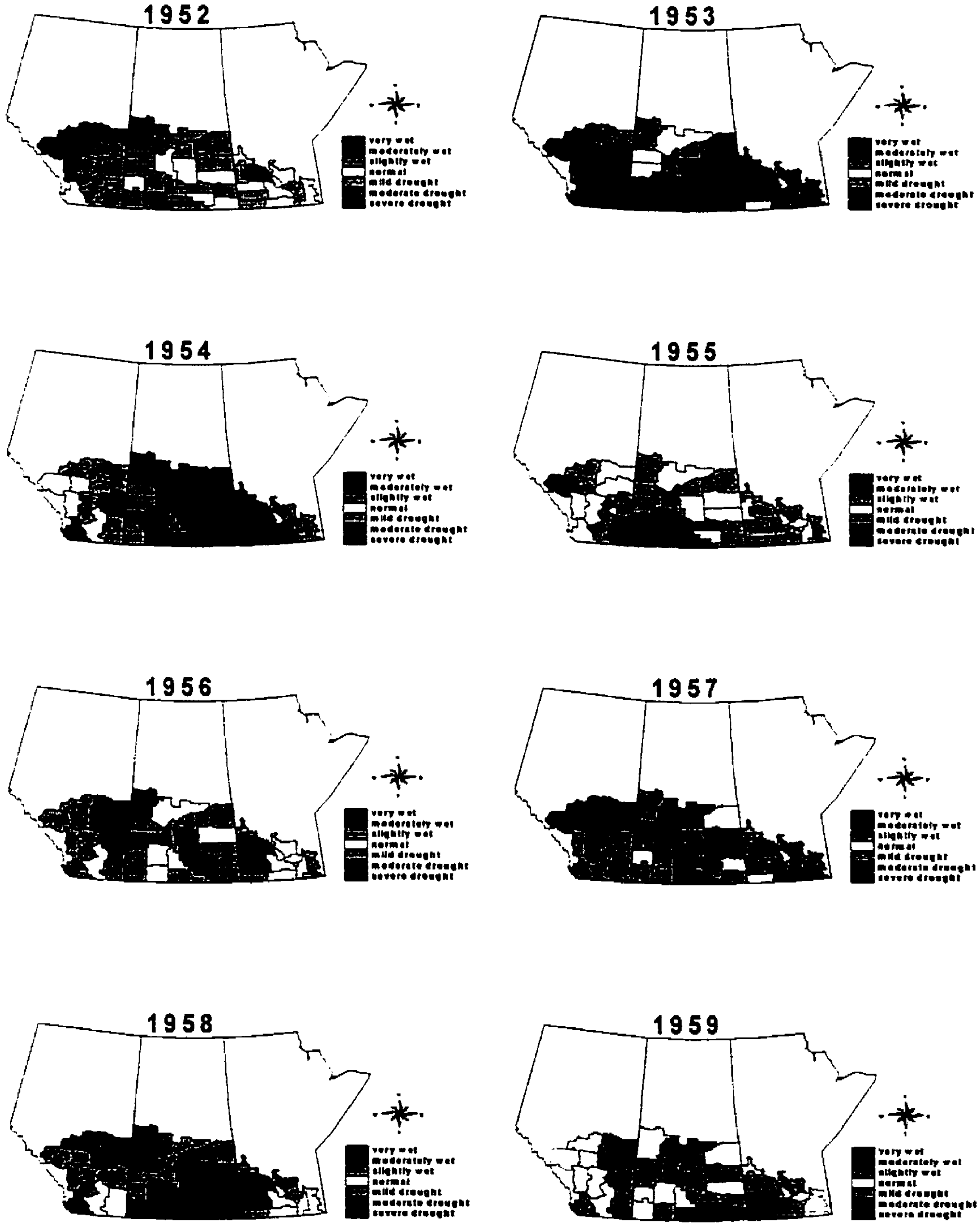

Figure 5.6 Annual growing season Moisture Anomaly Index (Z-index) maps: 1920-1999 (cont.)

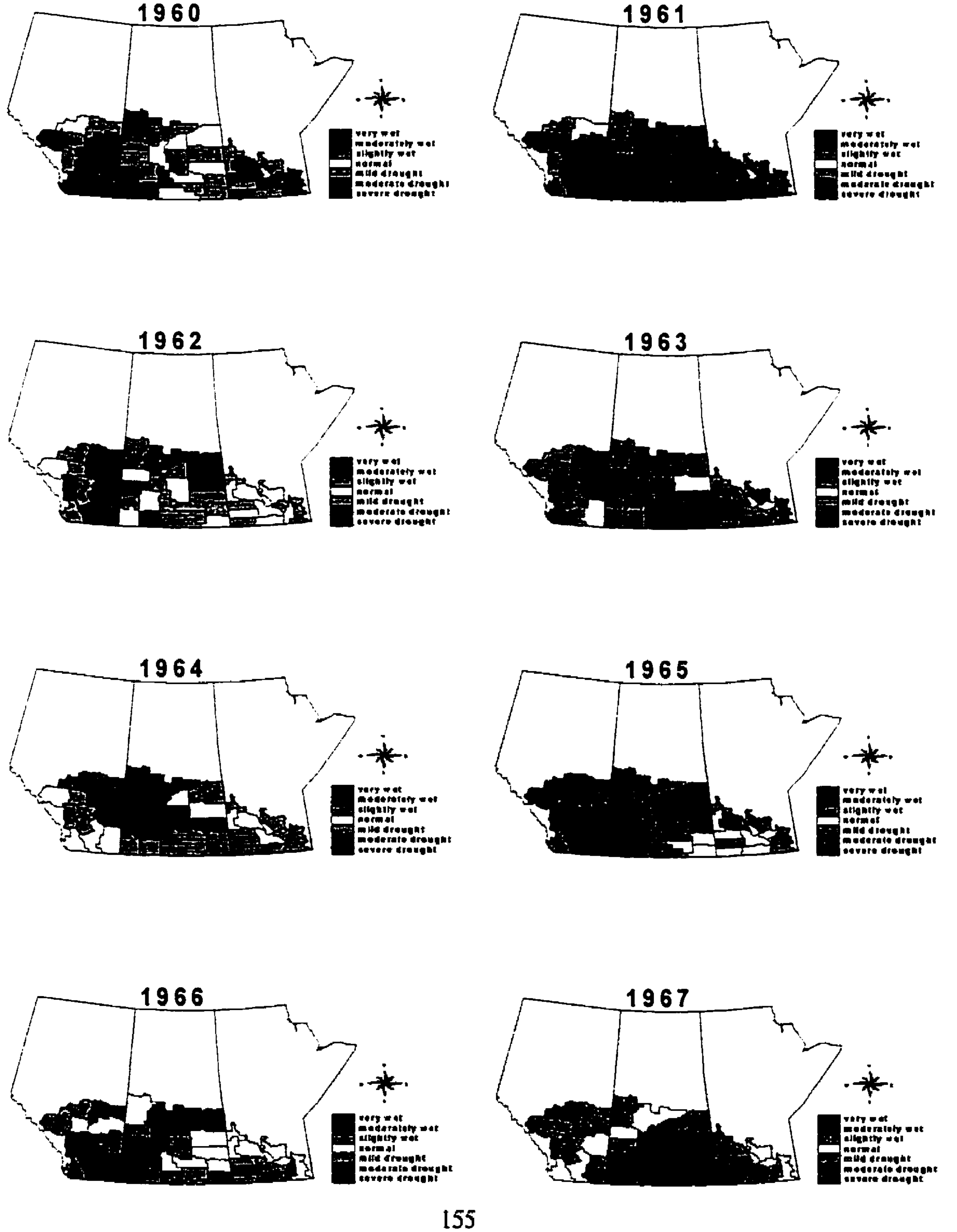

Figure 5.6 Annual growing season Moisture Anomaly Index (Z-index) maps: 1920-1999 (cont.)

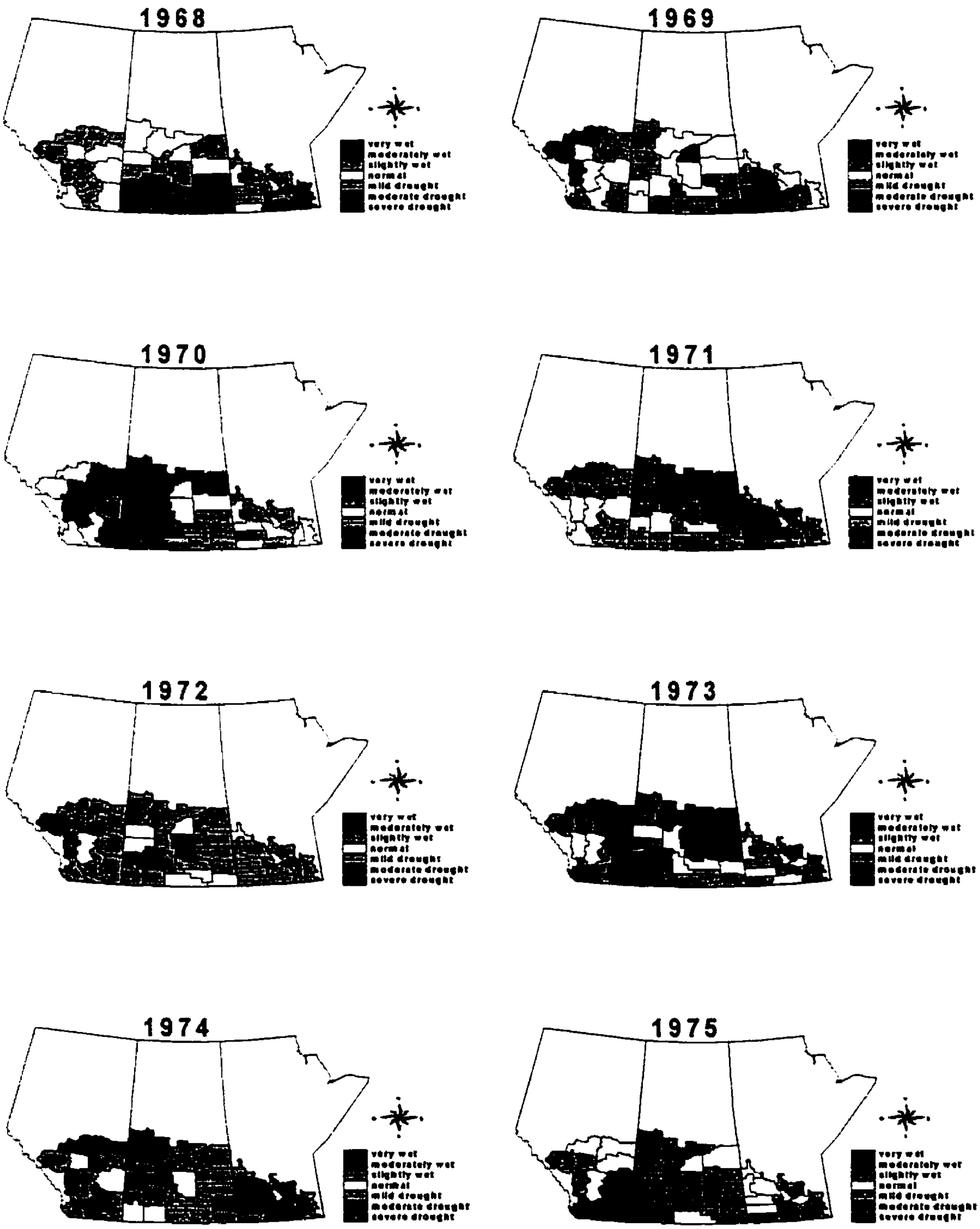

Figure 5.6 Annual growing season Moisture Anomaly Index (Z-index) maps: 1920-1999 (cont.)

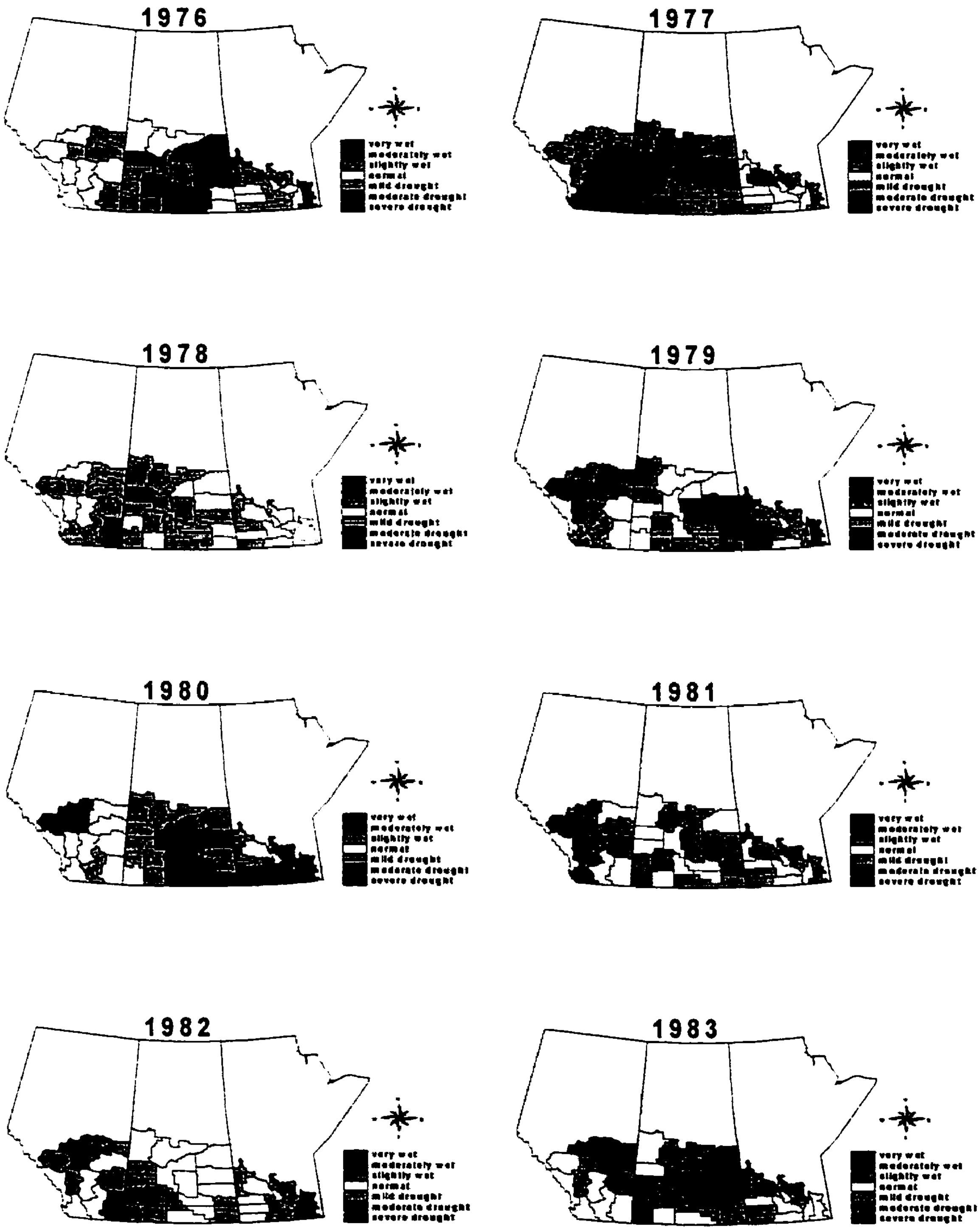

Figure 5.6 Annual growing season Moisture Anomaly Index (Z-index) maps: 1920-1999 (cont.)

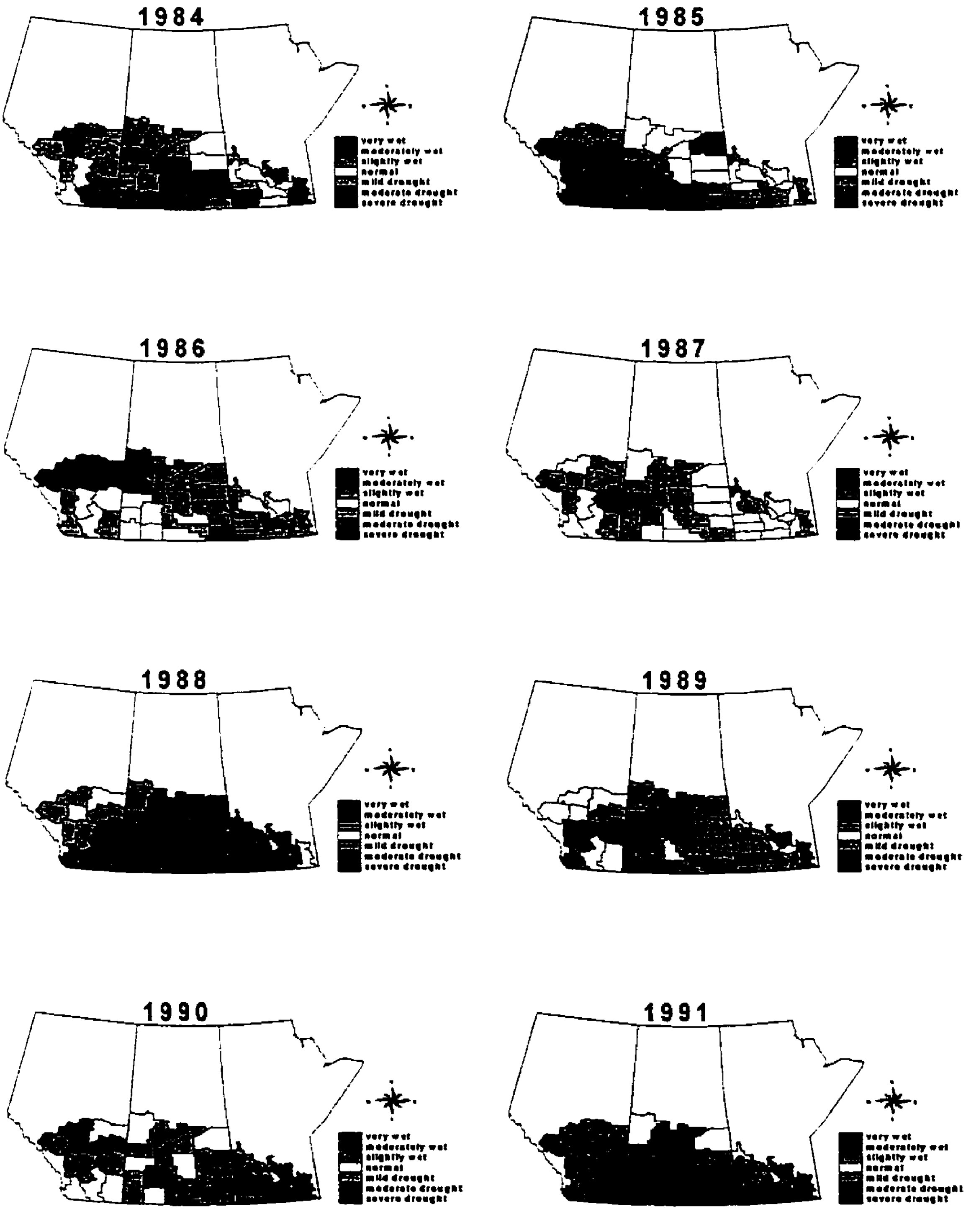

Figure 5.6 Annual growing season Moisture Anomaly Index (Z-index) maps: 1920-1999 (cont.)

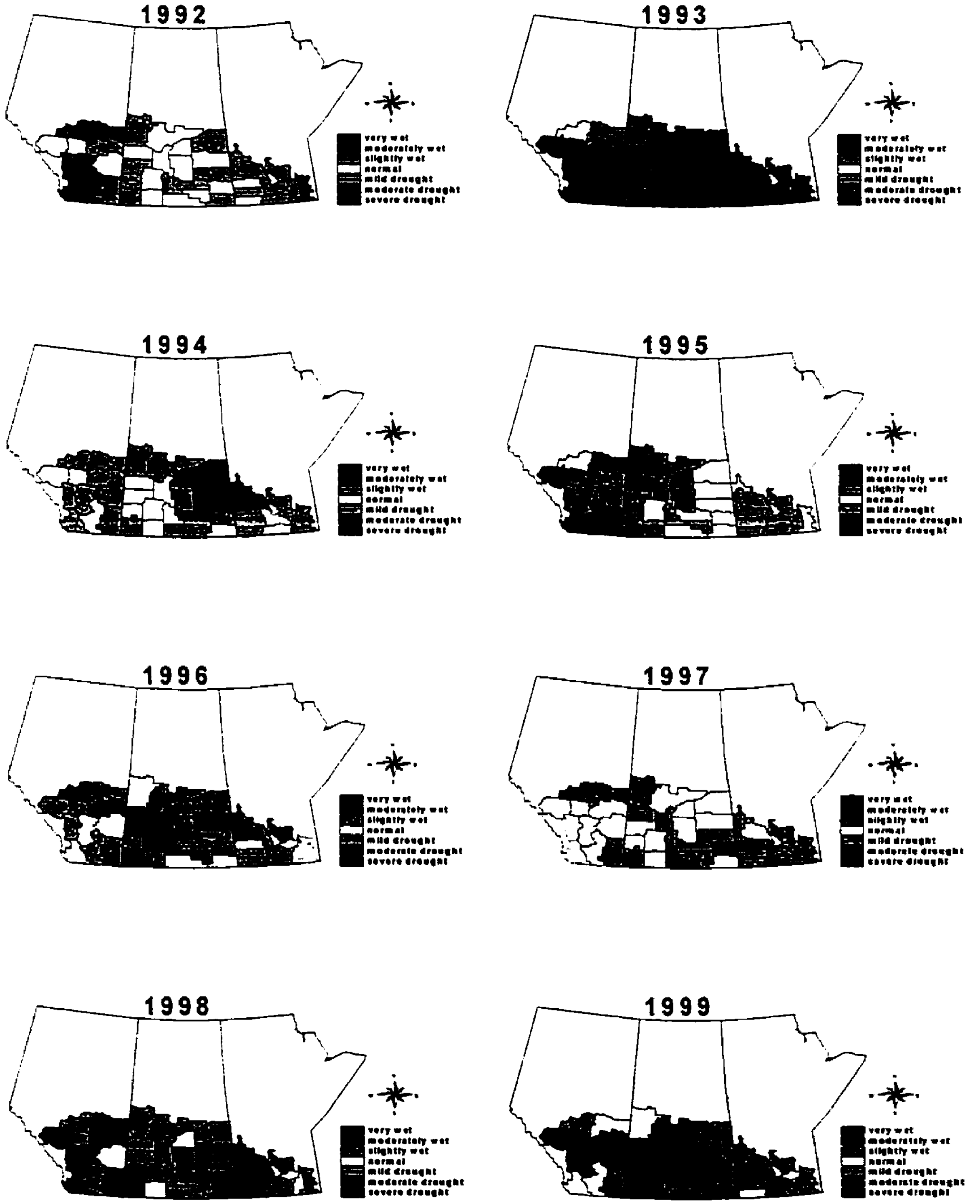

band of mild to moderate drought conditions extended from the southwestern corner of Alberta to the northeastern corner of Saskatchewan and Manitoba. Conditions on either side of this band of drought are classified as near normal or slightly wetter than normal. Another example of a spatially coherent pattern of drought occurred in 1985. A relatively uniform band of moderate to severe drought stretches from the northwestern corner of Alberta down to the southeast corner of Manitoba. To the north of this, conditions in Saskatchewan and Manitoba were normal or wetter than normal. The opposite situation is illustrated in 1966 when a distinct plume of wetter than normal conditions extends from southern Alberta through to the northern part of Saskatchewan. The crop districts on both sides of this band experienced normal or mild drought conditions. There are many other examples of spatially coherent linear patterns of drought.

These coherent linear patterns of drought are likely caused by changes in the location of the jet stream and storm tracks through the study region and the changes may be due to the presence of persistent ridges or troughs that are anchoring the jet stream and storm track. These ridges/troughs may in turn be linked to persistent SST anomalies in the Pacific.

There are also other spatially coherent patterns. For lack of a better term, the second pattern will be called drought or flood dominant. That is, the entire study region is essentially experiencing the same moisture conditions. One example of a drought dominant pattern occurred in 1929. Every crop district in the study area was classified as having drought conditions, with the exception of four crop districts that were experiencing near normal conditions. On the other hand, 1953 is an example a flood dominant pattern because the vast majority of the crop districts experienced very wet conditions. There are many other examples of drought or flood dominant patterns such as: 1936, 1937, 1941, 1942, 1954, 1961, 1965, 1977, 1988, 1991, 1993, and 1999. These years were selected because the prevailing conditions (drought or flood) appear to effect nearly all crop districts. Obviously, the selection of these years is somewhat subjective since it is based on a visual analysis of the patterns of drought occurrence. However, the underlying mechanism responsible for causing the drought (or flood) patterns during these years is probably different than the mechanism that is causing the linear patterns. The mechanism (or mechanisms) that are causing these drought dominant patterns are operating at a scale that influences the entire study region. Therefore, local convective activity and other small-scale control mechanisms can be ruled out. Many of the years that are given as examples of this type of pattern are extreme drought or flood years. The cause of the spatial pattern for many of these years, particularly the flood years, may be linked to ENSO. Six of the ten wettest years on the prairies occurred during El Niño events and the other four occurred during La Niña events (Table 5.6). ENSO appears to play a role in causing extremely wet years to occur. The signal is somewhat uncertain given that both El Niño and La Niña years appear to be important, but it may be related to the evolution of ENSO because La Niña events often occur following an El Niño. For example, an El Niño event occurred in 1953 and this was followed by a La Niña event in 1954. Coincidentally, 1954 happens to be the fourth wettest year on the prairies during the study period. Similarly, an El Niño event occurred in 1925, followed by a La Niña event in 1928. Also, an El Niño event occurred in 1939, followed by a La Niña event in 1942.

Table 5.6 Summary of the mean magnitude of the ten wettest growing seasons during 1920-1999 and whether there was an El Niño or La Niña event

Year	Mean Z-index Value	ENSO
1993	5.19	EN
1953	4.82	EN
1923	3.68	EN
1954	3.65	LN
1991	3.58	EN
1942	3.47	LN
1999	3.39	LN
1963	3.08	EN
1965	3.03	EN
1928	2.80	LN

There does not appear to be such a strong relationship between ENSO and extreme drought years. Only the drought during 1988 can be linked to a La Niña event. However, it is likely that other large-scale forcing functions are responsible for the dominant drought patterns.

The third type of drought pattern can be described as relatively random. It has very little spatial structure or evidence of a coherent pattern. It is essentially the exact opposite of the flood or drought dominant pattern. One example of this kind of pattern occurred in 1995 when drought conditions were present in northern Alberta and northwestern Saskatchewan, as well as in parts of Manitoba and very wet conditions were present in southern Alberta and parts of Saskatchewan. It seems logical to conclude that there is no single dominant mechanism controlling precipitation during years that display this type of random spatial pattern. In particular, these patterns may arise due to convective precipitation and as a result of natural variability in the climate system. It should be noted that large convective storms can significantly skew moisture patterns, particularly in years where there are very few stations being used to calculate the precipitation totals.

5.6 Temporal patterns of drought

The temporal patterns of drought, or drought cycles, that may be present in the eighty years of available data were analyzed using the Fast Fourier Transform (FFT) technique. Spectral density plots were produced for a representative crop district from each of the five drought regions (Figure 5.7). A series of cross amplitude graphs were also produced for each pair of regions (Figure 5.8).

Crop district MB1 was used to represent Cluster 1. Spectral analysis revealed that there were significant peaks in the density of Cluster 1 at roughly 2 years, 7 years, 9 years, and around 13 years (Figure 5.7). In fact, the spectral density actually has a rather broad peak between 7-10 years. These results are fairly consistent for all crop districts within Cluster 1.

Cluster 2 is represented by crop district SK4b and it has two significant peaks in spectral density. The first peak is at approximately 2 years and the second is at approximately 4 years. Unlike Cluster 1, there is not a strong peak between 7-10 years or between 10 and 20.

Cluster 3 is represented by crop district A7. Like Cluster 2, it has significant peaks in density at around 2 years and 4 years. It also has a rather broad plateau that spans from 7 years to about 15 years.

Cluster 4 is represented by crop district SK3as. It appears to be fairly similar to all of the previous clusters because it has peaks at around 2 and 4 years. The density then gradually climbs to form a broad plateau from about fifteen to the mid-twenties.

Cluster 5 is represented by crop district SK8b. It has a significant peak in density at about 2 years and it also has peaks between 7-10 years and between 15-20 years. The peak around 4 years that is present in many of the other clusters is not very prominent in Cluster 5.

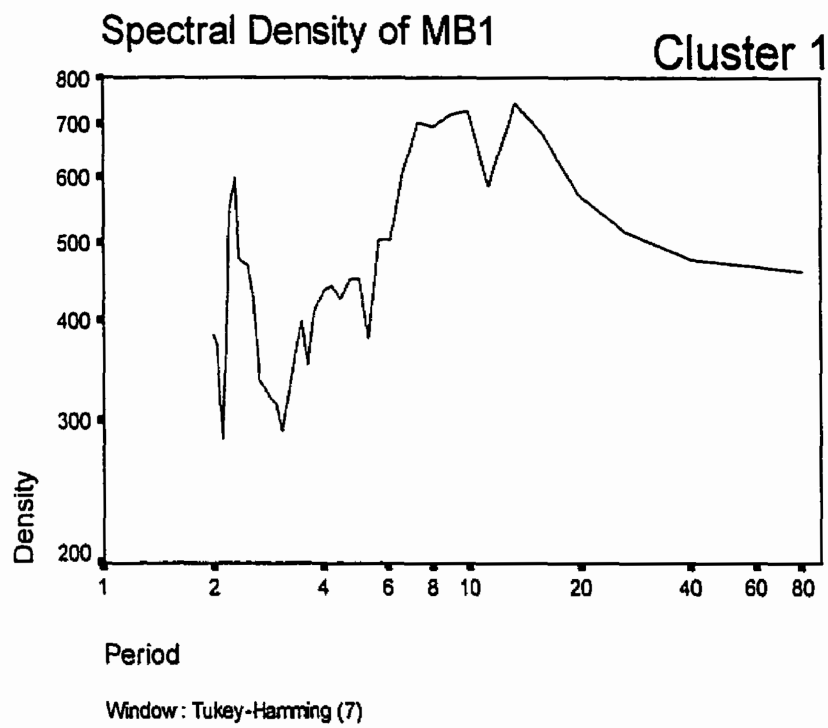

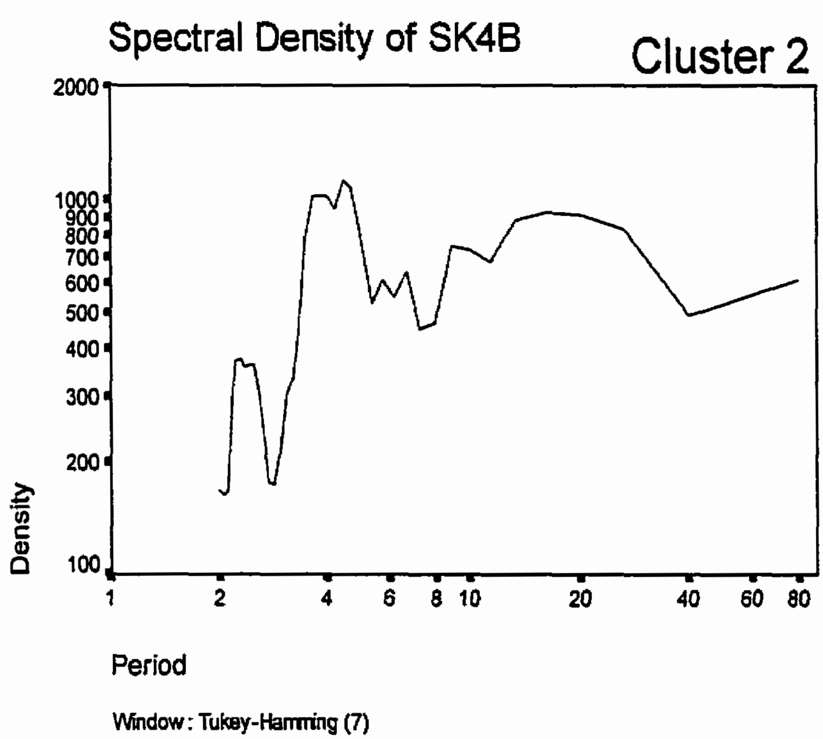

Figure 5.7 Spectral density plots (density power vs. period) for all five drought regions

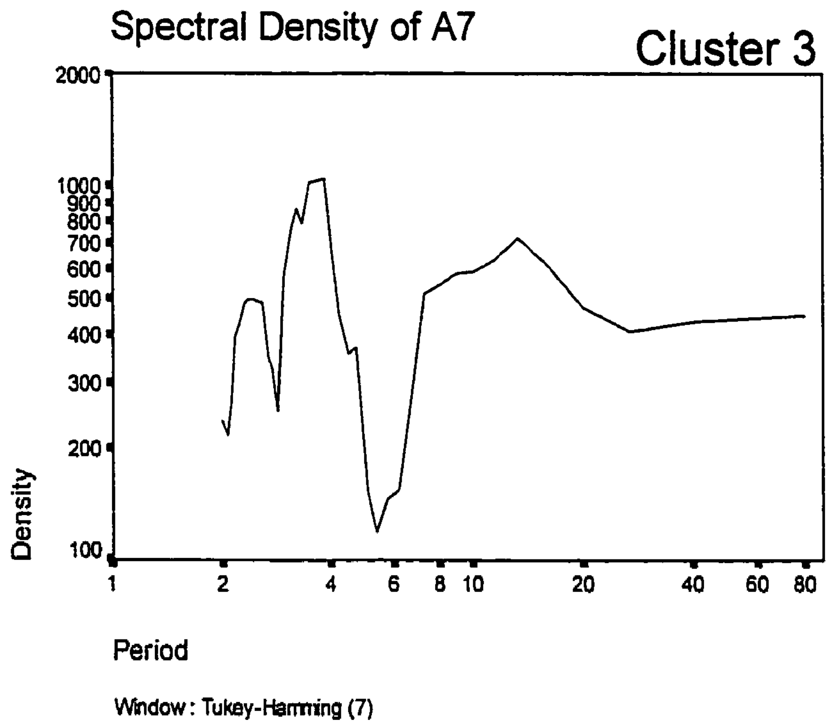

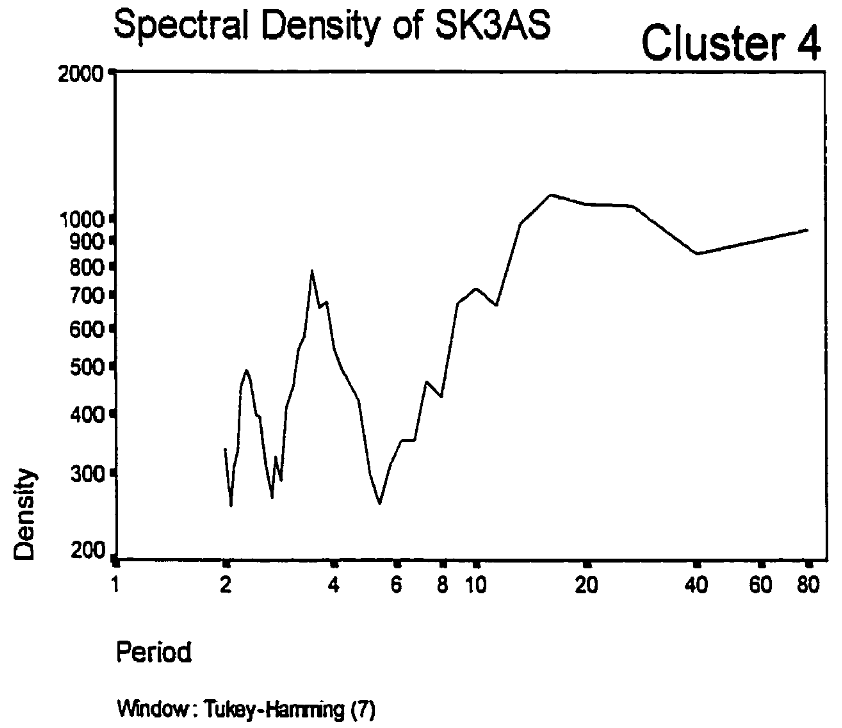

Figure 5.7 Spectral density plots (density power vs. period) for all five drought regions (cont.)

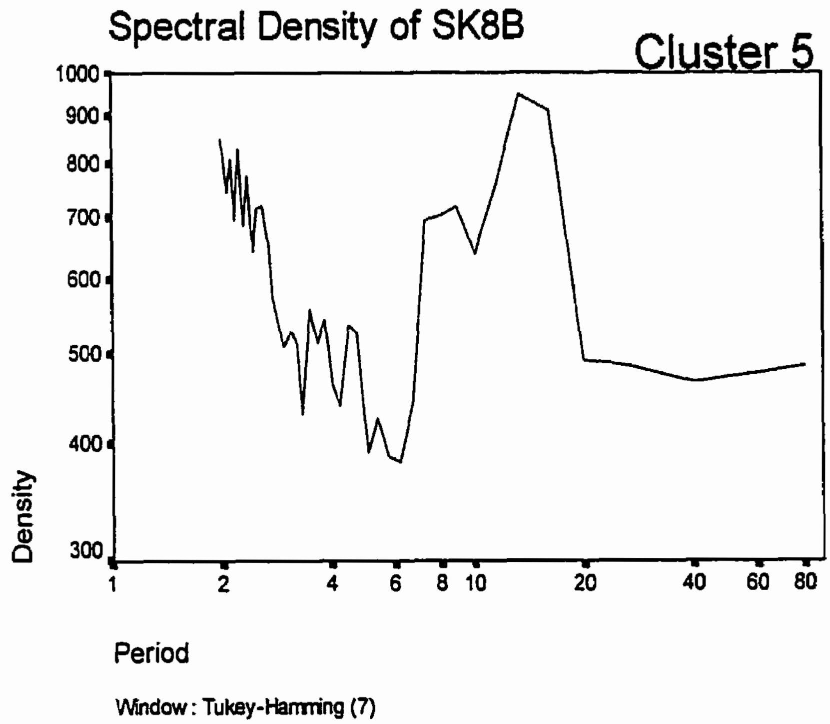

Figure 5.7 Spectral density plots (density power vs. period) for all five drought regions (cont.)

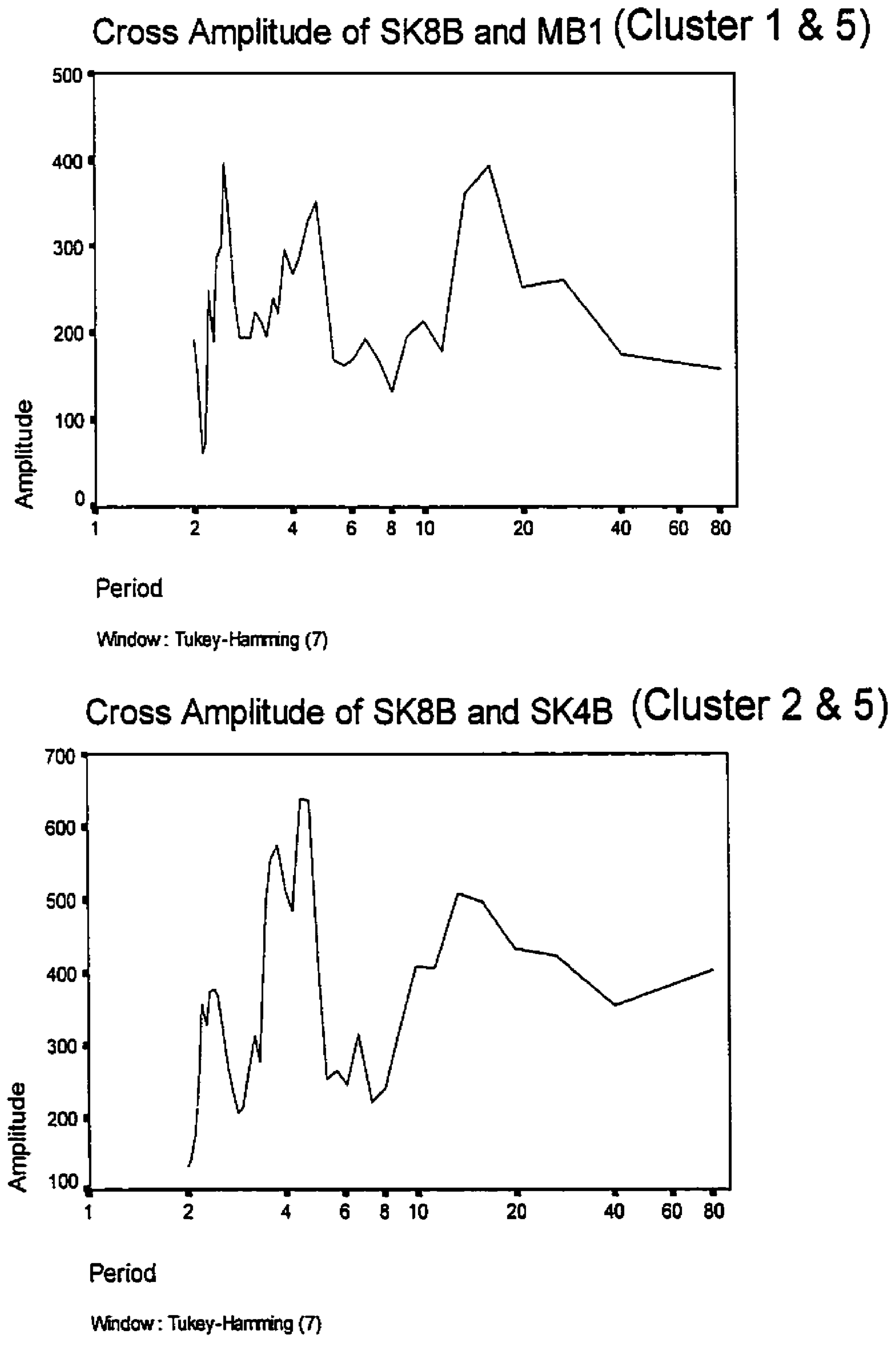

Figure 5.8 Cross amplitude plots (amplitude vs. period) comparing each of the other drought regions to Cluster 5 (SK8B)

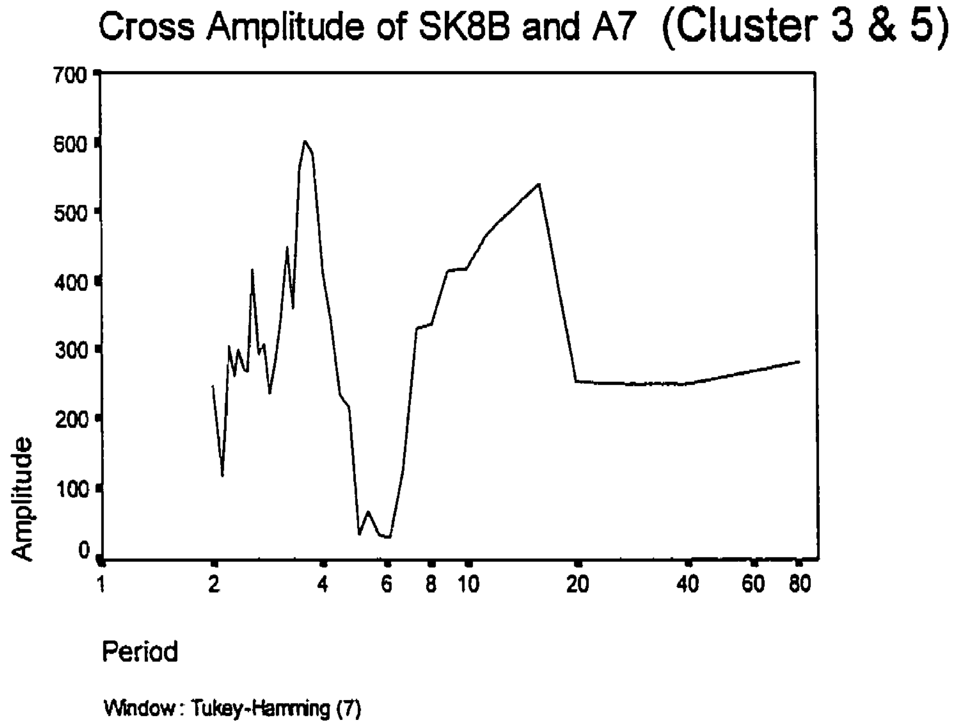

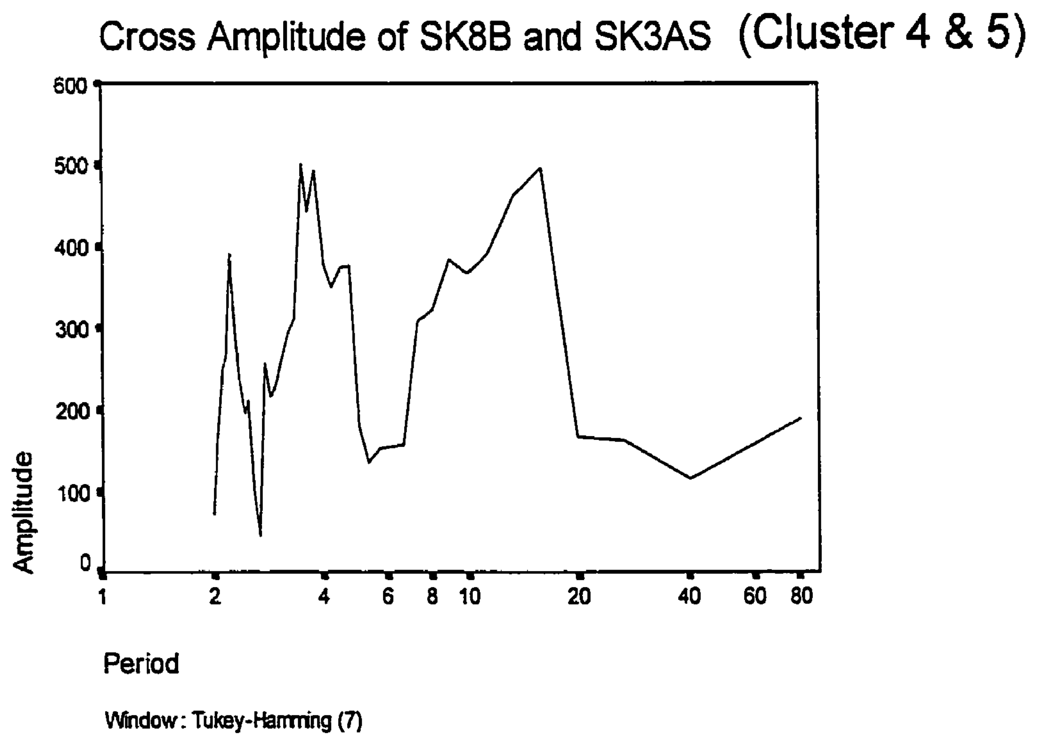

Figure 5.8 Cross amplitude plots (amplitude vs. period) comparing each of the other drought regions to Cluster 5 (SK8B)

Overall, it is apparent that all of the regions have a significant peak around 2 years. All of the regions also have a peak between 10-20 years, although the magnitude and width of this peak varies from region to region. Some of the clusters also have peaks between 7-10 years and around 4 years. A cross amplitude analysis was also carried out to quantitatively measure the agreement between regions.

The cross amplitude analysis (Figure 5.8) reinforces many of the conclusions that were drawn from a visual analysis of the spectral density plots for each region. All of the cross amplitude plots show strong and definite peaks at around two years. However, the signal is somewhat muddled in the cross amplitude plot of Cluster 3 and Cluster 5. There is also a strong, well-defined peak in the amplitude at about 4 years in all of the cross amplitude plots. Finally, there is a peak in the amplitude between 10-15 years. For the plots of Cluster 1 vs. Cluster 5 and Cluster 2 vs. Cluster 5, the amplitude begins to rise at around 8 years and then peaks between 10 and 15. For the plots of Cluster 3 vs. Cluster 5 and Cluster 4 vs. Cluster 5, the amplitude begins to rise at about 6 years and it has a minor peak at around 7 years and then continues to rise to a major peak at around 15 years.

The degree of agreement in the cross amplitude plots between all clusters is certainly striking. The quasi-2, 4, and 10-15 year oscillations are a common feature of the drought time series in all clusters and the majority of crop districts. There is also a fourth peak, with a 7-9 year oscillation, present in many of the drought spectra. The spatial coherence in the power spectra indicates that these oscillations in the drought record are more likely to be significant and not just random fluctuations that vary from station to station. Spatial coherence also means that all of the Canadian prairies are likely influenced by the same physical mechanisms. This type of spectral analysis of the drought time series is crucial because it may help to identify some of the significant factors that may be responsible for triggering drought conditions. In addition, if there are known periodicities in the prairie drought regime, they may have potential for drought forecasting.

The quasi-biennial oscillation is a common feature that is present in many precipitation time series around the world (Oladipo, 1987). The fundamental physical cause, or causes, of this oscillation are not clear. This oscillation is often attributed to the general atmospheric circulation and reversals in tropical stratospheric winds (Oladipo, 1987). It may also be related to large flux variations in the emission of ultraviolet rays by the sun; these variations have a period of about 26 months (Oladipo, 1987). Additionally, the quasi-biennial oscillation could be related to soil moisture conditions or other components of the local environment that contribute to year-to-year persistence. The literature does not give any clear indication of what mechanism might be responsible for the quasi-4-year oscillations, although in one study it has been suggested that oscillations having this return period may be related to ENSO (Oladipo, 1987). The 10-15 year oscillation is a significant feature in the drought spectra. Given the return period of this oscillation, it is possible that is may be linked to decadal-scale SST variability. Attributing this oscillation to a particular physical mechanism is beyond the scope of this study, nonetheless, this oscillation appears to be significant to the Canadian prairies.

A great deal of drought research has focused on looking for a link between sunspots and drought. In this study, there is no evidence of a 22-year oscillation in any of the drought spectra. This is of particular interest because of the long-standing debate about whether the 11-year sunspot cycle and the 22-year double sunspot cycle (Hale cycle) are related to drought (Oladipo, 1987; Padmanabhan and Ramachandra Rao, 1990). Although these cycles have been found in many other studies, there is still no conclusive evidence of how sunspots are related to drought conditions.

5.7 Chapter summary

A drought climatology for the crop-growing region of the Canadian prairies was developed by first dividing the study region into five relatively homogenous drought regions. These drought regions are composed of between 6 and 13 crop districts. The most drought vulnerable regions were Cluster 5 in north-western Saskatchewan and Cluster 2 in south-western Saskatchewan/south-eastern Alberta. Cluster 5 had the highest drought frequency. It experienced a moderate to severe drought during nearly 8% of the study period. That means that a moderate to severe drought had an average return period of thirteen years. Cluster 2 also has a high frequency of moderate to severe droughts. It experienced these conditions during 7% of the study period, or every fourteen years.

Not surprisingly, it was demonstrated that the severity and spatial extent of droughts on the Canadian prairies are strongly related. Overall, more than 77% of the variation in the spatial extent of drought events can be explained by drought severity. In other words, more severe droughts tend to cover larger areas.

The single most severe growing season drought on the Canadian prairies occurred in 1961. This drought covered more than 86% of the study region and the mean severity of the drought was -5.67. The second most severe drought to occur on the Canadian prairies was in 1988. The mean drought severity in 1988 was -4.58 and more than 77% of the study region was affected. Major droughts also occurred in many other years including 1929 (spatial extent = 65%; severity = -4.01) and 1937 (spatial extent = 69%; severity = -3.97).

The creation of a series of growing season drought maps illustrated that there are three major spatial patterns of drought on the Canadian prairies. The first pattern is linear in nature. Similar conditions extend in a line across the region and are surrounded on both sides by different conditions. The second pattern is flood or drought dominant. With this pattern, the same conditions are present in the entire study region. The final pattern is referred to as random and it is said to occur when there is no other distinct spatial pattern. Each of these patterns is likely linked to a different set of forcing factors.

Spectral analysis (FFT) revealed that there are a number of spatially consistent (present across the entire study region) periodicities in the drought index data. In particular, a quasi-biennial, quasi-4-year, and quasi-10-15 year oscillations are present across the study region. These oscillations may be the signature of a particular drought forcing function and therefore may be of use in drought forecasting.

CHAPTER 6
PREDICTION OF AGRICULTURAL DROUGHT CLIMATOLOGY ON THE CANADIAN PRAIRIES

6.1 Introduction

This chapter will explore the relationship between global teleconnections and drought on the Canadian prairies. Previous research has shown that there is a direct link between a number of these teleconnection patterns and precipitation and temperature anomalies on the Canadian prairies (Quiring, 1999; Quiring and Blair, 2000; Quiring and Blair, 2001).

The analysis will be carried out in two stages. The first stage is a composite analysis where five of the most severe growing season droughts will be used to create composites of a number of ocean and atmospheric variables. The second stage is a Principal Components Analysis (PCA) that will be used to quantify and support the findings of the composite analysis.

6.2 Composite analysis

The purpose of this section is to determine the surface boundary layer conditions and atmospheric and oceanic anomalies associated with severe growing season drought events. These composites will be used to illustrate some of the circulation and associated SST anomalies that occur coincident with severe growing season droughts, and in the seasons leading up to the drought. The five drought years used for the composite analysis were (in order of severity) 1961, 1988, 1958, 1967, and 1977.

6.2.1 Summer composites

The first and most obvious characteristic of severe droughts on the Canadian prairies is a decrease in the amount of precipitation. Figure 6.1 shows the spatial extent of the negative

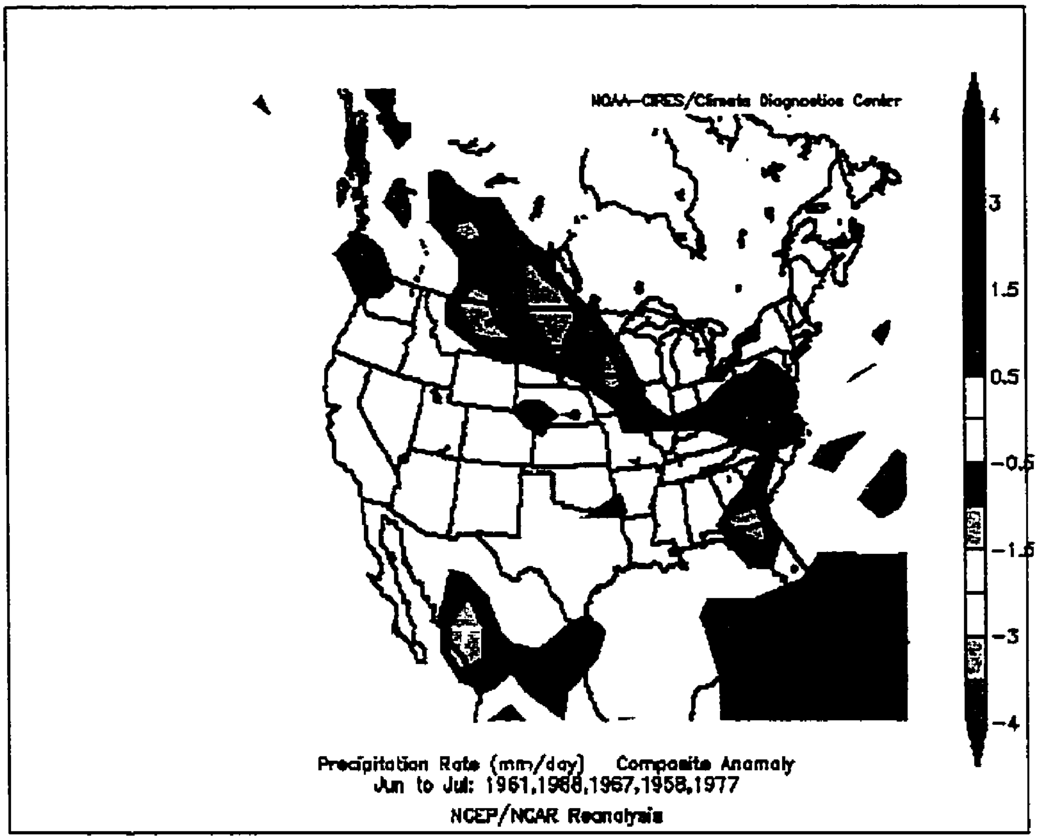

Figure 6.1 Composite growing season precipitation rate anomalies (mm/day)

precipitation rate anomaly (precipitation rate is determined by dividing the composite monthly precipitation anomaly (mm) by the number of days). Negative precipitation rate anomalies ranging from -0.5 to -1.5 mm/day cover much of Alberta, Saskatchewan, and southern Manitoba as well as extending south of the border into Montana, North Dakota, and parts of Minnesota and South Dakota. These negative precipitation anomalies also extend to the south and east along the East Coast of the United States. The coherence of these precipitation anomalies confirms the severity of the drought events chosen for the composite analysis. Interestingly, severe droughts in the Canadian prairies appear to coincide with drought events along the eastern coast of North America.

Increased surface temperatures (Figure 6.2) are also usually associated with severe growing season drought events because incoming solar energy becomes a sensible heat flux instead of a latent heat flux. The composite average temperature in the study region is approximately one degree Celsius warmer than normal. Surface temperature anomalies and OLR are closely related through Boltzmann's Law, since areas with higher surface temperatures have more available energy at the surface. Figure 6.3 shows the growing season OLR anomalies for North America. During severe drought events, there are strong positive OLR anomalies (W/m^2) over much of western North America. This anomaly pattern should be expected because there is typically less cloud cover during drought events (due to the persistent high pressure and strong subsidence) and therefore more long-wave radiation can escape relatively unimpeded.

The potential evaporation anomalies (W/m^2) (Figure 6.4) show that there is a wide band of above normal evaporation that stretches from northern British Columbia across the Prairie Provinces and down the east coast of the United States. The region of maximum potential evaporation anomalies (> 60 W/m^2) is centred over southern Alberta and Saskatchewan. These

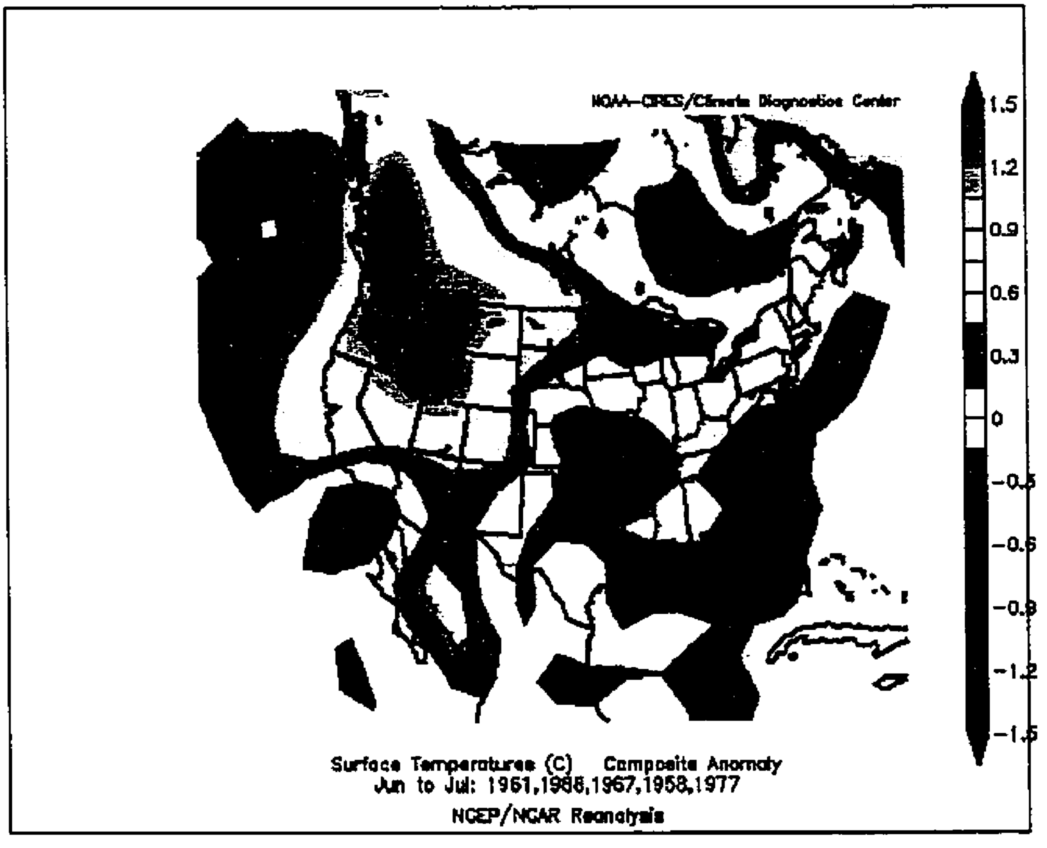

Figure 6.2 Composite growing season surface temperature anomalies

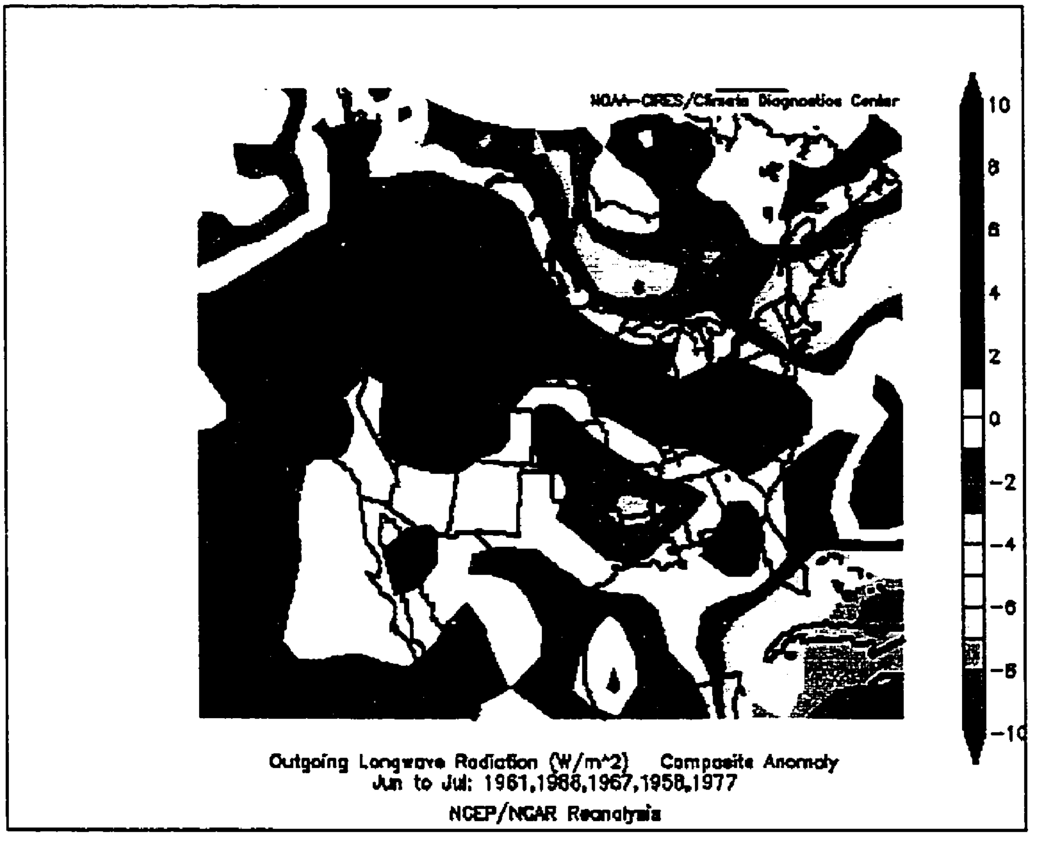

Figure 6.3 Composite growing season outgoing longwave radiation (OLR) anomalies (W/m^2)

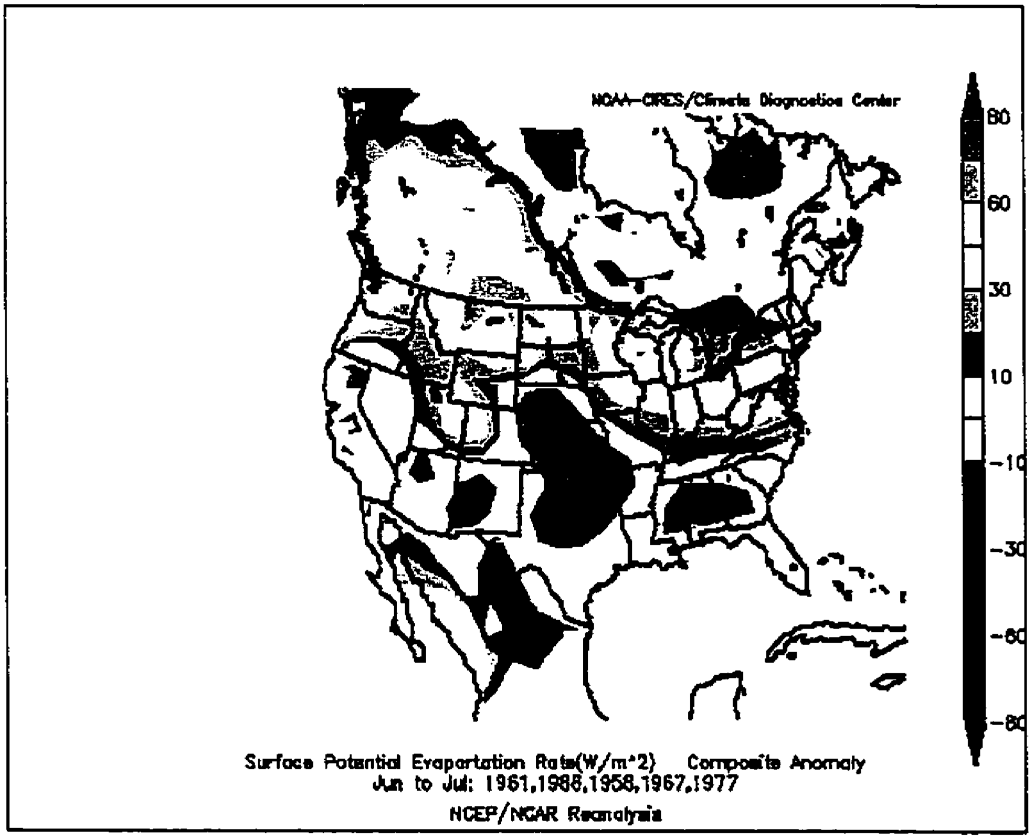

Figure 6.4 Composite growing season potential evaporation rate anomalies (W/m^2)

significantly higher rates of potential evaporation are a result of the higher amounts of energy available at the surface. The pattern is similar to that of the OLR anomalies.

Negative soil moisture anomalies also stretch from northern British Columbia across the Prairie Provinces and down the east coast of the United States (Figure 6.5). In addition, there is a band of negative soil moisture anomalies encompassing the mountains on the western side of North America. The area of maximum negative soil moisture departures covers southern Alberta and Saskatchewan and most of Montana. Boundary layer conditions, such as soil moisture, are particularly important because they play a role in initiating and sustaining severe drought events.

The pattern for relative humidity (Figure 6.6) is also similar to the pattern previously described for soil moisture, OLR, and evaporation rate. The composite relative humidity is about 5% below normal for the study region. This is due to the lack water available at the surface because of the lower than normal soil moisture levels and precipitation rates, coupled with higher than normal temperatures.

Figure 6.7 shows the summer tropical Pacific SST anomalies associated with severe prairies growing season droughts. The most striking feature in this figure is the anomalously cold water in the eastern equatorial Pacific (Niño-3 region). The composite anomaly is nearly one degree Celsius below normal during June and July. This indicates that severe drought on the Canadian prairies tends to coincide with La Niña-like conditions.

Figure 6.8 shows the summer global SST anomalies (note the different scale used to show global SST anomalies versus eastern equatorial SST anomalies) associated with severe drought conditions in the Canadian prairies. The negative anomaly covering a significant portion of the eastern equatorial Pacific can still be observed. There are also a number of other significant anomalies that are of interest. Firstly, there are a number of areas of positive SST anomalies off

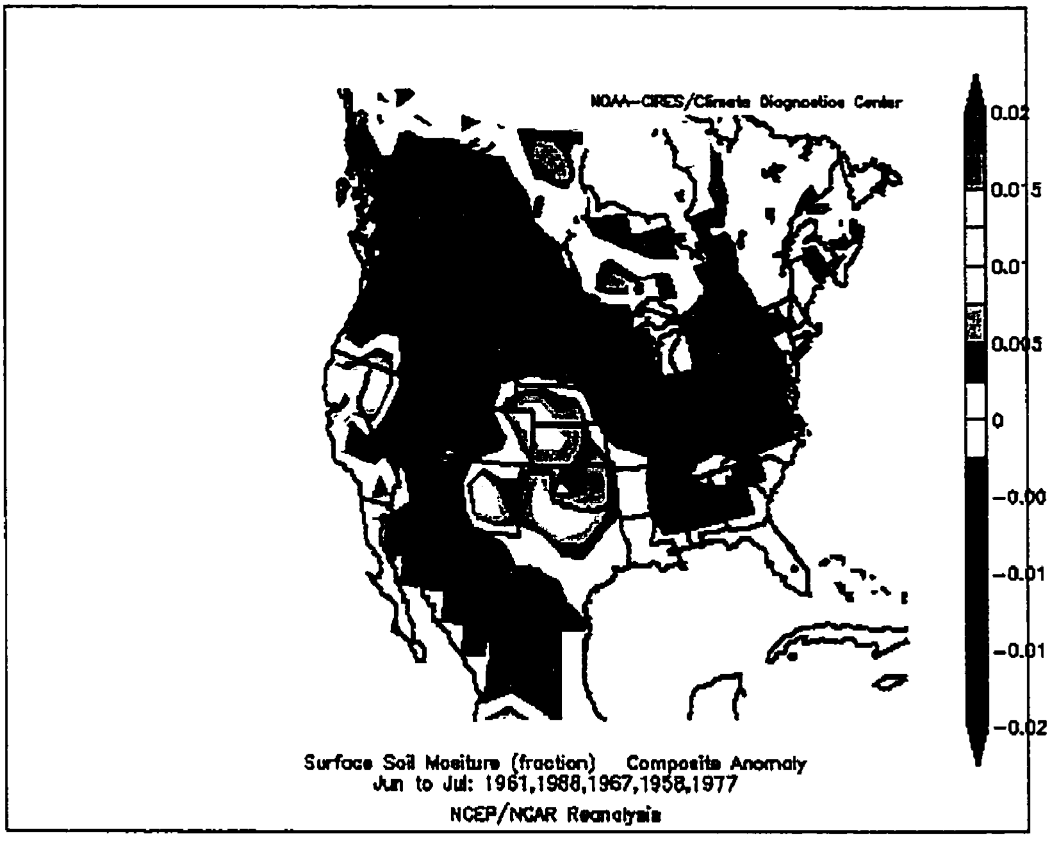

Figure 6.5 Composite growing season surface soil moisture anomalies

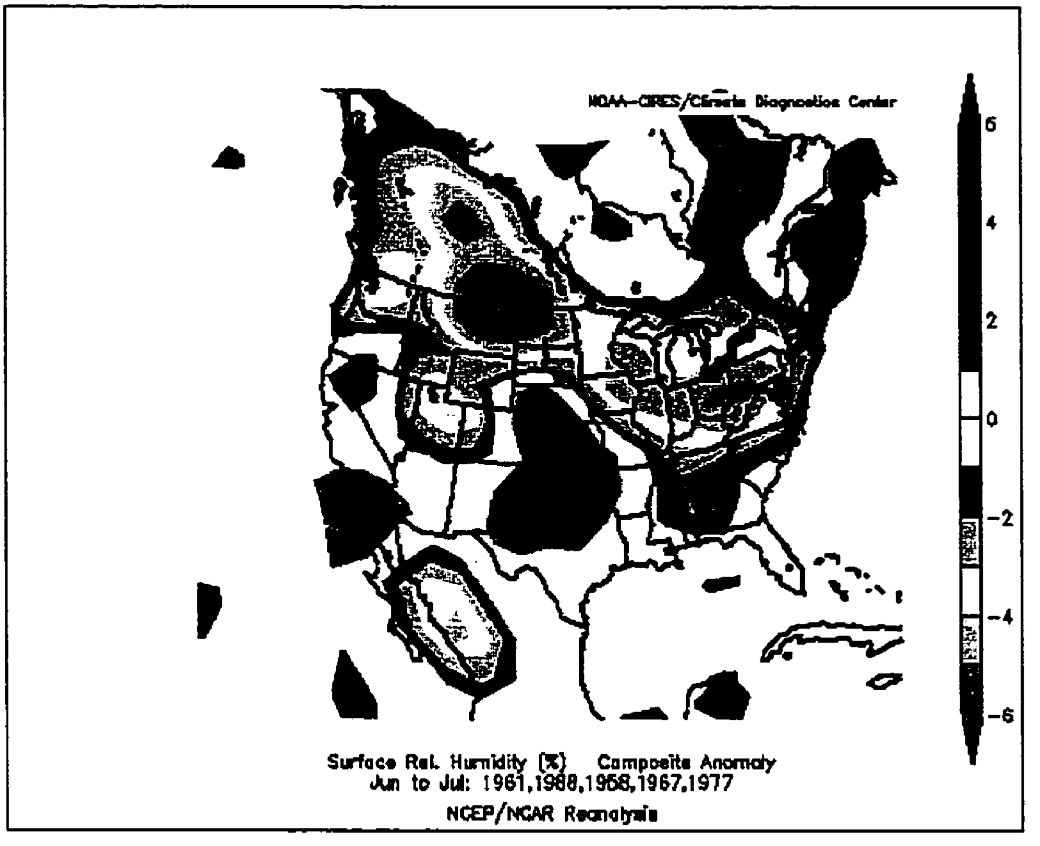

Figure 6.6 Composite growing season relative humidity anomalies (%)

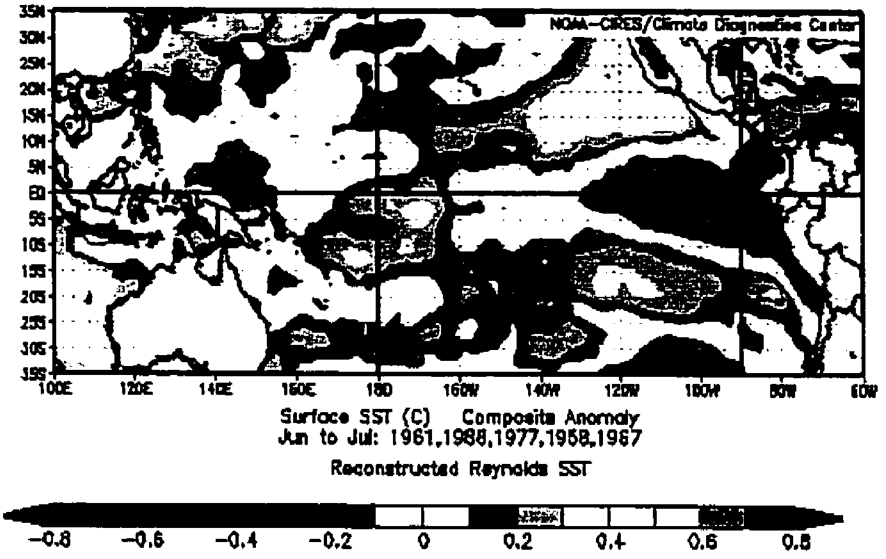

Figure 6.7 Composite growing season tropical Pacific SST anomalies

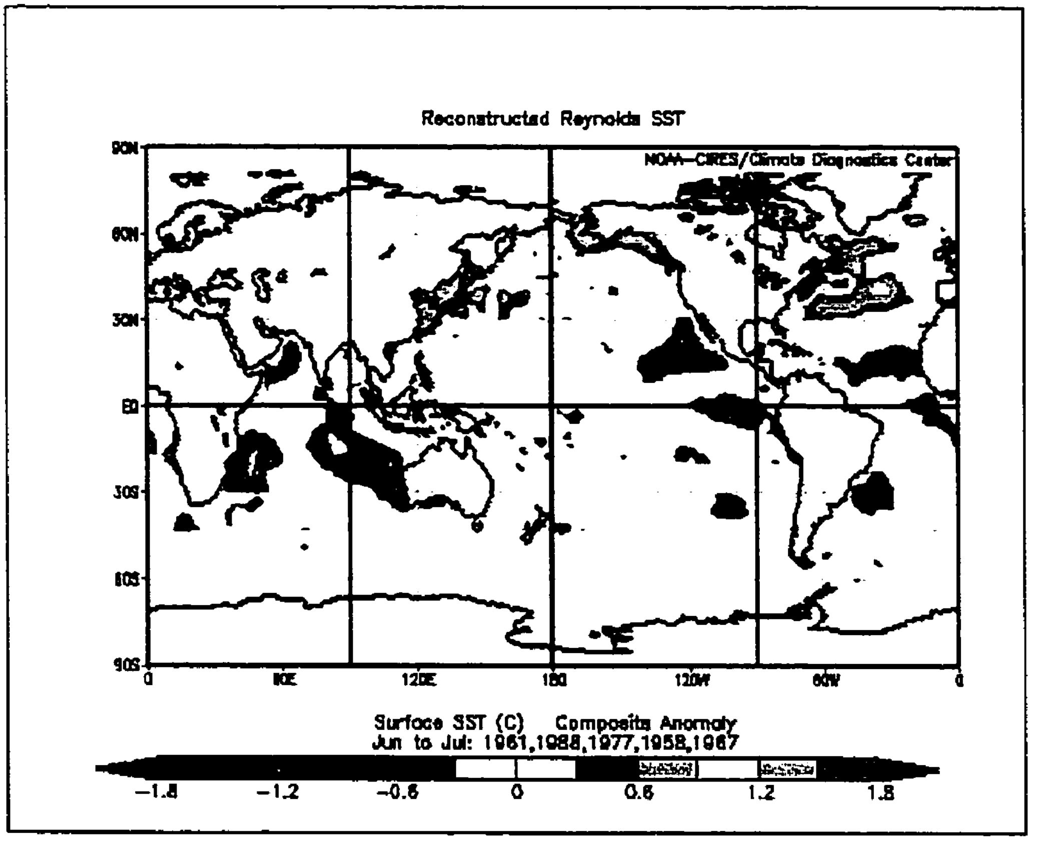

Figure 6.8 Composite growing season global SST anomalies

the west coast of North America from Oregon to Alaska. Indicating that positive SST anomalies off the west coast of North America tend to coincide with severe drought. There are also two other large regions where there are consistent positive SST anomalies, the first in the eastern Pacific around Japan, and the second in the North Atlantic extending south from Greenland to cover a significant portion of the North Atlantic. A pool of anomalously cool water is also present off the eastern United States coast. The SST anomalies in the Atlantic may be linked to the Arctic (North Atlantic) Oscillation and consequently related to severe drought on the Canadian prairies.

Figures 6.9, 6.10, and 6.11 show the composite geopotential height anomalies and composite mean geopotential height (m) of the 300, 500, and 700 mb surfaces over North America. Each of these figures illustrates that severe drought conditions on the Canadian prairies are associated with pronounced positive geopotential height anomalies centred over southern British Columbia and Washington, and pronounced negative geopotential height anomalies in northern Quebec. The strong upper level ridging over British Columbia and the western portion of the study region and strong upper level troughing in eastern North America creates a more meridional flow over the study region. There is also an extra trough present over California in the 700 mb composite mean geopotential height maps that is not present in the other upper level maps. According to Romolo (1998), this is a normal part of the mean 700 mb height pattern.

Composite mean sea-level pressure (MSLP) anomalies and mean MSLP (mb) for the growing season are shown in Figure 6.12. The dominant pattern that was clearly visible in the upper level data is not quite as clear when looking at the surface pressure map. Essentially there is still a persistent anomaly of higher than normal pressure in the west, but it is located just off the coast of British Columbia and over southern California. There is also still a persistent

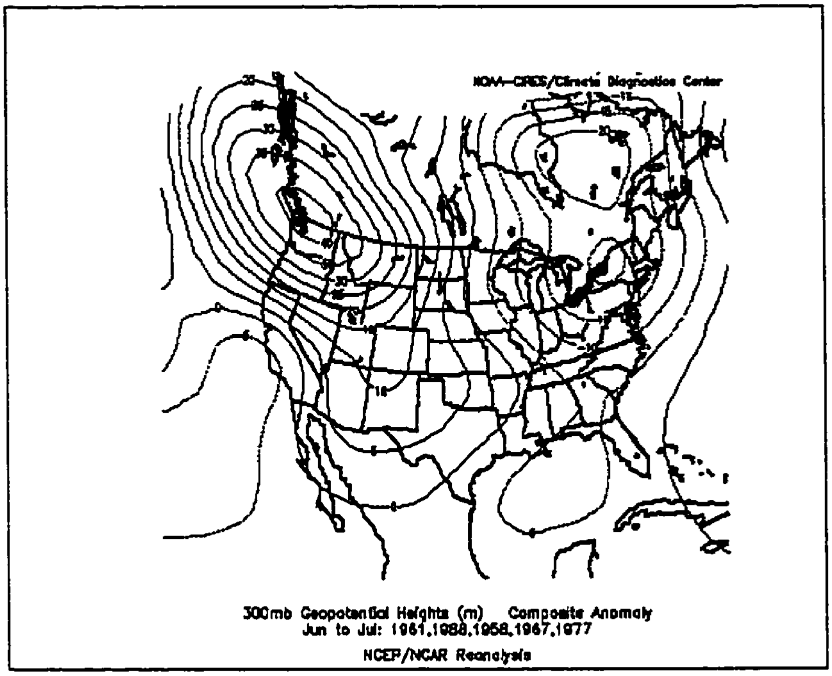

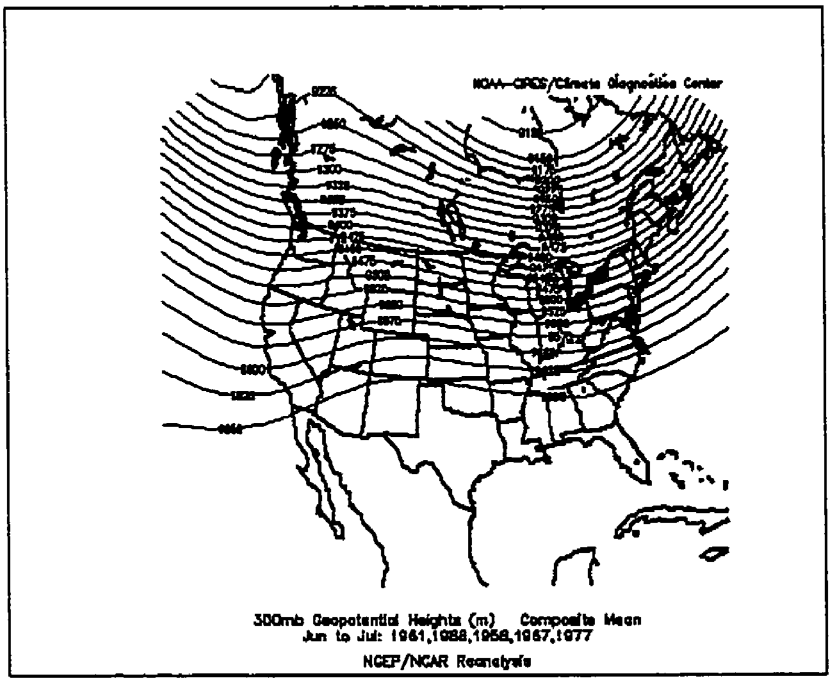

Figure 6.9 Composite growing season 300 mb geopotential height anomalies (m) and mean geopotential height (m)

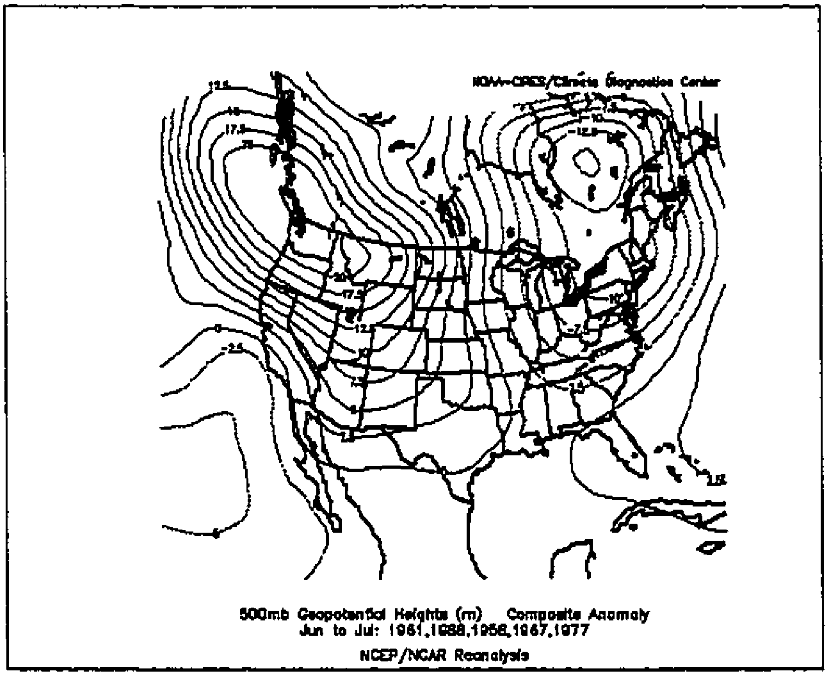

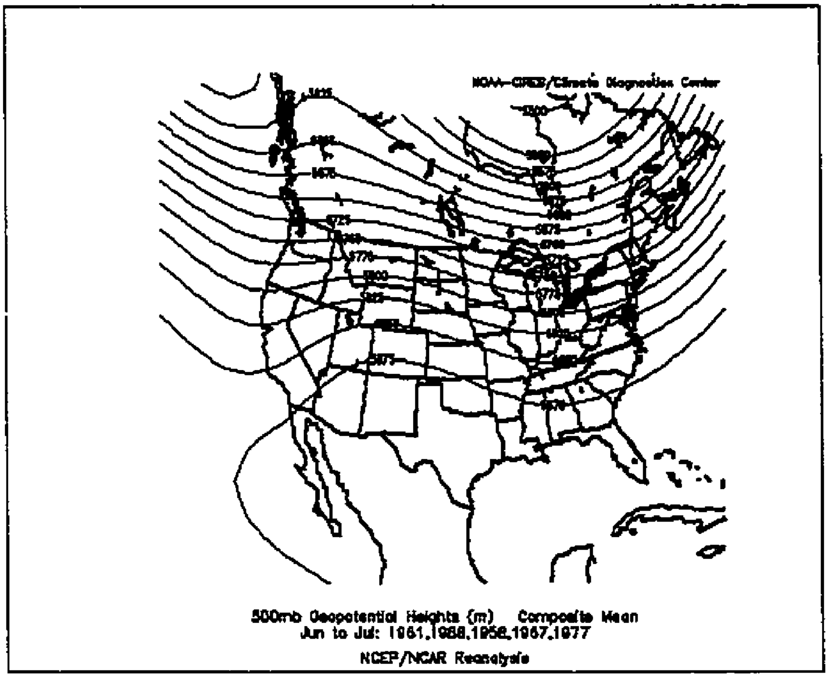

Figure 6.10 Composite growing season 500 mb geopotential height anomalies (m) and mean geopotential height (m)

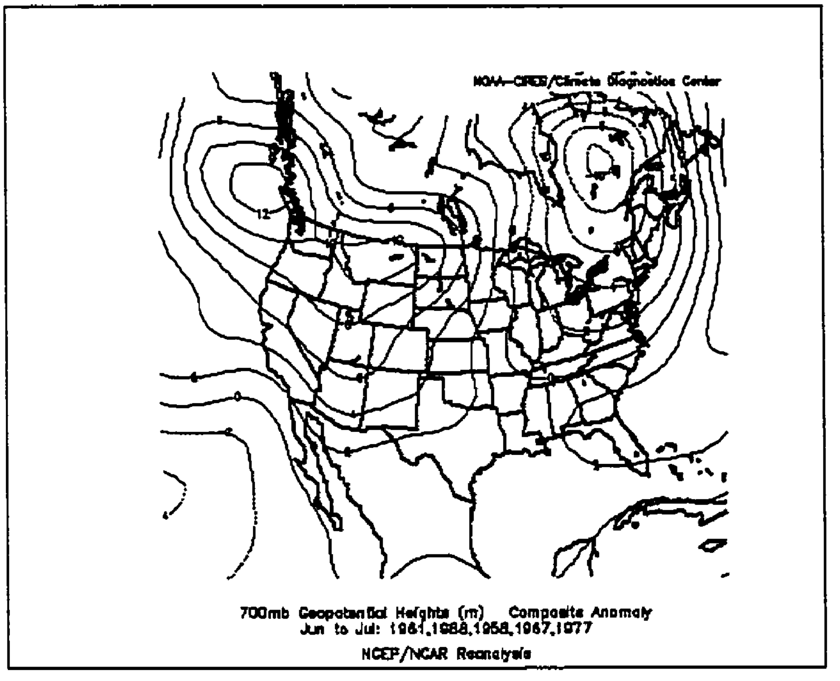

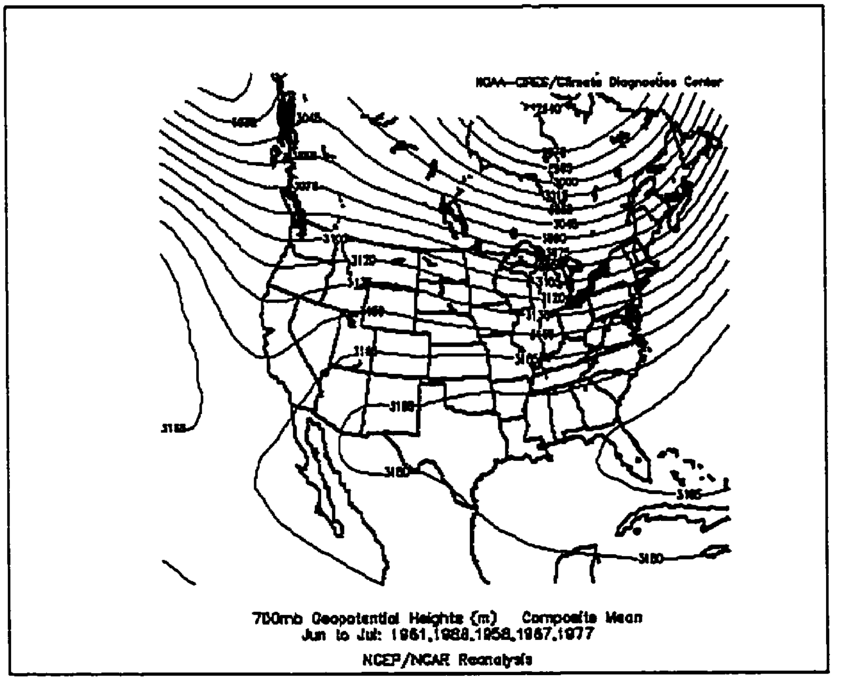

Figure 6.11 Composite growing season 700 mb geopotential height anomalies (m) and mean geopotential height (m)

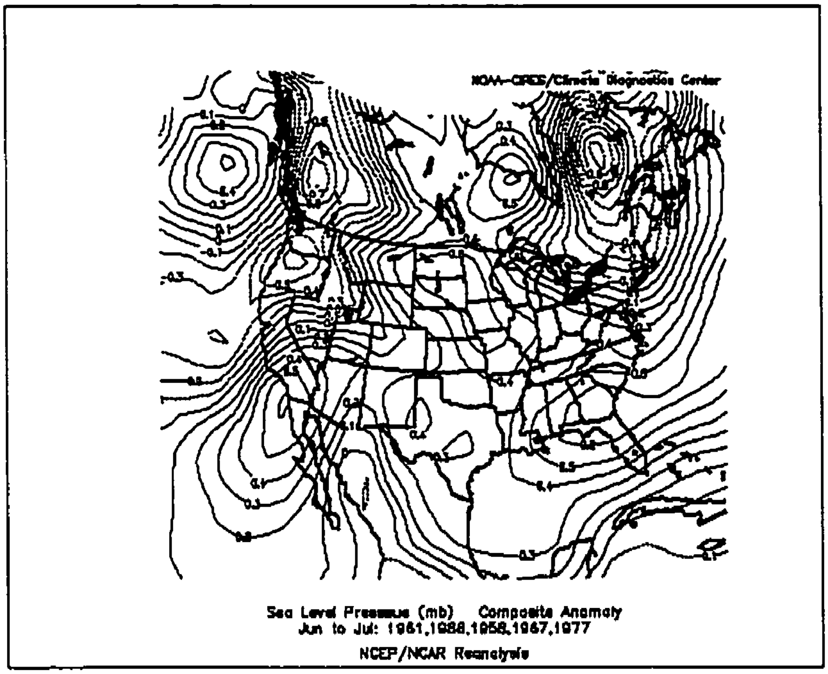

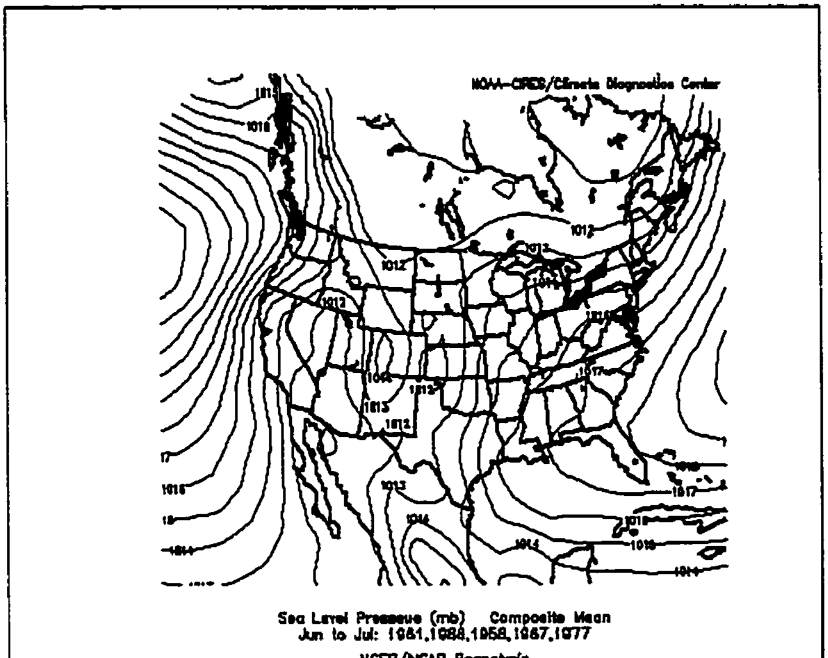

Figure 6.12 Composite growing season Mean Sea Level Pressure (MSLP) anomalies and mean MSLP (mb)

anomaly of lower than normal pressure located in northern Quebec. There is also a low-pressure anomaly over mainland British Columbia and a number of small anomalies of higher than normal pressure that run down the centre of the continent from northern Ontario to Texas. The MSLP maps are not as consistent or easy to interpret as the maps of upper level flow. In addition, the differences in the near-surface circulation are not very large, compared to the significantly anomalous conditions in the upper atmosphere.

It is worthwhile to include the MSLP in the composite analysis section because it provides a complete picture of the atmosphere, but the upper level maps are much more useful for interpretation and presentation. The upper level maps are particularly important because they are associated with changes in moisture transport, storm track positions, and the jet stream.

The polar jet stream is normally located along the polar front at an altitude of between 8000-10000 m (Romolo, 1998). The normal summer-time position of the jet stream is around 48°N (Trenberth and Guillemot, 1996). The 300 mb level was chosen because of its association with the jet stream. The position of the jet stream is taken as the core of the highest wind speeds at the 300 mb level. It is evident from the composite mean 300 mb geopotential height map (recall Figure 6.9) that the location of the jet stream over the study area, as determined by the area with the strongest pressure gradient along the polar front, is around 52°N. Therefore, during severe drought the jet stream tends to be located well to the north of its normal summer time position.

Figure 6.13 shows the composite 300 mb wind anomalies and mean winds (m/s). The location of the jet stream is denoted by the highest velocity winds on the mean wind composite map. The jet stream passes over top of the study region, but weakens in strength. The maximum velocity winds are found off the west coast of North America and from Ontario out to the east

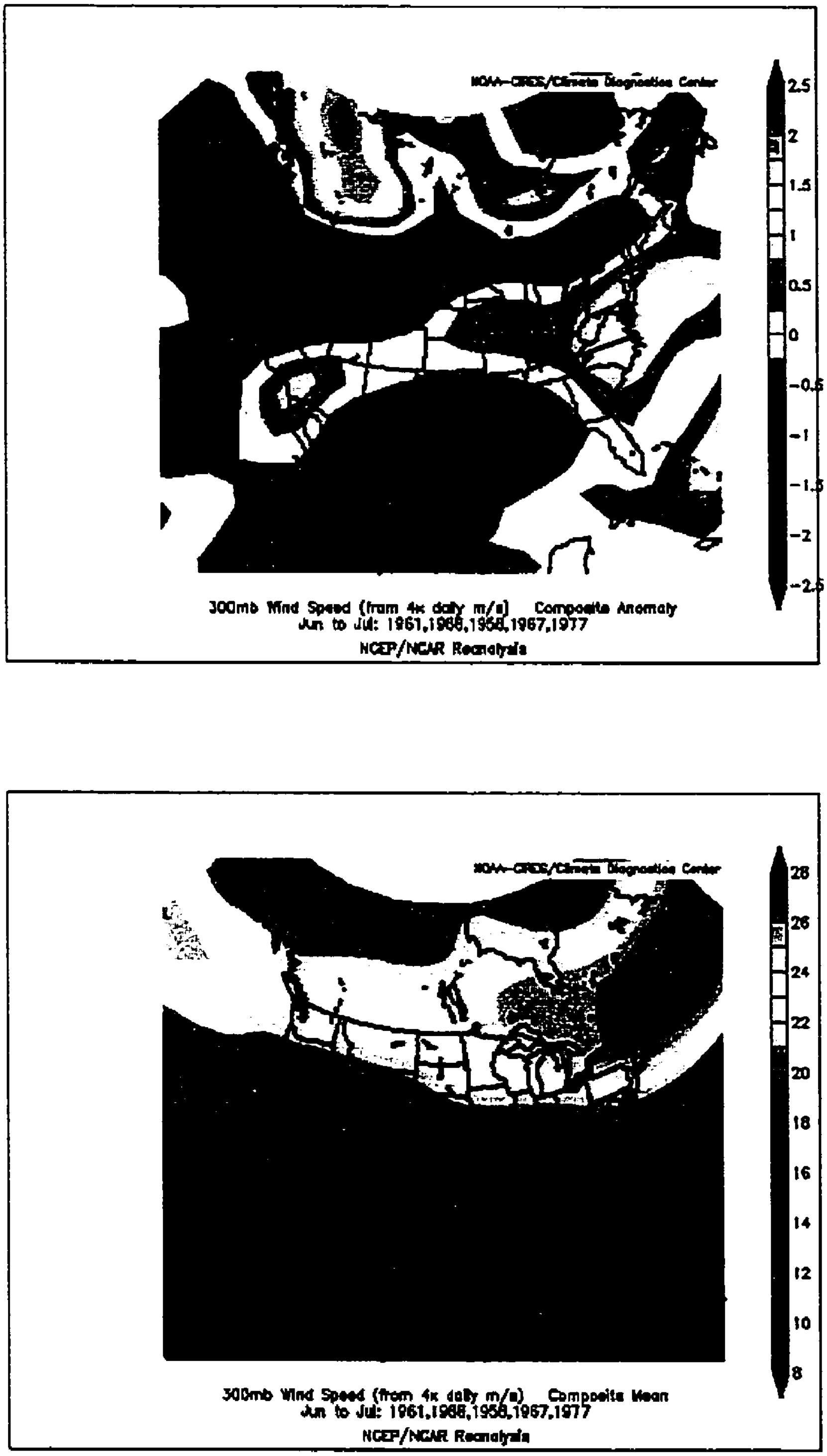

Figure 6.13 Composite growing season 300 mb wind speed anomalies and composite mean wind speed (m/s)

coast. During severe drought events, the wind velocities over the Canadian prairies are seen to decline slightly.

The 300 mb wind anomaly map also illustrates the shift in the position of the jet stream as compared to normal. There is a large band of below normal wind velocities that extends from off the west coast of British Columbia all the way across the United States and into Ontario. This band represents a more typical summer position of the jet stream. There is also a band of above normal wind velocity that extends down into the study region in a northwesterly direction. This illustrates how the flow over the study region has shifted to a more meridional regime.

6.2.2 Spring composites

Figure 6.14 shows the spring tropical Pacific SST anomalies associated with severe prairies growing season droughts. The composite shows that SSTs in the eastern equatorial Pacific are slightly above normal during the spring of severe drought years. However, a small tongue of colder than normal water is evident along the equator in the eastern Pacific.

Figure 6.15 shows the spring global SST anomalies associated with severe drought conditions on the Canadian prairies. There is a significant pool of colder than normal water in the centre of the northern Pacific. The surrounding water along the east coast of Asia, the west coast of North America, and just north of the equator is warmer than normal. This pattern of SST anomalies in the North Pacific is quite similar to that of the positive (warm) phase of the Pacific Decadal Oscillation (PDO). Much of the North Atlantic has above normal SSTs except for a band of cold water along the east coast of North America.

Figures 6.16, 6.17, and 6.18 show the composite geopotential height anomalies and composite mean geopotential height (m) of the 300, 500, and 700 mb surfaces for spring. Each of these figures shows that spring conditions prior to severe drought events on the Canadian

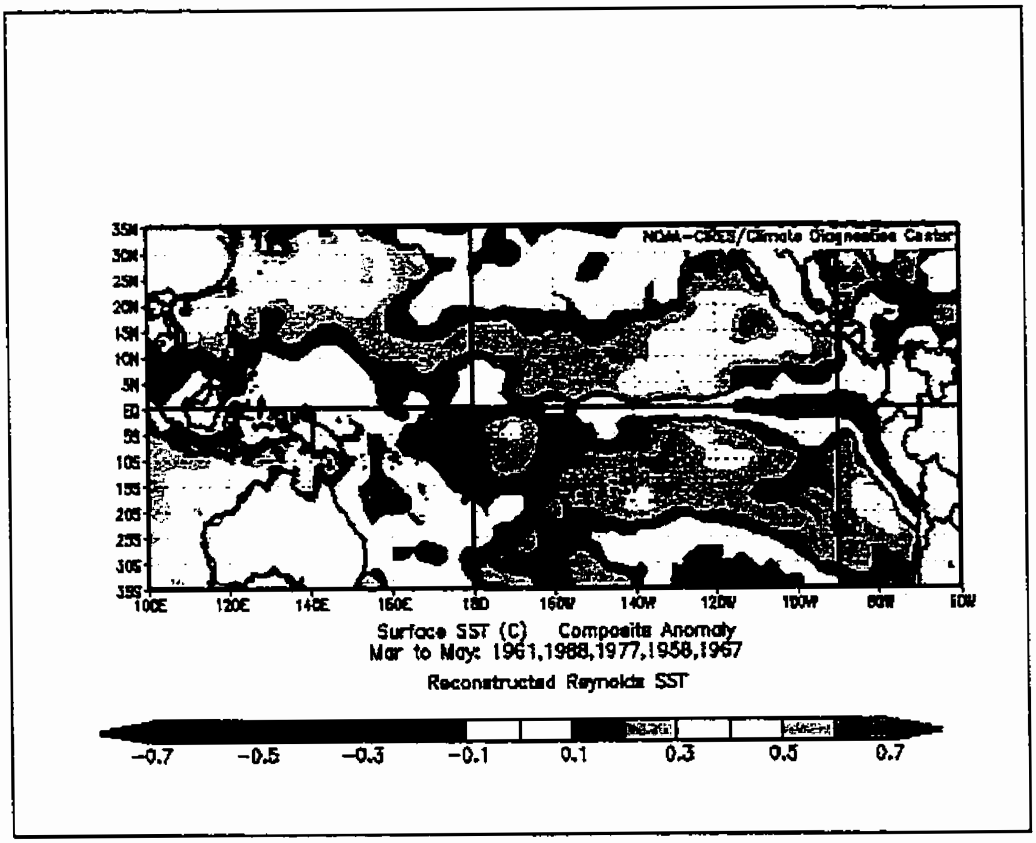

Figure 6.14 Composite spring tropical Pacific SST anomalies

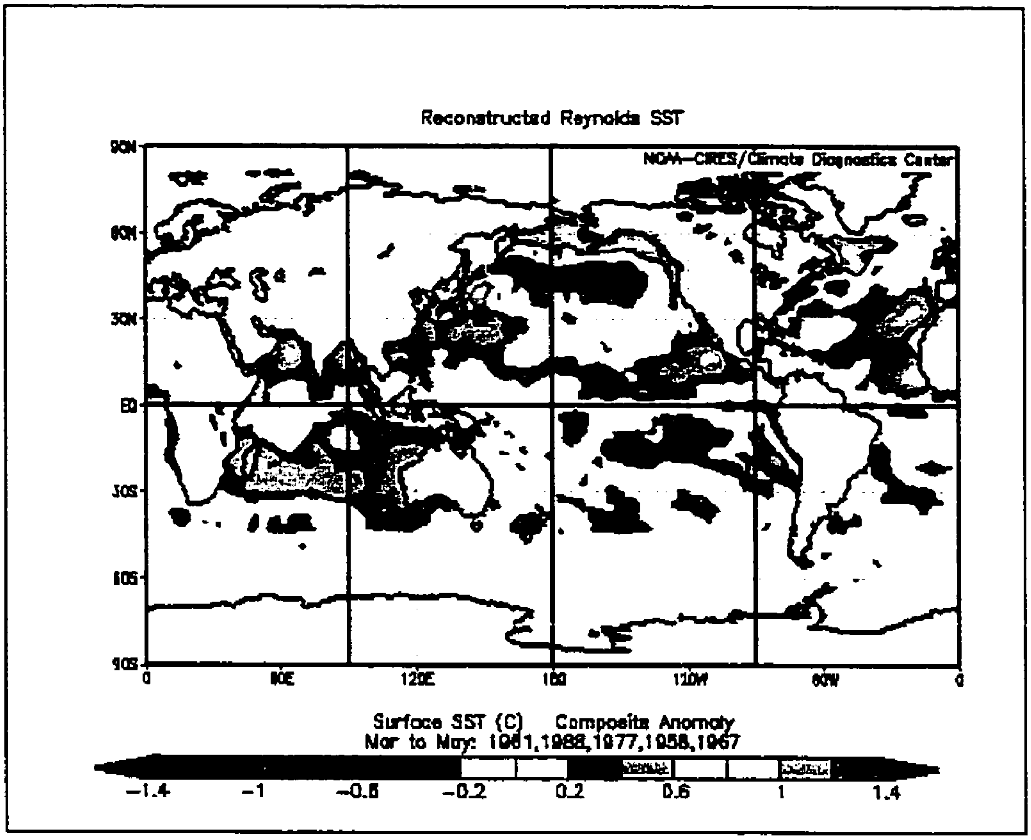

Figure 6.15 Composite spring global SST anomalies

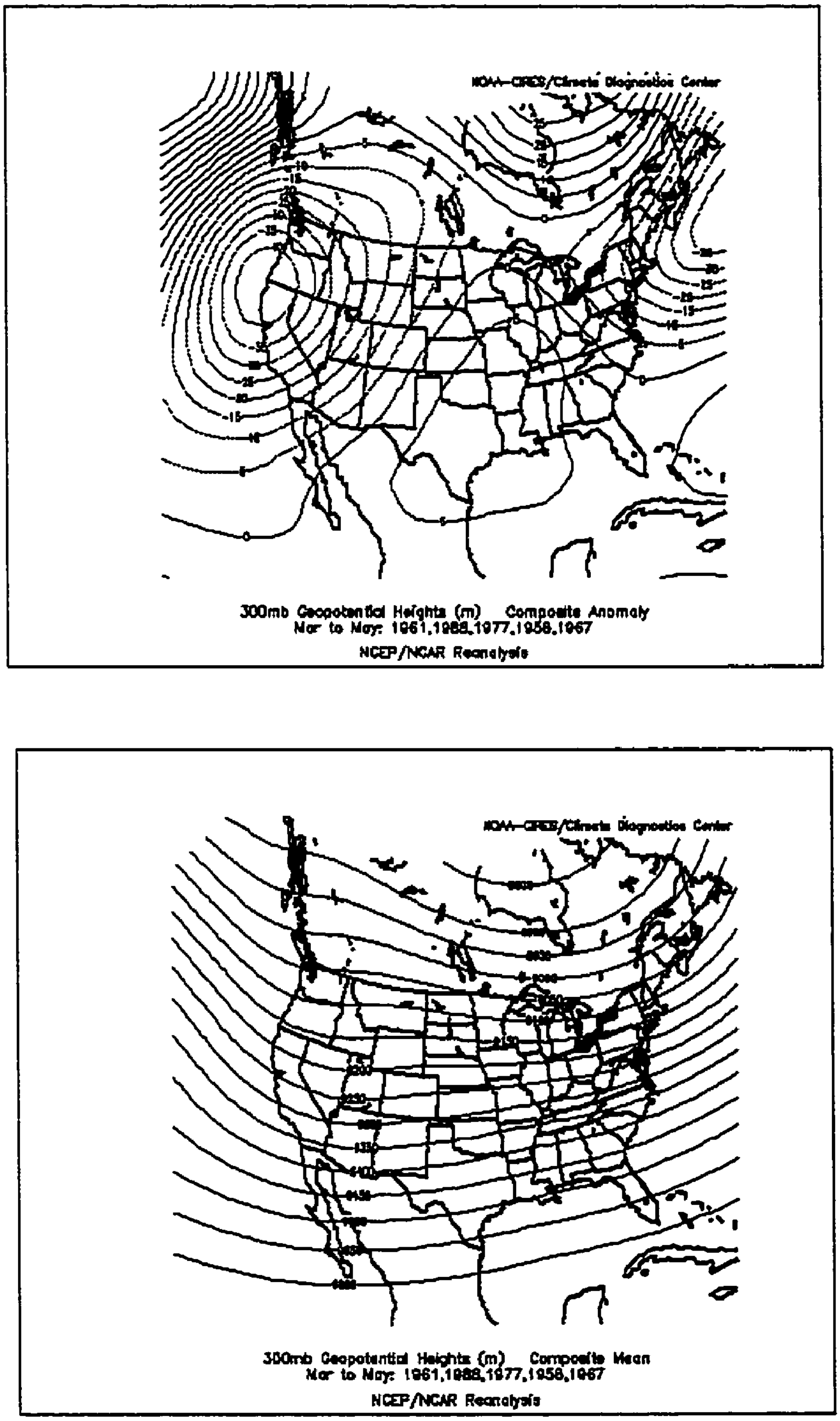

Figure 6.16 Composite spring 300 mb geopotential height anomalies (m) and mean geopotential height (m)

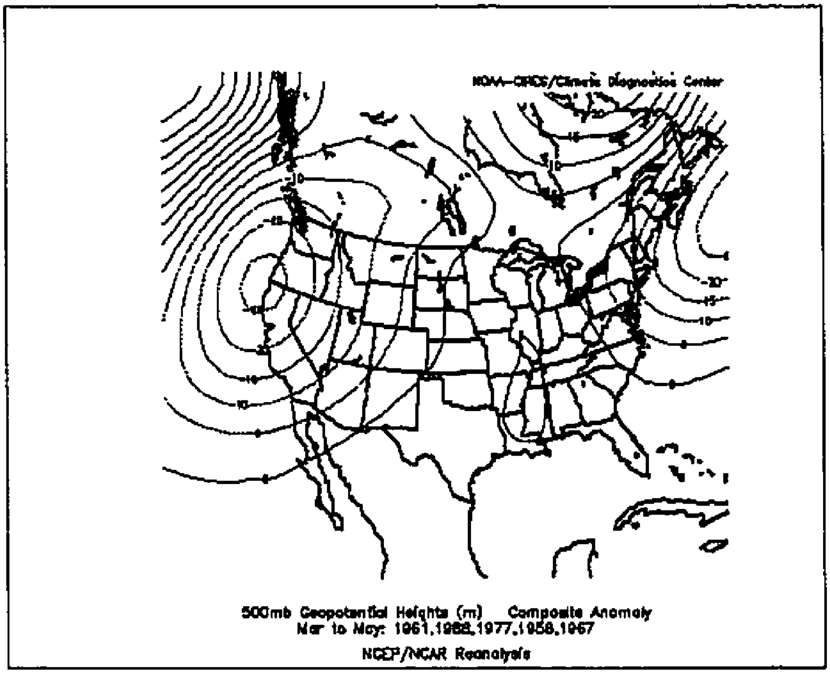

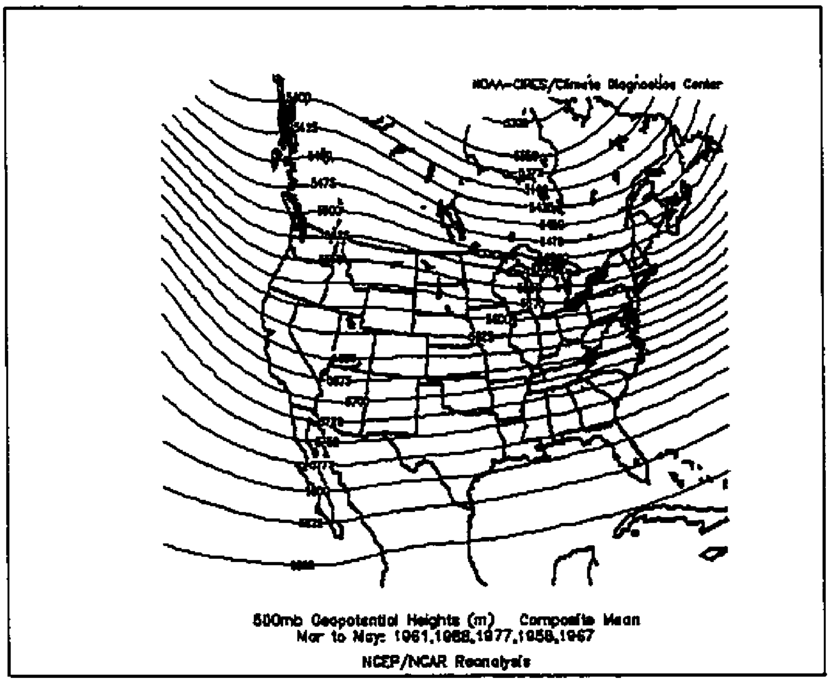

Figure 6.17 Composite spring 500 mb geopotential height anomalies (m) and mean geopotential height (m)

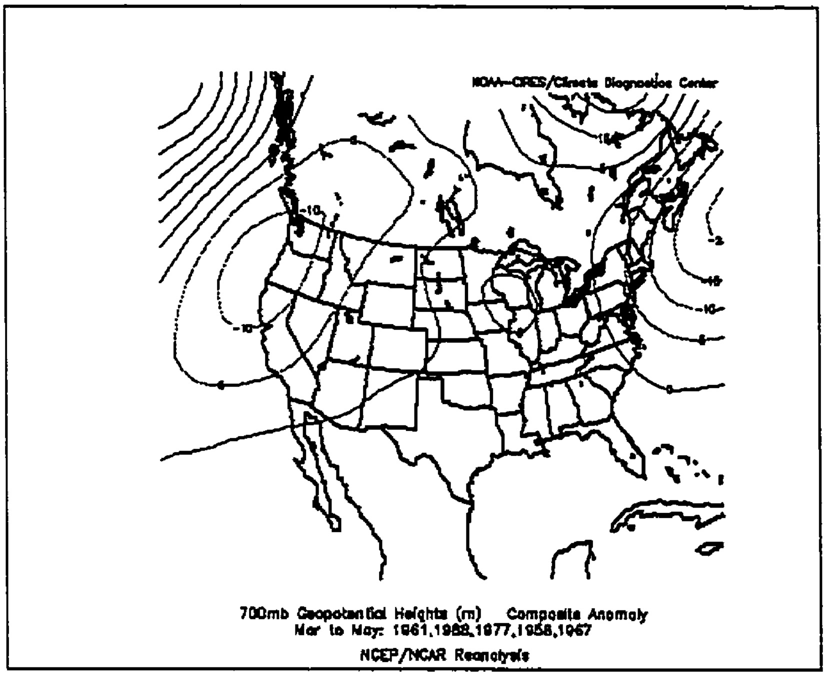

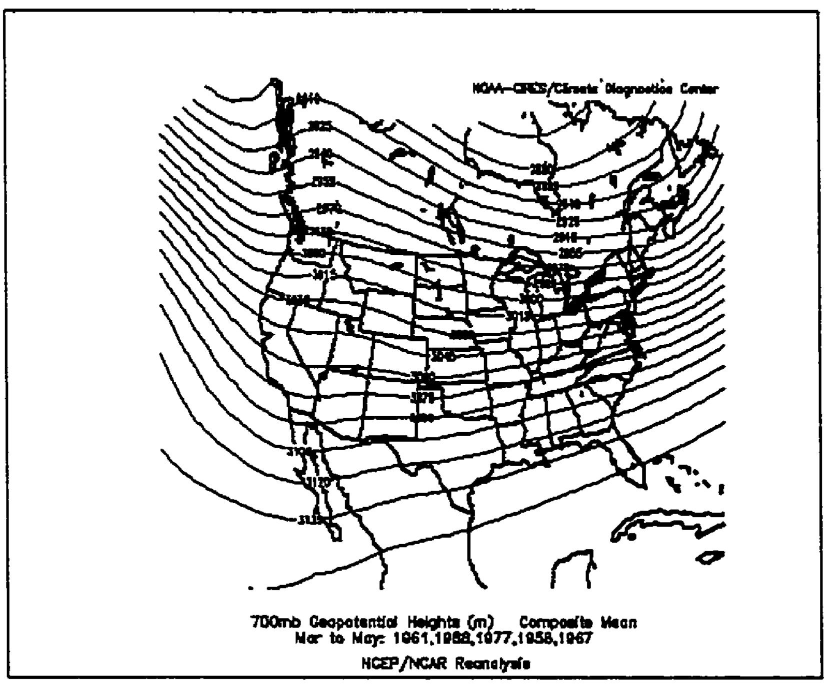

Figure 6.18 Composite spring 700 mb geopotential height anomalies (m) and mean geopotential height (m)

prairies are associated with pronounced negative geopotential height anomalies centred over the west coast of the United States. A weak trough is present over the west coast of North America and the ridge over the Rocky Mountains is much less pronounced than usual. There is also an accompanying negative geopotential height anomaly off the east coast of North America and a positive height anomaly over northern Quebec. These anomalies are present at all three levels of the atmosphere and are particularly interesting because they are opposite in sign to those that are present during the growing season.

Figure 6.19 shows the spring composite 300 mb wind anomalies and mean winds (m/s). During spring, the jet stream normally passes well to the south of the study region because it is only just beginning to make its way north. The 300 mb wind anomalies show a band of faster than normal wind speeds (+1 to +3 m/s) that stretches from the southwestern U.S. towards the northeast. North of the border, wind speeds are slightly lower than normal (-1 to -3 m/s). This indicates that the jet stream has been displaced slightly to the south of its normal spring-time position.

6.2.3 Winter composites

Figure 6.20 shows the winter tropical Pacific SST anomalies associated with severe prairies growing season droughts. Generally, the ocean temperature in the eastern equatorial Pacific during the winter prior to a severe growing season drought are nearly one degree above normal. A large pool of anomalously warm water dominates the eastern and central equatorial Pacific. These SST anomalies are indicative of El Niño conditions during the December to February period prior to a severe drought event.

Figure 6.21 shows the winter global SST anomalies associated with severe drought conditions in the Canadian prairies. Similar to spring, there is a significant pool of colder than

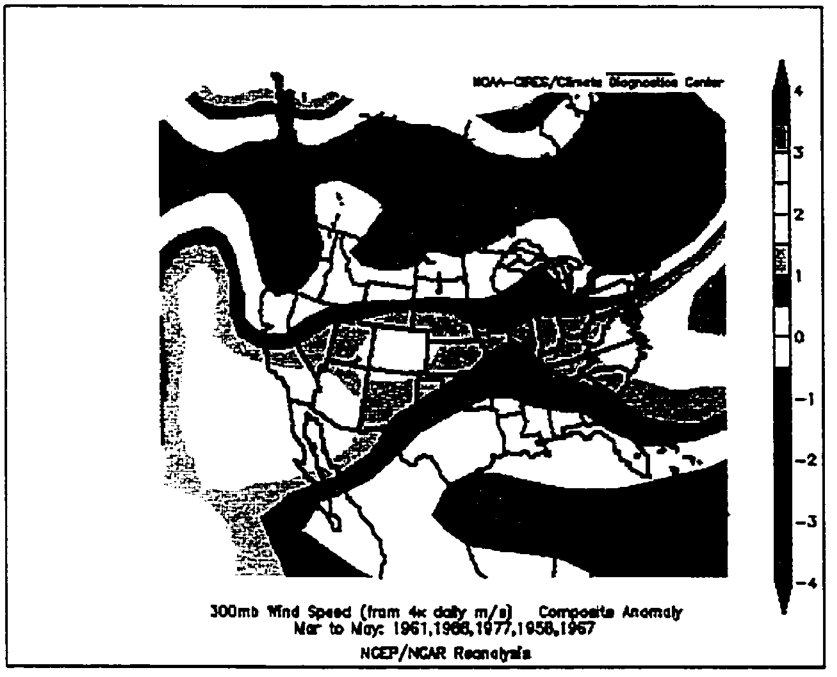

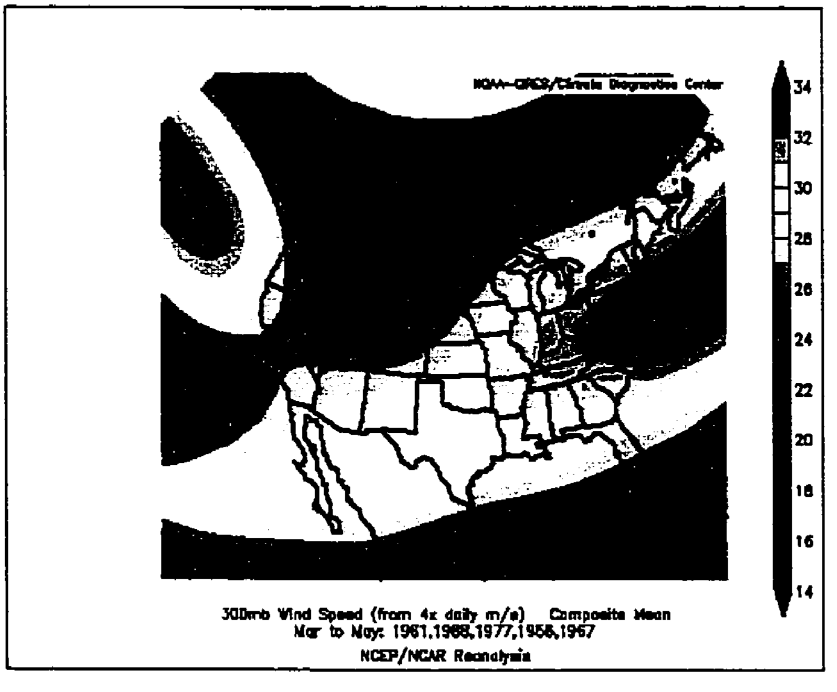

Figure 6.19 Composite spring 300 mb wind speed anomalies and composite mean wind speed (m/s)

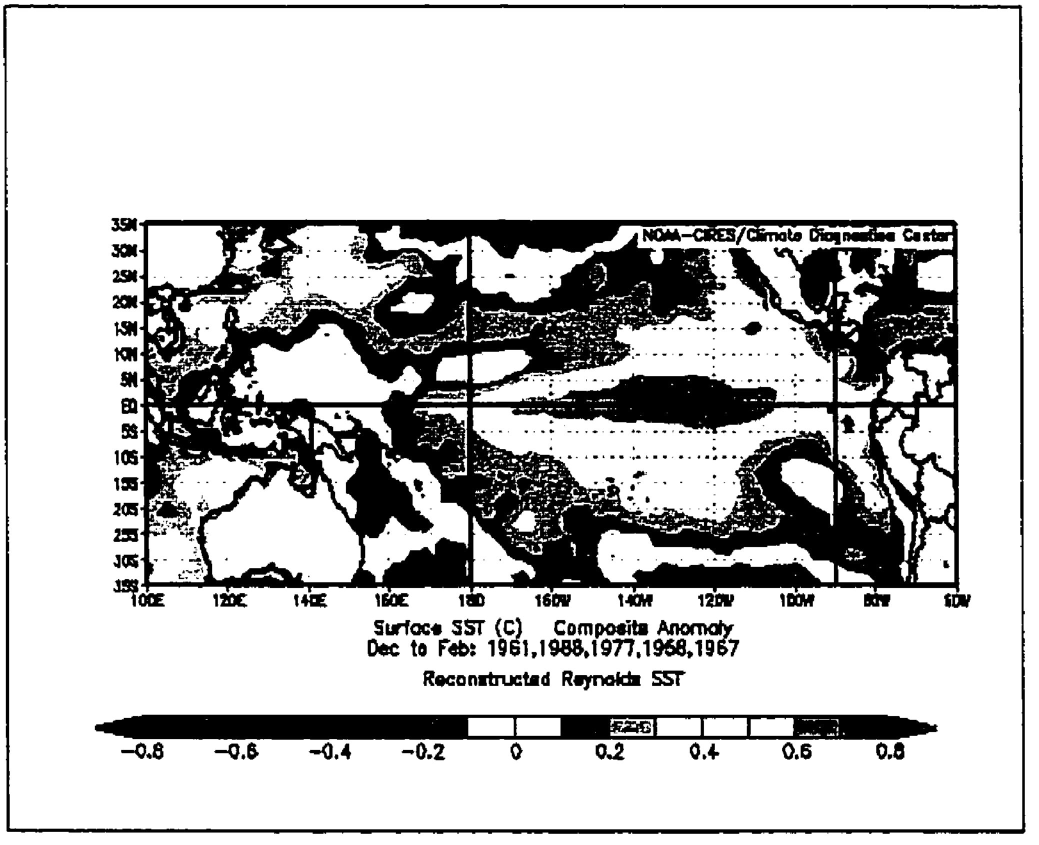

Figure 6.20 Composite winter tropical Pacific SST anomalies

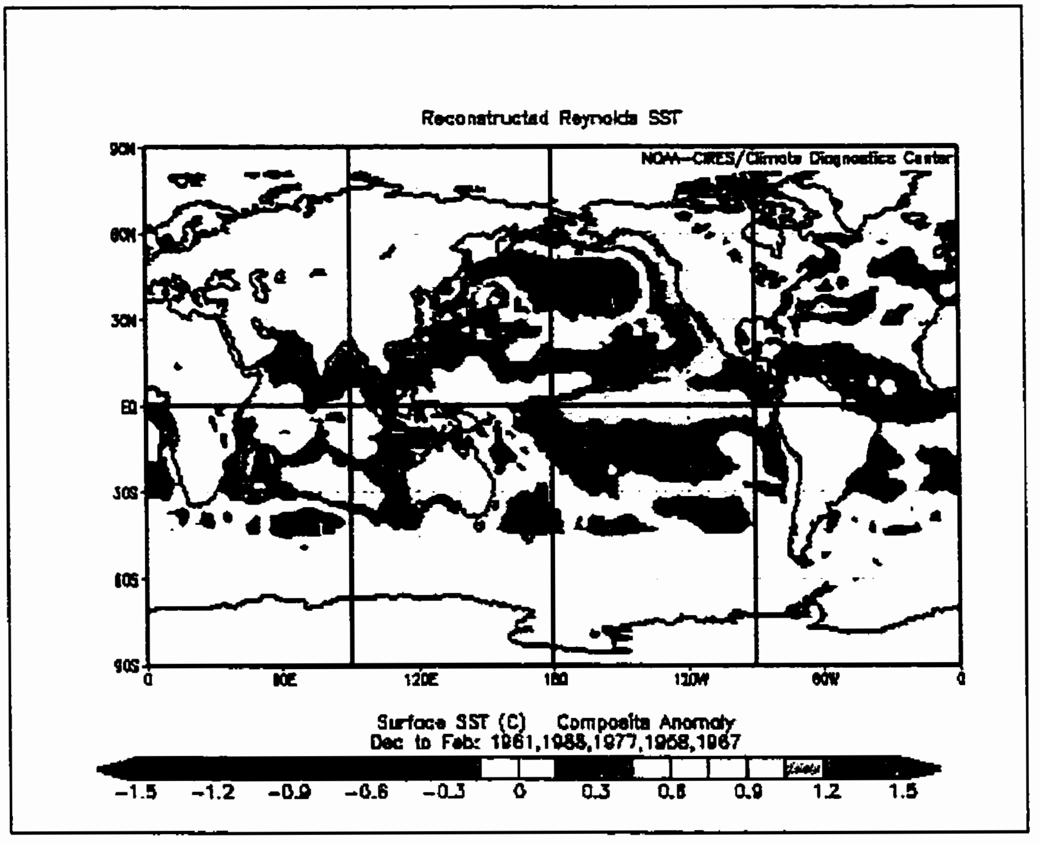

Figure 6.21 Composite winter global SST anomalies

normal water that is evident in the centre of the northern Pacific, but now it is even larger and more pronounced. Again similar to spring, the surrounding water around Japan, along the west coast of North America, and along the equator is warmer than normal. This pattern of SST anomalies in the North Pacific now almost exactly replicates that of the positive (warm) phase of the PDO. There is a significant region of warmer than normal SST in the Atlantic just north of the equator. A band of colder than normal water nearly stretches from the east coast of North America over to Europe.

Figures 6.22, 6.23, and 6.24 show the composite geopotential height anomalies and composite mean geopotential height (m) of the 300, 500, and 700 mb surfaces for winter. Each of these figures shows that winter conditions prior to severe drought events on the Canadian prairies are associated with pronounced negative geopotential height anomalies centred off the coast of Alaska and smaller positive height anomalies over the western United States. A pronounced negative geopotential height anomaly is also present to the east of the study region in the northeastern United States. The net result is that there is a more pronounced ridge over the west coast of North America and a more pronounced trough in eastern North America.

Figure 6.25 shows the winter composite 300 mb wind anomalies and mean winds (m/s). The 300 mb wind anomalies show a band of faster than normal wind speeds (up to +5 m/s) that stretches across Mexico and Florida. North of this, there is a band of lower than normal winds (up to -4 m/s) running parallel. This indicates that the jet stream has been displaced well to the south of its normal winter-time position.

6.2.4 Discussion

The composite analysis showed, not surprisingly, that the spatial pattern of anomalies for precipitation rate, OLR, evaporation rate, soil moisture, and relative humidity were quite similar

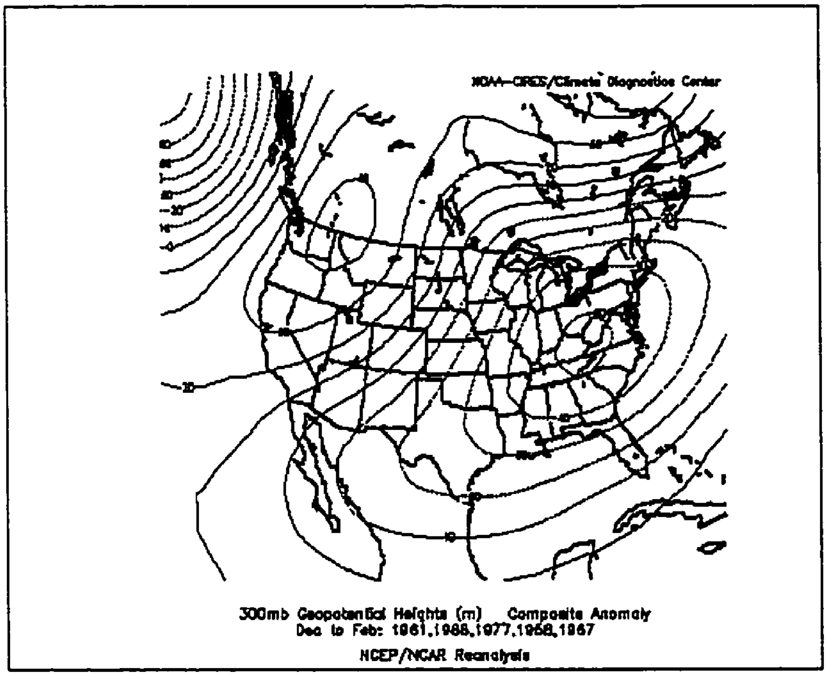

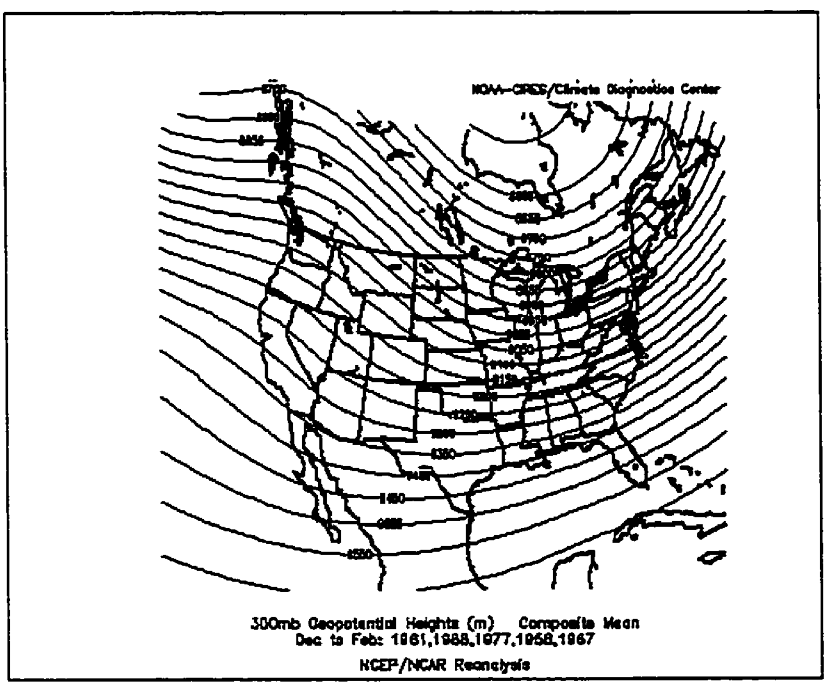

Figure 6.22 Composite winter 300 mb geopotential height anomalies (m) and mean geopotential height (m)

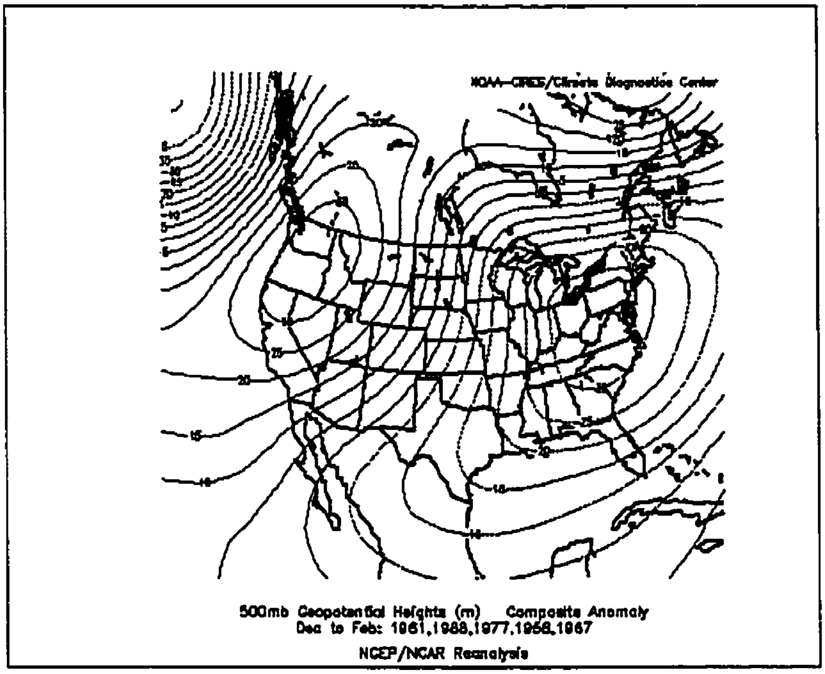

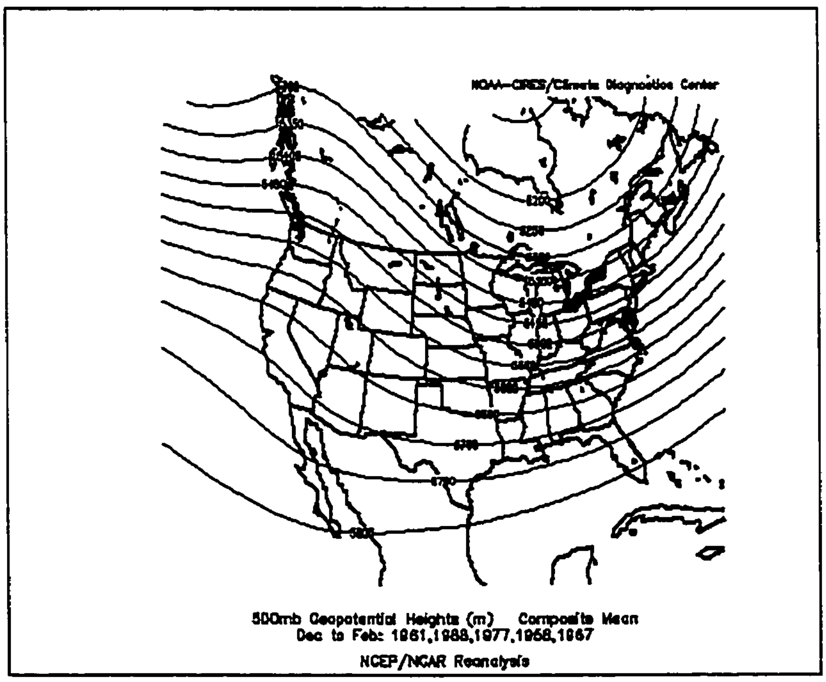

Figure 6.23 Composite winter 500 mb geopotential height anomalies (m) and mean geopotential height (m)

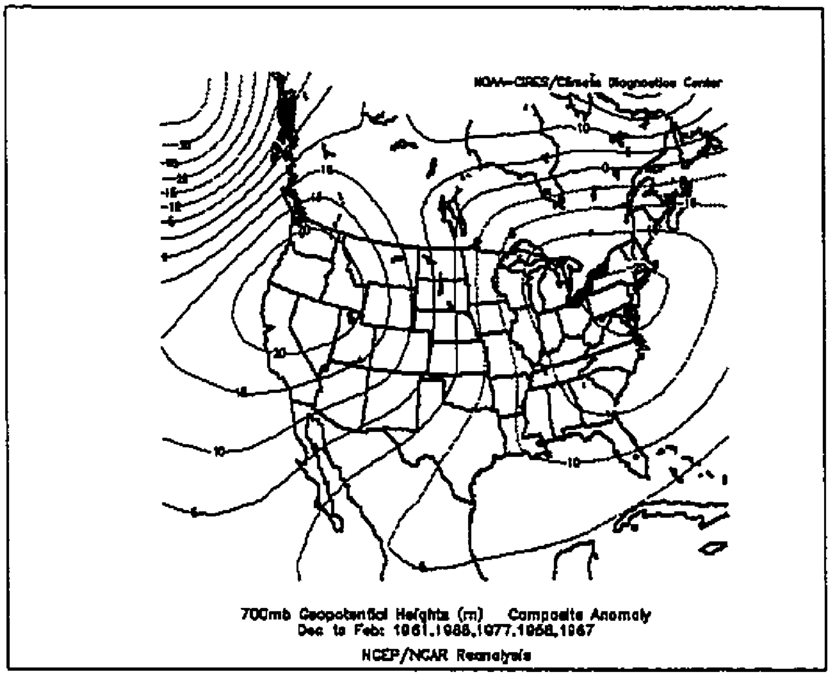

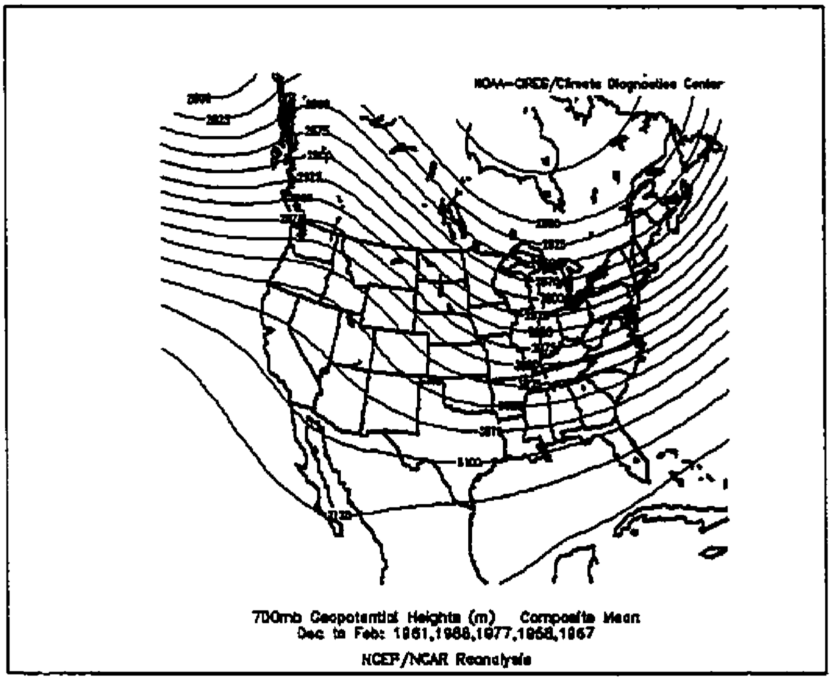

Figure 6.24 Composite winter 700 mb geopotential height anomalies (m) and mean geopotential height (m)

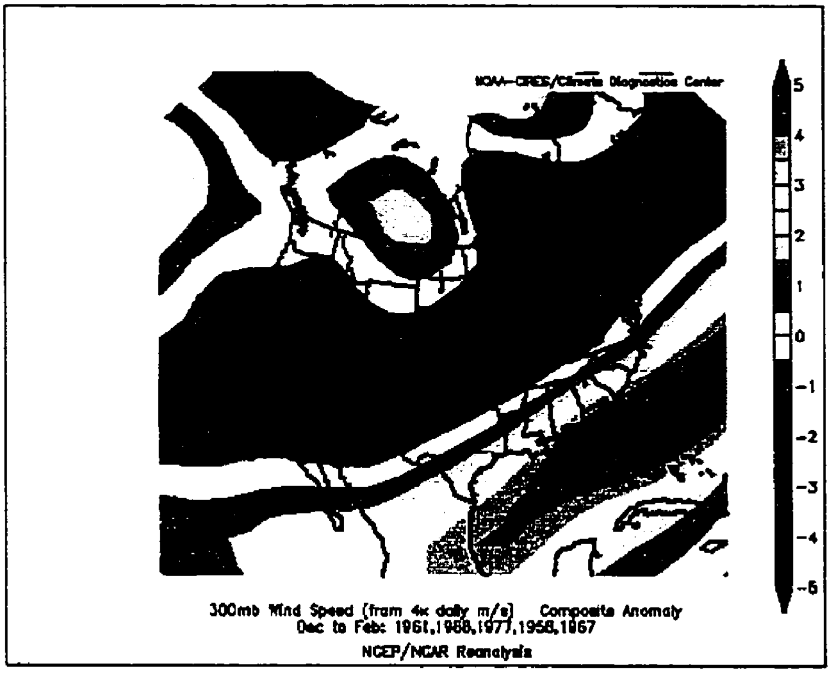

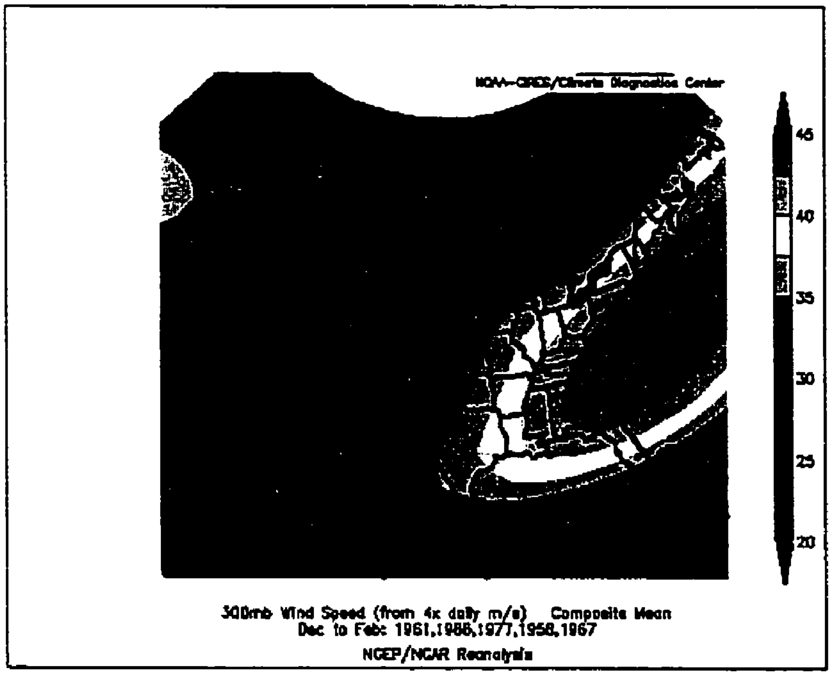

Figure 6.25 Composite winter 300 mb wind speed anomalies and composite mean wind speed (m/s)

over the study region. All of these variables are linked to each other through a complex series of feedback processes. A change in any one of these variables affects all of the others. In general, severe drought events on the Canadian prairies are associated with negative precipitation, soil moisture, and relative humidity anomalies, and positive temperature and OLR anomalies. During the five most severe droughts considered in this composite analysis, the drought-like conditions extended in a band from northern British Columbia through the Canadian prairies and all the way to the east coast of the United States. All of the variables showed a similar spatial pattern except for temperature. The higher than normal temperature anomalies were restricted to western North America, while most of eastern North America experienced cooler than normal conditions.

As the literature suggests, surface boundary layer conditions play a role in initiating and sustaining drought conditions of the Canadian prairies (Maybank *et al.*, 1995; Herring, 2000). This is probably due to the fact that the source of approximately 30% of the precipitation that falls in the during the growing season in the Canadian prairies is recycled rain (Raddatz, 2000). Thus, when there is very little available moisture at the surface, there is much less moisture available in the atmosphere. Feedback processes between the surface and the atmosphere tend to exacerbate the situation (drought causes drought) (Namias, 1960).

During the seasons leading up to severe drought events there is a dramatic seasonal evolution of SSTs in the tropical Pacific. During the winter there are strong positive SST anomalies over much of the central and eastern equatorial Pacific. These SST anomalies are indicative of El Niño-like conditions. This pattern of SST anomalies weakens during spring and by summer the pattern has reversed. The strong negative SST anomalies present in the eastern equatorial Pacific during the summer are associated with La Niña-like conditions. Therefore, severe drought events seem to be linked to a change in the phase of ENSO (a transition from El

Niño to La Niña). The change in the phase of ENSO may be as important as the presence of anomalously cold water in the eastern equatorial Pacific during drought events. The cold SST anomalies (La Niña-like conditions) cause a major disruption to the atmospheric heating in the tropics and this not only changes the location and intensity of the ITCZ, it also causes large-scale circulation anomalies that tend to favour the formation of drought conditions over the Canadian prairies (Trenberth and Guillemot, 1996).

There is also an interesting evolution of SST anomalies in the North Pacific. During the winter, the pattern of SST anomalies in the North Pacific resembles that of the positive phase of the PDO (recall that the PDO is the leading PC of North Pacific SST anomalies). This pattern of SST anomalies begins to weaken during spring, and, except for a pool of warmer than normal water along the west coast of North America, has almost completely dissipated by summer. The occurrence of the positive phase of the PDO prior to the growing season is of particular interest because authors such as Namias (1960, 1969, 1972, and 1986) and Bonsal *et al.* (1993) have shown that anomalously warm water off the coast of North America coupled with cool water in the central North Pacific produces a unique Rossby wave pattern that results in warm-dry conditions in western North America and cool-wet conditions in eastern North America. Although the SST anomalies have weakened by the summer, their effect may be felt because there is still a SST gradient. The gradient appears to be what is most responsible for producing the unique Rossby wave pattern (Namias 1960, 1969, 1972, and 1986; Bonsal *et al.*, 1993).

In the North Atlantic during winter, there is a region of slightly warmer than normal water in the central and southern (along the equator) portions and there is cooler than normal water along the western boundary of the basin (east coast of North America), and in a band that stretches across the Atlantic. By summer, the cool SST anomalies have almost entirely disappeared and the pool of warm water has shifted north into the central and northern regions. It is possible that these SST anomalies may be related to circulation anomalies in the Atlantic.

The composites indicate that growing season drought conditions are associated with a more meridional flow over North America. All of the summer geopotential height anomaly maps show a stronger than normal ridge to the west of the study region. The geopotential height anomalies at the 700 mb level are particularly important because of their association with atmospheric teleconnection patterns. Many of the teleconnection indices that are published by the CPC are calculated using 700 mb geopotential height anomalies and a RPCA technique developed by Barnston and Livezey (1986). In particular, the observed geopotential height anomalies in the upper level maps appear to be related to the PNA. The positive phase of the PNA is related to a higher than normal ridge over the Rocky Mountains and a deeper than normal trough over the eastern United States. The positive phase of the PNA is linked to increased meridional flow over the Canadian prairies. Romolo (1998) found that there is a strong and significant correlation between the PNA in April/May and spring precipitation (e.g., positive phase of the PNA is linked to below normal precipitation).

During the spring, conditions are reversed from the summer. A slight trough is now present over the west coast of North America due to negative geopotential height anomalies at the 300, 500, and 700 mb levels of the atmosphere. In winter, there is a large negative geopotential height anomaly centered off the coast of Alaska. This corresponds to a stronger than normal Aleutian Low (positive ALPI). There is also a pronounced trough in the eastern United States and a slightly stronger than normal ridge over North America. The net effect is that there is a more pronounced ridge and a deeper trough. The striking differences between the winter, spring, and summer conditions are probably related to a change in phase in one or more important atmosphere controls. Both winter and summer conditions feature a stronger than normal ridge and enhanced meridional flow. The winter conditions are strongly similar to the positive phase of the PNA, the PDO, AFI, and ALPI. If these conditions (a strong positive PDO with meridional flow during winter coupled with a change in the phase of ENSO) are typical of the ones which precede severe drought events they may be useful for drought forecasting.

The utility and importance of the jet stream is tied to its ability to change the mean flow as well as causing corresponding changes in atmospheric storm tracks. During the summer, when there is a strong ridge over the Rocky Mountains and the jet stream is shifted north of its normal position, storms tend to be preferentially steered around the study region. Colorado Lows are kept mainly to the south of the study region and Alberta Lows are steered north of the study region (Romolo, 1998). The WP is an important mode of low frequency variability in all months. The strong negative phase of the WP is associated with a more zonal flow of the Pacific Jet and the strong positive phase is associated with a more meridional flow of the Pacific Jet. The positive phase of the EP is related to a deeper than normal trough in western North America and enhanced westerlies. The negative phase confines the Pacific trough to the western Pacific and reduces the strength of the westerlies (more meridional). It is likely that these two teleconnection patterns may be important for predicting drought on the Canadian prairies given their connection with the position and strength of the jet stream. The southward shift in the position of the winter and spring jet stream may be related to the El Niño-like conditions that are present in the eastern equatorial Pacific and the related influence that it has on the position of the ITCZ.

6.3 Principal Components Analysis

6.3.1 Winter PCA

Three PCs were extracted from the set of winter teleconnection variables. The results are shown in Tables 6.1 and 6.2.

Table 6.1 Summary of the rotated PCA on winter teleconnection variables

	PC1	PC2	PC3
Eigenvalue	3.74	2.49	2.19
Percent of total variance explained (%)	33.95	22.63	19.90
Cumulative percent of total variance explained (%)	33.95	56.58	76.48

Table 6.2 Summary of the factor loadings for the rotated PCA on winter teleconnection variables

	Factor Loadings		
Variable	**PC1**	**PC2**	**PC3**
ALPI	**.822**	-.483	.089
Sunspots	-.415	.132	**.745**
PDO	**.948**	-.049	-.149
AO	-.247	**.729**	.149
EA	**.774**	.255	.149
WP	-.089	.273	**.772**
PNA	**.688**	**-.524**	-.313
North Atlantic SST	.286	-.299	**.764**
South Atlantic SST	.379	**.830**	.100
Niño-3 SST	.377	**-.716**	.499
Drought (Z-index)	**-.692**	.119	-.167

The first three PCs explained approximately 76% of the total variance. PC1 is of particular interest because it shows which variables are related to growing season drought conditions on the Canadian prairies. PC1 explains 34% of the total variance. The variables with the highest positive factor loadings are the PDO (.948), the ALPI (.822), the EA (.774), and the PNA (.688). The variable with the highest negative factor loading is the mean growing season Z-index value (-.692). The majority of variables that load highly on the first component are related to circulation and SST anomalies in the North Pacific.

The PDO is the variable that has the highest positive loading. As has been suggested by the composite analysis, severe drought events on the Canadian prairies tend to be associated with a pattern of SST anomalies in the North Pacific during the winter that is structurally similar to the positive (warm) phase of the PDO. Both the PDO and the mean growing season drought index are strongly correlated to PC1, but they have opposite signs. This indicates that positive phase of the PDO is related to a negative Z-index (drought).

The ALPI has the second highest positive loading with PC1. ALPI is a measure of the relative intensity of the Aleutian Low, a positive index value indicates a relatively strong, or intense Aleutian Low. The composite analysis established that a stronger than normal trough tends to occur off the coast of Alaska and over the Aleutians during the winter prior to severe drought events. The PCA shows that both the ALPI and the Z-index load strongly on PC1, but have opposite signs. This suggests that the presence of a stronger than normal Aleutian Low during the winter may be related to growing season drought conditions on the Canadian prairies.

The PNA also has a strong positive loading on PC1. The positive phase of the PNA is related to stronger than normal meridional flow over North America at the 700 mb level. The composite analysis established that pronounced anomalies in the 700 mb geopotential height field tend to occur in the winter prior to severe growing season drought events. In particular, a stronger than normal ridge tends to be present over western North America and a deeper than normal ridge tends to be present over eastern North America. Thus, flow is more meridional than normal. The PCA shows that the PNA and the Z-index both load strongly on PC1, but have opposite signs. This suggests that the presence of stronger than normal meridional flow over the study region may be related to growing season drought conditions on the Canadian prairies.

The EA pattern is the only teleconnection that is not related to the North Pacific that is strongly correlated to PC1. The EA is related to the strength of the jet stream over the Atlantic. It is more difficult to determine how this teleconnection relates to the results of the composite analysis and how it might be related to growing season drought conditions on the Canadian prairies.

The results of the PCA of winter teleconnections suggest that the status of North Pacific circulation and SST anomalies (as represented by the ALPI, PDO, and PNA) during the winter are related to growing season drought on the Canadian prairies. In particular, growing season drought events seem to be related to a stronger than normal Aleutian Low, atmospheric flow that is more meridional than normal, and North Pacific SST anomalies that are similar to those represented by the positive phase of the PDO during the winter.

It is not surprising that the results of the PCA also show that the PDO, PNA, and ALPI are strongly related to one another. In winter, all three of these variables loaded highly positive on PC1. This demonstrates that there is a strong coupling between SST and atmospheric flow in the North Pacific. Research by other authors has proven that SST anomalies associated with the positive phase of the PDO produce a more meridional flow over North America (Namias, 1960 and 1969; Bonsal *et al.*, 1993).

6.3.2 Spring PCA

Four PCs were extracted from the set of spring teleconnection variables and the results are shown in Tables 6.3 and 6.4.

Table 6.3 Summary of the rotated PCA on spring teleconnection variables

	PC1	PC2	PC3	PC4
Eigenvalue	3.28	2.61	2.52	1.93
Percent of total variance explained (%)	27.36	21.76	21.02	16.16
Cumulative percent of total variance explained (%)	27.36	49.12	70.14	86.30

Table 6.4 Summary of the factor loadings for the rotated PCA on spring teleconnection variables

	Factor Loadings			
Variable	**PC1**	**PC2**	**PC3**	**PC4**
PDO	**.701**	**.533**	.223	-.244
AO	**-.739**	**.565**	-.054	-.224
EA	.038	-.150	**.956**	-.126
EAJET	.071	.153	**.912**	.163
WP	.191	**.902**	.133	-.015
EP	**.849**	.158	.433	-.128
NP	**.805**	.063	-.212	.178
PNA	**.533**	.175	**.515**	.335
North Atlantic SST	.119	**.875**	-.147	.302
South Atlantic SST	**.699**	-.314	-.012	**-.600**
Niño-3 SST	.016	.183	.152	**.941**
Drought (Z-index)	.215	-.437	-.406	**.537**

The first four PCs explained approximately 86% of the total variance. PC1 explains approximately 27%, PC2 explains 22%, PC3 explains 21%, and PC4 explains 16% of the total variance. PC4 is of particular interest because the growing season drought index has a strong loading (.537) on this PC. The Niño-3 SST anomaly has the largest positive loading on PC4

(.941). The South Atlantic SST anomaly has a strong negative loading (-.600) on PC4.

The results of the composite analysis that indicate that a negative SST anomaly in the eastern equatorial Pacific during the spring is linked to major growing season drought events and this is supported by both the Z-index and Niño-3 SST loading positively on PC4. There also appears to be an inverse relationship between the South Atlantic SST anomalies and drought. Warmer SST anomalies in the South Atlantic are associated with more severe drought in the Canadian prairies. The exact mechanism by which this teleconnection manifests itself is not readily apparent.

The Z-index also has a moderate negative loading (-.437) on PC2. The WP is the variable that has the strongest positive loading (.902) with this PC and the North Atlantic SST variable also has a strong loading (.875). The PDO and AO are also related to this PC and they have loadings of .553 and -.565, respectively. It is more difficult to associate this group of variables with the results of the composite analysis due to the large number of variables that have strong loadings on this PC and the variety of the variables.

6.4 Chapter summary

The purpose of this chapter was to explore the relationship between global teleconnection patterns and the occurrence of agricultural drought on the Canadian prairies. The relationship between teleconnections and drought was examined using a composite analysis and a Principal Components Analysis (PCA). Examining severe droughts is particularly important because these are the events that tend to have a strong coherent climate signal. Thus, there are likely to be strong causal links between these events and atmospheric and oceanic anomalies.

The composite analysis showed, not surprisingly, that the spatial pattern of anomalies for precipitation rate, OLR, evaporation rate, soil moisture, and relative humidity were quite similar. As the literature suggests, surface boundary layer conditions seem to play an important role in initiating and sustaining drought conditions on the Canadian prairies through feedback processes between the surface and the atmosphere (Maybank *et al.*, 1995; Herring, 2000). The composite analysis also demonstrated that severe drought events are associated with a higher than normal ridge to the west of the study region during the growing season and a deeper than normal trough to the east of the study region. As a result, there is increased meridional flow over the Canadian prairies during the growing season. The position of the jet stream is also farther to the north than normal during severe drought. These changes in atmospheric flow cause associated changes in the location of storm tracks. During severe drought, storm tracks are steered preferentially to the north and to the south, away from the study region.

The composite analysis suggests that drought events are associated with a dramatic seasonal evolution of SSTs in the eastern equatorial Pacific. During the winter (December-January-February period), a pattern of strong positive SST anomalies usually exists. This pattern weakens during spring, and by summer it has completely reversed. This change in the phase of ENSO (a transition from El Niño-like conditions to La Niña-like conditions) may signal the onset of drought conditions. The La Niña-like conditions during the growing season is associated with a major disruption in the atmospheric heating of the tropics and this causes large-scale circulation anomalies that tend to favour the formation of drought conditions (Trenberth and Guillemot, 1996).

It is also interesting to note that the pattern of SST anomalies in the North Pacific during the winter, as shown by the composite analysis, resembles that of the positive phase of the PDO (recall that the PDO is the leading PC of North Pacific SST anomalies). This pattern of SST anomalies produces a unique Rossby wave pattern that results in increased meridional flow and warm-dry conditions in western North America (Namias, 1960 and 1969; Bonsal *et al.,* 1993).

The results of the PCA are important because they can be used to support the findings of the composite analysis. The PCA of winter teleconnections suggests that North Pacific circulation and SST anomalies (as represented by the ALPI, PDO, and PNA) are related to growing season drought on the Canadian prairies. In particular, growing season drought events seem to be related to a stronger than normal Aleutian Low, atmospheric flow that is more meridional than normal, and North Pacific SST anomalies that are similar to those represented by the positive phase of the PDO during the winter. In addition, growing season drought events also appear to be related to spring SST anomalies in the Niño-3 region of the eastern equatorial Pacific. The results also suggest that conditions in the Atlantic, such as South Atlantic SST anomalies and the East Atlantic (EA) pattern, may deserve consideration when attempting to produce a long-range drought forecast.

Obviously, all of the results stemming from the composite and PCA need to be more rigorously researched and verified before these relationships can be exploited in an operational long-range forecasting model. This chapter merely represents the first step in producing an agricultural drought forecasting model.

CHAPTER 7
CONCLUSIONS AND RECOMMENDATIONS

7.1 Conclusions

This study was undertaken to determine the best drought index for measuring agricultural drought in the Canadian prairies. This index was then used to produce an agricultural drought climatology for the region using data from 1920-1999. Finally, a composite analysis of severe drought events and a Principal Components Analysis were used to investigate the relationship between global teleconnection patterns and the occurrence of agricultural drought on the Canadian prairies.

The Moisture Anomaly Index (Z) was determined to be the 'best' index for measuring agricultural drought. The Z-index performed better than the PDSI, SPI, and NDI in both the growing season drought correlation analysis and the stepwise regression analysis. June moisture conditions were found to be the most important in determining Red Spring wheat yields, followed by July and May, respectively. Antecedent moisture conditions were shown to only explain a very small amount of the variance in wheat yields. The Moisture Anomaly Index value for June and July (Z67) explained the greatest amount of variance in yield.

There is a great deal of spatial variability in the strength of the relationship between Red Spring wheat yield and Z67 across the prairies and this index may not be suitable for use in all crop districts. It appears that factors other than moisture conditions dominate in northwestern Alberta and in the northern portion of the grain-growing region in Manitoba. The crop yield models could be improved if additional data sets were available that measured some of the other important variables that affect crop yield such as insects, extreme meteorological events (hail, wind, frost), and disease.

There is also considerable temporal variability in model performance in most crop districts. Many of the years where the model performs poorly can be attributed to an unequal distribution of precipitation. In some cases several large events significantly skew the precipitation totals. Poor model performance is also associated with years that have large gaps when no precipitation falls (particularly at the end June and the beginning of July). The timing of precipitation and its distribution (and intensity) throughout the growing season is just as critical (if not more critical) than the total amount of growing season precipitation. Also, large changes between June and July (dry June, wet July and vice versa) can cause the model to perform poorly since the net effect is to produce a Z-index value that is near zero.

The moisture conditions during the months of May and August also play a role in determining how accurately the model can predict Red Spring wheat yield. Extremely large or small amounts of May precipitation can cause yields to be lower than would otherwise be expected. August moisture conditions tend to be inversely correlated with yield since rain that falls at this point of the growing season does not significantly contribute to yield. Extremely large amounts of August precipitation can significantly decrease yield by delaying the harvest, causing crops to lodge, and causing grain that has been swathed to sprout, thus lowering the quality of yield.

Other sources of error include having an insufficient number of climate stations to produce a reliable spatial average of temperature and precipitation, or having an unequal spatial distribution of where crops are grown within a crop district. Also, the model tends to systematically over predict yield during severe drought events. Perhaps with a longer period of record that includes more severe drought years, the model would more accurately predict yield departures. It is also possible that the response of yield to moisture conditions may not be linear below a certain threshold. Model performance could also be improved if the Z-index was calculated on a weekly basis rather than monthly, and if the index was weighted to account for crop water demand (those weeks when the crop requires the most water would receive extra weighting).

A drought climatology for the crop-growing region of the Canadian prairies was developed by first dividing the study region into five relatively homogenous drought regions. These drought regions are composed of between 6 and 13 crop districts. Cluster 5 in north-western Saskatchewan and Cluster 2 in south-western Saskatchewan/south-eastern Alberta were determined to be the most drought prone regions. Cluster 5 experienced moderate to severe drought conditions during nearly 8% of the study period (an average return period of thirteen years). Cluster 2 experienced moderate to severe drought conditions during 7% of the study period (once every fourteen years). When the average number of moderate to severe drought and flood events are combined it is evident that approximately 16% of the study period for Clusters 2 and 5 (one out of six years) have growing season moisture conditions that are not well-suited for agriculture.

The severity and spatial extent of droughts on the Canadian prairies are inextricably linked. More than 77% of the variability in the spatial extent of drought events can be explained by drought severity. In other words, as the severity of a drought increases, the area that it affects also tends to increase.

The growing season drought of 1961 was the most severe drought on the Canadian prairies during the study period. More than 86% of the study region was affected by drought and the mean severity (Z-index) of the event was -5.67. The second most severe drought occurred during 1988. The mean drought severity was -4.58 and more than 77% of the study region was affected. Major prairie-wide droughts also occurred in a number of other years including 1929 (spatial extent = 65%; severity = -4.01), and 1937 (spatial extent = 69%; severity = -3.97). Moderate to severe drought conditions were present in at least one crop district during 62 of the 80 years. That is, there was in at least one crop district experiencing drought during 77.5% of the study period.

The major spatial patterns of drought on the Canadian prairies were examined through the creation of a series of growing season drought maps. Three major patterns were identified. The first pattern can be described as linear. It is usually characterized by a band of drought (flood) conditions extending across the region, flanked on either side by flood (drought) conditions. The second pattern is referred to as flood or drought dominant. With this pattern, the same conditions are present over the entire study region. The final pattern is referred to as random and it is said to occur when there is a lack of spatial coherence in the moisture conditions. Each of these patterns is likely linked to a different causal mechanism (set of forcing factors).

Temporal patterns of drought were examined by performing a spectral analysis on the drought index data. The results revealed a number consistent drought periodicities, in particular quasi-biennial, quasi-4-year, and quasi-10-15 year oscillations were present in the drought records of the entire study region. These oscillations may be the signature of a particular drought forcing function and therefore may be of use in drought forecasting.

The composite analysis showed that the spatial pattern of anomalies for precipitation rate, OLR, evaporation rate, soil moisture, and relative humidity were quite similar. The composite analysis demonstrated that severe drought events are associated with a higher than normal ridge to the west of the study region during the growing season and a deeper than normal trough to the east of the study region. As a result, there is increased meridional flow over the Canadian prairies during the growing season. During severe drought conditions, the position of the jet stream is farther to the north than normal. These changes in atmospheric flow cause storm tracks to be steered preferentially away from the study region.

The results of the PCA suggest that winter circulation and SST anomalies in the North Pacific (ALPI, PDO, and PNA) are related to growing season drought on the Canadian prairies. In particular, growing season drought events seem to be related to a stronger than normal Aleutian Low, atmospheric flow that is more meridional than normal, and North Pacific SST anomalies that are similar to those represented by the positive phase of the PDO during the winter. In addition, growing season drought events also appear to be related to spring SST anomalies in the Niño-3 region of the eastern equatorial Pacific. The seasonal evolution of SSTs in the eastern equatorial Pacific during severe drought events is particularly intriguing. The large positive SST anomalies that are present during the winter become strong negative SST anomalies by summer. This change in phase may be a signal of the onset of drought conditions. The PCA also suggests that conditions in the Atlantic, such as South Atlantic SST anomalies and the East Atlantic (EA) pattern, may deserve consideration when attempting to produce a long-range drought forecast.

All of the results generated from the composite and PCA analyses should be treated with caution. Both the composite and the PC analysis are only exploratory techniques. Composite analysis is a useful technique that aids in visualizing the conditions associated with severe drought events, however, the composites are influenced by the particular set of drought years that are chosen. For example, individual years may skew the composite if they are significantly stronger than the other years. This research represents just the first step towards producing an operational drought prediction model.

7.2 Utility of this study

This study furthers our understanding of agricultural drought in the Canadian prairies. First, a number of drought indices have been evaluated to determine which is the most appropriate for application in an agricultural context. This index could be calculated on an operational basis to provide the agricultural community with a measure of current moisture conditions across the Canadian prairies. This study also evaluated the strengths and weaknesses of the best drought index. This provides an opportunity to improve the accuracy of this index. In addition, this study highlights some of the physical mechanisms that are responsible for the genesis and perpetuation of drought conditions and explores the relationship between global teleconnection patterns and the occurrence of drought in the Canadian prairies. A number of these teleconnection patterns, specifically those related to SST and circulation in the North Pacific, to ENSO, and conditions in the Atlantic, appear to be related to the occurrence of severe prairie-wide drought events. Establishing the existence of these relationships lays the groundwork for the development of an operational long-range drought forecasting models for the Canadian prairies.

Of course, a great deal of research still needs to be done before an accurate forecasting model for the Canadian prairies can be produced. Particular emphasis needs to be placed on verifying the relationships between teleconnections and drought that are highlighted in this study, producing and validating forecast models, extending forecast lead-time, and finding ways to improve the forecast accuracy. Accurate long-range forecasts would be tremendously valuable for the agricultural community, and other sectors of the economy that are vulnerable to climate variability.

7.3 Recommendations for further research

Predictably this study raises a number of questions and opportunities for further research. Some suggestions are as follows:

1) Test and analyze additional drought indices. This study examined the performance of four droughts indices, but there are many others that may be useful in detecting the onset of drought and measuring drought severity (e.g., AVHRR-derived Vegatation Condition Index, Crop Moisture Index). Testing the performance of additional drought indices will insure that the most appropriate index for monitoring agricultural drought is adopted for operational use on the Canadian prairies.

2) Fine-tune existing drought indices or develop a hybrid drought index. Each of the drought indices employed in this study could be optimized to better reflect the conditions that are critical for crop growth. For example, the indices could be re-calculated on a time-scale that is more appropriate for agricultural applications (weeks or days versus months). It has also become evident that there are some areas where the drought indices need to be improved to better represent the climate of the Canadian prairies. The PDSI and Z-index algorithms could be modified to correct some of the problems that were mentioned in Sections 2.8.2 and 2.8.4 (e.g., PDSI does not account for frozen soil). Creating a hybrid index may also increase model performance by building on the strengths of a number of different drought indices. Making changes to the existing drought indices will require extensive and time consuming alterations to the models and rigorous testing and validation.

3) Consider other crops. This study only focused on the relationship between a series of agricultural drought indices and Red Spring wheat yield. It would be useful to extend this study to cover other crops that are important to the Canadian prairies such as Canola. The influence of moisture conditions on yield tends to be crop specific and a single agricultural drought index is probably not appropriate for all crops. Each crop uses moisture differently and has a unique reaction to moisture stress. Some crops are also more sensitive to moisture stress during a particular time of the year.

4) A validation of the relationship between global teleconnection patterns and the occurrence of growing season drought events should be carried out. These relationships could form the basis for operational drought forecast models.

5) An analysis of regional prairie drought patterns. This study just examined the relationship between teleconnection patterns and the drought dominant pattern (i.e., when drought conditions cover the whole study area). There is also a need to look at the linear/regional pattern of drought (only exhibits drought conditions in one part of the prairies). This spatial pattern of drought may be controlled by a different set of mechanisms.

6) An analysis of drought that utilizes environmental variables. Regional patterns of soil moisture, snow cover, and PET are an important drought forcing mechanism. These environmental variables were not explicitly covered in this study.

7) Develop a decision tree that determines when it is most appropriate to implement a drought model. This study indicates that the relationship between teleconnections and drought is dynamic. Therefore, a single model can not be blindly applied in all situations. Instead, a hybrid method using an analogue of previous severe drought years, indicator

variables, and a statistically-based teleconnection model may hold the most promise for drought prediction.

8) Examine drought patterns and conditions during all months and seasons. This study has only analyzed the growing season because of the interest in linking this to agricultural applications. Drought can occur during any season, and therefore, it would be useful to extend this study to analyze the patterns of drought frequency and severity in fall, winter, and spring as well.

REFERENCES

ACE (2000): Agricultural climate of the Eastern Canadian prairies, Agrometeorological Centre of Excellence. Available at: http://www.gov.mb.ca/agriculture/climate/waa00s00.html

Akinremi, O. O., S. M. McGinn, et al. (1996): Evaluation of the Palmer Drought Index on the Canadian prairies. Journal of Climate **9**: 897-905.

Alley, W. M. (1984): The Palmer Drought Severity Index: Limitation and assumptions. Journal of Climate and Applied Meteorology **23**: 1100-1109.

Arora, V. K., S. S. Prihar, et al. (1987): Synthesis of a simplified water use simulation model for predicting wheat yields. Water Resources Research **23**(5): 903-910.

Ash, G. H. B., C. F. Shaykewich, et al. (1992): Moisture risk assessment for spring wheat on the eastern Prairies: A water-use simulation model. Climatological Bulletin **26**(2): 65-78.

Ash, G. H. B., C. F. Shaykewich, et al. (2000): Agricultural climate of the Eastern Canadian prairies, Agrometeorological Centre of Excellence. **2001**.

Babb, J. C., M. L. Khandekar, et al. (1997): An analysis of PNA indices for forecasting summer weather over the Canadian prairies with implications for wheat yield and protein. Long-Range Weather and Crop Forecasting Workshop, Dorval, QB.

Barnett, T. P. and R. Preisendorfer (1987): Origins and levels of monthly and seasonal forecast skill for United States surface air temperatures determined by canonical correlation analysis. Monthly Weather Review **115**: 1825-1850.

Barnston, A. G. and R. E. Livezey (1987): Classification, seasonality, and persistence of low-frequency atmospheric circulation patterns. Monthly Weather Review **115**: 1083-1126.

Barnston, A. G., H. M. van den Dool, et al. (1994): Long-lead seasonal forecasts - Where do we stand? Bulletin of the American Meteorological Society **75**: 2097-2114.

Barry, R. G. and R. J. Chorley (1987): Atmosphere, Weather, and Climate. New York, Meuthuen.

Beamish, R. J., C. E. Neville, et al. (1997): Production of Fraser River sockeye salmon (Oncorhynchus nerka) in relation to decadal-scale changes in the climate and the ocean. Canadian Journal of Fisheries and Aquatic Science **54**: 543-554.

Bjerknes, J. (1969): Atmospheric teleconnections from the equatorial Pacific. Monthly Weather Review **97**: 163-172.

Blair, D. (1997): Short-period temperature variability at Winnipeg, Canada, 1872-1993: Characteristics and trends. Theoretical and Applied Climatology **58**: 147-159.

Bonsal, B. R., A. K. Chakravarti, et al. (1993): Teleconnections between North Pacific SST anomalies and growing season extended dry spells on the Canadian prairies. International Journal of Climatology **13**: 865-878.

Bonsal, B. R. and R. G. Lawford (1999): Teleconnections between El Niño and La Niña events and summer extended dry spells on the Canadian prairies. International Journal of Climatology **19**: 1445-1458.

Bonsal, B. R., X. Zhang, et al. (1999): Canadian prairie growing season precipitation variability and associated atmospheric circulation. Climate Research **11**: 191-208.

Bouten, W. (1995): Plant control on evapotranspiration: Models and measurements. The Role of Water and the Hydrological Cycle in Global Change. H. R. Oliver and S. A. Oliver. Berlin, Springer.

Burt, J. E. and G. M. Barber (1996): Time series analysis I. Elementary Statistics for Geographers, Guilford Press: 411-421.

Bushuk, W. (1982): Environment and grain quality components. Grainds and Oilseeds: handling, marketing, processing, 3rd Ed. Winnipeg, Canadian International Grain Institute: 463-472.

Cane, M. A. (1991): Forecasting El Niño with a geophysical model. Teleconnections Linking Worldwide Climate Anomalies, Cambridge University Press.

Chiew, F. H. S., T. C. Piechota, et al. (1998): El Nino/Southern Oscillation and Australian rainfall, streamflow, and drought: Links and potential for forecasting. Journal of Hydrology **204**: 138-149.

CPC (2001): Northern Hemisphere teleconnections patterns, Climate Prediction Centre. Available at: http://www.cpc.ncep.noaa.gov/data/teledoc/telepatcalc.html

Code, O. (1998): Statistics Canada, Ottawa. Personal Communication, February 4.

Cohen, S., E. E. Wheaton, et al. (1992): Impacts of Climatic Change Scenarios in the Prairie Provinces: A Case Study from Canada. Downsview, ON, Canadian Climate Center.

Cordery, I. and M. McCall (2000): A model for forecasting drought from teleconnections. Water Resources Research **36**(3): 763-768.

David, P. P., S. A. Wolfe, et al. (1999): Activity cycle of parabolic dunes from Seward sand hills, Saskatchewan. Holocene climate and environmental change in the Palliser Triangle. D. S. Lemmen and R. E. Vance, Geological Survey of Canada.

De Jong, R. and J. A. Sheilds (1988): Available water-holding capacity maps of Alberta, Saskatchewan, and Manitoba. Canadian Journal of Soil Science **68**: 157-163.

Deser, C. (2000): On the teleconnectivity of the "Arctic Oscillation". Geophysical Research Letters **27**(6): 779-782.

Dey, B. (1982): Nature and possible causes of droughts on the Canadian prairies. Journal of Climatology **2**: 233-249.

Eastin, J. D. and C. Y. Sullivan (1984): Environmental stress influences on plant persistence, physiology, and production. Physiological basis of crop growth and development. M. B. Tesar. Madison, WI, American Society of Agronomy: 201-236.

Garnett, E. R. and M. L. Khandekar (1992): The impact of large-scale atmospheric circulations and anomalies on Indian monsoon droughts and floods and on world grain yields - A statistical analysis. Agricultural and Forest Meteorology **61**: 113-128.

Garnett, E. R., M. L. Khandekar, et al. (1997): Teleconnections from Asia to the Canadian prairies: Implications for long-range weather and crop forecasting. Proceedings of the Fourteenth Annual Pacific Climate (PACLIM) Workshop, April 6-9, 1997. R. C. Wilson and V. L. Tharp.

Garnett, E. R., M. L. Khandekar, et al. (1998): On the utility of ENSO and PNA indices for long-lead forecasting of summer weather over the crop-growing region of the Canadian prairies. Theoretical and Applied Climatology **60**: 37-45.

Glantz, M. H. (1982): Consequences and responsibilities in drought forecasting: The case of Yakima, 1977. Water Resources Research **18**(1): 3-13.

Glantz, M. H. (1991): Introduction. Teleconnections Linking Worldwide Climate Anomlaies, Cambridge University Press.

Gray, W. M. and J. D. Sheaffer (1991): El Niño and QBO influences on tropical cyclone activity. Teleconnections Linking Worldwide Climate Anomalies, Cambridge University Press.

Gullet and Skinner (1992): The state of Canada's climate: Temperature change in Canada 1895-1991, Environment Canada: 36.

Guttman, N. B. (1998): Comparing the Palmer Drought Index and the Standardized Precipitation Index. Journal of the American Water Resources Association **34**(1): 113-121.

Guttman, N. B. (1999): Accepting the Standardized Precipitation Index: A calculation algorithm. Journal of the American Water Resources Association 35(2): 311-322.

Hayes, M. J. (1999): Drought indices, National Drought Mitigation Center. Available at: http://enso.unl.edu/ndmc/enigma/indices.htm

Herring, D. (2000): Dry times in North America, Earth Observatory, NASA. Available at: http://earthobservatory.nasa.gov/cgi-bin/printall?/Study/NAmerDrought/index.html

Herrington, R., R. Johnson, et al. (1997): Responding to Global Climate Change in the Canadian Prairies. Volume III of the Canada Country Study: Climate Impacts and Adaptation, Environment Canada.

Hurrell, J. W. (1996): Influence of variations in extratropical wintertime teleconnections on northern hemisphere temperature. Geophysical Research Letters 23(6): 665-668.

Janicot, S. (1992): Spatiotemporal variability of West African rainfall. Part I: Regionalization and typings. Journal of Climate 5: 489-511.

Janowiak, J. E. (1988): An investigation of interannual rainfall variability in Africa. Journal of Climate 1: 240-255.

Kavvas, M. L. and M. L. Anderson (1996): Extreme droughts. Hydrological Disasters. V. P. Singh. Drodrecht, Netherlands, Kulwer. 24: 127-160.

Kemp, D. D. (1982): The drought of 1804-1805 in central North America. Weather 37: 34-41.

Kerr, R. A. (1999): A new force in high-latitude climate. Science 284: 241-42.

King, J. R., V. V. Ivanov, et al. (1998): General circulation of the atmosphere over the North Pacific and its relationship to the Aleutian Low. Nanaimo, BC, Department of Fisheries and Oceans, Science Branch, Pacific Region, Pacific Biological Station: 18.

Kirtman, B. P., J. Shukla, et al. (1997): Multiseasonal predictions with a coupled tropical ocean-global atmosphere system. Monthly Weather Review 125: 789-808.

Knox, J. L. and R. G. Lawford (1990): The relationship between Canadian prairie dry and wet months and circulation anomalies in the mid-troposphere. Atmosphere-Ocean 28(2): 189-215.

Kumar, V. and U. Panu (1997): Predictive assessment of severity of agricultural droughts based on agro-climatic factors. Journal of the American Water Resources Association 33(6): 1255-1264.

Laird, K. R., S. C. Fritz, et al. (1996): Greater drought intensity and frequency before AD 1200 in the Northern Great Plains, USA. Nature 384: 552-554.

Lamb, P. J. and R. A. Peppler (1991): West Africa. Teleconnections Linking Worldwide Climate Anomalies, Cambridge University Press.

Lohani, V. K. and G. V. Loganathan (1997): An early warning system for drought management using the Palmer Drought Index. Journal of the American Water Resources Association **33**(6): 1375-1386.

Longley, R. W. (1952): Measure of the variability of precipitation. Monthly Weather Review **80**: 111-117.

Mantua, N. J., S. R. Hare, et al. (1997): A Pacific interdecadal climate oscillation with impacts on salmon production. Bulletin of the American Meteorological Society **78**: 1069-1079.

Maybank, J., B. Bonsal, et al. (1995): Drought as a natural disaster. Atmosphere-Ocean **33**(2): 195-222.

McFarlane, G. A., J. R. King, et al. (2000): Have there been recent changes in climate? Ask the fish. Progress in Oceanography **47**: 147-169.

McKee, T. B., N. J. Doeskin, et al. (1993): The relationship of drought frequency and duration to time scales. 8th Conference on Applied Climatology, Boston, MA, American Meteorological Society.

McKee, T. B., N. J. Doeskin, et al. (1995): Drought monitoring with multiple time scales. 9th Conference on Applied Climatology, American Meteorological Society.

Mo, K. C. and R. E. Livezey (1986): Tropical-extratropical geopotential height teleconnections during the northern hemisphere winter. Monthly Weather Review **114**: 2488-2515.

Monteverdi, J. P. (1978): A meteorological analysis of the variability of precipitation in the Great Plains, USA. Department of Geography, University of California- Berkeley.

Namias, J. (1960): Recent seasonal interactions between North Pacific waters and the overlying atmospheric circulation. Journal of Geophysical Research **64**: 631-646.

Namias, J. (1969): Seasonal interactions between the North Pacific ocean and the atmosphere during the 1960s. Monthly Weather Review **97**: 173-192.

Namias, J. (1972): Experiments in objectively predicting some atmospheric and oceanic variables for the winter of 1971-72. Journal of Applied Meteorology **71**: 1164-1174.

Namias, J. (1978a): Multiple causes of the North American abnormal winter 1976-77. Monthly Weather Review **106**(3): 67-83.

Namias, J. (1978b): Long-range weather and climate predictions. Geophysical Predictions. Washington, D. C., National Academy of Sciences: 103-114.

Namias, J. (1980): The art and science of long-range forecasting. EOS **61**(449-450).

Namias, J. (1986): Persistence of flow patterns over North America and adjacent ocean sectors. Monthly Weather Review **114**: 1368-1383.

Nicholls, N. and R. W. Katz (1991): Teleconnections and their implications for long-range forecasts. Teleconnections Linking Worldwide Climate Anomlaies, Cambridge University Press.

Nicholson, S. E. (1986): The nature of rainfall variability in Africa south of the equator. Journal of Climatology **6**: 515-530.

Nkemdirim, L. and L. Weber (1999): Comparison between the droughts of the 1930s and the 1980s in the southern Canadian prairies. Journal of Climate **12**: 2434-2450.

Oladipo, E. O. (1987): Power spectra and coherence of drought in the interior plains. Journal of Climatology 7: 477-491.

Padmanabhan, G. and A. Ramachandra Rao (1990): On the correlation between drought indices and solar activity. Theoretical and Applied Climatology **41**: 55-61.

Palmer, W. C. (1965): Meteorological drought. Washington, D.C., U.S. Weather Bureau.

Poole, M. A. and P. N. O'Farrell (1971): The assumptions of the linear regression model. Transactions of the Institute of British Geographers **52**: 145-158.

Quiring, S. M. (1999): The utility of global teleconnection indices for long-range crop forecasting on the Canadian prairies. Department of Geography. Winnipeg, MB, University of Winnipeg.

Quiring, S. M. and D. Blair (2000): The utility of global teleconnection indices for long-range crop forecasting on the Canadian prairies. Prairie Perspectives: Geographical Essays. J. I. Romanowski. Winnipeg, University of Manitoba. **3**: 23-61.

Quiring, S. M. and D. Blair (2001): Recent developments in teleconnection indices and their application in long-range forecasting. Long-Range Weather and Crop Forecasting Working Group IV, Regina, SK, Prairie Farm Rehabilitation Administration.

Raddatz, R. L. (1998): Anthropogenic vegetation transformation and the potential for deep convection on the Canadian prairies. Canadian Journal of Soil Science **78**: 657-666.

Raddatz, R. L. (2000): Summer rainfall recycling for an agricultural region of the Canadian prairies. Canadian Journal of Soil Science **80**: 367-373.

Rasmusson, E. M. (1991): Observational aspects of ENSO cycle teleconnections. Teleconnections Linking Worldwide Climate Anomalies, Cambridge University Press.

Riha, S. J., D. S. Wilks, et al. (1996): Impact of temperature and precipitation variability on crop model predictions. Climatic Change **32**: 293-311.

Romolo, L. (1998): The relationship between the Pacific/North American teleconnection pattern and spring precipitation on the Canadian prairies. Department of Geography. Saskatoon, SK, University of Saskatchewan.

Ropelewski, C. F. and M. S. Halpert (1986): North American precipitation and temperature patterns associated with the El Niño/Southern Oscillation (ENSO). Monthly Weather Review **114**: 2352-2362.

Ropelewski, C. F. and M. S. Halpert (1987): Global and regional scale precipitation patterns associated with the El Niño/Southern Oscillation. Monthly Weather Review **115**: 1606-1626.

Rosenberg, N. J. (1978): North American Droughts. Boulder, AAAS.

Saskatchewan Agriculture and Food (2000): Soil moisture. Available at: http://www.agr.gov.sk.ca/land_wat_clim/water/

Sauchyn, D. J. and A. B. Beaudoin (1998): Recent environmental change in the southwestern Canadian plains. Canadian Geographer **42**(4): 337-353.

Shabbar, A. and A. G. Barnston (1996): Skill of seasonal climate forecasts in Canada using canonical correlation analysis. Monthly Weather Review **124**: 2370-2385.

Shabbar, A. and M. Khandekar (1996): The impact of El Niño-Southern Oscillation on the temperature field over Canada. Atmosphere-Ocean **34**(2): 401-416.

Shaw, G. and D. Wheeler (1994): Statistical Techniques in Geographical Analysis. London, Fulton.

Soule, P. T. (1992): Spatial patterns of drought frequency and duration in the contiguous USA based on multiple drought event definitions. International Journal of Climatology **12**: 11-24.

Stahle, D. W., E. R. Cook, et al. (2000): Tree-ring data document 16th century megadrought over North America. EOS **81**(12): 124-125.

Stockton, C. W. and D. M. Meko (1983): Drought recurrence in the Great Plains as reconstructed from long-term tree-ring records. Journal of Climate and Applied Climatology **22**(1): 17-29.

Stone, R. C., G. L. Hammer, et al. (1996): Prediction of global rainfall probabilities using phases of the Southern Oscillation Index. Nature **384**: 252-255.

Strommen, N. D. and R. P. Motha (1987): An operational early warning agricultural weather system. Planning for drought: Toward a reduction of societal vulnerability. D. A. Wilhite, W. E. Easterling and D. A. Wood. Boulder, CO, Westview Press.

Sutton, R. T. and M. R. Allen (1997): Decadal predictability of North Atlantic sea surface temperature and climate. Nature **388**: 563-566.

Thompson, D. W. J. and J. M. Wallace (1998): The Arctic Oscillation signature in the wintertime geopotential height and temperature fields. Geophysical Research Letters **25**(9): 1297-1300.

Thompson, D. W. J. and J. M. Wallace (2000): Annular modes in the extratropical circulation. Part I: Month-to-month variability. Journal of Climate **13**: 1000-1016.

Thompson, D. W. J., J. M. Wallace, et al. (2000): Annular modes in the extratropical circulation. Part II: Trends. Journal of Climate **13**: 1018-1036.

Thornthwaite, C. W. (1948): An approach toward a rational classification of climates. Geophysical Review **38**: 55-94.

Titlow, J. K. (1987): A precipitation-based drought index for the Delaware river basin. Centerton, NJ, C.W. Thornthwaite Associates.

Trenberth, K. E. and C. J. Guillemot (1996): Physical processes involved in the 1988 drought and 1993 floods in North America. Journal of Climate **9**: 1288-1298.

Tribbia, J. J. (1991): The rudimentary theory of atmospheric teleconnections associated with ENSO. Teleconnections Linking Worldwide Climate Anomalies, Cambridge University Press.

Uppenbrink, J. (1997): Seasonal climate prediction. Science **277**: 1952.

Volkmar, K. M. and W. Woodbury (1995): Plant-water relationships. Handbook of Plant and Crop Physiology. M. Pessarakli, Marcel Dekker: 23-43.

Walker, G. T. (1923): Correlation in seasonal variations of weather III: A preliminary study of world weather. Memorandum of the Indian Meteorological Department **24**: 75-131.

Walker, G. T. (1924): Correlation in seasonal variation of weather IV: A further study of world weather. Memorandum of the Indian Meteorological Department **24**(275-332).

Wallace, J. M. and D. S. Gutzler (1981): Teleconnections in the geopotential height field during the northern hemisphere winter. Monthly Weather Review **109**: 784-812.

Wheaton, E. E., L. M. Arthur, et al. (1992): The prairie drought of 1988. Climatological Bulletin **26**: 188-205.

White, G. H., E. Kalnay, et al. (1993): The skill of precipitation and surface temperature forecasts by the NMC Global Model during DERF II. Monthly Weather Review **121**: 805-814.

Wilhite, D. A., W. E. Easterling, et al., Eds. (1987): Planning for drought: Toward a reduction of societal vulnerability. Boulder, CO, Westview Press.

Winter, T. C. and D. O. Rosenberry (1998): Hydrology of prairies pothole wetlands during drought and deluge: A 17-year study of the Cottonwood Lake wetland complex in North Dakota in the perspective of longer term measured and proxy hydrological records. Climatic Change **40**: 189-209.

Yarnal, B. and H. F. Diaz (1986): Relationships between extremes of the Southern Oscillation and the winter climate of the Anglo-American Pacific coast. Journal of Climatology **14(9)**: 947-967.

Yin, Z.-Y. (1994): Moisture condition in the south-eastern USA and teleconnection patterns. International Journal of Climatology **14**: 947-967.

APPENDIX A:
LIST OF ABBREVIATIONS AND ACRONYMS

Abbreviation/Acronym	Definition
AES	Atmospheric Environment Service
AFI	Atmospheric Forcing Index
ALPI	Aleutian Low Pressure Index
AO	Arctic Oscillation
AWC	available water content
BP	before present
bu/ac	bushels per acre
CAFEC	climatologically appropriate for existing conditions
CCA	canonical correlation analysis
CD	crop district
CDC	Climate Diagnostics Center
CGC	Canadian Grain Commission
CGCM	coupled general circulation model
CMI	Crop Moisture Index
CPC	Climate Prediction Center
CWB	Canadian Wheat Board
EA	East Atlantic Pattern
EAJET	East Atlantic Jet
ENSO	El Niño/Southern Oscillation
EOF	empirical orthogonal function
EP	Eastern Pacific Pattern
ET	evapotranspiration
FFT	Fast Fourier Transform
GCM	general (global) circulation model
HCM	hybrid coupled model
ICM	intermediate coupled model
ITCZ	Inter-Tropical Convergence Zone
kg/ha	kilograms per hectare
kPa	kilopascal
KWh	Kilowatt hours
L_s	evapotranspiration loss from the surface soil layer
L_u	evapotranspiration loss from the underlying soil layer
M	metre
mb	millibar
mm	millimetre
MSLP	Mean sea-level pressure
NA	North America
NAO	North Atlantic Oscillation

Abbreviation/Acronym	Definition
NDI	NOAA Drought Index
NDVI	Normalized Difference Vegetation Index
NH	Northern Hemisphere
NOAA	National Oceanographic and Atmospheric Administration
NP	North Pacific Pattern
P	precipitation
PC	principal component
PCA	Principal Components Analysis
PCI	Pacific Circulation Index
PDO	Pacific Decadal Oscillation
PDSI	Palmer Drought Severity Index
PE	potential evapotranspiration
PFRA	Prairie Farm Rehabilitation Administration
PNA	Pacific/North American Pattern
POP	principal oscillation patterns
PT	Pacific Transition
RPCA	Rotated Principal Component Analysis
SLP	sea-level pressure
SOI	Southern Oscillation Index
SPI	Standardized Precipitation Index
SST	Sea surface temperature
SWSI	Surface Water Supply Index
TNH	Tropical/Northern Hemisphere Pattern
USDA	United States Department of Agriculture
WP	Western Pacific Pattern
Z	Moisture Anomaly Index
Z67	June-July (growing season) Moisture Anomaly Index

APPENDIX B: CLIMATE STATIONS USED IN THE STUDY

This section contains a list of all of the climate stations that were used to calculate the mean daily temperature and precipitation for all 43 crop districts in the study region. The table shows the AES identification number, name, elevation, and location of each station. It also indicates whether the station supplied both temperature and precipitation data or just precipitation, and whether it is currently active.

Alberta 1:

STATION ID	STATION NAME	LAT	LONG	ELEVATION	ACTIVE	PPT-ONLY
3025764	SCHULER	50.30	-110.08	823	Y	
3030768	BOW ISLAND	49.73	-111.45	806	Y	
3030773	BOW ISLAND RIVERS DEV	49.87	-111.37	799		
3032640	FOREMOST	49.48	-111.45	884	Y	
3032928	GRASSY LAKE	49.83	-111.30	808		Y
3034480	MEDICINE HAT A	50.02	-110.72	717	Y	
3034489	MEDICINE LODGE LO	49.63	-110.32	1402	Y	
3035360	RALSTON	50.25	-111.17	770		Y
3035434	REDCLIFF	50.07	-110.77	741		Y
3035540	RONALANE	50.08	-111.57	716		
3035840	SEVEN PERSONS	49.83	-110.90	756		Y
3036235	SUFFIELD	50.22	-111.15	748		
3036240	SUFFIELD A	50.27	-111.18	770	Y	
3037520	WHITLA	49.87	-111.05	838		
3037600	WINNIFRED	49.90	-111.20	831		Y
3040049	ADEN	49.05	-111.32	1036	Y	
3040223	ALTAWAN	49.23	-110.02	945	Y	
3042148	EAGLE BUTTE	49.57	-110.37	1145	Y	
3042793	GLASSFORD	49.37	-110.70	834		
3042960	GROTON	49.20	-111.33	914		Y
3044200	MANYBERRIES CDA	49.12	-110.47	934		
3044923	ONEFOUR CDA	49.12	-110.47	935	Y	
304KFL0	FLORANN	49.27	-111.40	951		

Alberta 2:

STATION ID	STATION NAME	LAT	LONG	ELEVATION	ACTIVE	PPT-ONLY
3020864	BROOKS ONE TREE	50.63	-111.78	737		
3022143	DUCHESS	50.73	-111.90	755		
3022772	GEM	50.95	-112.18	764	Y	
3025010	PATRICIA	50.67	-111.67	732		
3030530	BARONS EXP ST	50.03	-113.17	961		Y
3030537	BASSANO DAM	50.78	-112.47	800		
3030838	BROOKS	50.58	-111.90	755		
3030840	BROOKS 1	50.57	-111.90	758		
3030QLP	BROOKS	50.55	-111.85	747	Y	
3031668	COALDALE	49.73	-112.63	862		

3032930	GRASSY LAKE RIVERS DEV	49.72	-111.70	830		Y
3033080	HAYS	50.10	-111.80	776		
3033500	IRON SPRINGS EXP ST	49.93	-112.60	837		Y
3033879	LETHBRIDGE	49.70	-112.85	903		
3033880	LETHBRIDGE A	49.63	-112.80	929	Y	
3033890	LETHBRIDGE CDA	49.70	-112.78	921	Y	
3034596	MONARCH	49.80	-113.15	945	Y	
3034820	NOBLEFORD EXP ST	49.88	-113.07	983		Y
3035350	RAINIER	50.37	-112.03	764		
3035420	RAYMOND	49.45	-112.70	957		
3036360	TABER	49.78	-112.12	808	Y	
3036490	TILLEY	50.45	-111.67			
3036680	VAUXHALL	50.07	-112.10	779		
3036681	VAUXHALL CDA	50.05	-112.13	779		
3036682	VAUXHALL CDA CS	50.05	-112.13	779	Y	
3041908	COUTTS	49.00	-111.95	1036		Y
3043667	KNIGHT LAKE	49.22	-112.53			
3044230	MASINASIN	49.13	-111.65	945	Y	
3044534	MILK RIVER	49.17	-111.53	975		
3046950	WARNER	49.28	-112.20	1010		Y
3046953	WARNER WEST	49.28	-112.23	1113	Y	
3047670	WRITING ON STONE PARK	49.08	-111.62	899		

Alberta 3:

STATION ID	STATION NAME	LAT	LONG	ELEVATION	ACTIVE	PPT-ONLY
3030665	BIG COULEE	49.75	-113.80	1325		
3031000	CALDWELL	49.17	-113.63	1286		
3031320	CARDSTON	49.13	-113.25	1193	Y	
3031342	CARMANGAY EXP ST 3	50.12	-113.33	939		Y
3031400	CARWAY	49.00	-113.37	1359	Y	
3031640	CLARESHOLM	50.00	-113.63	1012	Y	
3031805	CONNELLY CREEK	49.62	-114.23	1158		
3031920	COWLEY A	49.63	-114.08	1182		
3031924	COWLEY CREEBANK RANCH	49.57	-114.08	1171		Y
3031926	COWLEY OLIN CREEK	49.70	-114.07	1234	Y	Y
3031F5F	CLARESHOLM MEADOW CREEK	49.93	-113.75	1052	Y	Y
3032624	FIVE MILE CREEK	49.77	-113.85	1311	Y	
3032680	FORT MACLEOD	49.72	-113.40	950		
3032820	GLENWOODVILLE EXP ST	49.37	-113.52	1067		
3033281	HILL SPRING	49.28	-113.63	1183		
3033675	KYISKAP CREEK	49.90	-113.72	1067		Y
3034160	MAGRATH	49.42	-112.87	978		
3034720	MOUNTAIN VIEW	49.13	-113.63	1318	Y	Y
3035201	PINCHER CREEK	49.50	-113.95	1155		
3035202	PINCHER CREEK A	49.52	-114.00	1190		
3035208	PINCHER CREEK CR10	49.52	-114.00	1190	Y	
3035220	PINCHER CREEK TOWN	49.52	-113.97	1145		
3036099	STAVELY AAFC	50.18	-113.88	1364	Y	
3036100	STAVELY CDA	50.17	-113.87	1097		Y

3042040	DEL BONITA	49.03	-112.80	1158		
3042041	DEL BONITA	49.13	-112.82	1293		
3043667	KNIGHT LAKE	49.22	-112.73	1219		Y
3045293	POTHOLE MCINTYRE	49.22	-112.85	1158		
3047365	WHISKEY GAP	49.02	-112.95	1311		
3050600	BEAVER MINES	49.47	-114.17	1286		
3051165	CAMERON FALLS	49.05	-113.92	1311		
3051310	CARBONDALE LO	49.43	-114.37	1798	Y	
3051430	CASTLE	49.40	-114.33	1360	Y	
3053505	IRONSTONE LO	49.57	-114.47	2073		
3054120	LYNDON	50.02	-113.88	1250		
3054250	MAYCROFT	49.83	-114.25	1372		Y
3055237	POLL HAVEN AFS	49.03	-113.60	1615	Y	
3055980	SKYLINE RS	49.88	-113.97	1661		
3056214	WATERTON PARK GATE	49.13	-113.80	1296	Y	
3057000	WATERTON LAKES BELLY R	49.05	-113.70	1372		Y
3057243	WATERTON RIVER CABIN	49.12	-113.83	1281		
3057368	WHISTLER LO	49.33	-114.30	2163		
305J65G	CLARESHOLM TROUT CREEK	49.97	-113.87	1164		

Alberta 4:

STATION ID	STATION NAME	LAT	LONG	ELEVATION	ACTIVE	PPT-ONLY
3011760	COMPEER	51.97	-110.03	701		Y
3011820	CONSORT CDA EPF	52.03	-110.80	770		Y
3011840	CONSORT WADES	51.85	-110.77	753		
3011848	CONTRACOSTA LAKE	51.77	-111.55	792		
3014600	MONITOR	52.02	-110.55	732		Y
3014760	NACO	51.72	-110.80	732		
3014783	NEUTRAL VALLEY	52.13	-110.88	758		
3014788	NEW BRIGDEN EAST	51.68	-110.27	695		
3015165	PEMUKAN	51.98	-110.45	680		
3015799	SEDALIA EAST	51.65	-110.55	762		
3016817	VETERAN	52.00	-111.00	785		
3016960	WASTINA HEMARUKA	51.70	-111.12	793		
3016965	WASTINA YOUNGSTOWN	51.67	-111.12	762		
3017700	YOUNGSTOWN	51.42	-111.40	775		
301B460	ESTHER 1	51.67	-110.20	707	Y	
3020018	ACADIA VALLEY	51.18	-110.23	732		Y
3020020	ACADIA VALLEY EXP ST	51.08	-110.28	713		Y
3020025	ACADIA VALLEY MACTAVISH	51.20	-110.17	744	Y	
3020220	ALSASK	51.38	-110.03	701		Y
3020401	ATLEE	50.82	-110.95	793		
3020635	BERRY CREEK	51.37	-111.27			
3020636	BERRY CREEK	51.02	-111.03	732		
3020676	BIG STONE	51.17	-111.20	774		
3020680	BINDLOSS	50.68	-110.17	640		
3020690	BINDLOSS EAST	50.88	-110.18	655	Y	
3020717	BLOOD INDIAN CREEK	50.92	-111.07	640		
3020973	BULLPOUND CREEK	51.28	-111.88	793		Y
3021010	CALENDULA SIBBALD	51.48	-110.05	719		Y

3021465	CESSFORD	51.02	-111.55	701		
3022154	EAST BERRY CREEK	51.23	-111.35	792		Y
3022400	EMPRESS	50.97	-110.08		Y	
3022460	ESTHER	51.60	-110.23	747	Y	Y
3022500	EXCEL	51.50	-110.57	794		
3022616	FINNEGAN	51.18	-111.92	747		
3023000	HANNA	51.58	-111.85	823		
3023430	IDDESLEIGH	50.73	-111.32	770	Y	Y
3023560	JENNER	50.72	-111.20	762	Y	
3024960	OYEN	51.45	-110.48	777		
3024961	OYEN CAPPON	51.17	-110.52	793		
3024R60	OYEN AIRPORT	51.33	-110.48	761		
3025240	POLLOCKVILLE	51.08	-111.60	747		
3025762	SCAPA	51.87	-112.02	817	Y	
3025770	SCOTFIELD	51.58	-111.35	762	Y	
3025920	SIBBALD	51.47	-110.25	725	Y	

Alberta 5:

STATION ID	STATION NAME	LAT	LONG	ELEVATION	ACTIVE	PPT-ONLY
3020040	ACME CDA EPF	51.50	-113.42	905		
3021309	CARBON	51.48	-113.15	777		
3021940	CRAIGMYLE	51.77	-112.28	846	Y	
3022060	DELIA	51.58	-112.42	906		
3022120	DRUMHELLER	51.47	-112.72	687		
3022137	DRUMHELLER INSTITUTION	51.42	-112.68	814		
3022139	DRUMHELLER CITY	51.45	-112.70	688		
30221LG	DRUMHELLER EAST	51.43	-112.67	678		
3022778	GHOST PINE CREEK	51.65	-113.08	823		
3023400	HUSSAR	51.18	-112.58	937		Y
3023422	HUXLEY	51.90	-113.43	914	Y	Y
30254RJ	REDLAND	51.37	-113.07	853		Y
3025543	ROSEBUD	51.38	-113.00	887		Y
3026009	SLEEPY HOLLOW	51.48	-112.95	811		
3026275	SWALWELL	51.58	-113.35	908		Y
3026480	THREE HILLS	51.65	-113.30	841		
3026530	TROCHU EQUITY	51.78	-113.20	854		
3026540	TROCHU TOWN	51.83	-113.22	876	Y	
3026646	TWO BAR LAKE	51.28	-112.55	876		
302F4HF	THREE HILLS SOUTH	51.70	-113.32	860	Y	
3030300	ARMADA EXP ST	50.40	-112.68	911		Y
3030302	ARROWWOOD	50.73	-113.15	936		Y
3031348	CARMANGAY VILLAGE	50.13	-113.12	939	Y	Y
3032800	GLEICHEN	50.88	-113.05	905	Y	
3033138	HERRONTON EAST	50.60	-113.35	1067	Y	
3034166	MAJORVILLE	50.70	-112.65	914		Y
3034675	MOSSLEIGH	50.67	-113.28	1067	Y	Y
3035340	QUEENSTOWN	50.60	-112.98	945	Y	
3036085	STANDARD	51.15	-112.92	914		Y
3036200	STRATHMORE	51.05	-113.42	963		
3036208	STRATHMORE EAST	51.10	-113.22	930		

3036880	VULCAN	50.53	-113.07	991		
3036881	VULCAN	50.40	-113.25	1049	Y	

Alberta 6:

STATION ID	STATION NAME	LAT	LONG	ELEVATION	ACTIVE	PPT-ONLY
3021368	CARSTAIRS WEST	51.57	-114.28	1090		Y
3021950	CROSSFIELD	51.42	-114.17	1128		
3022083	DIDSBURY	51.67	-114.13	1006		
3023055	HARMATTAN	51.75	-114.38	1067		
3024150	MADDEN	51.50	-114.33	1143	Y	
3024920	OLDS	51.78	-114.10	1040	Y	
3026259	SUNDRE GARRINGTON	51.97	-114.45	991	Y	
3026260	SUNDRE RS	51.77	-114.63	1128		
3030796	BRAGG CREEK WEST	50.97	-114.62	1372		
3030GJJ	BLACKIE 2W	50.60	-113.68	1024		Y
3031093	CALGARY INT'L A	51.12	-114.02	1084	Y	
3031524	CHESTERMERE LAKE SOUTH	51.03	-113.78	1021		
3031676	COCHRANE	51.20	-114.43	1311	Y	
3031875	COP UPPER	51.08	-114.22	1235	Y	
3033240	HIGH RIVER	50.48	-114.17	1219	Y	
3033572	JUMPING POUND	51.08	-114.55			Y
3033956	LLOYD LAKE	50.87	-114.13	1128		Y
3034552	MILLARVILLE	50.72	-114.37	1250		
3034915	OKOTOKS	50.72	-113.98	1051		
3035233	POKAPPINI	50.42	-113.63	744		
3036640	TURNER VALLEY	50.72	-114.35	1238		
3036641	TURNER VALLEY RS	50.67	-114.28	1219		
303C642	KEOMA	51.25	-113.63	948	Y	

Alberta 7:

STATION ID	STATION NAME	LAT	LONG	ELEVATION	ACTIVE	PPT-ONLY
3010160	ALLIANCE	52.43	-111.78	716		
3010175	ALLIANCE SOUTH	52.42	-111.78	713	Y	
3010232	AMISK	52.68	-111.12	701		
3010890	BROWNFIELD	52.33	-111.47	747	Y	
3010991	CADOGAN	52.25	-110.53	665	Y	Y
3011440	CASTOR	52.22	-111.92	770		
3011441	CASTOR	52.13	-111.90	808		Y
3011479	CHAUVIN	52.72	-110.17	640		
3011880	CORONATION A	52.07	-111.45	791		
3011887	CORONATION CR10	52.08	-111.45	791	Y	
3011890	CORONATION	52.12	-111.45	789		
3012330	ELNORA SALEM	52.03	-112.13	826		
3012515	FABYAN	52.97	-111.00	698	Y	
3012652	FORESTBURG PLANT SITE	52.47	-112.12	663	Y	
3012992	HACKETT	52.15	-112.48	837	Y	
3012998	HALKIRK	52.28	-112.17	823		
3013040	HARDISTY	52.68	-111.30	625		
3013345	HORSESHOE LAKE	52.35	-110.73	658		

3013360	HUGHENDEN	52.52	-110.97	694		
3013361	HUGHENDEN	52.52	-110.97	694		
3014188	MANNVILLE SOUTH	53.10	-111.35	701		Y
3014520	METISKOW CDA EPF	52.40	-110.58	686		Y
3015287	POPLAR GLEN	52.87	-110.90	686	Y	
3015800	SEDGEWICK	52.88	-111.70	686		
3015808	SEDGEWICK TOWN	52.78	-111.70	663	Y	
3016119	STETTLER NORTH	52.33	-112.72	821	Y	
3016120	STETTLER	52.30	-112.70	823		
3016253	SULLIVAN LAKE	52.05	-111.95	811	Y	Y
3016932	WAINWRIGHT HEATH	52.83	-110.83	687		
301AR54	DAYSLAND	52.87	-112.28	689		
301NDR1	RED WILLOW	52.42	-112.57	783	Y	

Alberta 8:

STATION ID	STATION NAME	LAT	LONG	ELEVATION	ACTIVE	PPT-ONLY
3011953	DAKOTA WEST	52.73	-113.93	865	Y	
3015280	PONOKA	52.72	-113.77	857		Y
3015283	PONOKA SOUTH	52.65	-113.62	814		
3020120	ALIX	52.38	-113.17	788		
3020702	BISMARK	52.73	-113.87			Y
3020715	BLINDMAN	52.77	-114.48	960		Y
3020730	BLUFFTON	52.75	-114.28	908		Y
3020760	BOWDEN	51.98	-114.02	915		
3022078	DICKSON DAM	52.05	-114.22	980	Y	
3022158	ECKVILLE	52.38	-114.37	914		
3022159	ECKVILLE SOUTH	52.28	-114.38	960	Y	
3022325	ELNORA	51.97	-113.20	930	Y	Y
3022485	EVARTS	52.25	-114.22	942		Y
3023280	HILLSDOWN	52.17	-113.52	896		
3023665	KNEEHILL	51.92	-113.78	853		
3023720	LACOMBE CDA	52.47	-113.75	847		
3023722	LACOMBE CDA 2	52.45	-113.75	860	Y	
3024000	LOUSANA	52.08	-113.08	899		Y
3024210	MARKERVILLE	52.12	-114.13	914	Y	
3024572	MIRROR FLETCHER	52.45	-113.05	795		
3025170	PERBECK	51.97	-113.08	869		
3025222	PINE LAKE	52.17	-113.50	945		
3025440	RED DEER	52.28	-113.82	860		
3025441	RED DEER	52.30	-113.82	847	Y	
3025494	RIMBEY	52.63	-114.23	917		
3025K22	PINE LAKE NORTH	52.20	-113.48	899		Y
3026080	SPRINGDALE	52.80	-114.30	914		
3026259	SUNDRE GARRINGTON	51.97	-114.45	991	Y	
3026330	SYLVAN LAKE	52.35	-114.17	921		Y
302CCDB	HOADLEY	52.85	-114.20	914		Y

Alberta 9:

STATION ID	STATION NAME	LAT	LONG	ELEVATION	ACTIVE	PPT-ONLY
3010080	ALDER FLATS LO	52.80	-114.82	1076		
3010410	AURORA LO	52.65	-115.72	1341	Y	
3010534	BASELINE LO	52.13	-115.42	1897	Y	
3010712	BLACKSTONE LO	52.78	-116.35	1570	Y	
3011520	CHEDDERVILLE CDA EPF	52.20	-114.87	1036		
3011663	CLEARWATER	51.98	-115.25	1280	Y	
3014912	O CHIESE LO	52.78	-115.33	1113		
3015295	PRAIRIE CREEK RS	52.25	-115.30	1174		
3015520	ROCKY MTN HOUSE	52.38	-114.92	1015		
3015522	ROCKY MTN HOUSE A	52.43	-114.92	988		
3015524	ROCKY MTN HOUSE CR10	52.43	-114.92	988	Y	
3015530	ROCKY MOUNTAIN HOUSE	52.38	-114.92	969		
3016180	STRACHAN RS	52.25	-115.13	1113		
301C3D4	HORBURG	52.40	-115.20	1036	Y	
3020975	BURNSTICK LO	51.97	-114.78	1219		
3023800	LESLIEVILLE CDA EPF	52.40	-114.68	958		
3023971	LOBSTICK AUBUCHON	52.52	-114.73	1067	Y	
3050490	BALDY LO	52.55	-116.12	2083	Y	
30506GN	BIGHORN DAM	52.32	-116.33	1341	Y	
3050725	BLUEHILL LO	51.70	-115.22	1951	Y	
30516F5	CLINE LO	52.17	-116.18	2042	Y	
3053649	KISKA LO	52.30	-116.18	2073		
3053668	KOOTENAY PLAINS	52.18	-116.47	1359		
3054840	NORDEGG	52.47	-116.08	1402		
3054845	NORDEGG RS	52.50	-116.05	1320	Y	
3055379	RAM FALLS	52.08	-115.85	1641	Y	
3055485	RED DEER RS	51.67	-115.22	1451		
3055890	SHUNDA RS	52.48	-115.77	1433		
3057673	YA HA TINDA AFS	51.72	-115.57	1768	Y	

Alberta 10:

STATION ID	STATION NAME	LAT	LONG	ELEVATION	ACTIVE	PPT-ONLY
3010234	ANDREW	54.02	-112.23	610	Y	
3010535	BASHAW	52.68	-112.87	793		Y
3010558	BEAVER HILLS WEST	53.53	-112.53	770		Y
3010704	BITTERN LAKE	53.07	-113.00	745		
3010827	BRIARFIELD	53.73	-111.05	633		Y
3010900	BRUDERHEIM	53.78	-112.93	640		Y
3011239	CAMROSE	53.03	-112.80	675		
3011240	CAMROSE	53.03	-112.82	739	Y	
3011474	CHAILEY	53.55	-111.25	670	Y	
3012072	DEWBERRY	53.65	-110.60	616	Y	Y
3012275	ELK ISLAND NAT PARK	53.68	-112.87	716		
3012277	ELK ISLAND PARK	53.52	-112.90	724		
3013645	KINSELLA RANCH	53.00	-111.52	705	Y	
3013650	KITSCOTY	53.35	-110.33	670		
3013770	LAVOY	53.53	-111.87	670	Y	Y

3013961	LLOYDMINSTER A	53.32	-110.07	669	Y	
3013965	LLOYDMINSTER SEFTON PARK	53.08	-110.17	683	Y	Y
3013C44	HOLDEN SOUTH	53.08	-112.27	709	Y	Y
3013PFD	LAMONT	53.77	-112.85	710		
3014225	MARWAYNE	53.60	-110.23	594		
3014995	PARADISE VALLEY	53.12	-110.35	658	Y	
3015400	RANFURLY	53.45	-111.65	686		
3015405	RANFURLY 2NW	53.42	-111.73	673	Y	
3015879	SHALKA LAKE	53.80	-111.90	671		Y
3016494	TOFIELD NORTH	53.55	-112.75	701	Y	
3016590	TULLIBY LAKE	53.67	-110.13	574		
3016760	VEGREVILLE	53.48	-112.05	635		
3016761	VEGREVILLE CDA	53.48	-112.03	636		
3016790	VERMILION	53.37	-110.83	618		
3016800	VERMILION A	53.35	-110.83	619		
3016840	VIKING	53.10	-111.78	691		
3016845	VIKING NORTH 3	53.28	-111.77	676	Y	
3016954	WARWICK	53.65	-111.98	610		
3017665	WOSTOK	53.82	-112.48	652		
301B8LR	GOLDEN VALLEY	53.20	-110.15	640		

Alberta 11:

STATION ID	STATION NAME	LAT	LONG	ELEVATION	ACTIVE	PPT-ONLY
3010800	BRAZEAU LO	53.02	-115.42	1088	Y	
3010810	BREMNER	53.58	-113.28	678		Y
3010815	BRETON	53.17	-114.48	843	Y	
3010830	BRIGHTVIEW	52.98	-113.72	815	Y	
3010920	BUCK MOUNTAIN	53.02	-114.70	1061		
3011120	CALMAR	53.28	-113.85	720	Y	
3011854	COOKING LAKE	53.43	-113.12	743		
3012115	DRAYTON VALLEY	53.20	-114.98	853		
3012195	EDMONTON	53.55	-113.50	658		
3012208	EDMONTON CITY CENTRE A	53.57	-113.52	671	Y	
3012295	ELLERSLIE	53.42	-113.55	694		
3012659	FORT EDMONTON	53.52	-113.57	628		
3012710	FORT SASKATCHEWAN	53.72	-113.18	620		
3012990	GWYNNE	52.95	-113.18	768	Y	
3012P82	GIBBONS	53.82	-113.17	647		
3013060	HASTINGS LAKE	53.38	-112.88	762		
3013247	HIGHVALE	53.45	-114.47	747	Y	
3014565	MINISTIK SANCTUARY	53.37	-113.03	762		Y
3014870	NORTH COOKING LAKE	53.43	-113.18	741		
3014922	OLIVER TREE NURSERY	53.65	-113.37	648		
3016440	THORSBY	53.22	-114.05	744		
3016650	UNCAS	53.50	-113.03	750	Y	Y
3016900	WABAMUN	53.57	-114.47	729		Y
3017280	WETASKIWIN	52.97	-113.33	756		
3017286	WETASKIWIN SOUTH	52.97	-113.38	762	Y	
3017595	WINFIELD	52.95	-114.58	910	Y	

3060832	BRIGHTWOOD	53.50	-114.93	793		Y
3062451	ENTWISTLE	53.60	-114.98	780	Y	
3064157	MAGNOLIA	53.58	-114.88	755		Y
3064640	MOON LAKE	53.47	-114.98	762		

Saskatchewan 1a:

STATION ID	STATION NAME	LAT	LONG	ELEVATION	ACTIVE	PPT-ONLY
4010080	ALAMEDA CDA EPF	49.25	-102.28	580		
4010100	ALIDA	49.45	-101.80	585	Y	Y
4010240	ARCOLA CDA EPF	49.63	-102.53	604		Y
4010570	BENSON	49.45	-102.98	588	Y	
4011090	CANNINGTON MANOR	49.72	-102.03	629		
4011160	CARLYLE	49.63	-102.27	631		
4011250	CARNDUFF	49.22	-101.75	515	Y	Y
4012390	ESTEVAN	49.20	-103.07	566		
4012400	ESTEVAN A	49.22	-102.97	581	Y	
4012485	FERTILE	49.33	-101.45	511	Y	
4012790	GAINSBOROUGH	49.30	-101.53	518		Y
4013221	HEWARD	49.75	-103.15	625		
4013251	HIRSCH	49.18	-102.60	573		Y
4014050	KISBEY	49.55	-102.63	610		Y
4014142	LAMPMAN	49.45	-102.62	594		
4014870	MACOUN	49.23	-103.23	571	Y	Y
4015800	OXBOW	49.22	-102.17	582	Y	
4016520	REDVERS	49.58	-101.70	594		
4016521	REDVERS	49.60	-101.72	596	Y	
4016522	REDVERS	49.53	-101.70	587		
4018960	WILLMAR	49.42	-102.50	594	Y	Y
401G7R7	STOUGHTON	49.62	-103.07	610		Y

Saskatchewan 1b:

STATION ID	STATION NAME	LAT	LONG	ELEVATION	ACTIVE	PPT-ONLY
4010878	BROADVIEW	50.38	-102.55	597		
4010879	BROADVIEW	50.38	-102.68	602	Y	
4010880	BROADVIEW A	50.25	-102.53	620		
4012520	FLEMING CDA EPF	50.12	-101.53	541		Y
4012525	FLEMING SOUTH	50.03	-101.58	572		Y
4013030	GRENFELL	50.42	-102.93	599		
4013098	HANDSWORTH	49.83	-102.87	678	Y	
4014040	KIPLING	50.20	-102.73	671	Y	
4015045	MARYFIELD	49.83	-101.52	576	Y	
4015344	MOOSE MOUNTAIN RESERVOIR	49.88	-103.03	619		
4015360	MOOSOMIN	50.13	-101.67	576	Y	
4016842	ROCANVILLE	50.47	-101.55	479	Y	
4017910	SUMMERBERRY	50.48	-103.07	573		
4018506	WAPELLA	50.18	-102.13	602		
4018508	WAPELLA NEWFINLAND	50.45	-101.93	571		
4018678	WAWOTA	49.93	-101.97	643		

4018880	WHITEWOOD	50.35	-102.27	598	Y	
4019023	WOLSELEY	50.43	-103.28	594	Y	

Saskatchewan 2a:

STATION ID	STATION NAME	LAT	LONG	ELEVATION	ACTIVE	PPT-ONLY
4010150	AMULET	49.62	-104.73	728		
4011880	CREELMAN	49.80	-103.25	625		
4012493	FILLMORE	49.88	-103.43	619		Y
4013770	KHEDIVE	49.60	-104.50	651		
4015159	MIDALE	49.38	-103.30	587	Y	
4015160	MIDALE	49.40	-103.40	582		
4015863	PANGMAN	49.65	-104.55	649		
4018760	WEYBURN	49.65	-103.83	570	Y	
4019040	YELLOW GRASS	49.82	-104.18	580	Y	

Saskatchewan 2b:

STATION ID	STATION NAME	LAT	LONG	ELEVATION	ACTIVE	PPT-ONLY
4010540	BECHARD	50.05	-104.22	578		
4010568	BELLE PLAINE	50.45	-105.20	582		
4010840	BRIERCREST	50.15	-105.27	594		
4010984	BUFFALO POUND LAKE	50.55	-105.38	588	Y	
4011280	CARON	50.45	-105.87	579		
4011580	CLAYBANK	50.05	-105.22	643		
4011640	CONDIE	50.55	-104.77	572		Y
4012165	DAVIN 6	50.37	-104.15	648		Y
4012340	EDGELEY	50.60	-104.03	640		Y
4012720	FRANCIS	50.12	-103.92	603		
4013480	INDIAN HEAD CDA	50.55	-103.65	579	Y	
4014105	KRONAU	50.33	-104.30	594		
4015040	MARQUIS	50.62	-105.70	599		Y
4015258	MONTMARTRE	50.25	-103.47	678	Y	
4015320	MOOSE JAW A	50.33	-105.55	577	Y	
4015325	MOOSE JAW	50.35	-105.58			
4015648	ODESSA	50.33	-103.68	658		
4015920	PASQUA	50.33	-105.35	571		Y
4016080	PENSE	50.42	-105.00	577		
4016080	PENSE	50.42	-105.00	577		
4016320	QU'APPELLE	50.52	-103.88	650	Y	
4016322	QU'APPELLE 1	50.57	-103.98	663		
4016560	REGINA A	50.43	-104.67	577	Y	
4016960	ROWATT	50.22	-104.67	587		Y
4017281	SEDLEY	50.12	-104.10	590		
4018920	WILCOX	50.17	-104.33	585		
4019200	ZEHNER	50.63	-104.40	683	Y	

Saskatchewan 3an:

STATION ID	STATION NAME	LAT	LONG	ELEVATION	ACTIVE	PPT-ONLY
4011120	CARDROSS	49.82	-105.65	701		
4015400	MORTLACH EXP ST	50.45	-106.05	606		Y

STATION ID	STATION NAME	LAT	LONG	ELEVATION	ACTIVE	PPT-ONLY
4015867	PARKBEG	50.47	-106.07	610	Y	
4020720	BISHOPRIC	50.00	-105.78	680		
4021520	CHAPLIN	50.47	-106.65	672		
4021600	CODERRE	50.13	-106.37	685	Y	
4021850	COURVAL	50.17	-106.25	666		Y
4021851	COURVAL	50.18	-105.88	693	Y	
4022328	EASTLEIGH	50.28	-106.18	709	Y	
4022840	GILROY CDA EPF	50.83	-106.73	647		Y
4022960	GRAVELBOURG	49.88	-106.55	700		
4025242	MITCHELLTON	49.97	-105.63	716		Y
4025855	PALMER	49.87	-106.35	727		
4027440	SHAMROCK	50.18	-106.57	710		
4028360	VALJEAN	50.38	-106.55	671		Y

Saskatchewan 3as:

STATION ID	STATION NAME	LAT	LONG	ELEVATION	ACTIVE	PPT-ONLY
4011440	CEYLON	49.47	-104.60	713		
4011441	CEYLON	49.38	-104.65	753	Y	
4012050	DAHINDA	49.75	-105.00	725	Y	
4014138	LAKE ALMA	49.07	-104.25	724		
4015680	ORMISTON	49.72	-105.37	686		
4015716	OUNGRE	49.15	-103.75	604		
4016400	RADVILLE	49.50	-104.28	633		Y
4018120	TRIBUNE	49.25	-103.83	607		Y
4020280	ASSINIBOIA	49.73	-105.97	724		
4020286	ASSINIBOIA AIRPORT	49.73	-105.93	726	Y	
4024135	LAFLECHE	49.65	-106.57	750		
4024400	LIMERICK	49.50	-106.25	759		
4026480	READLYN	49.58	-105.67	676		
4029030	WOODROW	49.57	-106.78	730	Y	Y
4030569	BENGOUGH	49.38	-105.13	689		
4031844	CORONACH	49.12	-105.52	773	Y	
4032335	EAST POPLAR RIVER	49.00	-105.42	739		
4034380	LIDGETT	49.30	-106.58	914		Y
4035200	MINTON	49.17	-104.58	695		
4036844	ROCKGLEN (AUT)	49.17	-105.98	917	Y	
4038460	VICEROY CDA EPF	49.52	-105.37	725		
4038740	WEST POPLAR RIVER	49.00	-106.38	876	Y	

Saskatchewan 3bn:

STATION ID	STATION NAME	LAT	LONG	ELEVATION	ACTIVE	PPT-ONLY
4020560	BEECHY	50.77	-107.32	660	Y	
4020701	BIRSAY	51.08	-106.97	594		
4021025	CABRI	50.52	-108.45	678		
4022180	DEMAINE CDA EPF	50.90	-107.25	697		Y
4022368	ELROSE	51.13	-108.03	610	Y	
4023210	HERBERT	50.43	-107.22	701		
4023212	HERBERT 2	50.47	-107.27	710	Y	
4023240	HIGH POINT	50.98	-107.93	645	Y	Y

4023260	HODGEVILLE	50.12	-106.97	697		
4023360	HUGHTON	51.23	-107.92	613		
4024120	KYLE CDA EPF	50.73	-108.02	686		
4024714	LUCKY LAKE	50.95	-107.15	665	Y	
4025485	NEIDPATH	50.22	-107.10	777		
4026040	PENNANT	50.53	-108.23	730		
4026847	ROCK POINT	51.15	-107.27	725	Y	
4027000	RUSH LAKE	50.40	-107.40	712		
4027110	SANCTUARY	51.03	-108.05	610		
4027775	STEWART VALLEY	50.60	-107.80	727	Y	
4028035	SWIFT CURRENT	50.33	-107.75	744		
4028040	SWIFT CURRENT A	50.30	-107.68	818	Y	

Saskatchewan 3bs:

STATION ID	STATION NAME	LAT	LONG	ELEVATION	ACTIVE	PPT-ONLY
4020160	ANEROID	49.72	-107.30	754	Y	
4020772	BLUMENHOF	50.03	-107.77	899		
4021040	CADILLAC	49.72	-107.75	785		
4023160	HAZENMORE	49.58	-107.10	739		Y
4023263	HODGEVILLE 2	49.98	-106.93	724		Y
4023430	ILLERBRUN	49.88	-108.37	892		
4023520	INSTOW	49.72	-108.28	903		
4023800	KINCAID	49.67	-107.00	739	Y	
4025860	PAMBRUN CDA EPF	50.00	-107.43	777		
4027480	SHAUNAVON	49.65	-108.40	917		
4027485	SHAUNAVON 2	49.65	-108.42	914	Y	
4030800	BRACKEN CDA EPF	49.20	-108.10	888		Y
4031585	CLIMAX	49.20	-108.38	939		
4034910	MANKOTA	49.10	-107.02	830	Y	
4038116	TREELON	49.00	-108.38	902	Y	
4038400	VAL-MARIE	49.37	-107.85	808	Y	

Saskatchewan 4a:

STATION ID	STATION NAME	LAT	LONG	ELEVATION	ACTIVE	PPT-ONLY
4021996	CYPRESS HILLS	49.67	-109.47	1196	Y	
4022800	GARDEN HEAD	49.82	-108.57	905		
4023060	GULL LAKE CDA EPF	49.95	-108.47	907		
4024080	KLINTONEL	49.68	-108.92	1074		
4024919	MAPLE CREEK	49.90	-109.47	767	Y	
4024920	MAPLE CREEK	49.90	-109.48	764		
4031581	CLAYDON	49.13	-109.10	975		
4031760	CONSUL	49.30	-109.52	931		
4031776	CONSUL	49.30	-109.48	942		
4031999	CYPRESS HILLS PARK	49.65	-109.52	1271	Y	
4032000	CYPRESS HILLS PARK	49.67	-109.48	1372		
4032321	EASTEND CDA EPF SOUTH	49.37	-108.77	914		Y
4032323	EASTEND 2	49.52	-108.82	914		
4032510	FLAP JACK	49.53	-109.88	1036		

4032640	FORT WALSH	49.47	-109.57	1105		
4032766	FRONTIER	49.20	-108.57	901	Y	
4035120	MERRYFLAT	49.47	-109.77	1036		
4035480	NASHLYN	49.20	-109.52	945		
4036841	ROBSART	49.38	-109.35	962		Y
4037360	SENATE	49.27	-109.70	968		
4038490	VIDORA	49.35	-109.50	945		
4039000	WILLOW CREEK	49.02	-109.92	833		
4039001	WILLOW CREEK	49.08	-109.82	861		

Saskatchewan 4b:

STATION ID	STATION NAME	LAT	LONG	ELEVATION	ACTIVE	PPT-ONLY
4020020	ABBEY	50.70	-108.78	695	Y	
4021200	CARMICHAEL	50.05	-108.65	807		Y
4022680	FOX VALLEY	50.40	-109.43	709		Y
4022936	GOLDEN PRAIRIE	50.18	-109.80	747	Y	
4023053	GULL LAKE	50.27	-108.55	762		Y
4023500	INGEBRIGHT LAKE	50.37	-109.35	701		
4024160	LEADER	50.88	-109.55	671		
4024161	LEADER 2	50.88	-109.53	674		
4026175	PORTREEVE	50.88	-109.05	678	Y	
4026840	ROADENE	50.48	-108.75	723		
4027400	SHACKLETON CDA EPF	50.68	-108.68	709	Y	Y
4027960	SURPRISE	50.30	-109.98	762		
4028101	TOMPKINS	50.05	-108.80	811	Y	
4028500	WAPASHOE	50.07	-109.38	732		

Saskatchewan 5a:

STATION ID	STATION NAME	LAT	LONG	ELEVATION	ACTIVE	PPT-ONLY
4010310	ATWATER	50.82	-102.22	536	Y	
4010395	BALCARRES	50.78	-103.62	576	Y	Y
4010400	BANGOR	50.90	-102.28	526	Y	
4011888	CRESCENT LAKE	50.98	-102.42	505		
4011980	CUPAR	50.85	-104.27	556	Y	
4012309	DYSART	51.12	-103.98	640		
4012483	FENWOOD	51.15	-103.07	625	Y	
4012600	FORT QU'APPELLE	50.78	-103.80	486		
4012988	GRAYSON	50.70	-102.63	541	Y	
4013280	HUBBARD	51.10	-103.33	663		
4013660	KELLIHER	51.25	-103.75	671	Y	
4014145	LANGENBURG	50.90	-101.72	517	Y	
4014299	LEMBERG	50.60	-103.25	587		Y
4014320	LEROSS	51.30	-103.87	676		
4014325	LESTOCK	51.28	-103.95	676		
4014480	LIPTON	50.85	-103.77	602	Y	
4015100	MELVILLE	50.95	-102.80	558		
4016335	QUINTON	51.35	-104.42	623	Y	Y
4017095	SALTCOATS	50.97	-102.27	523	Y	
4017370	SERATH	51.17	-104.40	622	Y	

4018496	WALDRON	50.87	-102.47	530		Y
4019070	YORKTON	51.18	-102.52	498		
4019080	YORKTON A	51.27	-102.47	498	Y	

Saskatchewan 5b:

STATION ID	STATION NAME	LAT	LONG	ELEVATION	ACTIVE	PPT-ONLY
4010961	BUCHANAN	51.72	-102.83	503		
4011095	CANORA	51.63	-102.38	482		
4011846	COTE	51.52	-101.78	450	Y	
4012560	FOAM LAKE	51.63	-103.53	558		
4012561	FOAM LAKE	51.72	-103.55	544		
4012943	GOOD SPIRIT LAKE	51.50	-102.67	484	Y	
4013518	INSINGER	51.53	-103.08	539		
4013640	KAMSACK	51.57	-101.90	440		
4014100	KRISTNES	51.73	-103.63	532		
4014115	KUROKI	52.00	-103.45	585	Y	
4015020	MARGO	51.83	-103.33	544	Y	Y
4015870	PARKERVIEW	51.40	-103.27	637	Y	
4016185	PREECEVILLE	51.95	-102.65	518		
4016330	QUILL LAKE	52.07	-104.23	488		
4016335	QUINTON	51.37	-104.42	623		Y
4017704	SPALDING	52.37	-104.37	578		
4018074	THEODORE	51.50	-102.97	526		
4018098	TOGO	51.40	-101.58	559		Y
4019007	WISHART	51.57	-104.12	648		
4019035	WYNYARD	51.77	-104.20	561	Y	
4080260	ARRAN	51.97	-101.73	450		
4080262	ARRAN 23N	52.20	-101.63	450		
4083720	KELVINGTON	52.15	-103.55	559		
4084440	LINTLAW	52.08	-103.27	611		
4086000	PELLY	52.08	-101.87	509	Y	

Saskatchewan 6a:

STATION ID	STATION NAME	LAT	LONG	ELEVATION	ACTIVE	PPT-ONLY
4010358	AYLESBURY	50.93	-105.70	579		
4010360	AYLESBURY CDA EPF	51.00	-105.67	576		Y
4012040	DAFOE A	51.93	-104.57	540		
4012120	DAVIDSON	51.27	-105.98	619		
4012200	DILKE	50.87	-105.17	521		Y
4012300	DUVAL	51.17	-104.85	591	Y	
4012381	ESK	51.80	-104.85	542	Y	Y
4013038	GUERNSEY	51.78	-105.28	526		
4013040	GUERNSEY CDA EPF	51.82	-105.23	541		
4013270	HOLDFAST	51.00	-105.52	544	Y	
4013440	IMPERIAL	51.37	-105.53	556		
4013740	KENASTON	51.50	-106.27	616		Y
4014156	LAST MOUNTAIN CS	51.42	-105.25	497	Y	
4014322	LEROY	52.00	-104.63	533	Y	
4014360	LIBERTY	51.13	-105.33	495		

4014720	LUMSDEN	50.65	-104.87	497		
4015560	NOKOMIS	51.52	-105.00	526	Y	
4016450	RAYMORE	51.57	-104.58	564		
4016651	REGINA GILMOUR	50.57	-104.83	556	Y	Y
4017320	SEMANS	51.42	-104.73	562		
4017800	STRASBOURG	51.07	-104.95	544		
4018640	WATROUS	51.67	-105.47	541	Y	
4051636	COLONSAY	51.93	-105.77	543		
4058492	VISCOUNT	51.95	-105.63	547		
4059220	ZELMA	51.80	-105.93	541		Y

Saskatchewan 6b:

STATION ID	STATION NAME	LAT	LONG	ELEVATION	ACTIVE	PPT-ONLY
4050275	ASQUITH	52.13	-107.23	519		
4050500	BEAVER CREEK	51.97	-106.70	488		
4050768	BLACKSTRAP	51.78	-106.40	536		
4051147	CARLTON	52.80	-106.57	521	Y	
4051720	CONQUEST CDA EPF	51.52	-107.25	571		
4052210	DINSMORE	51.32	-107.33	644		
4052230	DONAVON	51.80	-107.18	533		
4052280	DUNDURN	51.80	-106.50	529		
4022360	ELBOW	51.12	-106.60	588		
4022361	ELBOW	51.13	-106.58	595		
4022363	ELBOW 2 NE	51.17	-106.55	605	Y	
4052933	GLENSIDE	51.47	-106.83	568		Y
4052956	GRASSWOOD	52.07	-106.63	503		
4053083	HAGUE	52.50	-106.48	520		
4053120	HARRIS	51.73	-107.58	578	Y	
405DJDN	LANGHAM 2W	52.37	-107.02	503	Y	
4054306	LENEY	51.88	-107.52	556		
4055043	MARTENSVILLE	52.33	-106.67	520		
4055165	MILDEN	51.43	-107.50	578	Y	
4055720	OUTLOOK	51.48	-107.05	541		
4055736	OUTLOOK PFRA	51.48	-107.05	541	Y	
4056920	ROSTHERN	52.67	-106.33	510		
4057120	SASKATOON A	52.17	-106.72	504	Y	
4027880	STRONGFIELD	51.33	-106.60	614		
4057920	SURBITON	51.33	-107.23	655		Y
4058000	SUTHERLAND CDA	52.15	-106.58	507		
4018160	TUGASKE	50.88	-106.30	607	Y	
4058390	VALLEY PARK	51.88	-106.82	526		
4058420	VANSCOY UPPER AIR	52.02	-107.03	510		

Saskatchewan 7a:

STATION ID	STATION NAME	LAT	LONG	ELEVATION	ACTIVE	PPT-ONLY
4040120	ALSASK	51.38	-110.00	701		
4020130	ALSASK HARDENE	51.33	-109.85	658		
4040180	ANGLIA	51.57	-108.17	567		
4040587	BICKLEIGH	51.30	-108.40	671	Y	

4022440	ESTON	51.15	-108.77	680		
4043215	HERSCHEL	51.68	-108.30	610		Y
4043888	KINDERSLEY	51.47	-109.15	681		
4043900	KINDERSLEY A	51.52	-109.18	694	Y	
4043920	KINDERSLEY KY	51.47	-109.17	683		
4044680	LOVERNA CDA EPF	51.65	-110.00	689		
4046879	ROSETOWN	51.62	-108.02	586	Y	
4046880	ROSETOWN CDA EPF	51.52	-107.88	591		
4047681	SOVEREIGN	51.52	-107.72	587	Y	Y
4047798	STRANRAER	51.70	-108.52	641		

Saskatchewan 7b:

STATION ID	STATION NAME	LAT	LONG	ELEVATION	ACTIVE	PPT-ONLY
4040600	BIGGAR	52.07	-107.98	671	Y	
4041088	CANDO	52.40	-108.27	710	Y	
4042188	DENZIL	52.30	-109.58	696		
4043653	KELFIELD	52.00	-108.58	685		
4043750	KERROBERT	51.97	-109.05	660	Y	
4044735	LUSELAND	52.08	-109.40	701		
4044800	MACKLIN	52.33	-109.95	667		
4047040	RUTHILDA	51.90	-108.52	695		Y
4047238	SCOTSTOWN	52.38	-109.40	685	Y	
4047240	SCOTT CDA	52.37	-108.83	660	Y	
4047644	SONNINGDALE	52.32	-107.77	716	Y	
4047050	ST DONATUS	51.98	-109.90	745		
4048320	UNITY	52.42	-109.08	640		
4048326	UNITY SOUTH	52.23	-109.20	655	Y	

Saskatchewan 8a:

STATION ID	STATION NAME	LAT	LONG	ELEVATION	ACTIVE	PPT-ONLY
4080200	ARCHERWILL EXP ST	52.43	-104.02	556		
4080250	ARMIT	52.83	-101.78	308		
4070365	AYLSHAM	53.20	-103.80	362	Y	
4076790	RIDGEDALE	53.05	-104.25	413		
4071612	CODETTE ELKHORN	53.25	-104.17	398		
4071680	CONNELL CREEK EXP ST	53.15	-103.32			Y
4083320	HUDSON BAY	52.87	-102.40	372		
4083321	HUDSON BAY A	52.82	-102.32	358		
4083323	HUDSON BAY 13W	52.88	-102.58	422	Y	
4074640	LOST RIVER	53.28	-104.33	375		
4085050	MCKAGUE	52.57	-103.83	539	Y	
4055080	MELFORT	52.87	-104.60	463		
4055085	MELFORT EXP FARM	52.82	-104.60	480		
4085241	MISTATIM	52.85	-103.23	482		
4075520	NIPAWIN 2	53.35	-104.02	358		
4075518	NIPAWIN A	53.33	-104.00	372	Y	
4086160	PORCUPINE PLAIN	52.65	-103.15	465		
4086180	PRAIRIE RIVER	52.87	-102.98	467		
4077557	SMOKY BURN	53.37	-103.17	319	Y	

4077560	SMOKY BURN EXP ST	53.33	-103.13	362		
4087640	SOMME EXP ST	52.62	-103.02	439		
4057757	STAR CITY	52.87	-104.33	465		Y
4057760	STAR CITY EXP ST	52.72	-104.33	469		Y
4078080	TISDALE	52.87	-104.00	450		
4078084	TISDALE SOUTH	52.75	-103.40	501	Y	
4078415	VALPARAISO	52.78	-104.20	462		Y
4088720	WEEKES	52.75	-102.83	422		

Saskatchewan 8b:

STATION ID	STATION NAME	LAT	LONG	ELEVATION	ACTIVE	PPT-ONLY
4052070	DANA RCAF	52.28	-105.77	617		
4052448	ETHELTON	52.77	-104.90	466		
4053264	HOEY	52.85	-105.78	473	Y	Y
4013400	HUMBOLDT	52.20	-105.10	567		
4013401	HUMBOLDT	52.27	-105.12	549	Y	
4053960	KINISTINO	52.95	-105.02	463		
4015440	MUENSTER	52.18	-105.00	579	Y	
4055450	MUSKIKI SPRINGS	52.32	-105.68	545		
4056120	PILGER	52.42	-105.15	552	Y	
4057070	ST LOUIS	52.92	-105.80	440		

Saskatchewan 9a:

STATION ID	STATION NAME	LAT	LONG	ELEVATION	ACTIVE	PPT-ONLY
4060620	BIG RIVER	53.83	-107.03	503		
4051080	CAMEO	53.28	-106.55	488		
4071560	CHOICELAND	53.50	-104.48	442		
4052671	FOXFORD	53.42	-105.12	468		
4042884	GLASLYN 2	53.42	-108.13	690		
4042920	GLENBUSH	53.23	-108.00	689		
4042921	GLENBUSH	53.10	-108.03	632		
4053080	HAFFORD EXP ST	52.72	-107.37	587		
4053090	HALCYONIA	52.50	-107.08	549		
4053200	HENRIBOURG EXP ST	53.37	-105.60	465		Y
4054110	KRYDOR	52.70	-107.03			
4054240	LEASK	53.02	-106.75	526		
4064312	LEOVILLE	53.55	-107.57	607		Y
4054795	MACDOWALL	53.02	-106.02	477	Y	
4055010	MARCELIN	52.92	-106.80	523	Y	
4045070	MEDSTEAD	53.35	-108.03	700		
4065172	MILDRED	53.33	-107.25	617		Y
4045600	NORTH BATTLEFORD A	52.77	-108.25	548	Y	
4055640	NORTHSIDE	53.53	-105.77	494		
4075840	PADDOCKWOOD EXP ST	53.52	-105.53	485		Y
4055880	PARKSIDE EPF	53.23	-106.58	515		
4056230	PRINCE ALBERT	53.17	-105.75	437		
4056240	PRINCE ALBERT A	53.22	-105.67	428	Y	
4046360	RABBIT LAKE	53.10	-107.87	704		
4056381	RADISSON 1	52.40	-107.42	520	Y	

4046977	RUDDELL	52.58	-107.85	538	Y
4077600	SNOWDEN EXP ST	53.53	-104.68	447	
4067720	SPIRITWOOD	53.37	-107.53	589	
4067723	SPIRITWOOD WEST	53.37	-107.55	584	Y
4068485	VICTOIRE	53.48	-107.03	521	
4058728	WEIRDALE	53.45	-105.25	474	
4078800	WHITE FOX EXP ST	53.45	-104.08	372	
4069010	WITCHEKAN	53.48	-107.55	579	

Saskatchewan 9b:

STATION ID	STATION NAME	LAT	LONG	ELEVATION	ACTIVE	PPT-ONLY
4040267	ARTLAND	52.78	-109.90	640	Y	
4040420	BATTLEFORD	52.68	-108.33	494		
4060452	BEACON HILL	54.33	-109.62	533	Y	
4041000	BUTTE ST PIERRE	53.45	-109.20	572	Y	
4041405	CARRUTHERS	52.90	-109.18	643		
4062240	DORINTOSH CDA EPF	54.33	-108.62	503		
4042338	EDAM	53.18	-108.77	549	Y	
4042760	FRENCHMAN BUTTE	53.58	-109.63	550		
4042880	GLASLYN CDA EPF	53.33	-108.27	690		
4062940	GOODSOIL	54.40	-109.23	506		
4043246	HILLMOND	53.43	-109.72	587	Y	
4044152	LASHBURN	53.03	-109.55	594	Y	
4044558	LLOYDMINSTER	53.30	-110.00	646		
4044562	LLOYDMINSTER 12E	53.28	-109.67	648		
4064590	LOON LAKE	54.03	-109.03	594		
4064600	LOON LAKE CDA EPF	54.05	-109.10	543	Y	
4065055	MEADOW LAKE	54.13	-108.43	481		
4065060	MEADOW LAKE 2	54.13	-108.43	494		
4065058	MEADOW LAKE A	54.13	-108.52	480	Y	
4045487	NEILBURG	52.80	-109.60	668		Y
4045660	ONION LAKE	53.87	-109.98			
4045975	PAYNTON	53.02	-108.95	561	Y	
4066090	PIERCELAND	54.35	-109.75	549		
4046200	PRINCE	52.97	-108.37	536		
4046280	PRONGUA	52.73	-108.55	563		Y
4047730	SPRUCE LAKE	53.53	-109.08	604		
4047080	ST WALBURG	53.63	-109.22	640		
4047081	ST WALBURG	53.72	-109.15	663		
4048240	TURTLEFORD	53.40	-108.95	587		
4048250	TURTLEFORD EPF	53.45	-109.00	587		
4048520	WASECA	53.13	-109.40	638	Y	

Manitoba 1:

STATION ID	STATION NAME	LAT	LONG	ELEVATION	ACTIVE	PPT-ONLY
5010180	BEDE	49.37	-100.93	442		
5010190	BELMONT	49.40	-99.43	447		Y
5010191	BELMONT	49.30	-99.45	482	Y	Y
5020320	BOISSEVAIN	49.23	-100.05	511		

5010538	CAMERON	49.47	-100.47	442	Y	
5010760	DELORAINE	49.30	-100.52	501		
5011080	GOODLANDS EXP ST	49.18	-100.58	500		
5011283	HARTNEY	49.50	-100.53	428		Y
5021480	KILLARNEY	49.18	-99.65	495	Y	
5011600	LYLETON	49.05	-101.18	460		Y
5011720	MELITA	49.33	-101.00	442		
501A7AR	MELITA	49.28	-100.98	446	Y	
5011762	MINTO	49.45	-100.05	477		Y
5022040	NINETTE	49.40	-99.63	417		
50220M0	NINETTE 1 NW	49.42	-99.65	419		
5022041	NINGA	49.23	-99.85	503		
5022065	PEACE GARDENS	49.00	-100.05	693	Y	
5012080	PIERSON	49.18	-101.27	469	Y	
5012340	REGENT	49.32	-100.37	501		
5012935	TURTLE MOUNTAIN	49.18	-100.33	655		
5012941	TURTLE MOUNTAIN 6	49.30	-100.32	503	Y	
5013120	WASKADA	49.03	-100.75	469		

Manitoba 2:

STATION ID	STATION NAME	LAT	LONG	ELEVATION	ACTIVE	PPT-ONLY
5010033	ALEXANDER	49.83	-100.30	427	Y	Y
5010485	BRANDON CDA	49.87	-99.98	363	Y	
5010524	BROOKDALE	50.02	-99.57	392	Y	Y
5010548	CARBERRY	49.87	-99.35	385		
5010554	CARROLL	49.55	-100.00	488		Y
5010868	ELKHORN	49.97	-101.23	499		
50110QFQ	ELKHORN 2 EAST	49.93	-101.20	498	Y	
5011051	GLENBORO	49.57	-99.33	372		
5011275	HARDING	50.03	-100.50	472		
5011280	HARGRAVE EXP ST	49.92	-101.10	488		Y
5011293	HILLVIEW	49.92	-100.55	427		
5011434	KENTON	49.98	-100.58	449	Y	Y
5012200	PIPESTONE EXP ST	49.57	-100.97			
5012333	RAPID CITY FORREST	50.02	-100.00	488		
5012400	RESTON	49.55	-101.10			
5012400	RESTON	49.55	-101.10	464		
5012439	RIVERS	50.03	-100.23	476		
5012440	RIVERS A	50.02	-100.32	473		
5012540	ST ALBANS	49.70	-99.55	360		
5012672	SHILO	49.78	-99.65	373		
5012719	SOURIS	49.65	-100.25	433	Y	
5012720	SOURIS	49.62	-100.27	427		
5012960	VIRDEN	49.83	-100.95	445	Y	
501K051	OAK LAKE	49.77	-100.63	431		Y

Manitoba 3:

STATION ID	STATION NAME	LAT	LONG	ELEVATIO N	ACTIVE	PPT-ONLY
5010216	BINSCARTH	50.58	-101.27	526	Y	

5010240	BIRTLE	50.43	-101.05	522	Y	
5010550	CARDALE	50.23	-100.33	556		
5010981	FOXWARREN	50.57	-101.07	552		
5011240	HAMIOTA	50.18	-100.62	518		
5011705	MCCONNELL	50.27	-100.60	541		Y
5011760	MINNEDOSA	50.27	-99.83	521		
5012054	OAKNER	50.10	-100.63	503	Y	
501233B	RAPID CITY	50.12	-99.93	546		Y
5012620	SANDY LAKE	50.50	-100.10	625	Y	
5012654	SHOAL LAKE CS	50.45	-100.60	561	Y	
5012676	SHOAL LAKE	50.48	-100.72	625		Y
5012677	SHOAL LAKE	50.45	-100.58	555		Y
5012796	STRATHCLAIR	50.40	-100.40	579	Y	
5013117	WASAGAMING	50.65	-99.93	627	Y	
501BMMA	RIVERS PETTAPIECE	50.12	-100.18	488	Y	
5040146	BASSWOOD	50.25	-100.03	583		
5041425	KELWOOD	50.62	-99.47	352		
5042000	NEEPAWA A	50.23	-99.50	388		
5042003	NEEPAWA CSC	50.23	-99.47	369		
5042005	NEEPAWA WATER	50.22	-99.47	358	Y	

Manitoba 4:

STATION ID	STATION NAME	LAT	LONG	ELEVATION	ACTIVE	PPT-ONLY
5010227	BIRDTAIL	50.82	-100.92	578		Y
5010310	BOGGY CREEK	51.60	-101.30	664	Y	
5011360	INGLIS	50.90	-101.23	594		
501205N	OLHA	50.67	-100.55	622		
5012471	ROBLIN	51.20	-101.45			
5012472	ROBLIN	51.23	-101.38	556		
5012500	ROSSBURN	50.67	-100.82	590		
501KE01	ROSSBURN 4 NORTH	50.75	-100.82	610	Y	Y
5012520	RUSSELL	50.77	-101.28	567		
5012680	SILVERTON EXP ST	50.77	-101.15	572		Y

Manitoba 5:

STATION ID	STATION NAME	LAT	LONG	ELEVATION	ACTIVE	PPT-ONLY
5040218	BIRCH RIVER	52.52	-100.92	268	Y	
5040FJ3	COWAN	52.03	-100.65	366	Y	
5040840	DURBAN EXP ST	51.93	-101.40	419		Y
5041440	KENVILLE EXP ST	52.00	-101.32	387		Y
5041560	LENSWOOD EXP ST	52.53	-101.00	305		Y
5041685	MAFEKING	52.68	-101.10	325	Y	
5042168	PINE RIVER	51.77	-100.32	302		
5042169	PINE RIVER SNOW RANCH	51.80	-100.57	378	Y	
5042800	SWAN RIVER	52.05	-101.22	347	Y	

Manitoba 6:

STATION ID	STATION NAME	LAT	LONG	ELEVATION	ACTIVE	PPT-ONLY
5040037	ALONSA	50.83	-99.05	274	Y	Y
5040060	AMARANTH	50.63	-98.72	259	Y	Y
5040121	ASHVILLE	51.28	-100.28	320		
5040EN5	CAYER	51.25	-99.08	259		
5040675	DAUPHIN	51.15	-100.03	292		
5040680	DAUPHIN A	51.10	-100.05	305	Y	
5040899	ETHELBERT	51.53	-100.38	343		Y
5040R73	FORK RIVER NORTH	51.57	-99.98	260	Y	Y
5040985	GILBERT PLAINS	51.10	-100.47	404	Y	
5041116	GRANDVIEW	51.12	-100.70	442	Y	Y
5041120	GRANDVIEW EXP ST	51.18	-100.80	465		Y
5041523	LAKE DAUPHIN	51.20	-99.55	264		
5041686	MAGNET	51.32	-99.48	264	Y	
5041707	MCCREARY	50.73	-99.42	297	Y	Y
50420E5	OCHRE RIVER	51.07	-99.78	280	Y	
5042425	RIDING MOUNTAIN PARK	50.70	-99.68	756		
5012423	RIDING MTN AUDY	50.72	-100.23	572		
5042485	RORKETON WEST	51.43	-99.73	266	Y	
5042610	STE ROSE	51.03	-99.38	274	Y	Y
5013117	WASAGAMING	50.65	-99.97			
5043158	WILSON CREEK WEIR CS	50.72	-99.53	351	Y	
5043226	WINNIPEGOSIS SOUTH EAST	51.60	-99.88	256		

Manitoba 7:

STATION ID	STATION NAME	LAT	LONG	ELEVATION	ACTIVE	PPT-ONLY
5040128	AUSTIN	49.90	-98.98	328		Y
5040165	BEAVER	50.02	-98.70	263		Y
5040166	BEAVER	50.05	-98.70	268	Y	Y
5010640	CYPRESS RIVER	49.55	-99.08	374	Y	
5040764	DELTA UNIVERSITY FS	50.18	-98.38	248	Y	
5040765	DELTA WATERFOWL RS	50.18	-98.30	248		
5020768	DOMAIN	49.62	-97.32	238		
5020870	ELM CREEK	49.72	-98.02	252		Y
5020913	FANNYSTELLE	49.80	-97.87	244	Y	Y
5041049	GLADSTONE	50.22	-98.95	270		
50410N0	GLADSTONE SOUTH	50.18	-99.02	282		
5041140	GRASS RIVER	50.52	-98.97	270		
5021285	HEADINGLY	49.88	-97.47	240		Y
5021302	HOLLAND	49.60	-98.88	381	Y	Y
5041400	KATRIME EXP ST	50.08	-98.68	270		Y
5041530	LANGRUTH	50.40	-98.55	250	Y	
5041670	MACDONALD	50.17	-98.50	250	Y	Y
5011680	MACDONALD A	50.08	-98.45	255		
5041684	MACGREGOR	49.90	-98.70	301		
5021695	MARQUETTE	50.02	-97.80	244	Y	

5022100	PIGEON LAKE	49.95	-97.60	238		
5042240	PLUMAS	50.38	-99.08			
5042241	PLUMAS	50.45	-99.00			
5012279	PORTAGE LA PRAIRIE	49.97	-98.30	261		
5012280	PORTAGE LA PRAIRIE	49.97	-98.30	261		
5012321	PORTAGE LA PRAIRIE CDA	49.95	-98.27	259	Y	Y
5022335	RATHWELL	49.68	-98.55	324	Y	
5042546	ST AMBROISE	50.23	-98.03	252	Y	
5022550	ST CLAUDE	49.65	-98.37	311	Y	Y
5022770	STARBUCK	49.73	-97.62	238	Y	
5012930	TREHERNE	49.63	-98.70	373		

Manitoba 8:

STATION ID	STATION NAME	LAT	LONG	ELEVATION	ACTIVE	PPT-ONLY
5020036	ALMASIPPI	49.55	-98.20	274		
5020040	ALTONA	49.10	-97.55	248	Y	
5010140	BALDUR	49.30	-99.33	450		
5020551	CARMAN	49.43	-98.15	282	Y	
5020555	CARTWRIGHT	49.10	-99.35	462		
5020625	CRYSTAL CITY	49.05	-98.97	465		Y
5020720	DEERWOOD	49.40	-98.32	338		
5020880	EMERSON	49.02	-97.20			
5020882	EMERSON AUT	49.00	-97.23	242	Y	
5021058	GNADENTHAL	49.10	-97.80	262		Y
5021160	GRAYSVILLE	49.50	-98.17	284		
5021220	GRETNA (AUT)	49.03	-97.57	253	Y	
5021395	KALEIDA	49.13	-98.47	478	Y	Y
5021565	LETELLIER	49.13	-97.30	240		Y
5021688	MANITOU	49.27	-98.48	488		
5021687	MANITOU STRANGE	49.25	-98.52	488	Y	
5021736	MIAMI ORCHARD	49.37	-98.28	330	Y	Y
5021840	MORDEN	49.18	-98.10	302		
5021848	MORDEN EXP FARM	49.18	-98.08	298		
5021920	MORRIS	49.35	-97.37	235		
5021965	MORRIS 2	49.43	-97.48	238	Y	Y
5021975	MYRTLE	49.40	-97.78	248	Y	
5022120	PILOT MOUND	49.20	-98.88	475		
5022125	PILOT MOUND PO	49.20	-98.90	475	Y	
5022245	PLUM COULEE	49.05	-97.80	265	Y	
5022480	ROLAND	49.42	-98.00	267		
5022492	ROSE ISLE	49.55	-98.35	309	Y	Y
5022490	ROSEBANK	49.37	-98.10	427		Y
5022623	SCHANZENFELD	49.13	-97.95	277	Y	Y
5022703	SNOWFLAKE	49.07	-98.65	474	Y	
5012710	SOMERSET	49.45	-98.62	488		
5022740	SPERLING	49.50	-97.70	243	Y	Y
5012545	ST ALPHONSE	49.45	-99.02	403	Y	
5022567	ST JEAN BAPTISTE	49.27	-97.40	238		Y

5012799	SWAN LAKE	49.40	-98.78	482

Manitoba 9:

STATION ID	STATION NAME	LAT	LONG	ELEVATION	ACTIVE	PPT-ONLY
5030160	BEAUSEJOUR 2	50.03	-96.47	251	Y	
5020810	DUGALD	49.87	-96.82	243		
5020880	EMERSON	49.07	-97.20	238		
5021054	GLENLEA U OF M RES STN	49.65	-97.12	234	Y	
5021205	GREEN RIDGE	49.17	-96.98	252	Y	Y
5031511	LA BROQUERIE	49.48	-96.53	290		Y
5021529	LANDMARK	49.67	-96.88	241		
5021689	MARCHAND	49.45	-96.38	305		
5021692	MARCHAND W4	49.43	-96.47	302		Y
5022043	NIVERVILLE	49.60	-97.05	237		
5022051	OAKBANK	49.93	-96.85	246	Y	
503B0NE	OSTENFELD	49.82	-96.48	274	Y	
5022056	OTTERBURNE	49.50	-97.05	238		Y
5022420	RICHER	49.65	-96.45	291		Y
5032495	ROSS	49.77	-96.43	274		
5022601	ST MALO	49.32	-96.97	245	Y	Y
5022606	ST PIERRE JOLYS	49.47	-97.02	281	Y	
502254Q	STE ANNE	49.67	-96.63	252	Y	
5022553	STE ELIZABETH	49.32	-97.17	239		Y
5032560	STE GENEVIEVE	49.75	-96.60	256		
5022780	STEINBACH	49.53	-96.77	254	Y	
5022797	STUARTBURN	49.12	-96.80	291	Y	Y

Manitoba 10:

STATION ID	STATION NAME	LAT	LONG	ELEVATION	ACTIVE	PPT-ONLY
5030155	BEAUSEJOUR	50.13	-96.22	302		
5030335	BRAINTREE 2	49.60	-95.62	316		Y
5030869	ELMA	49.77	-95.93	293		
5031200	GREAT FALLS	50.47	-96.00	249	Y	
503B0MF	NORTH JULIUS	50.07	-96.18	290		
5032160	PINAWA	50.22	-95.92	259		
5032162	PINAWA WNRE	50.18	-96.05	267	Y	
5022171	PINEY	49.03	-96.02	326		
5032360	RENNIE	49.85	-95.53	323	Y	
5032640	SEVEN SISTERS FALLS	50.12	-96.02	267		
5022759	SPRAGUE	49.02	-95.60	329	Y	
5022760	SPRAGUE	49.02	-95.60	329		
5022575	ST LABRE	49.35	-96.03	352		Y
5022798	SUNDOWN	49.02	-96.23	320	Y	Y
5023000	VITA	49.13	-96.57	302		
5023149	WHITEMOUTH LAKE	49.28	-95.75	351		
5023370	ZHODA	49.25	-96.52	305	Y	

Manitoba 11:

STATION ID	STATION NAME	LAT	LONG	ELEVATION	ACTIVE	PPT-ONLY
5021225	GROSSE ISLE	50.05	-97.43	245	Y	Y
5021227	GUNTON HATCHERY	50.28	-97.17	233		
5021992	NAROL	50.05	-96.97	231		
5022070	PETERSFIELD	50.32	-96.98	223		
5022630	SELKIRK	50.17	-96.87	226	Y	
50225DP	ST ANDREWS A	50.05	-97.03	231		
5022788	STONEWALL	50.12	-97.33	252		
502KGHG	STONEWALL	50.22	-97.32	248		Y
5022790	STONY MOUNTAIN	50.07	-97.23	245		
5022791	STONY MOUNTAIN	50.12	-97.17	236	Y	
5023110	WARREN	50.13	-97.63	248		

Manitoba 12:

STATION ID	STATION NAME	LAT	LONG	ELEVATION	ACTIVE	PPT-ONLY
5030080	ARBORG	50.93	-97.08	224	Y	
5040120	ASHERN	51.13	-98.37	263		
5040JK0	ASHERN NORTHWEST	51.20	-98.38	267	Y	Y
5030510	BROAD VALLEY	50.98	-97.47	259		
5030559	CHATFIELD	50.82	-97.50	266		
5040895	ERIKSDALE	50.83	-98.23	259		
5040896	ERIKSDALE 1	50.87	-98.13	268		
5030916	FISHER BRANCH	51.10	-97.55	247	Y	
5030982	FRASERWOOD	50.63	-97.22	256		
5031039	GIMLI	50.63	-97.02	223	Y	
5031040	GIMLI A	50.63	-97.05			
5041229	GYPSUMVILLE	51.67	-98.73	265		
5041230	GYPSUMVILLE	51.73	-98.67	260		
5031300	HODGSON	51.20	-97.58	231		
5031301	HODGSON 2	51.18	-97.45	232	Y	
5041587	LUNDAR	50.75	-97.93	267	Y	
5041800	MOOSEHORN	51.30	-98.62	250		
5041801	MOOSEHORN	51.28	-98.40	269		
5041804	MOOSEHORN COOK	51.28	-98.42	265		
5031991	NARCISSE	50.67	-97.65	273	Y	Y
504B0NM	OAK POINT	50.50	-98.02	250		
5043020	VOGAR	50.92	-98.75	250	Y	

APPENDIX C:
FORTRAN SOURCE CODE FOR DROUGHT INDICES

Palmer Drought Severity Index & Moisture Anomaly Index:

```
*-------------------------------------------------------------------
* This program computes the ORIGINAL Palmer Drought Index.
* This program was originally written BY Larry Batalden and
* Dr. S.M. McGinn and was later modified to incorporate the water
* balance and index computations used by Dr. K.H. Jones. This version
* of the palmer program computes indexes on a monthly basis.
*
* THIS CURRENT VERSION WAS MODIFIED FROM THAT USED FOR THE NAT CHRISTIE STUDY
* UNDERTAKEN BY Drs. Wole Akinremi and Sean McGinn. (1993-1995)
*
* Further edits made by Tim Papakyriakou/Steven Quiring (2001) affecting only the i/o
*

      PROGRAM PDI_vers1

      LOGICAL*1 REC_FLAG,FLAG_H11,FLAG_P04,FLAG_T04,FLAG_SN04
      LOGICAL*1 LUN_INFO,LUN_H11,LUN_T04,LUN_P04,LUN_SN04,LUN_OP
      INTEGER*2 IYR,IYR0,IYRN,IMO,IDY
      INTEGER*4 IREC,IREC0101,IREC1231,IT04,IP04,ISN04,IH11_EST
      INTEGER*4 IREC_H11,IOFFSET_H11,IRECMAX_H11
      INTEGER*4 IREC_T04,IOFFSET_T04,IRECMAX_T04
      INTEGER*4 IREC_P04,IOFFSET_P04,IRECMAX_P04
      INTEGER*4 IREC_SN04,IOFFSET_SN04,IRECMAX_SN04
      CHARACTER T04_FILE*24,P04_FILE*24,SN04_FILE*24,H11_FILE*25
      CHARACTER ROOT_T04*19,ROOT_P04*19,ROOT_SN04*19,ROOT_H11*19
      CHARACTER ROOT_INFO*24,ROOT_OP*22
      CHARACTER DATE9*9,TIME8*8

 INTEGER
   &       YR(1300),     ! year of observations
   &       MONTH(1300),  ! month of observations
   &       DAYS(1300),   ! # of days in that month
   &         CODE,       ! descriptor code       from input
   &         YY,         ! year                  from input
   &         MM,         ! month                 from input
   &         DD,         ! day                   from input
   &       MC,           ! month counter
   &       DC,           ! day counter
   &       NEXTMO,       ! month number for accumulating a month
   &                     !   of data when reading input
   &       INYEAR,       ! year of month of input
   &       J,            ! loop counter for months
   &       K,            ! loop counter
   &       YEAR1,        ! the first year of the data
   &       YRS           ! the # of yrs of data
```

```
REAL    I,      ! the heat index
&       W,      ! the available water capacity(MM)
&       SSPR,   ! soil moisture available at surface
&       SUPR,   !soil moisture available in underlyinglayer
&       TPRE(1300), ! total precipitation in MM
&       AVT(1300),  ! average monthly temperature in CELCIUS
&       ADT,    ! average daily temperature
&       MXT,    ! max daily temp        from input
&       MNT,    ! min daily temp        from input
&       RAIN,   ! daily rain in MM      from input
&       SNO,    ! daily snow in MM      from input
&       TP,     ! daily total precep in MM from input
&       GS,     ! daily ground snow in CM  from input
&       SUMP1,  ! total precipitation accumulator
&       SUMADT, ! daily avg temp accumulator
&       STDEV(12), ! Long term Mean Quarter Monthly Temperature
&       SUMSQ(12), ! Sum of square of precip
&       TSPE,   ! temp sum pe accumulator from input
&       MMT(12), ! Long term Mean Monthly Temperature
&       MADL(12), ! Monthly avg day length for each month
&       TEMPMADL, ! used to fill array of MADL
&       MHI(12), ! Monthly heat index
&       A1,     ! constant used to derive PE
&       LD      ! adjustment for day length
REAL
&       LONG,   ! longitude of station
&       CLAT,   ! latitude of station
&       LATD,   ! latitude (degrees) read from "STAT_DATA.DAT"
&       LATM,   ! latitude (minutes) read from "STAT_DATA.DAT"
&       LOND,   ! longitude(degrees) read from "STAT_DATA.DAT"
&       LONM,   ! longitude(minutes) read from "STAT_DATA.DAT"
&       PR(1300), ! potential recharge - amt of moisture
                ! required to bring soil to field capacity
&       PE(1300), ! potenial evapotranspiration for an
                ! individual month
&       PLS,    ! potential loss of soil moisture from the
                ! surface layer
&       PLU,    ! potential loss of soil moisture from the
                ! underlying layer
&       PL(1300), ! potential loss of soil moisture PLS + PLU
&       RS,     ! potential recharge on surface
&       LS,     ! computed moisture loss from the surface
&       SS,     ! moisture of surface at end of month
&       RU,     ! potential recharge on underlying
&       LU,     ! computed moisture loss from underlying
&       SU,     ! moisture of underlying at end of month
&       RO,     ! computed runoff
&       POT_RUN(1300), ! potential runoff - monthly
&       ET,     ! computed evapotranspiration for a month
&       R,      ! recharge; net gain in soil moisture
                ! during month
&       L       ! net loss of soil moisture during amonth

REAL
```

```
&         SUMET(12),      ! the sum of ET for each calendar month
&         SUMPE(12),      !           PE
&         SUMR(12),       !           R
&         SUMPR(12),      !           PR
&         SUMRO(12),      !           RO
&         SUMSP(12),      !           SP
&         SUML(12),       !           L
&         SUMPL(12),      !           PL
&         SUMP(12),       !           TPRE
&         ALPHA(12),      ! coefficient of evapotranspiration for
                  !  each calendar month
&         BETA(12),       ! coefficient of moisture recharge for
                  !  each calendar month
&         RHO(12),        !coefficient of runoff for each calendar

                  !  month
&         GAM(12),        ! coefficient of loss for each calendar
                  !  month
&         ETBAR(12),      ! long term mean evapotranspiration for a
&         PBAR(12),
                  !  calendar month
&         ETHAT,          ! Climatically Appropriate For Existing
                  ! Conditions (CAFEC) evapotranspiration
&         RHAT,           ! CAFEC soil moisture recharge
&         ROHAT,          ! CAFEC runoff
&         LHAT,           ! CAFEC soil moisture loss
&         PHAT(1300)      ! CAFEC precipitation

 REAL
&         SMD(1300),      ! moisture departure for a month
&         G(12),          ! a constant for each calendar month
&         X(1300),        ! the index of drought (or wet spell)
&         ALGSUM(12),     ! the algabraic sums of smd for eachmonth
&         SUMDBAR(12),    !soil moisture departure overrecordlength
&         KP(12),         ! the second approximation of K
&         ZBAR(12),       ! long term mean moisture anomaly index
&         ANZBAR,         ! sum of zbar
&         KK(12),         ! the climatic characteristic orweighting
                  !  factor for each calendar month
&         Z,              ! moisture anomaly index
&         SUMDK,TOTDK,    !sum of monthly DK and average DK
                  !for all the stations used for simulation
&         AVEDK           !this is the average DK (stations)

    CHARACTER*20
&         PROFILE,   ! name of input file to process
&         STNAME     ! name of station read from "STAT_DATA.DAT"
               !to get the latitude and longitude forstation
    CHARACTER*7
&         STNUM      ! station #  from input dat file
    CHARACTER*2
&         STPROV     ! province of station read from"STAT_DATA.DAT"

 LOGICAL
```

```
  &          ENDIN,     ! flag to indicate end of input file
  &          FOUND,     ! flag indicates that station was found in
  &          MOREDAT    !    "stat_data.dat"
   INTEGER MON(12),MONL(12),IMONTH,ITOTDY,ICOUNT
   DATA MON/31,59,90,120,151,181,212,243,273,304,334,365/
   DATA MONL/31,60,91,121,152,182,213,244,274,305,335,366/
C
C  You may have two input weather data. 1 for the 30 year
c calibration period to genrate the four constants - APLHA
c GAMMA, BETA AND RHO. The second data file will be the period
c of time for which you want to generate PDI. For most of my studies
c the two periods coincided and as such I had only one input data file.

   OPEN (UNIT=17,FILE='sk5b-2099.csv',STATUS='OLD')
   OPEN(UNIT=3,FILE='sk5b-pdsi.OUT',STATUS='UNKNOWN')
   ICOUNT=1
   TOTDK=0.


CCCCC --- The following values need to be checked prior to a run.
c
C  YOU HAVE TO CHANGE XLAT BELOW TO THE LATITUDE OF YOUR SITE
C  IN ORDER FOR THE THORNTHWAITE'S PE EQUATION TO WORK PROPERLY.
C  YOU CAN REMOVE THIS FROM HERE AND READ OFF YOUR INPUT TABLE.
C
       CLAT = 51.88
C
C
C THIS DEIFINES THE YEARS THAT WILL BE USED FOR CALIBRATION
C THIS PERIOD MUST BE AT LEAST 30 YEARS AND DOES NOT NECESSARILY
C HAVE TO COINCIDE WITH THE PERIOD FOR WHICH DROUGHT INDEX IS TO BE GENERATED.
C THIS PERIOD OF CALIBRATION IS ESSENTIAL TO GENRATE THE NECESSARY
C PARAMETERS AND CONSTANTS TO BE USED FOR CALCULATING PDI

    IYR0=1920
    IYRN=1999

    MC=0

C  "W" IS THE AVAILABLE WATER CAPACITY OF YOUR SOIL (AWC)
C THIS IS DEFINED AS THE FIELD CAPACITY MINUS WILTING POINT
C IF YOUR SOIL HAS A DIFFERENT VALUE THEN CHANGE "W" APPROPRAITELY.

    W=150
C
C ---  End of program initialization constants ------------
c

    YEAR1=IYR0
    YRS=1

*-- Initialize all the daily and monthly arrays to zero
*-- This will remove memory effect
   DO J= 1, 1300
```

```
     YR(J) = 0.0
     MONTH(J) = 0.0
     DAYS(J) = 0.0
     TPRE(J) = 0.0
     AVT(J) = 0.0
     PR(J) = 0.0
     PE(J) = 0.0
     PL(J) = 0.0
     POT_RUN(J) = 0.0
     PHAT(J) = 0.0
     SMD(J) = 0.0
     X(J) =0.0
    END DO    !INITIALIZE ARRAY OF 1300'S
   DO J= 1, 12
     MMT(J) = 0.0
     MADL(J) = 0.0
     MHI(J) = 0.0
     ALPHA(J) = 0.0
     BETA(J) = 0.0
     RHO(J) = 0.0
     GAM(J) = 0.0
     ETBAR(J) = 0.0
     STDEV(J) = 0.0
     SUMSQ(J) = 0.0
     PBAR(J) = 0.0
     G(J) = 0.0
     ALGSUM(J) = 0.0
     SUMDBAR(J) = 0.0
     KP(J)  = 0.0
     ZBAR(J) = 0.0
     KK(J)  = 0.0
    END DO    !INITIALIZE ARRAY OF 12'S
C-----------------------------------------------------
C AFTER INITIALIZING THE SITE PARAMERTES TO ZERO, IN CASE OF
C MULTI-SITE RUN, THEN START TO READ THE 30-YEAR CALIBRATION DATA
C FOR THE SITE OF YOUR INTEREST.
      MOREDAT = .TRUE.

C  THIS IS THE LOOP THAT READS YOUR INPUT WEATHER DATA
C  NOTE THE ORDER ON THE INPUT WEATHER VARIABLES!!!!!!
C  YEAR, JULIAN DAY, MAX TEMP, MIN TEMP, RAINFALL (mm)
C  TOTAL PRECIPITAION (mm)

      DO WHILE (MOREDAT)
READ(17,*,END=25)IYR,JDAY,PAX,PIN,RAIN,PCP

C-----------------------------------------------------
CC      DO 111 IYR=IYR0,IYRN

C Initialize the YEARLY variables DO THIS ON JAN 1
C  THE FIRST DAY OF THE YEAR - JULIAN DAY 1 (JDAY = 1)
    IF (JDAY.EQ.1) THEN
     DC = 1
     ITOTDY=1
```

```
    IMONTH=1
    NEXTMO =IMONTH
    INYEAR = IYR
    YY=IYR
    SUMP1 = 0.0
    SUMADT = 0.0
    YRS = YRS +1
    END IF
CC      DO 112  IREC=IREC0101,IREC1231

C  Assign the weather data to PROGRAM'S variables.
       MXT=PAX         ! maximum temperature
       MNT=PIN         ! minimum temperature
       TP=PCP          ! total precipitation
       RAIN=RAIN       ! rainfall amount

C --------- Loop to accumulate a month of data
          IF ((MXT .NE. 9999.0) .AND. (MNT .NE. 9999.0)) THEN
              ADT = (MXT + MNT)/2.0
              SUMADT = SUMADT + ADT
          END IF
          IF (TP .NE. 9999.0) THEN
              SUMP1 = SUMP1 + TP
          END IF
          DC = DC + 1
          ITOTDY=ITOTDY+1

C*****DETERMINE WHICH MONTH OF THE YEAR THE DATA READ FALLS INTO
C
    IF(MOD(YY,4).EQ.0.AND.ITOTDY.GT.MONL(IMONTH))THEN
       NEXTMO=NEXTMO+1
    ELSE IF(MOD(YY,4).GT.0.AND.ITOTDY.GT.MON(IMONTH)) THEN
       NEXTMO=NEXTMO+1
    END IF
C-----------------------------------------------
C------- ACCMULATE A MONTH OF DATA
    IF (NEXTMO.GT.IMONTH) THEN
       DC=DC-1
       MC = MC + 1
       TPRE(MC) = SUMP1
       AVT(MC) = SUMADT/DC
       YR(MC) = INYEAR
       MONTH(MC) = IMONTH
       DAYS(MC)=DC
       INYEAR =YY
       DC = 1
       SUMP1 = 0.0
       SUMADT = 0.0
       IMONTH=NEXTMO
    END IF
CC  112 CONTINUE  !END OF THE IREC0101 TO IREC1231
C
C  YEAR ACCUMULATOR
C
```

```
CC 111 CONTINUE     !FOR THE INPUT YEARS
     END DO       !FOR WHILE MORE DATA
 25   MOREDAT = .FALSE.

C THE READING AND PROCESSING OF THE CALIBRATION DATA ENDS HERE
C
C----------- Finished reading input file

    XYRS = FLOAT(YRS-1)
C SPLIT AWC INTO TOPSOIL AND SUBSOIL
    SSPR = 25.0
    SUPR = W - SSPR
    WRITE(3,*)' THIS IS THE OUTPUT FOR THIS STATION '
    WRITE(3,*)' Latitude is',' ',CLAT

CC     WRITE(3,101)ICOUNT,STN.CODE,STN.NAME,
CC    1  STN.LAT,STN.LNG,STN.ELEV
CC  101  FORMAT(1X,I4,4X,A7,1X,A28,3(2X,F7.2))
    WRITE(3,*)
C IT IS NOT CRUCIAL TO MAKE THE OUTPUTS BELOW. THEY WERE
C NECESSARY DURING THE INTIAL DEVELOPMENT OF THIS PROGRAM

     write (3,*) 'OUTPUT CONTAINS PE VALUES FROM THORNWAITE'
     write (3,*) 'used W = ',W
     write (3,*) 'used SSPR = ',sspr
     write (3,*) 'used SUPR = ',supr
     write (3,*)
C--------- Get the heat index
C      get a long term mean temperature for each calendar month
      DO J = 1, 12
        MMT(J) = 0.0
      END DO
      DO J = 1, MC
        MMT(MONTH(J)) = MMT(MONTH(J)) + AVT(J)
      END DO
       write (3,*) 'month, mean temp (cel)'
       write (3,*)
      DO J = 1, 12
        MMT(J) = MMT(J) / XYRS
         write (3,*) j,mmt(j)
         IF (MMT(J) .LT. 0.0) THEN
           MMT(J) = 0.0
        END IF
      END DO
 C* --------- compute heat index for each calendar month based on MMT
      I = 0.0
      DO J = 1, 12
        MHI(J) = (MMT(J) / 5.0) ** 1.514
        I = I + MHI(J)
      END DO
      WRITE (3,*) 'HEAT INDEX "I" WAS CALCULATED AS ',I
 C* --------- get A1
      A1 = 0.000000675*I**3-0.0000771*I**2+0.0179*I+0.492
      write (3,*) ' AND THE VALUE OF A1 IS  = ',a1
```

```
C* Loop to generate a mean average day length for each month
     write (3,*) 'THE MONTHLY AVERAGE DAY LENGHT FROM JAN TO DEC ARE:'
    DO J = 1, 12
       CALL DL(MONTH,YR,DAYS,J,TEMPMADL,LONG,CLAT)
        MADL(J) = TEMPMADL
        write (3,*)'   ', madl(j)
    END DO

* Loop to generate pe values for each month
    DO J = 1, MC
        LD = (MADL(MONTH(J)) / 12.0) * (DAYS(J) / 30.0)
      IF (AVT(J) .LT. 0.0) THEN
         PE(J) = 0.0
      ELSE
          PE(J) = 1.6 * LD * ((10.0 * AVT(J)) / I) ** A1
      END IF
    END DO

* PE has been calculated with celcius temperatures - Convert pe - cm
* to MM
C      write(3,*)
C*       write (3,*) ' I AM NOW CONVERTING PE IN CM TO MM'
      DO J = 1, MC
       PE(J) = PE(J) * 10.0
    END DO

* -------- Initialize the sum accumulators
    DO J= 1, 12
       SUMET(J) = 0.0
       SUMPE(J) = 0.0
       SUMR(J) = 0.0
       SUMPR(J) = 0.0
       SUMRO(J) = 0.0
       SUMSP(J) = 0.0
       SUML(J) = 0.0
       SUMPL(J) = 0.0
       SUMP(J) = 0.0
      END DO

* -------- Start computation for the WATER BALANCE
C NOTE THAT IF YOUR CALIBRATION PERIOD IS DIFFERENT FROM
C THE PERIOD FOR WHICH DROUGHT IS TO BE GENERATED THE WATER
C BALANCE MUST BE RECALCULATE (1) FOR THE 30-YEAR CALIBRATION PERIOD
C AND (2) FOR THE PERIOD OF INTEREST USIN A NEW INPUT DATA
     DO J = 1, MC
*        evaporation > precipitation   STRESS
        IF (TPRE(J) .LT. PE(J)) THEN
           LS = PE(J) - TPRE(J)
           IF (LS .GT. SSPR) LS = SSPR
           RS = -1.0 * LS
           LU = (PE(J) - TPRE(J) - LS) * SUPR / W
           IF (LU .LT. 0.0) LU = 0.0
           IF (LU .GT. SUPR) LU = SUPR
           RU = -1.0 * LU
```

```
          R = 0.0
          RO = 0.0
          L = LU + LS
*       evaporation = precipitation   EQUILIBRIUM
        ELSE IF (TPRE(J) .EQ. PE(J)) THEN
          RS = 0.0
          RU = 0.0
          LS = 0.0
          LU = 0.0
          R  = 0.0
          RO = 0.0
          L  = 0.0
*       evaporation < precipitation   RECHARGE
        ELSE
          RS = TPRE(J) - PE(J)
          IF (RS .GT. (25.0 - SSPR)) RS = 25.0 - SSPR
          LS = 0.0
          RU = TPRE(J) - PE(J) - RS
          IF (RU .LT. 0.0) RU = 0.0
          IF (RU .GT. (W - 25.0 - SUPR)) RU = W - 25.0 - SUPR
          LU = 0.0
          R = RS + RU
          RO = TPRE(J) - PE(J) - RS - RU
          IF (RO .LT. 0.0) RO = 0.0
          L = 0.0
        END IF

* -------- Complete Water Balance Accounting
        PR(J) = W - SUPR - SSPR
        ET = TPRE(J) + L
        IF (ET .GT. PE(J)) ET = PE(J)
        SS = SSPR + RS
        PLS = PE(J)
        IF (PLS .GT. SSPR) PLS = SSPR
        SU = SUPR + RU
        PLU = (PE(J) - PLS) * SUPR / W
        IF (PLU .GT. SUPR) PLU = SUPR
        PL(J) = PLS + PLU
        POT_RUN(J) = SSPR + SUPR
        SSPR = SS
        SUPR = SU

       SUMET(MONTH(J)) = SUMET(MONTH(J)) + ET
       SUMPE(MONTH(J)) = SUMPE(MONTH(J)) + PE(J)
       SUMR(MONTH(J)) = SUMR(MONTH(J)) + R
       SUMPR(MONTH(J)) = SUMPR(MONTH(J)) + PR(J)
       SUMRO(MONTH(J)) = SUMRO(MONTH(J)) + RO
       SUMSP(MONTH(J)) = SUMSP(MONTH(J)) + POT_RUN(J)
       SUML(MONTH(J)) = SUML(MONTH(J)) + L
       SUMPL(MONTH(J)) = SUMPL(MONTH(J)) + PL(J)
       SUMP(MONTH(J)) = SUMP(MONTH(J)) + TPRE(J)

 310   CONTINUE ! skip processing when data is missing
C BELOW IS A MONTHLY LISTING FOR THE ENTIRE PEORID ON INTEREST
```

```
write(3,*)
      write(3,308) YR(J), MONTH(J), AVT(J), TPRE(J),
   &           PE(J), ET, SSPR, SUPR, PR(J),
   &           R, PL(J), L, POT_RUN(J), RO

308  FORMAT(' ',I4,1X,I2,1X,12(F5.1,1X))
     END DO
* --------- end of phase I

* --------- Write the accumulators to the output file
     write(3,*)
     write (3,*) 'AT THE END OF PHASE I THE AVERAGES OF'
     write (3,*) 'PRECIP, PE, PR, R, PL, L, ET, AND RO'
     write (3,*) 'FOR THE MONTHS OF JAN TO DEC ARE:'
     write (3,*)
     write (3,*) 'PRECIP     PE     PR     R      PL
   1       L      ET      RO'
    do J = 1, 12
       write (3,35)j, sump(j)/XYRS, sumpe(j)/XYRS,
   &           sumpr(j)/XYRS, sumr(j)/XYRS, sumpl(j)/XYRS,
   &           suml(j)/XYRS, sumet(j)/XYRS, sumro(j)/XYRS
    end do
 35  FORMAT(5x,I5,8(F8.4, 1X))

* --------- Compute coefficients at beginning of Phase II on flowchart
    DO J = 1, 12
       IF ((SUMET(J) .EQ. 0.0) .AND. (SUMPE(J) .EQ. 0.0)) THEN
         ALPHA(J) = 1.0
       ELSE
        ALPHA(J) = SUMET(J) / SUMPE(J)
       END IF

       IF ((SUMR(J) .EQ. 0.0) .AND. (SUMPR(J) .EQ. 0.0)) THEN
         BETA(J) = 1.0
       ELSE
        BETA(J) = SUMR(J) / SUMPR(J)
       END IF

      IF ((SUMRO(J) .EQ. 0.0) .AND. (SUMSP(J) .EQ. 0.0)) THEN
         RHO(J) = 0.0
       ELSE
          RHO(J) = SUMRO(J) / SUMSP(J)
      END IF
       IF ((SUML(J) .EQ. 0.0) .AND. (SUML(J) .EQ. 0.0)) THEN
         GAM(J) = 0.0
       ELSE
        GAM(J) = SUML(J) / SUMPL(J)
       END IF

      ETBAR(J) = SUMET(J) / XYRS
      PBAR(J) = SUMP(J) / XYRS
     END DO
C-------------------------------------------------
C HERE IS THE END OF THE GENRATION OF CONSTANTS NEEDED FOR THE PDI
```

```
C IF YOUR CALIBRATION PERIOD IS DIFFERENT FROM YOUR PERIOD OF INTEREST
C THEN YOU WILL NEED TO OPEN A NEW WEATHER DATA HERE TO GENERATE THE
C THE SOIL MOISTURE BALANCE AND PDI USING THE CONSTANTS OBTAINED ABOVE
C-----------------------------------------------------------------


* --------- Write out the coefficients to the output file
   WRITE (3,*)
   write (3,*) ' THE VALUES OF THE FOLLOWING COEFFICIENTS '
   write (3,*) 'ALPHA, BETA, GAMMA, AND RHO '
   write (3,*) 'FOR THE MONTHS OF JAN TO DEC ARE:'
   write (3,*) ' ALPHA    BETA    GAMMA    RHO '
   do j = 1, 12
     write (3,40) alpha(j), beta(j), gam(j), rho(j)
   end do
   WRITE (3,*)
   WRITE (3,*)

 40   FORMAT (' ', 4(F8.4, 1X))

* --------- Page II-2 from literature

     DO J = 1, MC
       ETHAT = ALPHA(MONTH(J)) * PE(J)
       RHAT = BETA(MONTH(J)) * PR(J)
       ROHAT = RHO(MONTH(J)) * POT_RUN(J)
       LHAT = GAM(MONTH(J)) * PL(J)
       PHAT(J) = ETHAT + RHAT + ROHAT - LHAT

* --------- Compute small d
       SMD(J) = TPRE(J) - PHAT(J)
     END DO

* --------- Compute "G" for each of the 12 calendar months
    DO K = 1, 12
       G(K) = ((SUMPE(K) + SUMR(K) + SUMRO(K))
   &                / (SUMP(K) + SUML(K))) + 2.8

    END DO

     DO J = 1, MC
       ALGSUM(MONTH(J)) = ALGSUM(MONTH(J)) + SMD(J)
       SUMDBAR(MONTH(J)) = SUMDBAR(MONTH(J)) + ABS(SMD(J))
       IF (J .EQ. MC) THEN
         DO K = 1, 12
           ALGSUM(K) = ALGSUM(K) / XYRS
           SUMDBAR(K) = SUMDBAR(K) / XYRS
*            added next line to convert to millimeters
*             SUMDBAR(K) = 25.4 / SUMDBAR(K)
         END DO
       END IF
     END DO

    ANZBAR = 0.0
```

```
      DO K = 1, 12
        KP(K) = 1.5 * LOG10((G(K) * (25.4 / SUMDBAR(K)))) + 0.5
        ZBAR(K) = SUMDBAR(K) * KP(K)
       ANZBAR = ANZBAR + ZBAR(K)
      END DO
C THE OPTION IS YOURS HERE, YOU CAN USE 17.67 AS FOUND BY PALAMER
C OR YOU CAN USE 14.2 A VALUE MORE APPROPRAITE FOR THE PRAIRIE
C SEE AKINREMI ET AL 1996 - JOURNAL OF CLIMATE.

     DO K = 1, 12
CC          KK(K) = (17.67 / ANZBAR) * KP(K) * 25.4
        KK(K) = (14.2 / ANZBAR) * KP(K) * 25.4
     END DO

* --------- write out the monthly weighting factors
     write (3,*) 'THE MONTHLY WEIGHTING FACTORS FOR JAN TO DEC ARE:'
     write (3,*) ' SUMDBAR    KPRIME     K'

     SUMDK=0.
     do j = 1, 12
       write (3,45) sumdbar(j)/25.4, kp(j), kk(j)
     SUMDK = SUMDK + (SUMDBAR(j)/25.4 * KP(j))
     end do
     write (3,*)
     write (3,*) ' THE VALUE OF SUMDKPRIME IS', SUMDK
     write (3,*) ' THE NUMBER OF YEARS AND MONTH USED IS = ',XYRS,MC
  45 FORMAT(' ',3(f8.4, 1x))
* ---------- Loop to perform the rest of the calculations page II-3 (bottom)
      WRITE(3,*)
      WRITE (3,*)

      write (3,*) '  YEAR  MONTH     TPRE      PHAT
     1 Z(ANOMALY)  X(PDI) '
C ACTUAL CALCULATION OF PDI FOR YOUR PERIOD OF INTEREST BEGINS HERE
C THIS ASSUMES THAT YOU HAVE ALREADY CALCULATED KK AND SMD FOR EACH MONTH
     DO J = 1, MC
        Z = KK(MONTH(J)) * SMD(J)/25.4
        IF (J.EQ.1) THEN
          X(J) = Z/3.0
        ELSE
          X(J) = X(J-1) *0.897 + Z / 3.0
        ENDIF

        WRITE (3,30) YR(J),MONTH(J), TPRE(J),
     &             PHAT(J), Z, X(J)

     END DO
  30 FORMAT(5X,I4,2X,I2,5X,4(F8.2,2X))
* ---------- Formats

     TOTDK=TOTDK+SUMDK
     icount=icount+1
  41 FORMAT(I4,2F8.2)
C ------------------------------------------
```

```
C THE END OF THE NEW ADDITION
C-----------------------------------------------------------
C THE SUBROUTINE DROTFREQ GENRATES THE FREQUENCY OF DROUGHT ABOVE
C OR BELOW CERTAIN LEVEL OF PDI
C     CALL DROFREQ(X,YR,MONTH,MC)

  109 CONTINUE
      AVEDK=TOTDK/FLOAT(ICOUNT-1)
      write (3,*)
      write (3,*)
      write (3,*)
      write (3,*) 'THE OVERALL MEAN FOR ALL STATIONS IS',AVEDK
      write (3,*) 'THE TOTAL NUMBER OF STATIONS PROCESSED IS',ICOUNT-1
CC      CLOSE (LUN_INFO)
CC      CLOSE (LUN_T04)
CC      CLOSE (LUN_P04)
      CLOSE (UNIT=3)
      CLOSE (UNIT=3)
      END ! END OF THE PROGRAM MPAL

*-----------------------------------------------------------
*       returns the average monthly day length in hrs in the variable TEMPMADL
      SUBROUTINE DL(MONTH,YR,DAYS,MC,TEMPMADL,LONG,CLAT)

      IMPLICIT NONE

* ------------ FORMAL PARAMETERS ----------------
      INTEGER
     &          MONTH(1300),
     &          YR(1300),
     &          DAYS(1300),
     &        MC            ! current month being considered

      REAL
     &          TEMPMADL,    ! monthly average day length
     &        LONG,
     &        CLAT

* ------------ LOCAL VARIABLES ----------------
      REAL
     &        PI,
     &        MLON,
     &        C1(10),
     &        C2(10),
     &        LAT,
     &        DEC,
     &        EQT,
     &        PHI,
     &        HOUR,
     &        MIN,
     &        SUNA1,
     &        HANG,
     &        T,
     &        TSOL,
```

```
     &       ANG,
     &       LENG,
     &       SUMLEN    ! sum of the day lengths

      INTEGER
     &       I,
     &       N,
     &       J,
     &       JDAY,
     &       STJDAY(12),  !array of starting jday each calendar month
     &       ENDJDAY    ! the ending jday for particular month

      PI = 3.1416

*  -------- Set MLON according to CLAT
      IF (CLAT .GE. 105.0) THEN
          MLON = 105.0
       ELSE IF (CLAT .GE. 90.0) THEN
            MLON = 90.0
          ELSE
            MLON = 75.0
      END IF

      C1(1) = 0.3964
      C1(2) = 3.631
      C1(3) = 0.03838
      C1(4) = 0.07659
      C1(5) = 0.0
      C1(6) = -22.97
      C1(7) = -0.3885
      C1(8) = -0.1587
      C1(9) = -0.01021
      C2(1) = 0.002733
      C2(2) = -7.343
      C2(3) = -9.47
      C2(4) = -0.3289
      C2(5) = -0.1955
      C2(6) = 0.5519
      C2(7) = -3.02
      C2(8) = -0.07581
      C2(9) = -0.1245

*  -------- Initialize the starting julian day for each calendar month

        STJDAY(1) = 1
        STJDAY(2) = 32
        STJDAY(3) = 60
        STJDAY(4) = 91
        STJDAY(5) = 121
        STJDAY(6) = 152
        STJDAY(7) = 182
        STJDAY(8) = 213
        STJDAY(9) = 244
        STJDAY(10) = 274
```

```
      STJDAY(11) = 305
      STJDAY(12) = 335

* --------- Modify the starting julian day each calendar month for leapyrs

      IF (MOD(YR(MC),4) .EQ. 0) THEN
        DO J = 3, 12
          STJDAY(J) = STJDAY(J) + 1
        END DO
      END IF

* --------- Determine the ending julian day for the month being considered

     ENDJDAY = STJDAY(MONTH(MC)) + DAYS(MC) - 1

     SUMLEN = 0.0

* --------- Loop to accumulate the day length for each day of the month
*           being considered

      DO JDAY = STJDAY(MONTH(MC)), ENDJDAY

        LAT = CLAT * PI / 180.0
        DEC = C1(1)
        EQT = C2(1)

        DO I = 2, 5
          N = I - 1
          J = I + 4
          PHI = N * (2.0 * PI / 365.0) * JDAY
          DEC = DEC + C1(I) * SIN(PHI) + C1(J) * COS(PHI)
          EQT = EQT + C2(I) * SIN(PHI) + C2(J) * COS(PHI)
        END DO

        DEC = DEC * PI / 180.0
        EQT = EQT / 60.0

        SUNA1 = 0.0
        LENG  = 0.0

        DO HOUR = 0, 23

         DO MIN = 1, 60

         TSOL = (HOUR + MIN/60.0) - ((LONG - MLON) / 15.0) + EQT
         HANG = ABS(TSOL-12.0) * PI / 12.0
         T = SIN(LAT) * SIN(DEC) + COS(LAT) * COS(DEC) * COS(HANG)
            ANG = ASIN(T)
            HANG  = HANG * 180.0 / PI
            SUNA1 = ANG  * 180.0 / PI

            IF (SUNA1 .GT. -1.5) THEN
              LENG = LENG + 1.0
            END IF
```

```
      END DO

    END DO

    LENG = LENG/60.0
    SUMLEN = SUMLEN + LENG


  END DO

* --------- Set the Monthly Average Day Length on return
  TEMPMADL = SUMLEN / DAYS(MC)

 END ! subroutine DL - Returns to Program Palmer at calling point
```

Standardized Precipitation Index:

```
PROGRAM SPICOMPUTE
c
c This code was written by Ned Guttman and was obtained from
c ftp://www.ncdc.noaa.gov/pub/software/palmer/spinew.f
c
c Further modifications were made to the program by Steven Quiring (Feb. 2001)
c mainly to customize for available data
c
c ATTENTION: this program contains bugs that prevent compiling/running
c                  with the G77 compiler under the MSDOS(Windows) environment
c The bugs are related to the definition of two variables (amssng, derf)
c amssng- double precision vs. single precision
c derf- global vs. intrinsic
c

      parameter (nlen=7,maxyrs=80,amssng=-99.99,inunit=17,
     1  ibegyr=1920,iout=10,bmssng=-9.99,incode=2,ihist=1,icur=0,
     2  icuryr=1999,icurmo= 9)


c     This is the driver (main) program used to compute the
c     Standardized Precipitation Index (SPI). It computes
c     the probability of precipitation based on all available
c     input data. The time scales are 1,2,3,6,9,12,24-month
c     SPI values. These can be changed by changing the
c     "data nrun" statement. The parameter statement gives the
c     user the option of outputting sequential files for the period
c     of record or one file for all sites and time scales for a
c     specified year/month or both.
c
c     INPUT     nlen     number of time scales
c               maxyrs   maximum number of years of record
c               bmssng   input value for missing data
c               amssng   output value for missing data
c               incode   1 for integer input data; 2 for decimal
c               inunit   device number for input data
c               ibegyr   first year of data
c               ihist    1 to output arrays of sequential data (id, yr,
c                        12 monthly values); 0 to suppress these arrays
c               icur     1 to output only data for the specified
c                        year icuryr and month icurmo (id, yr, mo,
c                        nlen values) in the order corresponding to
c                        the data statement nrun; 0 to suppress
c               icuryr   year of output (see icur above)
c               icurmo   month of output (see icur above)
c               iout     device number for output data:
c
c     OUTPUT            *1   parameters, n-counts, etc for SPI(nlen)
c               *2   SPI(nlen)
c               *3   precip probabilities
c               *4   accumulated precip values
c               iout+5 SPI for all time scales for given yr/mo
```

```
c                   iout+6 precipitation probabilities for all
c                        time scales for given yr/mo
c                   iout+7 accumulated precip values for all
c                        time scales for given yr/mo
c
c                   the * indicates iout times nlen
c
c
c   OTHER ROUTINES CALLED
c     subroutine read
c     subroutine spipe3
c
c   CAVIAT
c     SPI values in central part of the precip distribution can
c     be considered to be accurate and reasonable if the number
c     of independent non-zero accumulated precipitation amounts
c     is greater than about 40; values in the tails of the
c     distribution can be considered accurate and reasonable
c     if the number of non-zero accumulated amounts is greater
c     than about 60.
c
c   NOTE
c     Look at READ subroutine to put input data in proper format.
c
c   written by Ned Guttman in January 1998; some of the software
c   and logic based on software provided by John Kleist, Colorado
c   State Univ.
c
c
      dimension pp(maxyrs*12),probne(maxyrs*12),
     1  pcpacc(maxyrs*12),pzero(12),spi(maxyrs*12),num(12),
     2  numpos(12),nrun(nlen),spiout(12),prob(12),pacc(12),
     3  curspi(nlen),curpro(nlen),curacc(nlen)
      double precision par1(12),par2(12),par3(12),xmom1(12),
     1  xmom2(12),xmom3(12),x(maxyrs),y(maxyrs*12),
     2  index(maxyrs*12),temparr(maxyrs+1)
       real amssng
      data nrun /1,2,3,6,9,12,24/
      do im=1,nlen
        curspi(im)=amssng
        curpro(im)=amssng
        curacc(im)=amssng
      enddo
      iread=0
           open(unit=inunit,file='sk5b-spi.csv',status='old')

      if(icur.eq.1) then
        write(iout+5,1014)(nrun(i),i=1,nlen)
        write(iout+6,1015)(nrun(i),i=1,nlen)
        write(iout+7,1016)(nrun(i),i=1,nlen)
      endif
 1014 format(' ID  YR MO SPI-',17(i2,5x))
 1015 format(' ID  YR MO PROB-',17(i2,6x))
 1016 format(' ID  YR MO ACCUM-',17(i2,7x))
```

```
l     if (iread.eq.1) goto 50
c
c     read input data
c
      call read(incode,pp,inunit,amssng,bmssng,ibegyr,maxyrs,id,iread)
      do 10 i=1,nlen
c
c     compute SPI values, probabilities, accumulated precip
c
       call spipe3 (nrun(i),pp,par1,par2,par3,pzero,spi,probne,
     1   pcpacc,xmom1,xmom2,xmom3,amssng,num,numpos,maxyrs,
     2   index,y,x,temparr)
c
c     write out monthly arrays of ncounts, lmoments, parameters,etc.
c
       do k=1,12
       write((iout*i)+1,1000)id,nrun(i),k,xmom1(k),xmom2(k),xmom3(k),
     1   par1(k),par2(k),par3(k),num(k),numpos(k),pzero(k)
1000   format (i4.4,2i3,6f13.8,2i5,f5.3)
       enddo
c
c      identify first and last non-missing data so that output
c      arrays do not contain a bunch of missing data.
c
       ifirst=1
20       if (spi(ifirst).eq.amssng) then
         ifirst=ifirst+1
         goto 20
        endif
       ilast=maxyrs*12
30       if (spi(ilast).eq.amssng) then
         ilast=ilast-1
         goto 30
        endif
       do im=1,12
        spiout(im)=amssng
        prob(im)=amssng
        pacc(im)=amssng
       enddo
       do 40 j=ifirst,ilast
        iy=(j-1)/12+ibegyr
        im=mod (j-1,12)+1
        spiout(im)=spi(j)
        prob(im)=probne(j)
        pacc(im)=pcpacc(j)
        if(icur.eq.1) then
          if(iy.eq.icuryr.and.im.eq.icurmo)curspi(i)=spiout(im)
          if(iy.eq.icuryr.and.im.eq.icurmo)curpro(i)=prob(im)
          if(iy.eq.icuryr.and.im.eq.icurmo)curacc(i)=pacc(im)
        endif
        if (im.eq.12.or.j.eq.ilast) then
c
c      write out arrays if ihist=1
c
```

```
         if(ihist.eq.1) then
          write ((iout*i)+2,1001)id,iy,(spiout(im),im=1,12)
          write ((iout*i)+3,1003)id,iy,(prob(im),im=1,12)
          write ((iout*i)+4,1002)id,iy,(pacc(im),im=1,12)
         endif
c
c      change the format statements for different output formats
c

1001   format (i4.4,i5,12f7.2)
1003   format (i4.4,i5,12f8.3)
1002   format (i4.4,i5,12f9.2)

         do im=1,12
          spiout(im)=amssng
          prob(im)=amssng
          pacc(im)=amssng
         enddo
        endif
40     continue
10     continue
c
c      write out array of current month spi for all id's
c
       if(icur.eq.1) then
        write(iout+5,1004)id,icuryr,icurmo,(curspi(im),im=1,nlen)
        write(iout+6,1005)id,icuryr,icurmo,(curpro(im),im=1,nlen)
        write(iout+7,1006)id,icuryr,icurmo,(curacc(im),im=1,nlen)
       endif
          do im=1,nlen
           curspi(im)=amssng
           curpro(im)=amssng
           curacc(im)=amssng
          enddo
1004   format (i4.4,i5,i3,17f7.2)
1005   format (i4.4,i5,i3,17f8.3)
1006   format (i4.4,i5,i3,17f9.2)
       goto 1
50     end


      SUBROUTINE READ(incode,pp,inunit,amssng,bmssng,ibegyr,
     1   maxyrs,jd,iread)
c
c     INPUT:  inprec    input data array: id,iyr,monthly integer
c                       precip amounts in hundredths
c             precin    input data array: id,iyr,monthly decimal
c                       precip amounts in hundredths
c             inunit    device number for reading input data
c             amssng    missing data code for output
c             bmssng    missing data code for input
c             incode    1 for integer; 2 for digital input data
c             ibegyr    earliest possible beginning year of data
c             maxyrs    maximum possible years of data
```

```
c
c     OUTPUT: pp        one dimensional array of precip data
c            jd        location identification number
c            iread      iread=1 indicates end of data file
c
c
      dimension pp(maxyrs*12),inprec(12),precin(12)
      if(incode.ne.1.and.incode.ne.2) STOP "INCODE ERROR"
      iread=0
c
c     set precip array to missing
c
1     do 10, i=1,maxyrs*12
       pp(i)=amssng
10     continue
      jd=0
20     continue

c
c     set input format to correspond to your input data source.
c     program assumes integer format (value is divided by 100
c     later in the program to get values to hundredths)
c

      if(incode.eq.1) then
       inmssng=bmssng
       read(inunit,*,end=40)id,iyr,(inprec(j),j=1,12)
c 1000  format (i1,i4,12i7)

c
c     check for new station id
c
       if (id.ne.jd.and.jd.ne.0) goto 30
       iy=iyr-ibegyr
       do im=1,12
         if(inprec(im).eq.inmssng) goto 23
c
c     convert integer precip to decimal precip (hundredths)
c
         pp(iy*12+im)=float(inprec(im))/100.0
 23     enddo
      else
       read(inunit,*,end=40)id,iyr,(precin(j),j=1,12)
c 1001  format (i1,i4,12f7.2)
       if (id.ne.jd.and.jd.ne.0) goto 30
       iy=iyr-ibegyr
       do im=1,12
         if(precin(im).eq.bmssng) goto 24
         pp(iy*12+im)=precin(im)
 24     enddo
      endif
      jd=id
      goto 20
 30    continue
```

```
      backspace (inunit)
      return
40    iread=1
      return
      end


      SUBROUTINE SPIPE3(nrun,pp,par1,par2,par3,pzero,spi,probne,
     1 pcpacc,xmom1,xmom2,xmom3,amssng,num,numpos,maxyrs,index,y,
     2 x,temparr)
c
c     INPUT: pp          one dimensional array of input data
c                   where input is monthly precip data
c                   beginning with a January value
c          nrun        length of moving totals
c          amssng        value for missing data
c          maxyrs        maximum possible number of years of
c                   data
c
c     OUTPUT: par1,par2,par3   parameters (mean, s.d., skewness) of
c                   Pearson Type III distribution used to
c                   fit the input data > 0
c          xmom1,xmom2,xmom3 l-moments of the input data > 0
c          pzero         relative  frequency of input data = 0
c          spi          standardized precip index
c          probne        probability of observed data <= x
c          pcpacc        data accumulated over length nrun
c          num          number of non-missing observations
c          numpos         number of non-zero observations
c
c     This program used the program of John Kleist, Colorado State
c     Univ., that computed spi values from a 2 parameter ML gamma
c     probability distribution, as a basis for the moving totals, etc.
c     code. I added the PE3 l-moment computations. The subroutines
c     and functions in upper case came from Jon Hosking, IBM.
c          Ned Guttman
c          Nov. 1997
c

      dimension pp(maxyrs*12),probne(maxyrs*12),pcpacc(maxyrs*12),
     1  pzero(12),spi(maxyrs*12),num(12),numpos(12)
      double precision par1(12),par2(12),par3(12),index(maxyrs*12),
     1  xmom1(12),xmom2(12),xmom3(12),xmom(3),para(3),
     2  y(maxyrs*12),x(maxyrs),temparr(maxyrs+1),
     3  cdfpe3,dlgamma,gamind,quastn
c
c
c     save par1,par2,par3 to 8 decimal places if you want to use
c     them later for any additional calculations...not keeping
c     enough decimal places leads to errors in probabilities!
c
c
c     the first nrun-1 index values will be missing
c
```

```
      do 10 j=1,nrun-1
        index(j)=amssng
        probne(j)=amssng
        pcpacc(j)=amssng
 10   continue
c
c     sum nrun precip values; store them in appropriate index location
C
c     if any value is missing, set the sum to missing
c
      do 30 j=nrun,maxyrs*12
        index(j)=0.0
        do 20 i=0,nrun-1
          if(pp(j-i).ne.amssng)then
            index(j)=index(j)+pp(j-i)
            pcpacc(j)=index(j)
          else
            index(j)=amssng
            probne(j)=amssng
            pcpacc(j)=amssng
            goto 30
          endif
 20     continue
 30   continue

c
c     to maintain seasonality, do everything by month
c
      do 50 i=0,11
        n=0
        nz=0
        np=0
        if (nrun.le.12) then
          do 40 j=nrun+i,maxyrs*12,12
            if(index(j).ne.amssng) then
c
c       this routine calculates lmoments and parameters of the PE3
c       distribution for all input data.  if you want to compute the
c       parameters for a specific period of record, then the limits
c       of j must be set appropriately for temparr. it is recommended
c       that for both monitoring and historical perspective that
c       all data be used for computing the probabilities, and that
c       the historical time series be the "latest" and most complete
c       output.
c
c       n-count for all non-missing data, including zeroes
c
              n=n+1
              if(index(j).gt.0) then
c
c       n-count for all non-missing, non-zero data; temparr is for
c       non-zero, non-missing precipitation
c
                np=np+1
```

```
              temparr(np)=index(j)
            else
c
c       n-count for all non-missing, zero data
c
              nz=nz+1
            endif
          endif
 40       continue
        elseif (nrun.gt.12) then
         j=nrun+i
c
c       step the sequence of data by the length of nrun to get
c       independent samples
c
         if (nrun.gt.12.and.nrun.le.24) nstep=24
         if (nrun.gt.24.and.nrun.le.36) nstep=36
         if (nrun.gt.36.and.nrun.le.48) nstep=48
         if (nrun.gt.48.and.nrun.le.60) nstep=60
         if (nrun.gt.60.and.nrun.le.72) nstep=72
 41       if (j.gt.maxyrs*12) GOTO 42
c
c        this routine calculates lmoments and parameters of the PE3
c        distribution for all input data.  if you want to compute the
c        parameters for a specific period of record, then the limits
c        of j must be set appropriately for temparr
c
           if(index(j).ne.amssng) then
             n=n+1
             if(index(j).gt.0) then
               np=np+1
               temparr(np)=index(j)
             else
               nz=nz+1
             endif
             j=j+nstep
             goto 41
           else
c
c        look for next non-missing nrun>12 value
c
             j=j+12
             goto 41
           endif
         endif
 42    im=mod(nrun+i-1,12)+1
        pzero(im)=float(nz)/float(n)
        num(im)=n
        numpos(im)=np
c
c      order the data
c
        call sort(temparr,x,np,maxyrs)
c
```

```
c     fit l-moments for non-zero precip; if 2nd moment=0, routine
c     fails and all 3 moments set to zero (condition indicates all
c     data values are equal).  also, if not enough non-zero data
c     (less than 3), routine fails and all moments set to zero.
c
      call samlmr(x,np,xmom,3,-0.00D0,0D0,ifail)
      xmom1(im)=xmom(1)
      xmom2(im)=xmom(2)
      xmom3(im)=xmom(3)
c
c     compute parameters of Pearson type III (3-parameter gamma); the
c     three parameters are the mean, s.d., skewness of the NON-ZERO data.
c     The mean for all the data is (1-pzero)*par1 or (1-pzero)*xmom1
c     since par1=xmom1
c
      call pelpe3(xmom,para,ifail)
c
c     if ifail not = 0, then all 3 parameters are set to zero
c     if routine fails, output is sent to unit 6 by pelpe3 routine
c
      par1(im)=para(1)
      par2(im)=para(2)
      par3(im)=para(3)
 50   continue
c
c     compute the probability (cdfpe3), take into account the
c     mixed distribution if pzero not equal to zero, truncate
c     the probability from .001 to .999, transform the probability to
c     spi (quastn). ifail=1 indicates invalid parameter 2 (negative).
c     if routines fail, output is sent to unit 6 by called routines.
c
      do 60 j=nrun,maxyrs*12
        im=mod(j-1,12)+1
        para(1)=par1(im)
        para(2)=par2(im)
        para(3)=par3(im)
c
c       set missing values to amssng
c
 61     if(index(j).eq.amssng) then
          probne(j)=amssng
          spi(j)=amssng
          goto 60
        endif
        if(index(j).ne.amssng) then
          index(j)=cdfpe3(index(j),para,ifail,amssng)
c
c       if cdf routine fails, set probne and spi = amssng
c
          if(ifail.ne.0) then
            index(j)=amssng
            goto 61
          endif
          y(j)=pzero(im)+(1-pzero(im))*index(j)
```

```
c
c       force the probabilities and therefore the spi to be bounded
c       by +/- 3.09
c
        if(y(j).gt..999)y(j)=.999
        if(y(j).lt..001)y(J)=.001
        probne(j)=y(j)
        index(j)=quastn(y(j))
        spi(j)=index(j)
      endif
 60   continue
      return
      end
c
c
      DOUBLE PRECISION FUNCTION CDFPE3(X,PARA,ifail,amssng)
C***********************************************************************
C*                                                                     *
C*  FORTRAN CODE WRITTEN FOR INCLUSION IN IBM RESEARCH REPORT RC20525, *
C*  'FORTRAN ROUTINES FOR USE WITH THE METHOD OF L-MOMENTS, VERSION 3' *
C*                                                                     *
C*  J. R. M. HOSKING                                                   *
C*  IBM RESEARCH DIVISION                                              *
C*  T. J. WATSON RESEARCH CENTER                                       *
C*  YORKTOWN HEIGHTS                                                   *
C*  NEW YORK 10598, U.S.A.                                             *
C*                                                                     *
C*  VERSION 3     AUGUST 1996                                          *
C*                                                                     *
C***********************************************************************
C
C  DISTRIBUTION FUNCTION OF THE PEARSON TYPE 3 DISTRIBUTION
C
C  OTHER ROUTINES USED: DERF,DLGAMA,GAMIND
C
      IMPLICIT DOUBLE PRECISION (A-H,O-Z)
      DOUBLE PRECISION PARA(3),DERF(X)

      real amssng

      DATA ZERO/0D0/,HALF/0.5D0/,ONE/1D0/,TWO/2D0/,FOUR/4D0/
      DATA RTHALF/0.70710 67811 86547 524D0/
C
C         SMALL IS USED TO TEST WHETHER SKEWNESS IS EFFECTIVELY ZERO
C
      DATA SMALL/1D-6/
C
      ifail=0
      CDFPE3=ZERO
      IF(PARA(2).LE.ZERO)GOTO 1000
      GAMMA=PARA(3)
      IF(DABS(GAMMA).LE.SMALL)GOTO 10
      ALPHA=FOUR/(GAMMA*GAMMA)
      Z=TWO*(X-PARA(1))/(PARA(2)*GAMMA)+ALPHA
```

```
      IF(Z.GT.ZERO)CDFPE3=GAMIND(Z,ALPHA,DLGAMA(ALPHA))
      IF(GAMMA.LT.ZERO)CDFPE3=ONE-CDFPE3
      RETURN
C
C         ZERO SKEWNESS
C
   10 Z=(X-PARA(1))/PARA(2)
      CDFPE3=HALF+HALF*DERF(Z*RTHALF)
      RETURN
C
 1000 WRITE(6,7000)
      ifail=1
      cdfpe3=amssng
      RETURN
C
 7000 FORMAT(' *** ERROR *** ROUTINE CDFPE3 : PARAMETERS INVALID')
      END
c
c
      SUBROUTINE PELPE3(XMOM,PARA,ifail)
C***********************************************************************
C*                                                                     *
C*  FORTRAN CODE WRITTEN FOR INCLUSION IN IBM RESEARCH REPORT RC20525, *
C*  'FORTRAN ROUTINES FOR USE WITH THE METHOD OF L-MOMENTS, VERSION 3' *
C*                                                                     *
C*  J. R. M. HOSKING                                                   *
C*  IBM RESEARCH DIVISION                                              *
C*  T. J. WATSON RESEARCH CENTER                                       *
C*  YORKTOWN HEIGHTS                                                   *
C*  NEW YORK 10598, U.S.A.                                             *
C*                                                                     *
C*  VERSION 3     AUGUST 1996                                          *
C*                                                                     *
C***********************************************************************
C
C  PARAMETER ESTIMATION VIA L-MOMENTS FOR THE PEARSON TYPE 3 DISTRIBUTION
C
C  PARAMETERS OF ROUTINE:
C  XMOM   * INPUT* ARRAY OF LENGTH 3. CONTAINS THE L-MOMENTS LAMBDA-1,
C           LAMBDA-2 AND TAU-3.
C  PARA   *OUTPUT* ARRAY OF LENGTH 3. ON EXIT, CONTAINS THE PARAMETERS
C           IN THE ORDER MU, SIGMA, GAMMA (MEAN, S.D., SKEWNESS).
C
C  OTHER ROUTINES USED: DLGAMA
C
C  METHOD: RATIONAL APPROXIMATION IS USED TO EXPRESS ALPHA, THE SHAPE
C  PARAMETER OF THE GAMMA DISTRIBUTION, AS A FUNCTION OF TAU-3.
C  RELATIVE ACCURACY OF THE APPROXIMATION IS BETTER THAN 3E-5.
C
      IMPLICIT DOUBLE PRECISION (A-H,O-Z)
      DOUBLE PRECISION XMOM(3),PARA(3)
      DATA ZERO/0D0/,THIRD/0.33333333D0/,HALF/0.5D0/,ONE/1D0/,TWO/2D0/
C
C         SMALL IS USED TO TEST WHETHER SKEWNESS IS EFFECTIVELY ZERO
```

```
C
   DATA SMALL/1D-6/
C
C      CONSTANTS USED IN MINIMAX APPROXIMATIONS
C
   DATA C1,C2,C3/ 0.2906D0, 0.1882D0, 0.0442D0/
   DATA D1,D2,D3/ 0.36067D0,-0.59567D0, 0.25361D0/
   DATA D4,D5,D6/-2.78861D0, 2.56096D0,-0.77045D0/
   DATA PI3,ROOTPI/9.4247780D0,1.7724539D0/
C
   ifail=0
   T3=DABS(XMOM(3))
   IF(XMOM(2).LE.ZERO.OR.T3.GE.ONE)GOTO 1000
   IF(T3.LE.SMALL)GOTO 100
   IF(T3.GE.THIRD)GOTO 10
   T=PI3*T3*T3
   ALPHA=(ONE+C1*T)/(T*(ONE+T*(C2+T*C3)))
   GOTO 20
 10 CONTINUE
   T=ONE-T3
   ALPHA=T*(D1+T*(D2+T*D3))/(ONE+T*(D4+T*(D5+T*D6)))
 20 CONTINUE
   RTALPH=DSQRT(ALPHA)
   BETA=ROOTPI*XMOM(2)*DEXP(DLGAMA(ALPHA)-DLGAMA(ALPHA+HALF))
   PARA(1)=XMOM(1)
   PARA(2)=BETA*RTALPH
   PARA(3)=TWO/RTALPH
   IF(XMOM(3).LT.ZERO)PARA(3)=-PARA(3)
   RETURN
C
C      ZERO SKEWNESS
C
 100 CONTINUE
   PARA(1)=XMOM(1)
   PARA(2)=XMOM(2)*ROOTPI
   PARA(3)=ZERO
   RETURN
C
c1000 WRITE(6,7000)
 1000 DO 1010 I=1,3
 1010 PARA(I)=ZERO
   ifail=1
   RETURN
C
 7000 FORMAT(' *** ERROR *** ROUTINE PELPE3 : L-MOMENTS INVALID')
   END
c
c
c
   SUBROUTINE SAMLMR(X,N,XMOM,NMOM,A,B,ifail)
C***********************************************************************
C*                                                                    *
C*  FORTRAN CODE WRITTEN FOR INCLUSION IN IBM RESEARCH REPORT RC20525, *
C*  'FORTRAN ROUTINES FOR USE WITH THE METHOD OF L-MOMENTS, VERSION 3' *
```

```
C*                                          *
C* J. R. M. HOSKING                                *
C* IBM RESEARCH DIVISION                                *
C* T. J. WATSON RESEARCH CENTER                              *
C* YORKTOWN HEIGHTS                                   *
C* NEW YORK 10598, U.S.A.                            *
C*                                          *
C* VERSION 3    AUGUST 1996                           *
C*                                          *
C***********************************************************************
C
C SAMPLE L-MOMENTS OF A DATA ARRAY
C
C PARAMETERS OF ROUTINE:
C X     * INPUT* ARRAY OF LENGTH N. CONTAINS THE DATA, IN ASCENDING
C             ORDER.
C N     * INPUT* NUMBER OF DATA VALUES
C XMOM  *OUTPUT* ARRAY OF LENGTH NMOM. ON EXIT, CONTAINS THE SAMPLE
C             L-MOMENTS L-1, L-2, T-3, T-4, ... .
C NMOM  * INPUT* NUMBER OF L-MOMENTS TO BE FOUND. AT MOST MAX(N,20).
C A     * INPUT* ) PARAMETERS OF PLOTTING
C B     * INPUT* ) POSITION (SEE BELOW)
C
C FOR UNBIASED ESTIMATES (OF THE LAMBDA'S) SET A=B=ZERO. OTHERWISE,
C PLOTTING-POSITION ESTIMATORS ARE USED, BASED ON THE PLOTTING POSITION
C (J+A)/(N+B)  FOR THE J'TH SMALLEST OF N OBSERVATIONS. FOR EXAMPLE,
C A=-0.35D0 AND B=0.0D0 YIELDS THE ESTIMATORS RECOMMENDED BY
C HOSKING ET AL. (1985, TECHNOMETRICS) FOR THE GEV DISTRIBUTION.
C
      IMPLICIT DOUBLE PRECISION (A-H,O-Z)
      DOUBLE PRECISION X(N),XMOM(NMOM),SUM(20)
      DATA ZERO/0D0/,ONE/1D0/
      ifail=0
      IF(NMOM.GT.20.OR.NMOM.GT.N)GOTO 1000
      DO 10 J=1,NMOM
   10 SUM(J)=ZERO
      IF(A.EQ.ZERO.AND.B.EQ.ZERO)GOTO 50
      IF(A.LE.-ONE.OR.A.GE.B)GOTO 1010
C
C         PLOTTING-POSITION ESTIMATES OF PWM'S
C
      DO 30 I=1,N
      PPOS=(I+A)/(N+B)
      TERM=X(I)
      SUM(1)=SUM(1)+TERM
      DO 20 J=2,NMOM
      TERM=TERM*PPOS
   20 SUM(J)=SUM(J)+TERM
   30 CONTINUE
      DO 40 J=1,NMOM
   40 SUM(J)=SUM(J)/N
      GOTO 100
C
C         UNBIASED ESTIMATES OF PWM'S
```

```
C
  50 DO 70 I=1,N
    Z=I
    TERM=X(I)
    SUM(1)=SUM(1)+TERM
    DO 60 J=2,NMOM
    Z=Z-ONE
    TERM=TERM*Z
  60 SUM(J)=SUM(J)+TERM
  70 CONTINUE
    Y=N
    Z=N
    SUM(1)=SUM(1)/Z
    DO 80 J=2,NMOM
    Y=Y-ONE
    Z=Z*Y
  80 SUM(J)=SUM(J)/Z
C
C       L-MOMENTS
C
 100 K=NMOM
    P0=ONE
    IF(NMOM-NMOM/2*2.EQ.1)P0=-ONE
    DO 120 KK=2,NMOM
    AK=K
    P0=-P0
    P=P0
    TEMP=P*SUM(1)
    DO 110 I=1,K-1
    AI=I
    P=-P*(AK+AI-ONE)*(AK-AI)/(AI*AI)
 110 TEMP=TEMP+P*SUM(I+1)
    SUM(K)=TEMP
 120 K=K-1
    XMOM(1)=SUM(1)
    IF(NMOM.EQ.1)RETURN
    XMOM(2)=SUM(2)
    IF(SUM(2).EQ.ZERO)GOTO 1020
    IF(NMOM.EQ.2)RETURN
    DO 130 K=3,NMOM
 130 XMOM(K)=SUM(K)/SUM(2)
    RETURN
C
 1000 ifail=1
    do i=1,3
     xmom(i)=0
    enddo
    WRITE(6,7000)
    RETURN
 1010 WRITE(6,7010)
    RETURN
 1020 ifail=1
    do i=1,3
     xmom(i)=0
```

```
      enddo
      WRITE(6,7020)
      RETURN
C
 7000 FORMAT(' *** ERROR *** ROUTINE SAMLMR : PARAMETER NMOM INVALID')
 7010 FORMAT(' *** ERROR *** ROUTINE SAMLMR :',
     * ' PLOTTING-POSITION PARAMETERS INVALID')
 7020 FORMAT(' *** ERROR *** ROUTINE SAMLMR : ALL DATA VALUES EQUAL')
      END
c
c
c
      DOUBLE PRECISION FUNCTION DERF(X)
C***********************************************************************
C*                                                                     *
C*  FORTRAN CODE WRITTEN FOR INCLUSION IN IBM RESEARCH REPORT RC20525, *
C*  'FORTRAN ROUTINES FOR USE WITH THE METHOD OF L-MOMENTS, VERSION 3' *
C*                                                                     *
C*  J. R. M. HOSKING                                                   *
C*  IBM RESEARCH DIVISION                                              *
C*  T. J. WATSON RESEARCH CENTER                                       *
C*  YORKTOWN HEIGHTS                                                   *
C*  NEW YORK 10598, U.S.A.                                             *
C*                                                                     *
C*  VERSION 3     AUGUST 1996                                          *
C*                                                                     *
C***********************************************************************
C
C  ERROR FUNCTION
C
C  BASED ON ALGORITHM 5666, J.F.HART ET AL. (1968) 'COMPUTER
C  APPROXIMATIONS'
C
C  ACCURATE TO 15 DECIMAL PLACES
C
      IMPLICIT DOUBLE PRECISION (A-H, O-Z)

      DATA ZERO/0D0/,ONE/1D0/,TWO/2D0/,THREE/3D0/,FOUR/4D0/,P65/0.65D0/
C
C         COEFFICIENTS OF RATIONAL-FUNCTION APPROXIMATION
C
      DATA P0,P1,P2,P3,P4,P5,P6/
     *  0.22020 68679 12376 1D3,    0.22121 35961 69931 1D3,
     *  0.11207 92914 97870 9D3,    0.33912 86607 83830 0D2,
     *  0.63739 62203 53165 0D1,    0.70038 30644 43688 1D0,
     *  0.35262 49659 98910 9D-1/
      DATA Q0,Q1,Q2,Q3,Q4,Q5,Q6,Q7/
     *  0.44041 37358 24752 2D3,    0.79382 65125 19948 4D3,
     *  0.63733 36333 78831 1D3,    0.29656 42487 79673 7D3,
     *  0.86780 73220 29460 8D2,    0.16064 17757 92069 5D2,
     *  0.17556 67163 18264 2D1,    0.88388 34764 83184 4D-1/
C
C         C1 IS SQRT(2), C2 IS SQRT(2/PI)
C         BIG IS THE POINT AT WHICH DERF=1 TO MACHINE PRECISION
```

```
C
      DATA C1/1.4142 13562 37309 5D0/
      DATA C2/7.9788 45608 02865 4D-1/
      DATA BIG/6.25D0/,CRIT/5D0/
C
      DERF=ZERO
      IF(X.EQ.ZERO)RETURN
      XX=DABS(X)
      IF(XX.GT.BIG)GOTO 20
      EXPNTL=DEXP(-X*X)
      ZZ=DABS(X*C1)
      IF(XX.GT.CRIT)GOTO 10
      DERF=EXPNTL*((((((P6*ZZ+P5)*ZZ+P4)*ZZ+P3)*ZZ+P2)*ZZ+P1)*ZZ+P0)/
     *  (((((((Q7*ZZ+Q6)*ZZ+Q5)*ZZ+Q4)*ZZ+Q3)*ZZ+Q2)*ZZ+Q1)*ZZ+Q0)
      IF(X.GT.ZERO)DERF=ONE-TWO*DERF
      IF(X.LT.ZERO)DERF=TWO*DERF-ONE
      RETURN
C
   10 DERF=EXPNTL*C2/(ZZ+ONE/(ZZ+TWO/(ZZ+THREE/(ZZ+FOUR/(ZZ+P65)))))
      IF(X.GT.ZERO)DERF=ONE-DERF
      IF(X.LT.ZERO)DERF=DERF-ONE
      RETURN
C
   20 DERF=ONE
      IF(X.LT.ZERO)DERF=-ONE
      RETURN
      END
c
c
c
      DOUBLE PRECISION FUNCTION DLGAMA(X)
C***********************************************************************
C*                                                                     *
C*  FORTRAN CODE WRITTEN FOR INCLUSION IN IBM RESEARCH REPORT RC20525, *
C*  'FORTRAN ROUTINES FOR USE WITH THE METHOD OF L-MOMENTS, VERSION 3' *
C*                                                                     *
C*  J. R. M. HOSKING                                                   *
C*  IBM RESEARCH DIVISION                                              *
C*  T. J. WATSON RESEARCH CENTER                                       *
C*  YORKTOWN HEIGHTS                                                   *
C*  NEW YORK 10598, U.S.A.                                             *
C*                                                                     *
C*  VERSION 3     AUGUST 1996                                          *
C*                                                                     *
C***********************************************************************
C
C  LOGARITHM OF GAMMA FUNCTION
C
C  BASED ON ALGORITHM ACM291, COMMUN. ASSOC. COMPUT. MACH. (1966)
C
      IMPLICIT DOUBLE PRECISION (A-H,O-Z)
      DATA SMALL,CRIT,BIG,TOOBIG/1D-7,13D0,1D9,2D36/
C
C         C0 IS 0.5*LOG(2*PI)
```

```
C      C1...C7 ARE THE COEFFTS OF THE ASYMPTOTIC EXPANSION OF DLGAMA
C
      DATA C0,C1,C2,C3,C4,C5,C6,C7/
     * 0.91893 85332 04672 742D 0, 0.83333 33333 33333 333D-1,
     * -0.27777 77777 77777 778D-2, 0.79365 07936 50793 651D-3,
     * -0.59523 80952 38095 238D-3, 0.84175 08417 50841 751D-3,
     * -0.19175 26917 52691 753D-2, 0.64102 56410 25641 026D-2/
C
C      S1 IS -(EULER'S CONSTANT), S2 IS PI**2/12
C
      DATA S1/-0.57721 56649 01532 861D 0/
      DATA S2/ 0.82246 70334 24113 218D 0/
C
      DATA ZERO/0D0/,HALF/0.5D0/,ONE/1D0/,TWO/2D0/
      DLGAMA=ZERO
      IF(X.LE.ZERO)GOTO 1000
      IF(X.GT.TOOBIG)GOTO 1000
C
C      USE SMALL-X APPROXIMATION IF X IS NEAR 0, 1 OR 2
C
      IF(DABS(X-TWO).GT.SMALL)GOTO 10
      DLGAMA=DLOG(X-ONE)
      XX=X-TWO
      GOTO 20
   10 IF(DABS(X-ONE).GT.SMALL)GOTO 30
      XX=X-ONE
   20 DLGAMA=DLGAMA+XX*(S1+XX*S2)
      RETURN
   30 IF(X.GT.SMALL)GOTO 40
      DLGAMA=-DLOG(X)+S1*X
      RETURN
C
C      REDUCE TO DLGAMA(X+N) WHERE X+N.GE.CRIT
C
   40 SUM1=ZERO
      Y=X
      IF(Y.GE.CRIT)GOTO 60
      Z=ONE
   50 Z=Z*Y
      Y=Y+ONE
      IF(Y.LT.CRIT)GOTO 50
      SUM1=SUM1-DLOG(Z)
C
C      USE ASYMPTOTIC EXPANSION IF Y.GE.CRIT
C
   60 SUM1=SUM1+(Y-HALF)*DLOG(Y)-Y+C0
      SUM2=ZERO
      IF(Y.GE.BIG)GOTO 70
      Z=ONE/(Y*Y)
      SUM2=((((((C7*Z+C6)*Z+C5)*Z+C4)*Z+C3)*Z+C2)*Z+C1)/Y
   70 DLGAMA=SUM1+SUM2
      RETURN
C
 1000 WRITE(6,7000)X
```

```
      RETURN
C
 7000 FORMAT(' *** ERROR *** ROUTINE DLGAMA :',
     *  ' ARGUMENT OUT OF RANGE :',D24.16)
      END
c
c
c
      DOUBLE PRECISION FUNCTION GAMIND(X,ALPHA,G)
C***********************************************************************
C*                                                                     *
C*  FORTRAN CODE WRITTEN FOR INCLUSION IN IBM RESEARCH REPORT RC20525, *
C*  'FORTRAN ROUTINES FOR USE WITH THE METHOD OF L-MOMENTS, VERSION 3' *
C*                                                                     *
C*  J. R. M. HOSKING                                                   *
C*  IBM RESEARCH DIVISION                                              *
C*  T. J. WATSON RESEARCH CENTER                                       *
C*  YORKTOWN HEIGHTS                                                   *
C*  NEW YORK 10598, U.S.A.                                             *
C*                                                                     *
C*  VERSION 3     AUGUST 1996                                          *
C*                                                                     *
C***********************************************************************
C
C  THE INCOMPLETE GAMMA INTEGRAL
C
C  BASED ON ALGORITHM AS239, APPL. STATIST. (1988) VOL.37 NO.3
C
C  PARAMETERS OF ROUTINE:
C  X      * INPUT* ARGUMENT OF FUNCTION (UPPER LIMIT OF INTEGRATION)
C  ALPHA  * INPUT* SHAPE PARAMETER
C  G      * INPUT* LOG(GAMMA(ALPHA)). MUST BE SUPPLIED BY THE PROGRAM,
C                  E.G. AS DLGAMA(ALPHA).
C
C  OTHER ROUTINES USED: DERF
C
      IMPLICIT DOUBLE PRECISION (A-H,O-Z)
      Double Precision Derf(X)
      DATA ZERO/0D0/,HALF/0.5D0/,ONE/1D0/,TWO/2D0/,THREE/3D0/,X13/13D0/,
     *  X36/36D0/,X42/42D0/,X119/119D0/,X1620/1620D0/,X38880/38880D0/,
     *  RTHALF/0.70710 67811 86547 524D0/
C
C         EPS,MAXIT CONTROL THE TEST FOR CONVERGENCE OF THE SERIES AND
C           CONTINUED-FRACTION EXPANSIONS.
C         OFL IS A LARGE NUMBER, USED TO RESCALE THE CONTINUED FRACTION.
C         UFL IS SUCH THAT EXP(UFL) IS JUST .GT. ZERO.
C         AHILL CONTROLS THE SWITCH TO HILL'S APPROXIMATION.
C
      DATA EPS/1D-12/,MAXIT/100000/,OFL/1D30/,UFL/-180D0/,AHILL/1D4/
      GAMIND=ZERO
      IF(ALPHA.LE.ZERO)GOTO 1000
      IF(X.LT.ZERO)GOTO 1010
      IF(X.EQ.ZERO)RETURN
C
```

```
      IF(ALPHA.GT.AHILL)GOTO 100
      IF(X.GT.ONE.AND.X.GE.ALPHA)GOTO 50
C
C     SERIES EXPANSION
C
      SUM=ONE
      TERM=ONE
      A=ALPHA
      DO 10 IT=1,MAXIT
      A=A+ONE
      TERM=TERM*X/A
      SUM=SUM+TERM
      IF(TERM.LE.EPS)GOTO 20
   10 CONTINUE
      WRITE(6,7020)
   20 ARG=ALPHA*DLOG(X)-X-G+DLOG(SUM/ALPHA)
      GAMIND=ZERO
      IF(ARG.GE.UFL)GAMIND=DEXP(ARG)
      RETURN
C
C     CONTINUED-FRACTION EXPANSION
C
   50 CONTINUE
      A=ONE-ALPHA
      B=A+X+ONE
      TERM=ZERO
      PN1=ONE
      PN2=X
      PN3=X+ONE
      PN4=X*B
      RATIO=PN3/PN4
      DO 70 IT=1,MAXIT
      A=A+ONE
      B=B+TWO
      TERM=TERM+ONE
      AN=A*TERM
      PN5=B*PN3-AN*PN1
      PN6=B*PN4-AN*PN2
      IF(PN6.EQ.ZERO)GOTO 60
      RN=PN5/PN6
      DIFF=DABS(RATIO-RN)
      IF(DIFF.LE.EPS.AND.DIFF.LE.EPS*RN)GOTO 80
      RATIO=RN
   60 PN1=PN3
      PN2=PN4
      PN3=PN5
      PN4=PN6
      IF(DABS(PN5).LT.OFL)GOTO 70
      PN1=PN1/OFL
      PN2=PN2/OFL
      PN3=PN3/OFL
      PN4=PN4/OFL
   70 CONTINUE
      WRITE(6,7020)
```

```
 80 ARG=ALPHA*DLOG(X)-X-G+DLOG(RATIO)
    GAMIND=ONE
    IF(ARG.GE.UFL)GAMIND=ONE-DEXP(ARG)
    RETURN
C
C     ALPHA IS LARGE: USE HILL'S APPROXIMATION (N.L. JOHNSON AND
C     S. KOTZ, 1970, 'CONTINUOUS UNIVARIATE DISTRIBUTIONS 1', P.180)
C
C     THE 'DO 110' LOOP CALCULATES 2*(X-ALPHA-ALPHA*DLOG(X/ALPHA)),
C     USING POWER-SERIES EXPANSION TO AVOID ROUNDING ERROR
C
 100 CONTINUE
    R=ONE/DSQRT(ALPHA)
    Z=(X-ALPHA)*R
    TERM=Z*Z
    SUM=HALF*TERM
    DO 110 I=1,12
    TERM=-TERM*Z*R
    SUM=SUM+TERM/(I+TWO)
    IF(DABS(TERM).LT.EPS)GOTO 120
 110 CONTINUE
 120 WW=TWO*SUM
    W=DSQRT(WW)
    IF(X.LT.ALPHA)W=-W
    H1=ONE/THREE
    H2=-W/X36
    H3=(-WW+X13)/X1620
    H4=(X42*WW+X119)*W/X38880
    Z=(((H4*R+H3)*R+H2)*R+H1)*R+W
    GAMIND=HALF+HALF*DERF(Z*RTHALF)
    RETURN
C
 1000 WRITE(6,7000)ALPHA
    RETURN
 1010 WRITE(6,7010)X
    RETURN
C
 7000 FORMAT(' *** ERROR *** ROUTINE GAMIND :',
   *  ' SHAPE PARAMETER OUT OF RANGE :',D16.8)
 7010 FORMAT(' *** ERROR *** ROUTINE GAMIND :',
   *  ' ARGUMENT OF FUNCTION OUT OF RANGE :',D16.8)
 7020 FORMAT(' ** WARNING ** ROUTINE GAMIND :',
   *  ' ITERATION HAS NOT CONVERGED. RESULT MAY BE UNRELIABLE.')
    END
c
c
c
    DOUBLE PRECISION FUNCTION QUASTN(F)
C***********************************************************************
C*                                                                     *
C*  FORTRAN CODE WRITTEN FOR INCLUSION IN IBM RESEARCH REPORT RC20525, *
C*  'FORTRAN ROUTINES FOR USE WITH THE METHOD OF L-MOMENTS, VERSION 3' *
C*                                                                     *
C*  J. R. M. HOSKING                                                   *
```

```
C* IBM RESEARCH DIVISION                        *
C* T. J. WATSON RESEARCH CENTER                     *
C* YORKTOWN HEIGHTS                           *
C* NEW YORK 10598, U.S.A.                   *
C*                             *
C* VERSION 3    AUGUST 1996                   *
C*                             *
C***********************************************************************
C
C QUANTILE FUNCTION OF THE STANDARD NORMAL DISTRIBUTION
C
C BASED ON ALGORITHM AS241, APPL. STATIST. (1988) VOL.37 NO.3
C
   IMPLICIT DOUBLE PRECISION (A-H,O-Z)
   DATA ZERO/0D0/,HALF/0.5D0/,ONE/1D0/
   DATA SPLIT1/0.425D0/,SPLIT2/5D0/,CONST1/0.180625D0/,CONST2/1.6D0/
C
C     COEFFICIENTS OF RATIONAL-FUNCTION APPROXIMATIONS
C
   DATA A0,A1,A2,A3,A4,A5,A6,A7,B1,B2,B3,B4,B5,B6,B7/
  *                   0.33871 32872 79636 661D  1,
  * 0.13314 16678 91784 377D  3, 0.19715 90950 30655 144D  4,
  * 0.13731 69376 55094 611D  5, 0.45921 95393 15498 715D  5,
  * 0.67265 77092 70087 009D  5, 0.33430 57558 35881 281D  5,
  * 0.25090 80928 73012 267D  4, 0.42313 33070 16009 113D  2,
  * 0.68718 70074 92057 908D  3, 0.53941 96021 42475 111D  4,
  * 0.21213 79430 15865 959D  5, 0.39307 89580 00927 106D  5,
  * 0.28729 08573 57219 427D  5, 0.52264 95278 85285 456D  4/
   DATA C0,C1,C2,C3,C4,C5,C6,C7,D1,D2,D3,D4,D5,D6,D7/
  *                   0.14234 37110 74968 358D  1,
  * 0.46303 37846 15654 530D  1, 0.57694 97221 46069 141D  1,
  * 0.36478 48324 76320 461D  1, 0.12704 58252 45236 838D  1,
  * 0.24178 07251 77450 612D  0, 0.22723 84498 92691 846D -1,
  * 0.77454 50142 78341 408D -3, 0.20531 91626 63775 882D  1,
  * 0.16763 84830 18380 385D  1, 0.68976 73349 85100 005D  0,
  * 0.14810 39764 27480 075D  0, 0.15198 66656 36164 572D -1,
  * 0.54759 38084 99534 495D -3, 0.10507 50071 64441 684D -8/
   DATA E0,E1,E2,E3,E4,E5,E6,E7,F1,F2,F3,F4,F5,F6,F7/
  *                   0.66579 04643 50110 378D  1,
  * 0.54637 84911 16411 437D  1, 0.17848 26539 91729 133D  1,
  * 0.29656 05718 28504 891D  0, 0.26532 18952 65761 230D -1,
  * 0.12426 60947 38807 844D -2, 0.27115 55568 74348 758D -4,
  * 0.20103 34399 29228 813D -6, 0.59983 22065 55887 938D  0,
  * 0.13692 98809 22735 805D  0, 0.14875 36129 08506 149D -1,
  * 0.78686 91311 45613 259D -3, 0.18463 18317 51005 468D -4,
  * 0.14215 11758 31644 589D -6, 0.20442 63103 38993 979D-14/
C
   Q=F-HALF
   IF(DABS(Q).GT.SPLIT1)GOTO 10
   R=CONST1-Q*Q
   QUASTN=Q*(((((((A7*R+A6)*R+A5)*R+A4)*R+A3)*R+A2)*R+A1)*R+A0)
  *     /(((((((B7*R+B6)*R+B5)*R+B4)*R+B3)*R+B2)*R+B1)*R+ONE)
   RETURN
 10 R=F
```

```
      IF(Q.GE.ZERO)R=ONE-F
      IF(R.LE.ZERO)GOTO 1000
      R=DSQRT(-DLOG(R))
      IF(R.GT.SPLIT2)GOTO 20
      R=R-CONST2
      QUASTN=(((((((C7*R+C6)*R+C5)*R+C4)*R+C3)*R+C2)*R+C1)*R+C0)
     *    /(((((((D7*R+D6)*R+D5)*R+D4)*R+D3)*R+D2)*R+D1)*R+ONE)
      GOTO 30
   20 R=R-SPLIT2
      QUASTN=(((((((E7*R+E6)*R+E5)*R+E4)*R+E3)*R+E2)*R+E1)*R+E0)
     *    /(((((((F7*R+F6)*R+F5)*R+F4)*R+F3)*R+F2)*R+F1)*R+ONE)
   30 IF(Q.LT.ZERO)QUASTN=-QUASTN
      RETURN
C
 1000 WRITE(6,7000)F
      QUASTN=ZERO
      RETURN
C
 7000 FORMAT(' *** ERROR *** ROUTINE QUASTN :',
     * ' ARGUMENT OF FUNCTION INVALID')
      END
c
c
c
      SUBROUTINE SORT(temparr,X,N,maxyrs)
C***********************************************************************
C*                                                                     *
C*  FORTRAN CODE WRITTEN FOR INCLUSION IN IBM RESEARCH REPORT RC20525, *
C*  'FORTRAN ROUTINES FOR USE WITH THE METHOD OF L-MOMENTS, VERSION 3' *
C*                                                                     *
C*  J. R. M. HOSKING                                                   *
C*  IBM RESEARCH DIVISION                                              *
C*  T. J. WATSON RESEARCH CENTER                                       *
C*  YORKTOWN HEIGHTS                                                   *
C*  NEW YORK 10598, U.S.A.                                             *
C*                                                                     *
C*  VERSION 3     AUGUST 1996                                          *
C*                                                                     *
C***********************************************************************
C
C  SORTS THE ARRAY X INTO ASCENDING ORDER
C
C  PARAMETERS OF ROUTINE:
C  X     *IN/OUT* ARRAY OF LENGTH N. CONTAINS THE NUMBERS TO BE SORTED.
C                 ON EXIT, CONTAINS THE SORTED NUMBERS.
C  N     * INPUT* NUMBER OF ELEMENTS TO BE SORTED
C
C  METHOD USED IS SHELL SORT WITH SEQUENCE OF INCREMENTS AS IN
C  D.F.KNUTH (1969) 'THE ART OF COMPUTER PROGRAMMING', VOL.3, P.95
C
      IMPLICIT DOUBLE PRECISION (A-H,O-Z)
      DOUBLE PRECISION X(N),temparr(maxyrs+1)
      IF(N.LE.1)RETURN
      do i=1,n
```

```
   x(i)=temparr(i)
  enddo
  J=4
  DO 10 I=1,100
  J=3*J+1
  IF(J.GE.N)GOTO 20
10 CONTINUE
20 CONTINUE
  M=(J/3)
  DO 60 MM=1,100
  M=M/3
  IF(M.EQ.0)RETURN
  DO 50 I=M+1,N
  TEST=X(I)
  J=I
  DO 30 JJ=1,100
  J=J-M
  IF(J.LE.0)GOTO 40
  IF(TEST.GE.X(J))GOTO 40
30 X(J+M)=X(J)
40 CONTINUE
50 X(J+M)=TEST
60 CONTINUE
  END
```

NOAA Drought Index:

```
        PROGRAM NOAA2
*
* This program is from Titlow (1987) and has been modified for
* use with existing data
*
*
*       Fortran version of the NOAA Drought Index
*
*
*       Variable list:
*       @ MMN       = MONTHLY MEAN PRECIPITATION
*       @ WMN       = WEEKLY MEAN PRECIPITATION (ASSUMED TO BE 1/4 OF MONTHLY
TOTAL)
*       NODAYS      = NUMBER OF DAYS IN EACH FILE
*       NREC  = INDIVIDUAL RECORD NUMBER, INPUT FILE
*       @ KYR = YEAR OF RECORD
*       @ N   = WEEK NUMBER, 1-52
*       @ PRCP      = DAILY PRECIPITATION
*       @ PREC      = WEEKLY PRECIPITATION
*       @ PAVG      = WEEKLY NORMAL PRECIPITATION
*       NA1   = FIRST WEEK OF ACCUMULATION PERIOD
*       PSUM  = SUM OF PREC
*       PRAVG = SUM OF PAVG
*       CT    = PERCENT, PSUM OF PAVG
*       NUM   = NUMBER OF WEEKS IN INPUT FILE
*       CTDRW       = DROUGHT WARNING COUNTER
*       CTDRE = DROUGHT EMERGENCY COUNTER
*       @DRGRH      = DROUGHT LEVEL ARRAY FOR GRAPH
*       @W    = WEEK ARRAY FOR ARRAY
*       Z     = LENGTH OF DROUGHT COUNTER
*       @DEF  = FIRST WEEK OF TWO CONSECUTIVE WEEKS IN DROUGHT EXITING CRITIERIA
*       @WKAVG      = WEEK AFTER DROUGHT PERCENTAGE SURPASSES 65%
*             THAT MUST RECEIVE NORMAL PRECIPITATION
*       @     = AN ARRAYED VARIABLE
*
*
*
              INTEGER NODAYS,NUM,CTDRW,CTDRE,CTDRWH
              CHARACTER*25 NAME
              REAL PRCP(29220),WMN(12),MMN(12),WKAVG
              REAL PRECAR(4174),PAVGAR(4174),DEF(30)
              INTEGER YR(29220),MNTH(29220),DY(29220),P,Z
              INTEGER KYRARR(4174),NARR(4174),DRGRH(5000),W(5000)
*
* open I/O files
*
              open(unit=17, file='sk5b-noaa.csv', status='old')
              open(unit=20, file='sk5b-mppt.csv', status='old')
              open(unit=3, file='sk5b-noaa.out', status='unknown')
              open(unit=2, file='sk5b-noaa2.out', status='unknown')
```

```
*
* set number of weeks in 1920-99
*
            num = 4174
*
*       SET DROUGHT COUNTERS TO ZERO
*
            CTDRW=0
            CTDRE=0
            CTDRWH=0
*
*       READ IN YEAR, MONTH, JULIAN DAY, and DAILY PRECIPITATION RECORD FOR 1920-99
*
            DO 1 I=1,29220
                READ(17,*) yr(I),mnth(I),DY(I),PRCP(I)
1           CONTINUE
*
*       READ IN MONTHLY MEAN PRECIPIATION VALUES AND CONVERT TO WEEKLY (DIVIDE BY
FOUR)
*
            DO 2 J=1,12
                READ(20,*) MMN(J)
                WMN(J)= MMN(J)/4.0
2           CONTINUE
*
*       COMPUTE THE WEEKLY ACTUAL AND AVERAGE PRECIPITATION, AND YEAR FOR EACH
WEEK NUMBER
*
*           KYRARR(1)=1950
            DO 3 K=1,4174
                L=(K-1)*7
                PRECAR(K)=0.0
                PAVGAR(K)=0.0
                NARR(K)=K
                DO 4 M=1,7
                    PRECAR(K)= PRECAR(K) + PRCP(M+L)
4               CONTINUE
                KYRARR(K)=YR(M+L)
                PAVGAR(K)= PAVGAR(K) + WMN(MNTH(M+L))
3           CONTINUE
*
*       INITIALIZE COUNTING VARIABLE
*
            NREC=0
*
*       WRITE OUTPUT CAPTIONS
*
*
            WRITE(2,40)
40          FORMAT(/,12X,8X, 'WKLY PRECIP',3X,'NORM PRECIP',4X,'PCT OF')
*
            WRITE(2,50)
50      FORMAT(1X,'YEAR',6X,'WEEKS',4X,'LAST',4X,'SUM',3X,'LAST',4X,'SUM',4X,'NORMAL')
*
```

```
*       NON-DROUGHT LOOP
*
500             NREC= NREC+1
                PSUM=0.0
                PRAVG=0.0
*
*       TWELVE-WEEK COUNTER
*
                DO 100 I=1,12
                        IF(NREC .GT. NUM) GOTO 400
*
                        KYR=KYRARR(NREC)
                        N=NARR(NREC)
                        PREC=PRECAR(NREC)*(((FLOAT(I)-1.0)*0.04545)+0.5)
                        PAVG=PAVGAR(NREC)*(((FLOAT(I)-1.0)*0.04545)+0.5)
*
                        IF(I .EQ. 1) NA1=N
*
                        PSUM=PSUM+PREC
                        PRAVG=PRAVG+PAVG
                        NREC=NREC+1
100                     CONTINUE
*
*       PERCENTAGE CALCULATION AND DROUGHT WARNING BRANCH
*
150                     PCT=100.0*(PSUM/PRAVG)
                        IF(PCT .LT. 58.0) GOTO 300
*
*       DROUGHT WATCH CHECK
*
                IF(PCT.GE.58.0.AND.PCT.LE.62.0)THEN
                        WRITE(2,14) KYR,NA1,N,PREC,PSUM,PAVG,PRAVG,PCT
                        W(N-11)=N
                        DRGRH(N-11)=1
                        WRITE(3,13) W(N-11),DRGRH(M-11)
                        CTDRWH=CTDRWH+1
                ELSE
                        WRITE(2,10) KYR,NA1,N,PREC,PSUM,PAVG,PRAVG,PCT
                        W(N-11)=N
                        DRGRH(N-11)=O
                        WRITE(3,13) W(N-11),DRGRH(N-11)
                ENDIF
                NREC=NREC-12
                GOTO 500
*
*       POST-DROUGHT RECOVERY AND RESET
*
200             WRITE(2,10) KYR,NA1,N,PREC,PSUM,PAVG,PRAVG,PCT
                W(N-11)=N
                DRGRH(N-11)=O
                WRITE(3,13) W(N-11),DRGRH(N-11)
                NREC=NREC-11
                GOTO 500
*
```

```
*       DROUGHT WARNING MODE:
*       WEEKS BEYOND THE 12 WEEK PERIOD ARE ACCUMULATED UNTIL PCT .GE. 65 FOR TWO
WEEKS PLUS
*       SECOND WEEK ARE RECEIVING NORMAL PRECIPITATION
*
300         Z=1
*
*       DROUGHT EMERGENCY CHECK
*
310         IF(PCT .LT. 45.0.AND.DRGRH(N-12).GT.1)THEN
                WRITE(2,12) KYR,NA1,N,PREC,PSUM,PAVG,PRAVG,PCT
                W(N-11)=N
                DRGRH(N-11)=3
                WRITE(3,13) W(N-11),DRGRH(N-11)
                CTDRE=CTDRE+1
            ELSE
                WRITE(2,11) KYR,NA1,N,PREC,PSUM,PAVG,PRAVG,PCT
                W(N-11)=N
                DRGRH(N-11)=2
                WRITE(3,13) W(N-11),DRGRH(N-11)
                CTDRW=CTDRW+1
            ENDIF
            KYR=KYRARR(NREC)
            N=NARR(NREC)
            PREC=PRECAR(NREC)
            PAVG=PAVGAR(NREC)
*
*       NEXT WEEK IN RECORD IS ADDED
*
            PSUM=PSUM+PREC
            PRAVG=PRAVG+PAVG
*
            PCT=100.0*(PSUM/PRAVG)
            DEF(Z)=PCT
*
*       DECISION BRANCH FOR CONITUATION OF DROUGHT
*       (GOTO 200-CONTINUATION OF DROUGHT)
*       (GOTO 310-DROUGHT ENDS)
*
            IF(PCT .GE. 65.0.AND.DEF(Z-1).GT.65.0)THEN
                WKAVG=PAVGAR(NREC)
                IF(PRECAR(NREC).GE.WKAVG)GOTO 200
            ENDIF
*
            NREC=NREC+1
            NEWNUM=NUM+1
            IF(NREC .GT. NEWNUM) GOTO 400
            Z=Z+1
            GOTO 310
*
*
400         WRITE(2,666)CTDRWH
            WRITE(2,444)CTDRW
            WRITE(2,555)CTDRE
```

```
666         FORMAT(/,1X,'NO. OF DROUGHT WATCH PERIODS = ',1X,I4)
444         FORMAT(/,1X,'NO. OF DROUGHT WARNING PERIODS = ',1X,I4)
555         FORMAT(/,1X,'NO. OF DROUGHT EMERGENCY PERIODS = ',1X,I4)
*
*
10          FORMAT(1X,I4,2X,I4,1X,'-',I4,4F7.2,F10.2)
14          FORMAT(1X,I4,2X,I4,1X,'-',I4,4F7.2,F10.2, ' DR. WATCH ')
11          FORMAT(1X,I4,2X,I4,1X,'-',I4,4F7.2,F10.2, ' DR. WARN. ')
12          FORMAT(1X,I4,2X,I4,1X,'-',I4,4F7.2,F10.2, ' DR. EMERG. ')
13          FORMAT(1X,I4,1X,I1)
*
*
            STOP
            END
```